UNIVERSIDADE DE LISBOA
FACULDADE DE CIÊNCIAS

# Novel dynamics and functions of Fibronectin in early vertebrate development

*" Documento Definitivo"*

**Doutoramento em Biologia**

Especialidade de Biologia do Desenvolvimento

Patrícia Gomes de Almeida

Tese orientada por:

Prof. Dr. Sólveig Thorsteinsdóttir

Prof. Dr. Isabel Palmeirim

Prof. Dr. Raquel P. Andrade

Documento especialmente elaborado para a obtenção do grau de doutor

2018

UNIVERSIDADE DE LISBOA

FACULDADE DE CIÊNCIAS

# Novel dynamics and functions of Fibronectin in early vertebrate development

**Doutoramento em Biologia**

Especialidade de Biologia do Desenvolvimento

Patrícia Gomes de Almeida

Tese orientada por:

Prof. Dr. Sólveig Thorsteinsdóttir, Prof. Dr. Isabel Palmeirim, Prof. Dr. Raquel P. Andrade

Júri:

Presidente:

- Doutora Maria Manuela Gomes Coelho de Noronha Trancoso, Professora Catedrática e Presidente do Departamento de Biologia Animal da Faculdade de Ciências da Universidade de Lisboa

Vogais:

- Doutor Theodoor Henri Smit, *Professor*, *Department of Medical Biology* da *Amsterdam University Medical Center*, Holanda;
- Doutora Cristina Maria Santos Alves de Carvalho Barrias, Investigadora Principal, Instituto Nacional de Engenharia Biomédica da Universidade do Porto;
- Doutora Maria José Cardoso Oliveira, Investigadora Principal, Instituto Nacional de Engenharia Biomédica da Universidade do Porto;
- Doutora Ana Teresa Fernandes Nunes Tavares, Investigadora Pós-Doutoramento, Nova Medical School | Faculdade de Ciências Médicas da Universidade Nova de Lisboa;
- Doutora Maria Leonor Tavares Saúde, Professora Auxiliar Convidada, Faculdade de Medicina da Universidade de Lisboa;
- Doutora Solveig Thorsteinsdóttir, Professora Associada com Agregação, Faculdade de Ciências da Universidade de Lisboa (orientadora).

Documento especialmente elaborado para a obtenção do grau de doutor

Fundação para a Ciência e Tecnologia - SFRH/BD/86980/2012

2018

The work presented in this dissertation was developed with the support from the Fundação para a Ciência e Tecnologia, through a PhD Fellowship (SFRH/BD/86980/2012), and Projects PTDC/SAU-OBD/103771/2008, PTDC/BEXBID/5410/2014, UID/BIA/00329/2013, UID/BIM/04773/2013 and PPBI-POCI-01-0145-FEDER-022122.

*The most beautiful things in the world cannot be seen or touched, they are felt with the heart.*
— Antoine de Saint-Exupéry, The Little Prince

## Acknowledgements

Completar uma viagem como esta não seria possível sem ter imenso a agradecer a uma verdadeira multidão, dentro e fora do laboratório.

Em primeiríssimo lugar quero agradecer à Sólveig, por depositar a sua confiança em mim e ter aceite embarcar nesta viagem comigo, remando sempre incansavelmente para a frente independentemente dos desafios e dificuldades que fomos encontrando pelo caminho. Obrigada por me teres dado a conhecer a incrível e sempre fascinante Biologia do Desenvolvimento e por me transmitires o teu entusiasmo e paixão pela Ciência, guardarei isso sempre! Mas acima de tudo, agradeço por me teres orientado não só com sabedoria e inteligência, mas com amizade e carinho. Obrigada pela tua paciência infindável, compreensão, positivismo, e principalmente pela constante disponibilidade e apoio incondicional, científico ou não.

Tenho de fazer um agradecimento muito especial também à super co-orientadora Raquel. Obrigada por me teres acolhido com tanto carinho e entusiasmo, e me receberes sempre com um enorme abraço e energia positiva contagiante. Um obrigado especial também por toda a tua compreensão, disponibilidade e generosidade ímpares; mas, acima de tudo, por uma amizade muito especial que ultrapassa o laboratório e a ciência, e o apoio nos momentos mais difíceis. Obrigada do fundo do coração por tudo, foi e é um privilégio trabalhar contigo.

E porque fui orientada por um elenco de luxo, um enorme obrigado também à Isabel, por me receberes sempre com um sorriso, por também me acolheres e me ensinares as tuas artes! É um orgulho poder dizer que fui orientada não por uma, não duas, mas três pessoas e cientistas extraordinárias, com quem aprendi tanto, não só sobre Ciência, mas sobre humanidade. Um gigante obrigado.

Além disso, tive a sorte de estar inserida também não num, mas dois grupos fantásticos, a quem tenho tanto a agradecer. Ao André pela constante boa disposição, “caaaaalma” e animação musical! Ao Luís, por tornar sempre o dia mais divertido e enriquecer as conversas sobre os mais variados temas, mas acima de tudo por estar sempre disponível para ajudar no que for preciso, científico, eletrónico ou pessoal. À “não-chefe” Gabriela também sempre animada, com boas conversas e boas gargalhadas, e uma palavra de apoio quando é necessária. Mesmo não sendo BD oficial, à enorme Marta Palma, pela tua constante disponibilidade, seja para um abraço, para me fazeres chorar a rir, para animares os almoços ou para me ajudares num problema, qualquer que ele seja. Esta viagem não seria a mesma sem a tua energia positiva inesgotável! Ao meu “Maninho” Tomás, por estares sempre presente e disponível, incondicionalmente, para tudo! À Lisa, por me ter acolhido com tanto carinho, no laboratório e na vida. Aos enormes Gil, Cristina e Rita, pelo fantástico ambiente de laboratório, companheirismo e principalmente por estarem sempre disponíveis tanto para ajudar no laboratório como para tornar o dia-a-dia mais feliz. Vocês são os maiores. À Inês

Rodrigues, porque sempre que te encontro é uma *fiesta*! Obrigada por teres sempre uma palavra amiga. Um obrigado especial à (Mediana) Isabel Duarte, por me ensinar tanto, como cientista e como pessoa, e me dar um incentivo e apoio especial, sempre. Adoro as tuas idiossincrasias (nunca vou esquecer isto! Mas é verdade). Um obrigado especial aos "gurus" da microscopia, Gabriel e Cláudia! À Cláudia também por todo o apoio e amizade fora da microscopia. E claro, aos membros passados do laboratório – Rifes, Gonçalo, Raquel Vaz, Rachel, Marianne – que partilharam parte desta viagem comigo. Por fim, mas não por último, à minha incansável companheira de luta e "*sister from another mister*" Andreia. Nunca poderei pôr por palavras o quanto te estou grata, por tanta coisa, ao longo de tantos anos, dentro e fora do laboratório. A tua energia inesgotável, boa disposição, otimismo e companheirismo no dia-a-dia dum laboratório são inigualáveis, és a melhor colega de laboratório que alguém pode desejar. Mas, muito, muito mais que isso, és uma pessoa extraordinária e das melhores amigas que alguém pode ter. Obrigada por tudo.

Quero agradecer também em especial a todas as pessoas que contribuíram para que me sentisse em casa, mesmo distante. Obrigado à Susana, João, Ana, Tomás e Cristina, o maior da aldeia Bitro (ahaha!) e claro, à Suki! Obrigada por me acolherem em vossa casa e tornarem uma fase turbulenta da minha viagem numa real *Sitcom*, pelo apoio e ajuda nas grandes e pequenas coisas e por me manterem sã na fase final. Um obrigado também muito especial à Ana Patrício, por me deixar "invadir" a sua casa, com imensa generosidade e compreensão. Obrigada também aos enormes Ramiro, Isabel e Martel, não só pela excelente companhia, mas também pelas conversas e discussões – filosóficas, científicas, da vida, enfim. Vocês são inspiradores e foi um privilégio aprender tanto convosco. Um obrigado especial à Bruna e ao Celso, por serem um raio de sol nos dias sombrios e nos fazerem sempre sentir bem; ao Marco Campinho pela boa disposição e *pep talks*; e ao Pedro Andrade, pelo carinho, boa disposição, por me fazer sempre rir e por me fazer sentir em casa.

Tenho de agradecer também a todo um outro exército "fora da ciência" que foi contribuindo para me manter sã ao longo desta caminhada. Um agradecimento muito especial aos meus *Friends Against Humanity* – à Andreia, mais uma vez; à Rachel pela companhia e incentivo, e por estares sempre presente ao longo destes anos, *no matter what*; à Raquel, pela amizade, disponibilidade e apoio incondicionais, sempre; ao Nelson, pela boa disposição e por me fazer rir e sentir bem mesmo nos dias mais difíceis; à Diana, pelo companheirismo e pela partilha, em especial do piano!; ao Tiago, pela forma serena e bem disposta como encaras e relativizas tudo, e por também me fazeres rir à gargalhada com as coisas mais totós; e à Xana, por uma amizade e apoio incondicionais de três décadas (!!), obrigada por estares sempre ao meu lado, a vida toda (mesmo a aturar conversas infindáveis sobre ciência e minudências das dinâmicas de um laboratório). Um agradecimento especial também aos meus companheiros de uma vida Bruno e Mariana, por serem um refúgio para onde sei que posso fugir para conseguir sarar feridas, sempre; Joana e Andreia, que mesmo não percebendo exactamente o que se passa com "as minhas galinhas" que me fazem estar tão ausente, mantêm a sua companhia e apoio; à Inês Fragata e ao Carlos (e agora também ao Filipe!), por serem os meus *geeks* preferidos e das melhores pessoas deste mundo, com quem tenho a sorte de partilhar esta vida; ao Gonçalo (fixe), pela tua preocupação e pelas palavras amigas quando menos espero; à Joana, pela companhia, apoio e *cheerleading*!, independentemente de quantos quilómetros estão entre nós, continuas próxima sempre; e às minhas restantes tontas Inês, Catarina, Sofia e Margarida, e também Catarina Dourado, por me trazerem sempre lufadas de ar fresco ao longo deste percurso quando nos fomos encontrando.

Um obrigado do fundo do coração à minha família, em especial aos meus pais e avós, pelo apoio inesgotável e incondicional a todos os níveis, por serem um porto seguro, por acreditarem e investirem em mim, por me ensinarem o que é ter força, resiliência e profissionalismo, mas também ética, generosidade e humanidade. Nunca poderei expressar o quão grata vos estou por tudo.

Por fim, mas nunca por último, tenho de agradecer especialmente ao Lucas, por tudo o que não posso colocar por palavras, por toda a paciência, apoio, amor, gargalhadas, companheirismo, todos os dias, independentemente dos quilómetros que nos separam. Obrigada por seres o melhor companheiro que poderia ter não só nesta viagem, mas na vida.

## Abstract

The metameric body plan of vertebrates is established during somitogenesis, one of the most complex morphogenetic events during development. Somites epithelialize periodically from the anterior-most presomitic mesoderm, and this rhythmicity is thought to be controlled by cyclic traveling waves of gene expression that sweep the tissue anteriorly. Although the spatial and temporal regulation of somitogenesis has been extensively studied, how the periodicity of genetic oscillations is translated into periodic somite epithelialization remains elusive. Furthermore, while knockout experiments have implicated the extracellular matrix component fibronectin in somite formation, much of the roles of its qualitative features deriving from its assembly state are still unknown.

The aim of this thesis is to re-address the role of fibronectin during paraxial mesoderm development, particularly during somite morphogenesis. In **Chapter 2**, we describe fibronectin production and assembly dynamics during early embryogenesis and found that it is highly dynamic throughout paraxial mesoderm development, as different forms of fibronectin assembly (autocrine *vs* paracrine) correlate with exquisite morphogenetic events. In **Chapter 3** we re-address the role of fibronectin during somite formation *in vivo*. We show that an intact fibronectin matrix and downstream mechanotransduction signaling are required for correct segmentation clock dynamics and somite morphogenesis. Our results suggest that the fibronectin matrix and its downstream chemical and mechanical cues couple genetic oscillations with timely somite morphogenesis. In **Chapter 4** we investigate the role of fibronectin in somite maturation. We demonstrate that normal fibronectin assembly is required for correct Sonic hedgehog signaling in the somite, which in turn controls fibronectin production in this tissue, suggesting that fibronectin and Sonic cooperate to orchestrate somite patterning and differentiation.

This thesis demonstrates that fibronectin is a dynamic pivotal player regulating paraxial mesoderm development. It also highlights the previously unappreciated importance of the extracellular matrix and its derived mechanical cues during embryonic development.

**Keywords**: fibronectin, paraxial mesoderm, somite, extracellular matrix, mechanotransduction.

## Resumo

O padrão metamérico do plano corporal dos vertebrados é estabelecido na somitogénese, um dos mais complexos eventos morfogenéticos do desenvolvimento. Os sómitos epitelizam a partir da parte anterior da mesoderme pré-somítica de forma periódica, num processo controlado por ondas cíclicas de expressão génica que percorrem este tecido numa direcção posterior-anterior. Embora muitos estudos se tenham focado no controlo temporal e espacial da somitogénese, os mecanismos pelas quais estas oscilações genéticas se traduzem na morfogénese periódica dos sómitos são em grande parte desconhecidos. Por outro lado, foi demonstrado que a matriz extracelular de fibronectina é crucial à formação dos sómitos, mas o impacto das suas características qualitatitvas neste processo é também desconhecido.

Esta tese tem como objectivo reavaliar o papel da fibronectina durante o desenvolvimento da mesoderme paraxial, em particular na morfogénese dos sómitos. No **Capítulo 2**, analisamos a dinâmica de produção e montagem da fibronectina durante o desenvolvimento precoce, demonstrando que a montagem da matriz de fibronectina é extremamente dinâmica durante as várias fases de desenvolvimento da mesoderme paraxial, correlacionando com o seu rearranjo e maturação. No **Capítulo 3** analisamos o papel da matriz de fibronectina na formação de sómitos *in vivo*, mostrando que esta matriz e respectiva mecanotransdução são cruciais para a dinâmica do relógio de segmentação e morfogénese do sómito. Estes resultados apontam a matriz de fibronectina como o agente responsável à coordenação das oscilações genéticas com a formação periódica do sómito. No **Capítulo 4**, mostramos que a matriz de fibronectina é necessária à sinalização Sonic hedgehog nos sómitos, que por sua vez controla a produção de fibronectina neste tecido, sugerindo que ambos colaboram na padronização e diferenciação do sómito.

Os resultados desta tese demonstram que a fibronectina tem um papel fundamental na regulação do desenvolvimento da mesoderme paraxial, e evidencia a importância da matriz extracelular no desenvolvimento.



**Palavras-chave**: fibronectina, mesoderme paraxial, matriz extracelular, mecanotransdução

## Resumo alargado

Uma das características mais proeminentes dos vertebrados é o padrão metamérico do seu plano corporal, particularmente evidente no arranjo segmentar da sua coluna vertebral. Este padrão segmentado tem origem durante a formação dos sómitos, um dos mais complexos e regulados eventos morfogenéticos do desenvolvimento precoce dos vertebrados. Os sómitos são segmentos esféricos de mesoderme paraxial localizados de cada lado das estruturas axiais, que se formam periodicamente a partir da região mais anterior da mesoderme pré-somítica e dão mais tarde origem às vertebras e costelas do esqueleto axial, ao músculo esquelético, derme, entre vários outros tecidos. Assim, é fundamental que a somitogénese ocorra de forma robusta e precisa, uma vez que qualquer problema neste processo origina uma situação patológica grave.

A periodicidade da formação de cada par de sómitos é acompanhada por oscilações do relógio de segmentação, constituído por ondas cíclicas de expressão génica que percorrem a mesoderme pré-somítica da zona posterior para a zona anterior. O período de cada ciclo destas ondas de expressão corresponde ao período necessário à formação de cada par de sómitos, sugerindo que estes processos estão intimamente relacionados. De facto, um conjunto alargado de genes envolvidos principalmente na via de sinalização Notch, mas também nas de Fgf (*Fibroblast growth factor*) e Wnt, foram descritos como fazendo parte deste relógio de segmentação em vários animais modelo, sugerindo que se trata de um processo conservado. Na ausência de determinados genes do relógio, em particular genes ligados à via Notch, a segmentação ocorre de forma irregular e desordenada, demonstrando a sua importância neste processo. Quando as ondas de expressão destes genes chegam à zona anterior da mesoderme pré-somítica, estas abrandam e estabilizam, de forma a que a sua banda de expressão mantida na zona anterior da mesoderme pré-somítica corresponde à fenda do próximo segmento. No entanto, os mecanismos através dos quais a estabilização das ondas do relógio se traduzem na ativação periódica da morfogénese da fenda somítica não são bem compreendidos.

Todos os tecidos e órgãos do embrião estão rodeados por matriz extracelular, de constituição e topologia específicas. Durante décadas, a matriz foi considerada como um constituinte passivo e estrutural do espaço extracelular, sem nenhuma relevância no comportamento e funções celulares para além da separação de tecidos e da manutenção da sua integridade. No entanto, a deleção genética de vários componentes da matriz são deletérias ainda *in utero*, e estudos mais recentes em culturas celulares vieram mostrar que a composição, densidade, topologia e rigidez de uma dada matriz tem um papel instrutivo na regulação das funções celulares, desde a sua migração e alteração de forma à sua proliferação ou diferenciação.

Durante todo o seu desenvolvimento, a mesoderme paraxial está associada a uma matriz extracelular de fibronectina que aumenta progressivamente de complexidade durante a maturação do tecido. Esta matriz de fibronectina está implicada na somitogénese, uma vez que embriões de ratinho cujo gene codificante para esta proteína (*Fn1*) foi eliminado formam alguma mesoderme paraxial, mas esta não segmenta. Este fenótipo é comum a outros animais-modelo com deficiências na matriz de fibronectina, sugerindo que a necessidade de uma matriz de fibronectina intacta para a normal formação de sómitos é transversal aos vertebrados. Embora esta matriz esteja claramente implicada na formação morfológica de sómitos, pouco se sabe sobre a sua função neste contexto, uma vez que a deleção do gene e a consequente ausência da proteína mascara os potenciais papéis de características relevantes da matriz, incluindo a sua complexidade e rigidez. A isto acresce o facto de muitos dos processos envolvidos no controlo temporal e espacial da somitogénese permanecerem obscuros, incluindo os mecanismos de estabilização das oscilações do relógio na mesoderme anterior, bem como a sua tradução na formação temporal de fendas somitícas regulares. Desta forma, o principal objectivo desta tese é clarificar quais as dinâmicas e funções da matriz extracelular de fibronectina ao longo do desenvolvimento da mesoderme paraxial, desde a sua formação à especificação dos derivados somíticos, com especial foco nos eventos morfológicos e moleculares inerentes à formação dos sómitos.

No **Capítulo 2**, analisamos a dinâmica de produção e montagem da fibronectina durante o desenvolvimento precoce dos embriões de galinha e ratinho, desde a gastrulação até à organogénese. Descrevemos que tecidos expressam o gene codificante para fibronectina, *Fn1* e, portanto, produzem a proteína, e que tecidos montam a matriz fibrilar, analisando também o padrão de expressão do mRNA e a localização dos seus receptores específicos, as integrinas $\alpha 5$ e $\alpha v$. Neste Capítulo demonstramos que a montagem da matriz de fibronectina pode ser parácrina em vários contextos ao longo do desenvolvimento precoce, em que um tecido particular expressa *Fn1* e produz a proteína, que por sua vez é recebida por um tecido adjacente que não produz fibronectina, mas procede à sua montagem, constituindo uma forma particular de comunicação entre tecidos. Os resultados obtidos neste Capítulo demonstram ainda que a produção e montagem da matriz de fibronectina é consideravelmente dinâmica durante o desenvolvimento da mesoderme paraxial, correlacionando com os vários eventos morfogenéticos sofridos pelo tecido ao longo da sua maturação. De facto, demonstramos que a montagem de fibronectina é autócrina nas células da linha primitiva e no esclerótomo já após sofrer a sua característica transição epitélio-mesênquima, sendo por sua vez parácrina nas células do epiblasto aquando da gastrulação e na mesoderme pré-somítica, no coração, na notocorda, no miótomo, bem como no tubo digestivo. Dada a relevância da matriz de fibronectina nos vários tecidos analisados, e sendo a sua montagem um evento parácrino em vários contextos ao longo do desenvolvimento, propomos que a montagem da matriz de fibronectina constitui um evento de comunicação celular de significância igualável à da sinalização via morfogénios.

No **Capítulo 3**, reavaliamos o papel da matriz de fibronectina na formação dos sómitos, analisando também o seu potencial papel na regulação do relógio de segmentação. Para este efeito, recorremos à cultura de explantes posteriores de embrião de galinha bem como à electroporação de embriões de galinha *ex vivo*, interferindo directamente desta forma com a montagem da matriz de fibronectina, a sua ligação a integrinas e a actividade e regulação do citoesqueleto, interferindo assim com a maquinaria de mecanotransdução das células da mesoderme pré-somítica. Os resultados obtidos neste capítulo experimental demonstram que a matriz de fibronectina e a sua ligação a integrinas, bem como a sua via intracelular de mecanotransdução, são cruciais para a correcta dinâmica do relógio de segmentação e a morfogénese da fenda somítica. Estes resultados evidenciam a importância da fibronectina na regulação da somitogénese, e apontam para um novo papel desta matriz na coordenação das oscilações do relógio com a morfogénese periódica dos sómitos. Também implicam a via de mecanotransdução ligada a integrinas nestes dois processos, constituindo mais um exemplo a adicionar aos recentes estudos que demonstram que a informação biomecânica providenciada pela matriz extracelular tem um papel instrutivo e fundamental não só em culturas celulares, mas também durante o desenvolvimento *in vivo*.

No capítulo experimental final, **Capítulo 4**, avaliamos o papel da matriz de fibronectina na maturação do sómito, uma vez que este está rodeado de uma densa matriz de fibronectina da qual não se conhecem as funções específicas. Os resultados obtidos neste Capítulo demonstram que a matriz de fibronectina é crucial para a normal sinalização Sonic hedgehog nos sómitos, uma das principais vias de sinalização envolvidas na sua diferenciação, responsável pela determinação do esclerótomo. Por outro lado, demonstramos também que a produção desta matriz de fibronectina é regulada por sinais derivados da notocorda, incluindo o próprio Sonic hedgehog, sugerindo que a fibronectina e Sonic colaboram para regular a padronização e diferenciação do sómito ventral, especificando o esclerótomo.

O trabalho apresentado nesta tese ilustra a natureza dinâmica da montagem e funções da matriz extracelular de fibronectina durante o desenvolvimento precoce dos vertebrados, em particular no desenvolvimento e morfogénese da mesoderme paraxial. Este trabalho contribui para a crescente consciencialização da relevância da matriz extracelular no desenvolvimento, sendo não só um suporte estrutural, mas também um agente activo e fundamental para a correcta embriogénese. Finalmente, os resultados obtidos nesta tese evidenciam ainda a importância da integração do estudo da mecanobiologia com o estudo do desenvolvimento, uma vez que a informação mecânica recebida pelos tecidos embrionários tem também um papel na sua maturação e desenvolvimento.

# Contents

# List of Figures

**Chapter 1: Introduction**



**Chapter 2: Fibronectin assembly during early embryo development: a versatile communication system between cells and tissues**

**Chapter 3: A fibronectin-dependent mechanotransduction pathway in control of the chick embryo segmentation clock**

**Chapter 4: Crosstalk between Sonic hedgehog signaling and Fibronectin matrix during somite morphogenesis**



**Chapter 5: Discussion**

# List of Abbreviations and Acronyms

| | |
|---|---|
| **AKT** | (Ak) Thymoma viral proto-oncogene |
| **A-P** | Antero-posterior |
| **ADAM** | A Disintegrin and Metalloproteinase |
| **BMP** | Bone Morphogenetic Protein |
| **bHLH** | Basic Helix-Loop-Helix |
| **Cdc42** | Cell Division Cycle 42 |
| **D-V** | Dorso-ventral |
| **Dll** | Delta-like |
| **DOC** | Deoxycholate |
| **ECM** | Extracellular Matrix |
| **EGF** | Epidermal Growth Factor |
| **EGFR** | Epidermal Growth Factor Receptor |
| **EMT** | Epithelial to Mesenchymal Transition |
| **ERK** | Extracellular signal–Regulated Kinases |
| **FAK** | Focal Adhesion Kinase |
| **FGF** | Fibroblast Growth Factor |
| **FN** | Fibronectin |
| **GAG** | Glycosaminoglycan |
| **GTPases** | Guanosine Triphosphatases |
| **HER** | Hairy/Enhancer of Split related |
| **HES** | Hairy/Enhancer of Split |
| **HOX** | Homeobox containing transcription factors |
| **ILK** | Integrin-Linked Kinase |
| **IPP** | ILK, PINCH and Parvin |
| **JAG** | Jagged |
| **JNK** | c-Jun N-terminal Kinase |
| **Lnfg** | Lunatic fringe |
| **M-L** | Medio-lateral |
| **MAML** | Mastermind-like |
| **MAPK** | Mitogen-Activated Protein Kinases |
| **MET** | Mesenchymal to Epithelial Transition |
| **Mesp** | Mesoderm Posterior |
| **MLKC** | Myosin light chain kinase |
| **MMP** | Matrix Metalloproteinase |
| **MRCK** | Myotonic Dystrophy Kinase-related |

| | |
|---|---|
| **Ncad** | N-cadherin / Cadherin-2 |
| **NICD** | Notch Intracellular Domain |
| **NMMII** | Non-muscle Myosin II |
| **PAK** | p21-associated Kinase |
| **PAPC** | Paraxial protocadherin |
| **Pax** | Paired-box |
| **PCP** | Planar Cell Polarity |
| **PDGF** | Platelet-Derived Growth Factor |
| **Phall** | Phalloidin F-actin staining |
| **PINCH** | Particularly Interesting Cys-His-rich |
| **PORD** | Progressive Oscillatory Reaction-Diffusion model for somite formation |
| **PSEN** | Presenilin |
| **PSI** | Plexin-sempahorin-integrin Domain |
| **PSM** | Presomitic Mesoderm |
| **PTB** | Phosphotyrosine Binding Domain |
| **RA** | Retinoic Acid |
| **Rac1** | Ras-related C3 botulinum substrate 1 |
| **RGD** | Arginine-Glycine Aspartic acid |
| **RhoA** | Ras homolog A |
| **RBPJκ** | Recombination signal sequence-binding protein κ |
| **ROCK** | Rho-associated protein kinase |
| **Shh** | Sonic Hedgehog |
| **Src** | Cellular homolog of transforming gene of Rous sarcoma virus |
| **TBX** | T-Box transcription factor |
| **TGFβ** | Transforming Growth Factor Beta |
| **VEGF** | Vascular Endothelial Growth Factor |
| **VEGFR** | Vascular Endothelial Growth Factor Receptor |
| **Wnt** | Wingless/Integrated Family Members |
| **YAP** | Yes-associated protein |
| **ZO-1** | Zonula Occludens-1 |

# Chapter 1

## Introduction

*Remember to look up at the stars and not down at your feet. Try to make sense of what you see and wonder about what makes the universe exist. Be curious.*
— Stephen Hawking

# I. General Introduction

## 1. Paraxial mesoderm development

All vertebrates have a characteristic metameric body plan, most prominently visible in the arrangement of the vertebral column and associated muscles, essential for vertebrate locomotion. This characteristic segmented pattern of the vertebrate body plan has its origin in the formation of somites, which is one of the most complex and tightly regulated morphogenetic events of early development. Somites are repeated spheres of paraxial mesoderm that form periodically at each side of the axial structures. They give rise to the distinctly segmented vertebral column and also contribute to a variety of other tissues, including the skeletal muscles of trunk and limbs and the dermis of the back. This segmental pattern of the somites also dictates the metameric arrangement of blood vessels and the peripheral nervous system (Christ et al., 2004). Somite formation must therefore be tightly controlled in space and time, as failures in this process may result in several pathologies (Andrade et al., 2007). Given its importance and complexity, it is thus of no surprise that somite formation has fascinated embryologists for the past 170 years (Remak, 1850). Here I will review paraxial mesoderm development, from its origin during gastrulation to somite differentiation, focusing mainly on chick (*Gallus gallus*) and mouse (*Mus musculus*) development, but also referring to amphibians (*Xenopus laevis*) and fish (*Danio rerio*) when appropriate.

### 1.1. Paraxial mesoderm formation

*1.1.1 Gastrulation*

In 1986, developmental biologist Lewis Wolpert argued that “It is not birth, marriage, or death, but gastrulation which is truly the most important time in your life”. Indeed, gastrulation is the developmental process through which the three embryonic germ layers – endoderm, mesoderm and ectoderm – form and which will give rise to all the different tissues and organs of the body (Fig. 1.1; Gilbert, 2006). Before gastrulation, the amniote embryo is composed of the dorsally located epiblast, and the hypoblast lying ventrally. In birds and mammals, all three germ layers come from the epiblast, which in the posterior region of the embryo forms a thickening in the midline called the primitive streak (Fig. 1.1). The anterior portion of the primitive streak is slightly thicker and forms the embryonic organizer, called the Hensen’s node in avian embryos and simply the node in mammalian embryos (Fig. 1.1). Soon after primitive streak formation, Hensen’s node is displaced anteriorly, extending the primitive streak towards the future anterior region of the embryo. Because of its position in the midline, the formation of the primitive streak establishes all embryonic axes – antero-posterior (A-P), dorso-ventral (D-V), medio-lateral (M-L) and left-right. Concomitantly

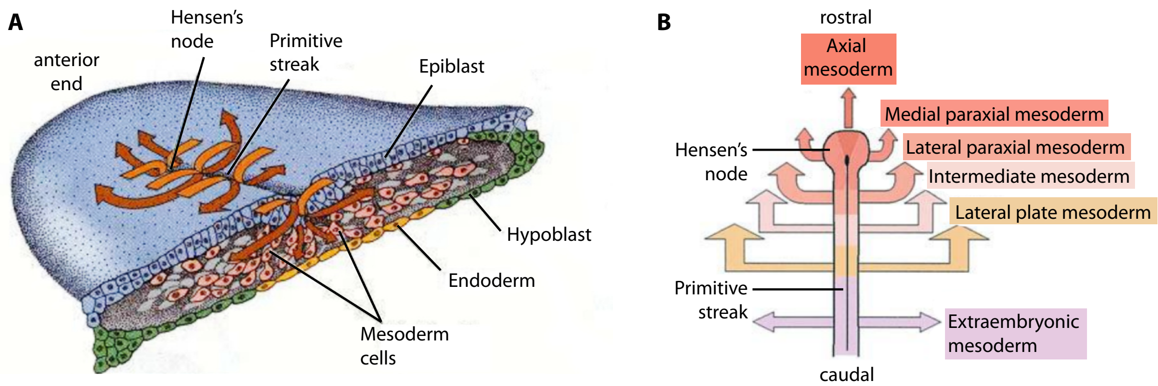


**Fig. 1.1. Gastrulation in the avian embryo and fate map of mesodermal cells. (A)** Illustrative representation of gastrulation in the avian embryo. Epiblast cells ingress either though Hensen's node and migrate anteriorly, giving rise to dorsal endoderm and head and axial mesoderm, or they ingress through the primitive streak, after which they originate endoderm or migrate laterally, giving rise to paraxial, intermediate, lateral and extraembryonic mesoderm. Adapted from Gilbert, 2006. **(B)** Fate map of a HH4 chick embryo, demonstrating that cells from Hensen's node and different axial positions on the primitive streak give rise to different mesodermal compartments later in development. Adapted from Stern, 2004.

with the formation of the primitive streak, epiblast cells go through an orderly epithelial to mesenchymal transition (EMT). Cells in Hensen's node ingress ventrally and migrate anteriorly, while cells in the primitive streak ingress ventrally through the streak and migrate laterally (Fig. 1.1). The A-P position of epiblast cells and the timing of their ingression will define their fate and final position in the embryo: cells ingressing earlier will give rise to more anterior structures, while cells ingressing later will develop into more posterior tissues (Fig. 1.1). Similarly, primitive streak cells closest to Hensen's node will give rise to medial structures, while cells located more posteriorly in the streak will form lateral structures (Freitas et al., 2001; Psychoyos and Stern, 1996; Schoenwolf et al., 1992; Stern, 2004).

When the primitive streak reaches its full A-P extension, Hensen's node starts regressing posteriorly, leaving behind precursors of dorsal endoderm and axial mesoderm along its journey (Iimura et al., 2007; Psychoyos and Stern, 1996). Once formed, anterior structures will immediately begin their developmental program. At the same time, gastrulation continues more posteriorly where undifferentiated cells are still being added to posterior tissues, which will consequently mature and differentiate later in development. This results in an A-P gradient of maturity of embryonic structures, with anterior tissues being more developed than those located more posteriorly (Sawada and Aoyama, 1999).

The mesoderm formed during gastrulation can be subdivided into four regions which are distinguished by their position relative to the embryo midline (Fig. 1.2; Gilbert, 2006). The axial mesoderm is deposited in the midline and will form the cephalic prechordal mesoderm and the notochord. Flanking each side of the axial mesoderm is the paraxial mesoderm, composed of a cephalic non-segmented region, the segmented somites and the presomitic mesoderm (PSM). Located immediately lateral to the paraxial mesoderm is the intermediate mesoderm, which will originate the urogenital system. Finally, the lateral-most

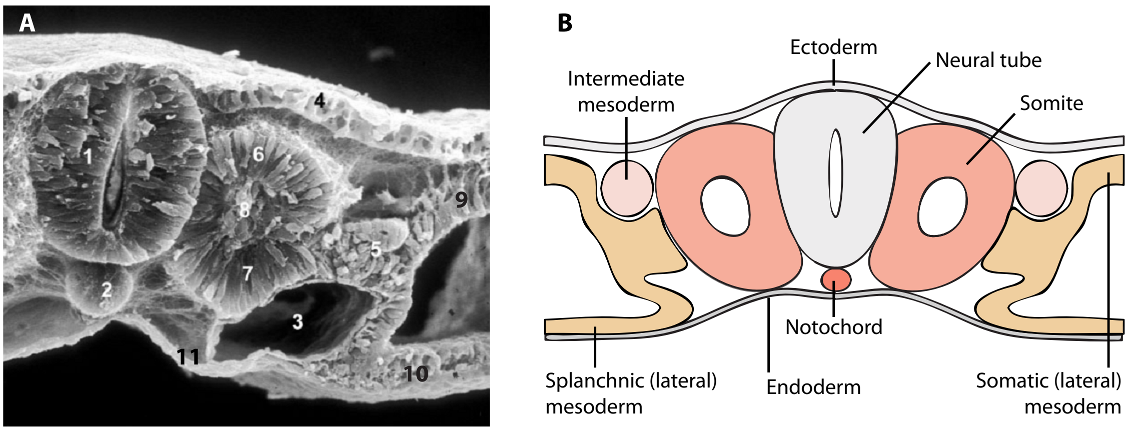


**Fig. 1.2. Mesoderm derivatives in the vertebrate embryo. (A)** Scanning electron microscopy image of a transverse section of a 48-hour chick embryo. 1 – Neural tube; 2 – Notochord; 3 – Dorsal aorta; 4 – Ectoderm; 5 – Intermediate mesoderm; 6 – Epithelial somite (dorsal); 7 – Epithelial somite (ventral); 8 – Mesenchymal somitocoel; 9 – Lateral plate mesoderm (somatic); 10 – Lateral plate mesoderm (splanchnic); 11 - Endoderm. Adapted from Christ et al. 2007. **(B)** Schematic representation of a transverse section of a 48-hour chick embryo. Adapted from Dietrich et al., 1997.

mesodermal structure is the lateral plate mesoderm, which becomes further subdivided into the dorsal somatic mesoderm and the ventral splanchnic mesoderm, and will contribute to many different tissues and organs, including the connective tissue of the limbs and the circulatory system.

### *1.1.2 Commitment of Paraxial mesoderm precursors*

Mesodermal precursors are specified in the primitive streak, and this commitment is reflected by the expression of Brachyury (or T, from Tail), a transcription factor from the T-box family (Wilkinson et al., 1990). Brachyury activation is dependent on both Wnt and Fibroblast Growth Factor (Fgf) signaling in the primitive streak (Ciruna and Rossant, 2001; Sun et al., 1999; Yamaguchi et al., 1999), and is required for the correct gastrulation of mesodermal precursors – in its absence, epiblast cells fail to ingress and migrate (Wilkinson et al., 1990; Wilson et al., 1995). Indeed, Wnt3a and Brachyury are both essential for promoting the mesenchymal morphology and mesodermal fate of ingressing epiblast cells (Yamaguchi et al., 1999).

Paraxial mesoderm precursors also activate the expression of an additional T-box transcription factor, Tbx6, in a Brachyury-dependent manner (Chapman et al., 1996). Once activated, the maintenance of both Brachyury and Tbx6 expression depends on Wnt3a signaling (Yamaguchi et al., 1999). In addition to promoting paraxial mesoderm development (Takemoto et al., 2011), Tbx6 also acts as a negative regulator of neuronal fate, as Tbx6-null embryos form two ectopic Sox2-expressing neural tubes at the expense of paraxial mesoderm (Chapman and Papaioannou, 1998).

Thus, while paraxial mesoderm precursors are specified by their A-P position in the primitive streak and the timing of their ingression, commitment to paraxial mesoderm is reinforced molecularly through the expression of both Brachyury and Tbx6, which further regulate paraxial mesoderm development. It is important to note that the mouse Tbx6 and the avian Tbx6L (Tbx6-like) are not homologous (Knezevic et al., 1997; Kondoh and Takemoto, 2012). While both genes share high sequence similarity in their T-box domain, the rest of their sequence is highly divergent. Nevertheless, both genes share the same function in paraxial mesoderm commitment and development (Chapman et al., 1996; Knezevic et al., 1997; Sheng et al., 2003), and may thus be considered functionally comparable.

During gastrulation, the precursors of the paraxial mesoderm are located both in and adjacent to the primitive streak, just caudal to the Hensen's node (Fig. 1.1; Hatada and Stern, 1994; Iimura et al., 2007; Psychoyos and Stern, 1996). These precursors start to ingress while the primitive streak is still extending anteriorly and continue their ingression as Hensen's node regresses, contributing to paraxial mesoderm throughout the axis. Remarkably, cells of the medial and lateral portions of the PSM have different origins. Precursors of the medial portion of the PSM reside more anteriorly in the primitive streak, and behave as a pool of resident stem cells which remains in the streak and contributes with mesodermal cells throughout the full A-P length of the tissue (Iimura et al., 2007). In contrast, the lateral portion of the PSM is generated by continuous ingression of epiblast cells through the streak. (Iimura et al., 2007).

The posterior regression of Hensen's node occurs concomitantly with embryo growth and is completed by stage HH12 in the chick embryo (16-somite stage, Hamburger and Hamilton, 1992; Schoenwolf, 1979). From this stage onwards, new mesodermal cells enter the caudal tissues through the tailbud. The tailbud is the most posterior structure of the elongating embryo and is a functional remnant of Hensen's node and the primitive streak, which contains neural and mesodermal precursors (Catala et al., 1995; Catala et al., 1996).

## 1.2. The presomitic mesoderm and somites

During gastrulation through the tailbud, the PSM maintains its relative length as the embryo grows caudally, with the tailbud continuously providing new cells to the caudal end of the PSM, while the anterior end of the tissue segments into epithelial somites (Fig. 1.3). Cells entering the PSM divide once or twice before being incorporated into a somite, which occurs around 20h after they entered the PSM (Stern et al., 1988).

PSM cells are highly dynamic and motile, frequently changing neighbors – however, in the anterior two thirds of the PSM, these movements are restricted to about the length of 1 presumptive somite (Kulesa and Fraser, 2002; Stern et al., 1988). In fact, soon after entering the tissue from the tailbud, PSM cells remain in approximately the same axial position, being displaced anteriorly as the embryo grows (Fig. 1.3; Bénazéraf et al., 2010; Kulesa and Fraser, 2002). This displacement is accompanied by changes in the maturation of PSM cells from caudal to rostral. Accordingly, in the posterior two thirds of the PSM, cells remain undifferentiated and proliferative, while in the anterior third crucial aspects of somite maturation are already being defined (Saga and Takeda, 2001; Saga et al., 1997; Takahashi et al., 2000). Importantly, these cells are already changing their expression profile and morphology to prepare for being incorporated into a somite (Saga and Takeda, 2001). Spatial positioning of future segment boundaries and the period at which boundaries will form is defined in the rostral PSM prior to morphological segmentation, as is the establishment of the rostro-caudal polarity of the prospective somite (see sections 1.2.6, *Notch signaling and Mesp2 activation* and 1.3.1, *Boundary formation* for more details). Additionally, the anterior-most end of the PSM is already undergoing morphological boundary formation and epithelialization of its peripheral cells (Martins et al., 2009).

Somite formation is characteristic of vertebrates, but the rhythm at which somites form varies widely between species. One new somite pair forms every 30 minutes in the zebrafish (Schröter et al., 2008), 90 minutes in the chick (Palmeirim et al., 1997), 2 hours in the mouse (Tam, 1981) and between 4 to 6 hours in humans (Bailey and Dale, 2015). The length of the PSM and total number of segments formed are also species-specific: while the zebrafish forms a total of 33 somite pairs, humans form around 38-44 pairs, mice have a total of 65 pairs, and the corn snake (*Pantherophis guttatus*) has more than 300 (Gomez et al., 2008). These changes in segment number are of evident evolutionary importance, as for example different segment numbers in fish allow distinct modes of swimming, enabling adaptation to different environments (Hubaud and Pourquié, 2014). Intriguingly, while it was long believed that somite formation would only stop after complete exhaustion of PSM

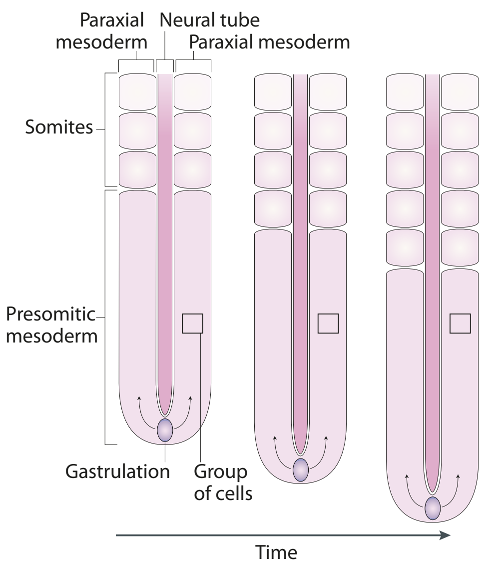


**Fig. 1.3. PSM development during embryo elongation**. The PSM maintains its length as the embryo grows caudally, with new cells being added in the caudal end of the embryo, while somites bud off from the anterior PSM. Once in the PSM, the cells remain approximately at the same axial position (square) whereas their relative position within the PSM is progressively displaced anteriorly until they are incorporated into a somite. Adapted from Hubaud and Pourquie, 2014.

tissue, that is not the case. Indeed, somite formation stops before complete segmentation of the PSM, leaving a portion of unsegmented tissue in the caudal tip of the embryo (Tenin et al., 2010). The mechanism by which somitogenesis comes to a halt is still unknown.

### *1.2.1 Somite nomenclature*

Christ and Ordahl (1995) defined a nomenclature system able to distinguish between different “ages” of the somites of a given embryo. As mentioned above, the PSM and somites show an A-P gradient of maturity whereby cells in the PSM and somites become more mature as they are “displaced” anteriorly (Fig. 1.3). This system was later refined by Pourquié and Tam (2001) (Fig. 1.4; Christ and Ordahl, 1995; Pourquié and Tam, 2001). Arabic numerals are used to identify somites according to their relative position to the rostral end of the embryo. For example, the first 5 anterior somites (somites 1 to 5) give rise to the occipital bone in both chick and mouse embryos (Fig. 1.4, Christ and Ordahl, 1995). Conversely, the “age” of a given somite is defined by Roman numerals and reflects their relative distance to the anterior end of the PSM (Fig. 1.4; Pourquié and Tam, 2001). Thus, the forming somite in the anterior PSM is defined as somite 0 (S0), while already formed somites which are anterior to S0 are numbered SI, SII, SIII (somite one, two, and three, respectively) and so forth. Thus, at any given developmental stage, the most recently formed somite is SI, which will later develop into SII, SIII, SIV etc. as more somites form caudal to it. In addition, presumptive somites in the PSM are also numbered according to their relative position to S0, identified by negative Roman numerals. Thus, these are somites S-I (somite minus one),

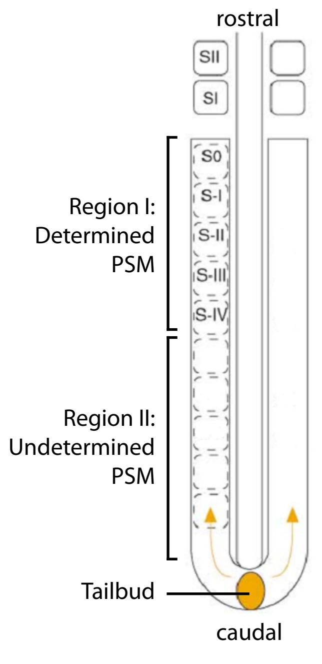


**Fig. 1.4. Nomenclature system for somite staging**. Adapted from Pourquie and Tam, 2001.

S-II, S-III, S-IV etc (Fig. 1.4). While the PSM is not segmented, this nomenclature is useful to distinguish events occurring in the posterior-most undifferentiated PSM vs. the anterior third of the PSM (S-IV to S-I), where PSM cells start their molecular and morphological segmentation program (see section 1.2.2, *Gradients in the PSM* for more details).

### *1.2.2 Gradients in the PSM*

As development proceeds, cells in the posterior PSM progressively change their relative position within the PSM, becoming more and more anterior with the development and growth of the embryo. PSM cells are thought to start their differentiation program when they reach a given axial position in the anterior PSM (Saga and Takeda, 2001). The transition between these two cellular states is thought be accomplished by the action of different morphogen gradients in the PSM, which define an axial level where PSM cells switch from an undifferentiated state to a differentiating state. This is the so-called determination front (Fig. 1.5; Hubaud and Pourquié, 2014).

The first morphogen gradient to be implicated in this A-P maturation gradient was the *Fgf8* mRNA gradient. Cells in the posterior PSM have more mRNA for *Fgf8* compared to cells in its anterior end in zebrafish, chick and mouse embryos (Dubrulle and Pourquié, 2004; Dubrulle et al., 2001; Naiche et al., 2011; Sawada et al., 2001). Both *Fgf8* and *Fgf4* are transcribed in gastrulating cells, but their transcription stops as these cells enter the caudal PSM. This pool of *Fgf* mRNA is then gradually degraded over time, as the relative position of the cells in the PSM is displaced anteriorly. This results in a posterior to anterior gradient

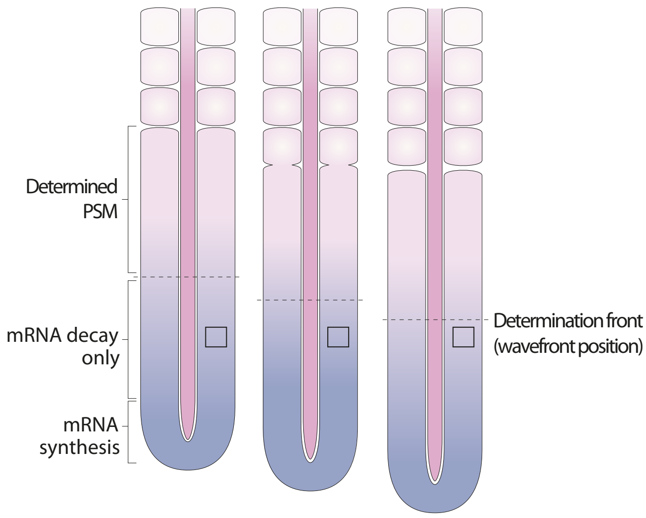


**Fig. 1.5. Gradient formation and determination front positioning**. Fgf/Wnt transcripts are produced in the tailbud and progressively degraded in the PSM. As the embryo extends caudally, cells become dislocated more anteriorly (square) and receive progressively lower levels of Fgf/Wnt signaling as the determination front moves posteriorly. Adapted from Hubaud and Pourquie, 2014.

of Fgf signaling, with higher levels of Fgf activity in posterior PSM and negligible levels in the anterior PSM (Dubrulle and Pourquié, 2004). This Fgf gradient was later found to have a role in segmentation as overexpression of *Fgf8* in the chick PSM results in either formation of smaller somites or absence of somites, indicating that high levels of Fgf inhibit somite formation (Dubrulle et al., 2001). Conversely, if the Fgf signaling pathway is inhibited in the avian PSM, the resulting somites are bigger. These results indicate that Fgf signaling has a role in both maintaining PSM cells undifferentiated and defining the size of the somites. Accordingly, conditional knockout of *Fgfr1*, which is the only Fgf receptor in the PSM, in the mouse, results in the loss of dynamic cyclic gene expression (see section 1.2.3, *The segmentation clock*, for more details) and eventual arrest of somite formation (Wahl et al., 2007).

Wnt3a also shows a posterior to anterior gradient of mRNA expression in the PSM, which is accompanied by an expression gradient of the Wnt target *Axin2* and the nuclear localization of β-catenin (Aulehla et al., 2003; Aulehla et al., 2008). When a Wnt ligand binds to its transmembrane Frizzled receptor, β-catenin translocates from the cytoplasm to the nucleus, where it acts as a transactivator of LEF/TCF transcription factors, promoting the transcription of Wnt target genes (Schambony et al., 2004). If β-catenin is constitutively active in the nucleus of PSM cells, the undifferentiated domain of the PSM expands anteriorly and no somitic borders are formed, although the segmentation clock keeps oscillating (Aulehla et al., 2008; see section 1.2.3, *The segmentation clock*, for more details). This phenotype was shown to be indirectly controlled by Fgf signaling, suggesting that both pathways cooperate to maintain the immature state of the posterior PSM (Aulehla et al., 2008). Accordingly, constitutive expression of *Axin2*, a Wnt antagonist, in the mouse embryo results in bigger somites, while increasing Wnt3a levels generates smaller somites. These phenotypes resemble those of blocking or increasing Fgf signaling, respectively (Aulehla et al., 2003). Similarly, in the zebrafish, reducing the Wnt gradient without affecting mesoderm production shifts the segmenting domain of the PSM caudally and results in the production of larger somites. Thus, the determination front is defined by a threshold of Fgf and Wnt activity, which dictates the axial level in the PSM where cells leave their naïve state and start differentiating.

The determination front is further strengthened by an opposing gradient of Retinoic acid (RA) activity (Diez del Corral et al., 2003). RA is thought to be produced in recently formed somites by Raldh2, an enzyme that catalyzes RA synthesis (Aulehla and Pourquié, 2010; Niederreither et al., 1997), and degraded in the posterior PSM by Cyp26a1, an enzyme which metabolizes RA, resulting in an anterior to posterior gradient of RA in the PSM (Abu-Abed et al., 2001; Fujii, 1997; Sakai et al., 2001). This gradient appears to counteract that of Fgf signaling: when RA is absent in the quail embryo, the Fgf8 expression domain shifts anteriorly and the resulting somites are smaller (Diez del Corral et al., 2003). This is also observed when RA levels are reduced in both mouse and zebrafish embryos (Kawakami et al., 2005; Kumar and Duester, 2014). Conversely, treatment with an RA agonist strongly reduces Fgf8 levels (Diez del Corral et al., 2003). However, the mechanism by which RA controls Fgf levels is unclear. Importantly, the posterior edge of RA activity in the PSM is rather sharp and not graded, and downregulation of Cyp26a1 expression in the PSM does not result in caudally-extended RA activity (Wahl et al., 2007). Moreover, the Fgf8 gradient results from increased mRNA decay and not from differential transcription. RA has no known role in the regulation of mRNA stability, although it interacts directly with Fgf8 promoter in the PSM (Kumar and Duester, 2014). Finally, deficiency in Rdh10, which also controls RA activity, has no effect on either Fgf8 expression nor segmentation in the mouse (Cunningham et al., 2015).

Thus, gradients of Fgf/Wnt and possibly RA activity define two different regions of the PSM: region I, which is maintained undetermined by high Fgf/Wnt levels and is thus termed the undifferentiated PSM; and region II, located anteriorly to the determination front and is called the determined PSM, which in the chick embryo spans from S-IV to S0 (Fig. 1.4 and 1.5; Saga and Takeda, 2001).

*1.2.3 The segmentation clock*

The periodicity of somite formation suggests that the segmentation of the PSM is controlled by an intrinsic oscillator (Cooke and Zeeman, 1976). The first evidence for the existence of such an oscillator was reported in the chick embryo, where *Hairy1*, the avian homolog of the *Drosophila* pair rule gene *hairy*, was expressed in varying patterns along the PSM of embryos of the same developmental stage (Palmeirim et al., 1997). These different *Hairy1* expression patterns were found to reflect distinct phases of a cyclic wave of expression that repeats itself every 90 min, which in turns corresponds to the time needed for a new somite pair to form in the chick. The authors found that *Hairy1* expression sweeps the PSM from posterior to anterior which culminates in the stabilization of its expression in a single band corresponding to the posterior region of the next presumptive somite (Fig. 1.6 A; Palmeirim et al., 1997; Resende et al., 2014). Concomitantly with the formation of this anterior stripe of stable *Hairy1* expression, a new expression domain arises in the posterior PSM, corresponding to the next phase of the cycle. The dynamic expression pattern of *Hairy1* was confirmed about 10 years later, when Masamizu and colleagues drove the expression of a luciferase reporter in the mouse PSM under the control of the promoter of *Hes1*, the murine homolog of *Hairy1*. The reporter clearly showed traveling waves of *Hes1* expression sweeping the PSM from posterior to anterior, its stabilization in S0 and its disappearance upon somite formation (Masamizu et al., 2006), while *Hes1* mRNA becomes restricted to the caudal portion of the somite (Jouve et al., 2000). Importantly, the period of one *Hes1* cycle also corresponds to the period of formation of one somite pair in the mouse (i.e., around 2 hours). The propagation of this wave is independent of both cell movement and division

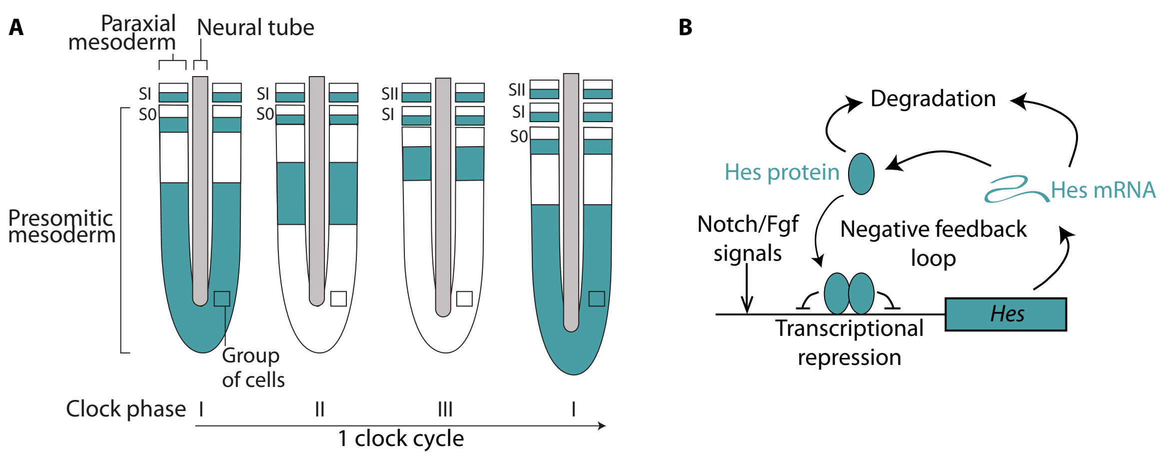


**Fig. 1.6. Segmentation clock oscillations. (A)** Schematic representation of the distinct phases of the segmentation clock cycle, represented by the oscillating expression of *Hairy1*. *Hairy1* transcriptional oscillations propagate in a posterior to anterior direction (Phase I to III), slowing down in the anterior PSM (Phase II-III) and arriving at the rostral-most PSM concomitantly with somite formation (Phase I). This expression pattern is a kinematic wave, in which individual PSM cells periodically turn on and off the expression *Hairy1* mRNA (square). Adapted from Resende et al., 2014. **(B)** Schematic representation of the negative feedback underlying cyclic *Hes* expression. Fgf and Notch signals induce the synthesis of Hes mRNA and proteins. These proteins will then mediate their own transcriptional repression. Both Hes mRNA and proteins are unstable, and together with their transcriptional repression, this results in their rapid disappearance from the cell. This in turn allows for the next cycle of *Hes* activation, thus driving oscillatory Hes mRNA and protein expression. Adapted from Harima et al., 2014.

(Palmeirim et al., 1997). Furthermore, these oscillations are tissue autonomous, as cultured PSMs isolated from the surrounding tissues still express dynamic *Hairy1* (Palmeirim et al., 1997).

After this initial discovery, hundreds of genes with oscillating behavior have been found in the PSM of zebrafish, frog, snake, chick and mouse embryos, suggesting that this oscillatory behavior of genes in the PSM is evolutionarily conserved (Gomez et al., 2008; Krol et al., 2011; Li et al., 2003). These cyclic genes constitute the so-called segmentation clock. The most conserved clock genes are those encoding for proteins of the Hairy and enhancer of split family (HES, which includes Hes, Her and Hairy), which are transcriptional repressors downstream of the Notch pathway. Importantly, at least one HES gene has an oscillatory behavior in the PSM of zebrafish, mouse and chick embryos, suggesting that the HES gene family is at the core of the vertebrate segmentation clock. In fact, only *Hes1* and *Hes7* orthologs have been found to be cyclic in all studied species, while other genes can be cyclic or non-cyclic depending on the species (Krol et al., 2011). In addition to the cyclic components and targets of the Notch pathway, such as *Lunatic fringe* (*Lnfg*), *Nrarp* or *Delta-like 1* (*Dll1;* Dequeant et al., 2006; Forsberg et al., 1998; Kageyama et al., 2018) the other oscillating genes in the vertebrate PSM were found to belong to just two more signaling pathways, namely that of Fgf and Wnt (Dale et al., 2006; Dequéant et al., 2006; Krol et al., 2011).

*1.2.4 How to establish oscillations*

Remarkably, the oscillation of segmentation clock gene expression is initiated during gastrulation, long before somitogenesis takes place (Freitas et al., 2001; Ishimatsu et al., 2010; Jouve et al., 2002; Riedel-Kruse et al., 2007). In the PSM, cells in different axial positions will be in different phases of the expression cycle (Fig. 1.6 A). The pattern of oscillation has specific features: (1) a wave of gene expression travels the PSM from posterior to anterior; (2) as this wave reaches the anterior PSM, it slows down and arrests immediately rostral or caudal to the region that will become the future segment boundary; and (3) these waves are cyclic, being repeated every time a new somite pair forms (Oates et al., 2012).

Although many genes exhibit oscillatory behavior in the PSM, the likely candidates for generating single cell oscillations are the HES genes, which repress the transcription of many segmentation clock genes, including their own (Harima et al., 2014; Kageyama et al., 2012; Schröter et al., 2012). This generates a negative feedback loop that gives rise to the cyclic pattern of genetic oscillations (Fig. 1.6 B; Novák and Tyson, 2008). Accordingly, knockdown of *Hes7* in the mouse leads to alteration of the cyclic expression profiles of both Notch- and Fgf-related segmentation clock genes (Bessho et al., 2001; Ferjentsik et al., 2009), although Wnt activity remains cyclic suggesting that *Hes7* does not regulate Wnt-mediated oscillations. Conversely, while the activation of *Hes7* expression in the posterior PSM is Fgf-dependent, its rostral propagation is dependent on Notch signaling (Ferjentsik et al., 2009; Niwa et al., 2007). *Hes7* appears to be the only non-redundant player in the clock machinery of the mouse, since double knockout of *Hes1* and *Hes5* does not lead to segmental defects nor altered clock oscillations (Bailey and Dale, 2015). Importantly, *Hes7* is the only HES in the mouse whose expression is specifically restricted to the PSM. The cycle of genetic activation and repression is accomplished by the rapid degradation of HES proteins, making their repressive activity transitory (Fig. 1.6 B). These proteins have a short half-life, which is a crucial feature for the generation of oscillating gene expression patterns: extending the half-life of Hes7 from 22 to 30 minutes in the mouse while maintaining its repressor activity leads to a progressive loss of oscillations (Hirata et al., 2004).

The period of oscillations is defined by the time it takes for mRNA transcription, intron splicing, nuclear export, translation and post-translation protein modifications, and mRNA and protein decay. While transcription has been found to be rapid and contribute little to this delay, intron splicing has a significant contribution to the period of oscillations. For instance, the expression of an *Hes7* reporter from which all the introns were removed results in a shorter interval (19 minutes shorter than wildtype *Hes7*) between its expression and translation, abolishing its oscillatory behavior and leading to major segmental defects (Takashima et al., 2011). Only reducing the number of *Hes7* introns results in a reduction of the clock period by 5 minutes, and the formation of extra vertebrae (Harima et al., 2013).

Synchronization of oscillations by neighboring PSM cells is dependent on Notch-Delta signaling (Delaune et al., 2012; Herrgen et al., 2010; Soza-Ried et al., 2014). When components of the Notch pathway are knocked out in the mouse embryo, the oscillatory behavior of segmentation clock genes is lost (Ferjentsik et al., 2009; Zhang et al., 2002). In the zebrafish, loss of Notch components leads to progressive loss of coherent oscillations, and segmentation clock genes become expressed in a salt-and-pepper manner, indicating loss of synchrony (Jiang et al., 2000; Oates and Ho, 2002). Indeed, mathematical modeling predicts that Notch-based feedback loops support the building of waves of coherent oscillations between neighboring PSM cells at the tissue level (Lewis et al., 2009). However, reciprocal Notch activation and repression does not completely account for the pacemaker – segmentation clock genes downstream of the Wnt pathway oscillate in a Notch-independent manner (Aulehla et al., 2003; Feller et al., 2008). Conversely, the Fgf pathway seems to be upstream of both Wnt and Notch in controlling the segmentation clock (Niwa et al., 2011; Wahl et al., 2007).

The dynamics of the segmentation clock are complex, as genes belonging to the different signaling pathways cycle in or out of phase depending on the A-P region of the PSM. For instance, waves of Notch target genes and pERK (a downstream target of Fgf signaling) sweep the posterior PSM in-phase, while becoming progressively out of phase when reaching the anterior-most PSM, which is positive for Notch components but negative for pERK, causing a phase-shift (Hubaud and Pourquié, 2014; Niwa et al., 2011). Conversely, components of the Wnt and Notch pathway oscillate out of phase in the posterior PSM, but progressively become in-phase when their wave of expression arrives in the anterior PSM (Sonnen et al., 2018). Additionally, segmentation clock genes from different signaling pathways show different dynamics: while *Dusp4* and *Axin2* (downstream of Fgf and Wnt, respectively) display a dynamic on/off expression in the posterior PSM, waves of *Lnfg* (downstream target of Notch) sweep the full length of the PSM continuously (Aulehla et al., 2003; Forsberg et al., 1998; Niwa et al., 2011). Recent evidence also suggests that clock oscillations are faster in the caudal PSM and slower in the rostral PSM, adding more complexity to the system (Niwa et al., 2011; Shih et al., 2015).

### *1.2.5 Models for somite formation*

The fact that somites form in a periodic fashion has intrigued embryologists for decades, and models for somite formation were proposed in as early as 1917 (Kulesa et al., 2007). The Clock and Wavefront model proposed by Cooke and Zeeman in 1976 was the first to postulate the existence of an oscillator controlling the pace of somite formation (Cooke and Zeeman, 1976). According to this model, the correct spatiotemporal formation of somites is accomplished by the combining activities of two different components: (1) an internal oscillator, intrinsic to PSM cells, which oscillate between a permissive and a non-permissive state; and (2) a traveling wavefront of maturation that moves posteriorly in the PSM, which defines the region where oscillations will arrest and the next somite will form. While the presence of oscillating genetic activity in the PSM was only first discovered 20 years after Cooke and Zeeman proposed the Clock and Wavefront model, since then many experimental studies have provided further evidence in favor of this model, making it the most widely accepted model for somite formation (see sections 1.2.2, *Gradients in the PSM* and 1.2.3, *The segmentation clock*, for more details).

The oscillations of segmentation clock genes are presumed to constitute the Clock, in which neighboring cells synchronize their genetic oscillations and a cyclic wave of expression coherently travels from posterior to anterior in the PSM. Conversely, the Wavefront corresponds to the determination front established by Fgf/Wnt posterior to anterior gradients, which are displaced caudally as the embryo grows, maintaining the caudal PSM cells with oscillating activity and undifferentiated. Thus, during the period of formation of one somite pair, a kinematic wave of expression of segmentation clock genes will travel the PSM from its caudal to its rostral end, while the determination front moves posteriorly as the embryo is elongating (Fig. 1.7 A). When PSM cells are hit by this determination front, cells that are in the same phase of the clock cycle will arrest their oscillations, and eventually form a new somite. This model also postulates that the size of the segment is defined by the distance travelled by the wavefront during one cycle of the clock.

Although the Clock and the Wavefront have been long regarded as independent entities, recent evidence is emerging suggesting that these players cross-talk, supporting the more recent "phase-shift" models (Fig. 1.7 B). In these models, the clock is a periodic inductive signal (the oscillations of the segmentation clock) and the wavefront is a periodic

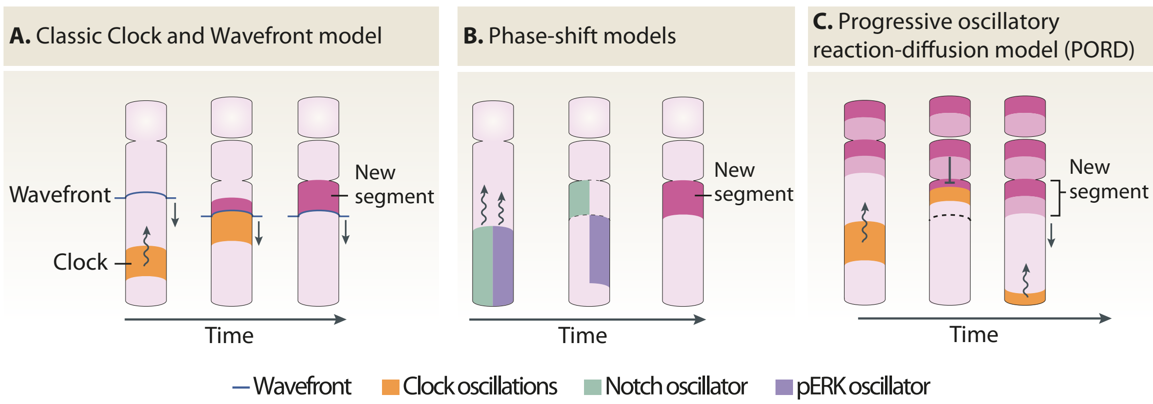


**Fig. 1.7. Theoretical models for somite formation. (A)** The classic Clock and Wavefront model. The new segment is defined by the length travelled by the wavefront (blue line) when the next clock cycle (orange) arrives at the anterior PSM. **(B)** Phase-shift models. The new segment is defined by a shift in different oscillators. In the mouse, the Notch oscillator (green) travels further rostral than the pERK oscillator (purple), and the next segment is defined when the Notch oscillator reaches a pERK negative area. **(C)** PORD model. The travelling wave of oscillatory clock activity is stabilized in the anterior PSM by the repressive action of the last formed stripe, thus defining the next segment. Adapted from Hubaud and Pourquié, 2014.

competency signal, whose position is influenced by the clock. Indeed, as referred previously, some targets of both Fgf and Wnt signaling have been found to oscillate in the PSM – genes from the Wnt pathway oscillate out of phase with Notch signaling in the posterior PSM, becoming in-phase with Notch cycles when arriving in the anterior PSM. Conversely, Fgf and Notch downstream targets oscillate in phase in the posterior PSM, but in the anterior region, oscillations of Notch-related genes move more anteriorly in respect to pERK (downstream of Fgf) oscillations, creating a shift (Fig. 1.7 B). Thus, the somite is determined in the region of the anterior PSM that has Notch oscillations, but no pERK signaling (Fig. 1.7 B).

Mathematical modeling has shown that the slowing down of clock oscillations does not need to be coupled with traveling morphogen gradients, as the coupling between oscillators may be sufficient to transform these oscillations into spatial patterns. In this model, the wavefront is a phase gradient of the clock, and not a separate player (Murray et al., 2011). A recent model proposed by Cotterel et al. (2015) called the Progressive Oscillatory Reaction-Diffusion (PORD) model is a challenge to the Clock and Wavefront (Cotterell et al., 2015). Indeed, they found that both molecular oscillations and a traveling wavefront participate in somitogenesis, particularly in stripe formation. However, these stripes are defined by the diffusion of a repressor molecule secreted by the adjacent stripe, and thus the wavefront is an emergent property of the system rather than a causal agent (Fig. 1.7 C). Importantly, this model does not rely on positional information provided by morphogen gradients. Moreover the authors provide experimental evidence that Fgf may block MET caudally, thus serving as a means to regulate the proper timing of the MET in the anterior PSM (Cotterell et al., 2015).

### *1.2.6 Notch signaling and Mesp2/Meso1 activation – Defining the boundary and rostro-caudal polarity of the future somite*

The activation of Notch signaling starts with the interaction between a transmembrane Notch receptor of one cell and a Delta/Jagged ligand in the membrane of a neighboring cell. The affinity of this interaction is modulated by Fringe, a glycosyltransferase that can either promote or inhibit Notch signaling. Binding of the ligand to Notch leads to its cleavage by the action of both the ADAM-family of metalloproteases and γ-secretase. Cleavage of the Notch receptor by the γ-secretase complex releases the Notch Intracellular Domain (NICD), which is translocated to the nucleus and associates with RBPJκ (recombination signal sequence-binding protein κ), creating a transcriptional activator complex and promoting the transcription of Notch target genes (Fig. 1.8; Borggrefe and Oswald, 2009; Totaro et al., 2018).

Notch signaling is undoubtedly implicated in somite formation, since mice carrying null mutations for various components of the pathway show somite defects. These include mutations in genes encoding for the Notch1 and Notch2 receptors (Huppert et al., 2005; Swiatek et al., 1994), the ligands Dll1 (Hrabě de Angelis et al., 1997) and Dll3 (Kusumi

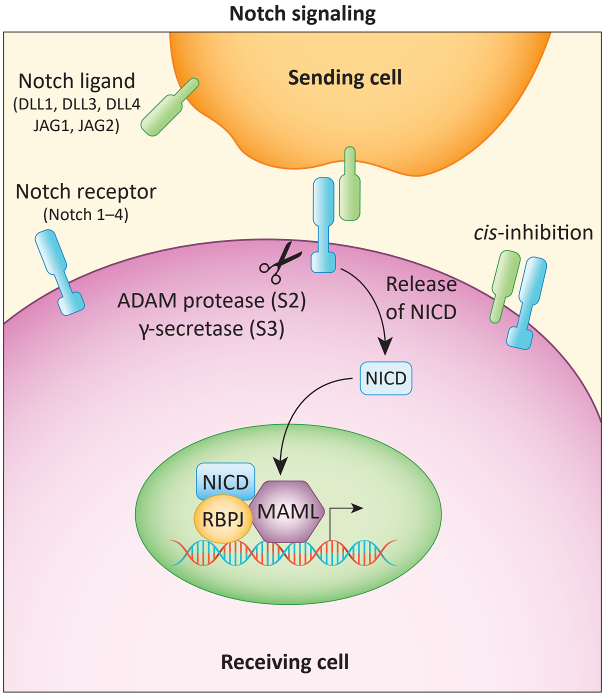


**Fig. 1.8. Notch signaling cascade**. Binding of ligands (green) on one cell to the Notch receptor (blue) of a neighboring cell induces the proteolytic cleavage of the NICD through the action of ADAM proteases extracellularly and the presenilin-dependent γ-secretase complex intracellulary. NICD then translocates to the nucleus, where it associates with RPBJ and MAML to drive the transcription of its target genes. These may be their own negative regulators such as Hes or Fringe. Interaction between a receptor and ligand on the same cell results in cis-inhibition of Notch signals. DLL – Delta-like. JAG – Jagged. NICD – Notch intracellular domain. RBPJ - recombination signal sequence-binding protein. MAML - Mastermind-like. Adapted from Totaro et al., 2018.

et al., 1998), the γ-secretase component Presenilin 1 (Psen1; Wong et al., 1997), the Notch modulator Lnfg (Dale et al., 2003; Evrard et al., 1998; Zhang and Gridley, 1998), the transcriptional co-activator RBPJκ (Ferjentsik et al., 2009) and the *Hes7* target gene (Bessho et al., 2001). Remarkably, the somite defects of these mutants include not only deficient segmentation clock oscillations, but also defective morphogenesis of somites, which exhibit abnormal shape, size and rostro-caudal polarity, leading to the formation of fused vertebrae and deficient patterning of peripheral nerves. Thus, Notch signaling has several roles during somite specification, morphogenesis and maturation – it regulates and is part of the segmentation clock, coordinates segment boundary formation, and has a role in specifying the rostral and caudal compartments of the future somite. These outputs of Notch signaling in the PSM are a consequence of the cyclic activation of one of its target genes, the bHLH transcription factor *Mesp2* in the mouse, *Meso1* in the chick, or *mespa/mespb* in the zebrafish (Buchberger et al., 1998; Saga et al., 1997; Sawada et al., 2000). Oscillating Notch signaling periodically activates *Mesp2* expression (or that of its homologs) in the S-II and/or S-I in the PSM of these embryos. This is accomplished by interactions of high levels of NICD with the transcription factor Tbx6 in a region with low pERK (Fig. 1.9; Hubaud and Pourquié, 2014; Niwa et al., 2011; Saga, 2012). Accordingly, high levels of Fgf in the posterior PSM repress *Mesp2* expression, even in the presence of Tbx6, which is expressed evenly throughout the PSM with its anterior-most border corresponding to S-I (Delfini et al., 2005; Dubrulle et al., 2001; Niwa et al., 2011; Saga, 2012; Sawada et al., 2001). When the cyclic wave of NICD arrives upon this region where pERK is low, both NICD and Tbx6 activate *Mesp2* expression in a band that corresponds to the length of one presumptive somite (Fig. 1.9). Mesp2 then activates *Ripply2* expression which promotes the degradation of Tbx6 protein in this region, shifting the anterior border of *Tbx6* expression one somite length posteriorly. This defines the region where the next wave of NICD will interact with Tbx6 to activate *Mesp2* expression during the next cycle (Fig. 1.9; Dahmann et al., 2011; Saga, 2012; Yasuhiko et al., 2006). The anterior border of *Mesp2* expression coincides with the region of the PSM that will later form a segment boundary, suggesting that Mesp2 has a role in positioning the future somitic cleft (Fig. 1.9, Morimoto et al., 2005; Oginuma et al., 2010). Indeed, *Mesp2*-null mice have disorganized somites, with irregularly positioned segment boundaries (Saga et al., 1997). Thus, molecular segmentation of the PSM precedes morphological boundary formation.

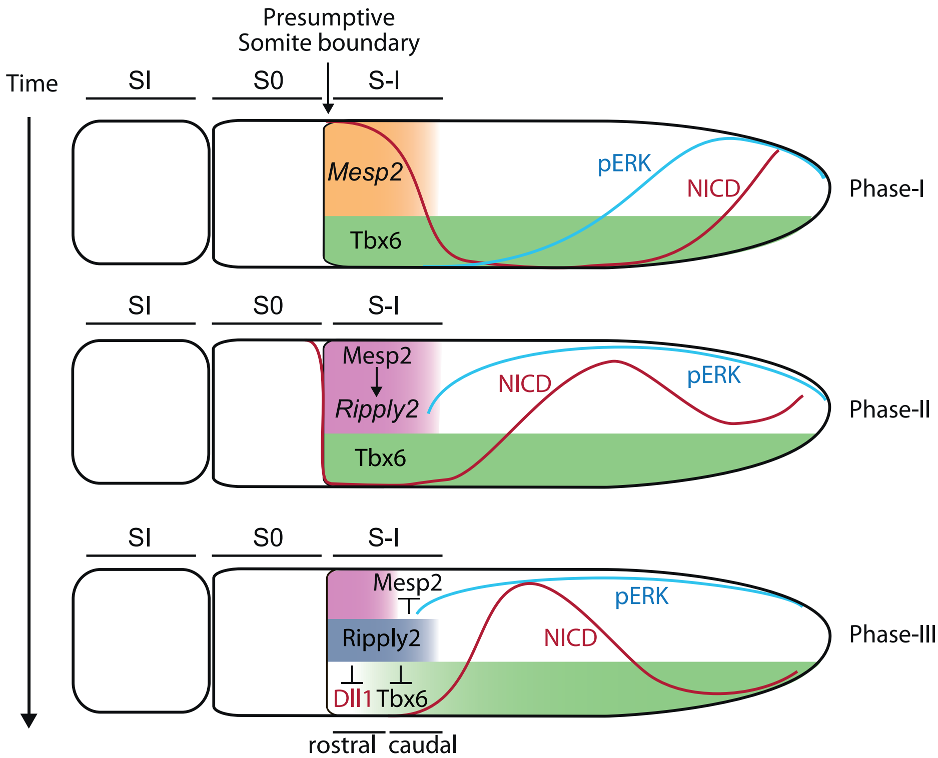


**Fig. 1.9. Mesp2 activation in the mouse embryo.** Schematic representation of the sequential molecular events leading to Mesp2 (Meso1 in chick) activation and function. During Phase I of the segmentation clock oscillations, low pERK signals in S-I (S-II in chick) create a permissive environment for high Notch signaling which, combined with Tbx6 protein (geen), induces the transcription of *Mesp2* (orange). Mesp2 protein (purple) then activates *Ripply2* transcription during Phase II, and Ripply protein (blue) induces Tbx6 degradation in Phase III, leading to a posterior shift of one-somite length in its anterior domain. Ripply2 also negatively regulates *Dll1* and *Mesp2* expression. Mesp2 thus becomes restricted to the rostral half of S-I. Adapted from Saga, 2012.

Soon after its activation in S-I/S-II, *Mesp2* expression is further restricted to the rostral half of the presumptive segment in a process induced by Mesp2 itself, as Ripply2 also mediates its repression, confining Mesp2 to the rostral region of the presumptive segment (Fig. 1.9). Mesp2 also activates *Lnfg* and represses *Dll1*, thus inhibiting Notch signaling in this domain (Saga, 2012). This results in the restriction of *Dll1* expression to the caudal domain of the future somite, where Dll1 activates Notch signaling . Together, these signaling events provide the foundation for the establishment of the rostro-caudal polarity of the future somite, which occurs when cells are still in the unsegmented PSM. Accordingly, the entire somite of *Mesp2*-null mice has a caudal identity  (Takahashi et al., 2003).

*Mesp2* in the rostral domain of the future segment contributes to the establishment of rostral identity by activating the expression of *Tbx18*, a T-box transcription factor that specifies the rostral compartment of the future somite. Conversely, the presumptive caudal half maintains *Dll1* expression and thus activates both Notch signaling and the expression of *Uncx4.1*, which is restricted to this caudal domain in both chick and mouse somites (Mansouri et al., 1997; Schrägle et al., 2004). *Uncx4.1* is a paired homeobox gene that specifies the proximal ribs and pedicles of the future vertebrae (Leitges et al., 2000; Mansouri et al., 2000). This rostro-caudal imprinting is established in the anterior PSM. If the anterior (but not the posterior) PSM is dissected out, rotated along the A-P axis and transplanted to a recipient embryo, somites originating from this transplanted PSM will maintain their original rostro-caudal specification (Palmeirim et al., 1998).

It is relevant to note that the regulation of *Dll1* expression in the posterior PSM, where *Dll1* presents oscillatory behavior, is different from that of *Dll1* expression in the caudal domain of the future somite. Indeed, both are differentially regulated by the Notch pathway, as *Dll1* expression in caudal domain of the prospective somite is Psen1-dependent, while *Dll1* expression in the posterior PSM is Psen1-independent (Takahashi et al., 2003). This suggests that Notch signaling has two modes of action depending on the axial position in the PSM. Indeed, these different modes of Notch signaling culminate in different outputs. First, it mediates the oscillatory activity of segmentation clock genes in the posterior PSM. Second, it induces both cyclic *Mesp2* activation in the S-I/S-II, thus defining the future segment border in the anterior PSM, and it specifies the rostro-caudal polarity of the future somite. However, it is important to note that the specification of the rostro-caudal polarity of the presumptive somites in the anterior PSM is dependent on cyclic Notch activity, and not just the presence of Notch-signaling *per se*. Mouse embryos expressing a constitutively active form of NICD throughout the total length of the PSM, thus abolishing *Lnfg*, *Hes7* and *Spry2* oscillations (but not those of *Axin2*), show caudalized somites – *Uncx4.1* is expressed throughout the whole segment, and *Tbx18* is completely absent (Feller et al., 2008). Thus, the segmentation clock not only defines the time and space for correct somite formation, but also somitic A-P polarization in the rostral PSM.

## 1.3. Somite morphogenesis

### *1.3.1 Boundary formation*

The formation of somitic boundaries is a complex, tightly regulated morphogenetic event, whereby strictly choreographed cellular rearrangements establish a cleft in the anterior PSM, and cells immediately anterior to this cleft begin epithelializing (Kulesa and Fraser, 2002; Martins et al., 2009). While Notch signaling is required for determining the position of future segment boundaries in the unsegmented anterior PSM (i.e., where the initial cleft in the anterior PSM will form), ectopic activation of Notch signaling in the S-II region is sufficient to induce ectopic clefts, suggesting it also has a role in its morphogenesis (Sato et al., 2002). Since Mesp2 activation is under the control of Notch signaling and its anterior border of expression coincides with the future segment cleft (Morimoto et al., 2005), Mesp2 is in a position to mediate morphological segmentation as an output of Notch signaling. This is further supported by the somitic phenotype of *Mesp2*-null mice, which have deficient somitic boundaries (Saga et al., 1997). The patterning events that define the region of the anterior PSM where the future segment boundary will form are followed by a rapid MET of the posterior cells of the nascent somite. This MET is instructed by the *Mesp2*-expressing cells immediately juxtaposed posteriorly to the nascent boundary. The cells instructed by Mesp2 will thus compose the posterior region of the forming somite (S0), which is the region that undergoes full epithelialization first (Fig. 1.10; Martins et al., 2009; Sato et al., 2002; Takahashi et al., 2005).

Mesp2 induces the formation of this morphological boundary by activating the Eph-ephrin signaling pathway (Fig. 1.10). Ephs are tyrosine kinase transmembrane receptors which bind to membrane-bound Ephrin ligands on neighboring cells, eliciting a variety of cellular responses, including repulsion, adhesion or differentiation (Cayuso et al., 2015). In the chick embryo, *Meso1* upregulates EphA4 in the cells just posterior to the next forming boundary (Watanabe et al., 2009). EphA4 in the membrane of these cells interacts with the EphrinB2 receptor on the cells immediately anterior (and juxtaposed) to them. It has been proposed that signaling via the EphA4 receptor induces a repulsive behavior in the cells caudal to the forming cleft, while EphrinB2 signaling in the cells rostral to the border inhibits Cdc42 activity, which normally inhibits MET (Nakaya et al., 2004), in these cells and thus promotes their epithelialization (Watanabe et al., 2009). This MET is also dependent on the tight regulation of Rac1 levels, since both elevated or reduced levels of Rac1 disrupt the epithelialization of the posterior cells of the nascent somite (Nakaya et al., 2004). Accordingly, zebrafish *fss* mutants, in which the EphA4/EphrinB2 signaling pathway is disrupted, have no somitic boundaries and restoring EphA4/EphrinB2 signaling in the PSM is sufficient to drive boundary formation, further implicating this pathway in the process (Barrios et al., 2003). Moreover, epithelialization of border cells is recovered,

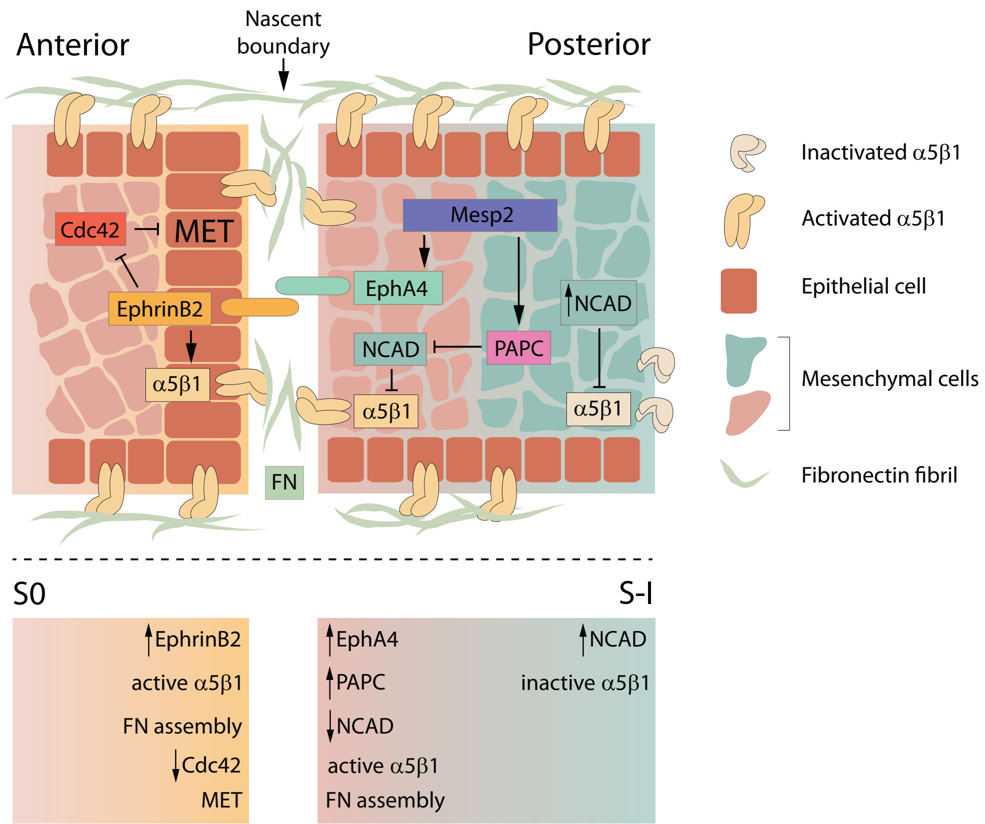


**Fig. 1.10. Induction and morphogenesis of the somitic boundary**. S-I expresses Mesp2, which induces the formation of the next segment boundary in at least two ways. First, it activates PAPC transcription and PAPC protein stimulates the endocytosis of N-cadherin in the anterior region of S-I. The removal of N-cadherin in turn alleviates the N-cadherin-mediated inhibition of integrin α5β1 activation. Second, Mesp2 activates EphA4 expression in the anterior region of S-I and EphA4 protein binds to EphrinB2 on the cells in S0, i.e. immediately anterior to the EphA4-positive cells . EphrinB2 induces the activation of α5β1 on these cells and inhibits Cdc42 activity. EphA4 and EphrinB2 induce cellular repulsion, generating a gap between caudal S0 and anterior S-I cells, which is further stabilized through the assembly of a fibronectin matrix built by the activated α5β1 integrins. Decreased Cdc42 levels is also thought to allow for the mesenchymal-to-epithelial (MET) transition of posterior S0 cells, which epithelialize and further detach from the S-I.

although complete somitic epithelialization is not fully restored (Barrios et al., 2003; see section 1.3.2, *Somite epithelialization*, for more details).

After the morphological boundary is established, the maintenance of its integrity is strengthened by other pathways downstream of Mesp2. In addition to EphA4, Mesp2 also activates Paraxial protocadherin (PAPC; Fig. 1.10). PAPC is a cycling gene under the control of Notch signaling in the PSM of both chick and mouse embryos and is required for the epithelial organization of the cells of segment borders (Chal et al., 2017; Rhee et al., 2003). When PAPC is upregulated in the cells immediately posterior to the forming boundary, it promotes the endocytosis of N-cadherin (Ncad), which is expressed by all PSM cells. Ncad mediates PSM cell-cell adhesion and has been shown in zebrafish to maintain integrin α5β1 in an inactive state (Jülich et al., 2015). In the dorsal and ventral edges of the PSM, where cells do not contact with neighbors and there is space in the interface where they connect to the adjacent tissues, integrins are liberated from the repressive activity of Ncad and adopt an active conformation. This allows the building of fibronectin matrix, that is first restricted to the dorsal and ventral sides of the PSM. However, when endocytosis of Ncad is promoted by PAPC activity in the cells posterior to the nascent boundary, EphrinB2 promotes integrin clustering in the cells anterior to the nascent cleft, which then become activated and start building the fibronectin matrix necessary for boundary maintenance (Fig. 1.10, see section 3.6, *Importance of fibronectin in somitogenesis,* for more details).

It is important to note that while Notch signaling is upstream of Mesp2/Meso1 activation, and thus plays a pivotal role in establishing the signaling cascades that culminate in boundary formation, it is still under debate whether its oscillatory behavior is required for these processes. In *Hes7*-null mice, constitutively active NICD is found throughout the PSM and the cyclic behavior of Notch-regulated genes is disrupted, but somitic boundaries still form in these mice albeit with abnormal spacing, suggesting boundary positioning is asynchronous and randomized (Ferjentsik et al., 2009). Accordingly, mice expressing activated NICD throughout the PSM have discernable segment boundaries, although somites are irregularly shaped and sized (Feller et al., 2008). However, conflicting results were reported in another study (Oginuma et al., 2010), where the authors found that it is the oscillatory activity of NICD and not its anterior sharp boundary that is needed for *Mesp2* upregulation and boundary formation. Thus, although there is a clear relationship between the segmentation clock and regulation of the machinery mediating somitic boundary positioning, it is still unclear how the temporal oscillations of the clock translate into spatially and temporally regulated boundary formation.

### *1.3.2 Somite epithelialization*

Somite formation is characterized by a MET, in which mesenchymal cells from the anterior PSM epithelialize into an aster-like somite, surrounding a mesenchymal core, the somitocoel. Similarly to what was observed in the segment boundary, downregulation of Cdc42 and intermediate levels of Rac1 are necessary for the correct epithelialization of the whole segment (Nakaya et al., 2004). In fact, blocking Cdc42 leads to hyper-epithelialization of somitic cells with fewer mesenchymal cells in the somitocoel, whereas somitic cells remain mesenchymal when Cdc42 levels are increased (Nakaya et al., 2004). Also, cells with increased or inhibited Rac1 fail to epithelialize correctly, suggesting that Rac1 activity must be tightly regulated (Nakaya et al., 2004).

Albeit seemingly concomitant, boundary formation and somite epithelialization are two separate processes. This is illustrated by the somitic phenotype of mice null for the bHLH gene *Paraxis*, in which segment boundaries are formed normally (and, importantly, segmentation clock oscillations also occur normally; Burgess et al., 1996). However, these segments fail to epithelialize and are thus blocks of mesenchymal cells, suggesting that boundary formation and somite epithelialization are decoupled. In addition, these segments lacked normal rostro-caudal polarity (Johnson et al., 2001). *Paraxis* is expressed in from S-III to SI and is maintained in the epithelial somites in mouse, chick (Barnes et al., 1997), zebrafish (Shanmugalingam and Wilson, 1998) and *Xenopus* (Carpio et al., 2004; Tseng and Jamrich, 2004), and seems to mediate somite epithelialization through the control of Rac1 levels (Nakaya et al., 2004; Rowton et al., 2013). Thus, epithelialization of somites requires more than just making boundaries between paraxial mesoderm cells in a regular spatio-temporal fashion.

Live imaging studies in the chick embryo have added more information about the dynamics of boundary formation and somite epithelialization. These studies have shown that cells in the PSM are highly dynamic and can be observed to move out of the *Meso1* expression domain in S-I and to migrate across the border from one presumptive somite to another (Kulesa and Fraser, 2002; Martins et al., 2009). Furthermore, somite epithelialization in the chick embryo was found to take much longer than the 90 min period of somite formation (Martins et al., 2009). In fact, cells in the rostral PSM do not all epithelialize simultaneously. The first cells to organize into a cuboidal epithelium (the first epithelialization event) are the medial PSM cells and this process starts already around S-IV. Then by S-II, this first epithelialization event has spread to the dorsal and ventral sides of the anterior PSM (Martins et al., 2009). When the cleft starts forming in S0, cells elongate into spindle-shaped cells (the second stage of epithelialization). This epithelialization event sweeps along the forming border and progressively spreads to all sides as S0 detaches from the PSM as SI. The anterior border of SI epithelializes after the posterior border undergoes its MET and the lateral border is the side that epithelializes last, at SII stage (Martins et al., 2009). Thus, in reality, the epithelialization process starts long before border formation, at around S-II, and spans a period of about 6 hours, until the somite reaches SII stage (Martins et al., 2009).

Somite integrity is maintained through the action of cell-cell adhesion molecules. N-cadherin is present throughout the paraxial mesoderm and becomes enriched in the apical side of the epithelial somitic cells of both chick and mouse embryos (Duband et al., 1987; Linask et al., 1998). Mice null for N-cadherin show fragmented somites, but normally spaced somitic boundaries and R-C polarity, as seen by normal *Uncx4.1* expression and the presence of epithelioid cells (Horikawa et al., 1999; Radice et al., 1997). Importantly, somites fragmented in the rostro-caudal interface of the somite, suggesting that N-cadherin activity is crucial for maintaining the integrity of the somitic epithelium, in particular in connecting the rostral and caudal halves of the somite, which aggregate independently of each other when separated in culture (Horikawa et al., 1999).

Somite epithelialization has recently been described as being independent of the segmentation clock (Dias et al., 2014). In this study, posterior primitive streak explants were treated with Noggin, a BMP (Bone Morphogenetic Protein) inhibitor, and subsequently transplanted to the extraembryonic region of a host chick embryo. High BMP levels in the posterior primitive streak specify lateral plate mesoderm, while the anterior primitive streak, from which the paraxial mesoderm derives, shows low levels of BMP. Accordingly, this manipulation effectively converted the posterior primitive streak explant into paraxial mesoderm, since after 9-12 hours of incubation, about 6-14 ectopic somites formed in a grape-like structure in the absence of cyclic expression of segmentation clock genes. Importantly, these somites presented normal shape and size, but lacked rostro-caudal polarity. These results confirm that segmentation clock oscillations have a role in regulating the precise timing of somite formation in a linear array, since the somites resulting from these posterior primitive streak explants form simultaneously and in a "bunch of grapes" manner (Dias et al., 2014). Moreover, this also confirms that the rostro-caudal polarity of the future somite, established in the anterior PSM, is dependent on the activity of the segmentation clock.

In conclusion, while segmentation clock oscillations, the establishment of rostro-caudal polarity, segment boundary specification and formation, and somite epithelialization occur in the anterior PSM, these events are distinct, but interdependent, and can be experimentally decoupled. The tight temporal and spatial control of these processes requires a complex network of players and safe-guard mechanisms, ensuring that somite specification and morphogenesis occurs at the right space and the right time. The tight and intricate regulation of these different processes allows normal development of the vertebral column and makes somitogenesis one of the most complex morphogenetic events in vertebrate embryogenesis and, therefore, one of the most fascinating and challenging to study.

## 1.4. Somite patterning

### *1.4.1. The Hox code and axial specification*

Depending on the axial position of the somite, the resulting sclerotome will give rise to cervical, thoracic, lumbar, sacral or caudal vertebrae, which have different morphological traits. For example, thoracic vertebrae have ribs, while lumbar vertebrae are denser and larger, and sacral vertebrae have fused lateral protrusions (Mallo et al., 2010). This axial specification occurs very early during paraxial mesoderm development, long before morphological segmentation occurs. This is illustrated by classical transplantation experiments where the PSM of a prospective thoracic region was grafted to a different axial position of a host embryo, developing into rib-containing vertebrae according to its original axial positioning in the donor embryo (Kieny et al., 1972). Interestingly, this only applies to sclerotomal derivatives, as the myogenic precursors originated by the donor PSM develop according to the new location in the host tissue (Chevallier et al., 1977; Stern and Keynes, 1987).

This early specification of axial identity is mediated by the colinear activation of homeobox-containing Hox transcription factors, first discovered in the fruit fly (Alexander et al., 2009). Hox genes are organized in clusters, more specifically in four different clusters in the case of vertebrates, resulting from genome duplication events (Fig. 1.11). In mammals, 39 Hox genes are organized into 13 paralogous groups. The spatial collinearity of Hox gene expression reflects their colinear position in the chromosomes. Also, Hox genes within a given cluster are expressed from 3' to 5' in a temporally defined way, so that the first activated genes are expressed early in the primitive streak, while the last genes are expressed much later, restricted to the posterior end of the growing embryo. The so called "Hox code" imprints the final axial position on PSM cells, although the morphological translation of this blueprint is only detectable much later, upon vertebrae development. It is possible that this axial specification occurs even earlier, during gastrulation – accordingly, the Hox code has been found to control the ingression of cells though the primitive streak during mesoderm formation, suggesting that they may exert axial identity in the ingressing cells (Iimura and Pourquié, 2006).

Although extensive studies on Hox function have been made in the last decades, it is still not clear how the Hox code blueprints axial identity to the paraxial mesoderm, and how it intercommunicates with the other signaling systems acting on paraxial mesoderm

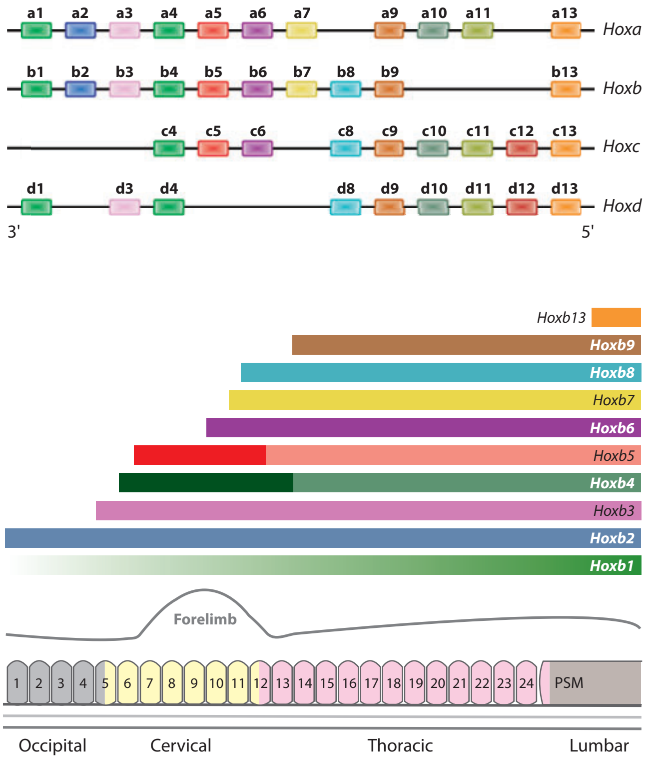


**Fig. 1.11. The Hox code.** *Top*. Hox genes are organized into four clusters - *Hoxa*, *Hoxb*, *Hoxc*, and *Hoxd* – which are in separate chromosomes. The linear arrangement of the *Hox* genes within each cluster reflects the spatial and temporal initiation of their expression, and location of the anterior border of their expression domain – for example, genes from the first paralogous group (Hoxa1, *Hoxb1*, and *Hoxd1*) are expressed earlier and more anteriorly, while genes from the last group (*Hoxa13*, *Hoxb13*, *Hoxc13*, and *Hoxd13*) are the most posterior and last to be activated; *Bottom*. Schematic representation of the somitic expression of *Hox* genes from the *Hoxb* cluster along the A-P axis of the embryo. The different Hox signature of each somite will define the types of vertebrae they will develop into, here exemplified with either occipital, cervical, thoracic or lumbar. Adapted from Alexander et al., 2009.

development. Altering the gradient of Fgf in the chick PSM results in abnormal Hox gene expression (Dubrulle et al., 2001), and some Hox genes have been found to have a cyclic behavior in the mouse PSM (Zákány et al., 2001), possibly under the control of Notch signaling via Dll1 and Lnfg (Cordes et al., 2004).

### *1.4.2 Somite differentiation*

In contrast to the A-P polarity of the somite, which is defined while cells are still in the PSM, the dorso-ventral (D-V) and medio-lateral (M-L) polarities only become determined after the somite has formed, at around SIII stage. The polarization of the somite in the D-V and M-L axes is dependent on the surrounding tissues, which secrete morphogens that specify the different somitic compartments that will give rise to different types of tissues.

Dorso-ventral patterning of the somite depends on the tissues ventral and dorsal to it. Sonic hedgehog (Shh) secreted by the notochord and by the floor plate of the neural tube signals to the ventral somite to determine the sclerotome (Buttitta et al., 2003; Fan and Tessier-Lavigne, 1994; Fan et al., 1995; Marcelle et al., 1997; Stafford et al., 2011). The sclerotome contains the progenitors of cartilage and bone of the vertebrae and ribs (Fig. 1.12; Christ et al., 2004). This specification of the ventral somite involves a downregulation of *Pax3* and the expression of *Pax1* at around SIV and *Pax9* soon after (Borycki et al., 1997; Ebensperger et al., 1995; Monsoro-Burq, 2005). At around SX stage in the avian embryo, the ventral somite undergoes an EMT and becomes mesenchymal (Balling et al., 1996; Monsoro-Burq, 2005; Rifes and Thorsteinsdóttir, 2012). Conversely, dorsalizing signals from the overlying ectoderm and the roof plate of the neural tube, including Wn3a, Wnt1 and Wnt6 and BMP4, specify the dorsal compartment of the somite (Bothe et al., 2007; Dietrich et al., 1997). This dorsal region of the somites, the dermomyotome, remains epithelial for longer and retains *Pax3* expression (Cairns et al., 2008). The dermomyotome will give rise to the myotome, the first embryonic skeletal muscle, as well as to all muscle stem cells which generate the skeletal muscles of trunk and limbs. It also contains dermal and brown fat progenitors and cells capable of differentiating into endothelial and smooth muscle cells (Buckingham and Rigby, 2014). Finally, communication between the myotome and the dorsal sclerotome leads to the specification of the syndetome, an area containing the progenitors of the axial tendons (Brent et al., 2003).

Somite derivatives are further subdivided along the medio-lateral axis, with midline structures specifying medial fates, and the lateral plate mesoderm inducing lateral fates (Christ et al., 2007). This is accompanied by a slight rotation of the somite which accompanies the closing of the embryo's lateral folds, such that the medial domain becomes dorso-medial (also called epaxial) and the lateral region becomes ventro-lateral (also called hypaxial; Fig. 12; Brand-Saberi et al., 1996). The medial sclerotome gives rise to the vertebrae bodies and intervertebral discs, while the ribs originate from the lateral sclerotome (Christ et al.,

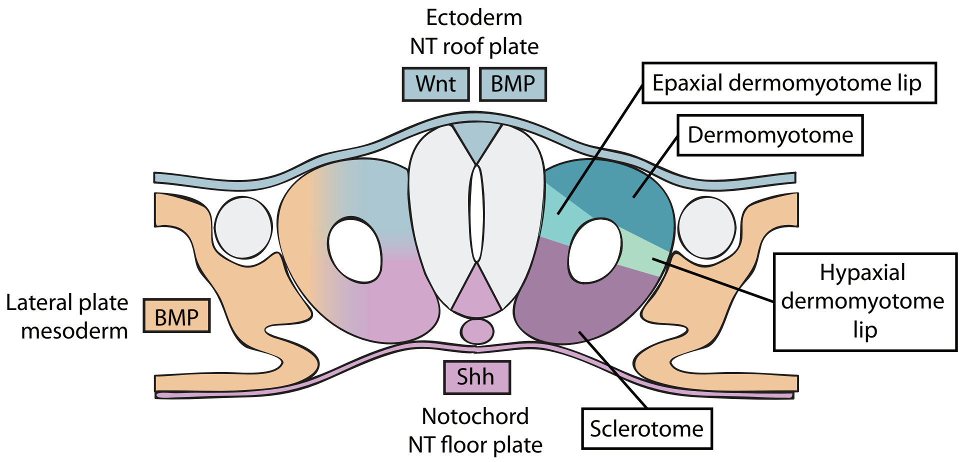


**Fig. 1.12. Schematic representation of the dorso-ventral and medial lateral patterning of the somite**. For clarity, the morphogen gradients received by the somite are represented on the left and the resulting somite derivatives are represented on the right. Wnt and BMP signals from the ectoderm and the roof plate of the neural tube (blue) specify dorsal structures (dermomyotome). Shh from the notochord (violet) induces the ventral somite to form the sclerotome. Intermediate levels of both dorsal and ventral signals induce the epaxial domain of the dermomyotome to form the epaxial dorsomedial lip, while lateralizing BMPs from the lateral plate mesoderm (orange) specify the hypaxial lip. Adapted from Dietrich et al., 1997.

2004; Christ et al., 2007). Similarly, the epaxial lip of the dermomyotome and myotome will originate the deep muscles of the back, while the hypaxial domain gives rives to intercostal, lateral and ventral muscles, as well as the diaphragm, limb and tongue muscles, depending on their A-P position (Babiuk et al., 2003; Deries and Thorsteinsdóttir, 2016; Deries et al., 2010; Murphy and Kardon, 2011; Sambasivan et al., 2011). These D-V and M-L patterning events depend entirely on the surrounding tissues and are not an emergent property of the somite. Experiments where early epithelial somites are rotated in the D-V or M-L axis result in a patterning consistent with the new orientation, suggesting that re-specification of dorsal, ventral, medial and lateral fates occurs when the environment changes (Aoyama and Asamoto, 1988; Ordahl and Le Douarin, 1992).

## 1.5. Somite derivatives

### *1.5.1 Dermomyotome*

The dermomyotome remains epithelial until HH18 in the chick and E11.0 in the mouse, retaining the expression of both *Paraxis* and *Pax3* and activating the expression of *Pax7* (Dietrich et al., 1997; Endo, 2015; Scaal and Christ, 2004; Thorsteinsdóttir et al., 2011). The dermomyotome forms a sheet of epithelial tissue that stretches and grows above the sclerotome in a dorsolateral direction (Fig. 1.13; Buckingham and Rigby, 2014). Its four edges bend slightly in the direction of the sclerotome, forming the dermomyotome lips. The medial-most region of the dermomyotome (so-called dorsomedial lip) is where myogenesis starts, with the activation of the expression of myogenic regulatory factors, including *MyoD*

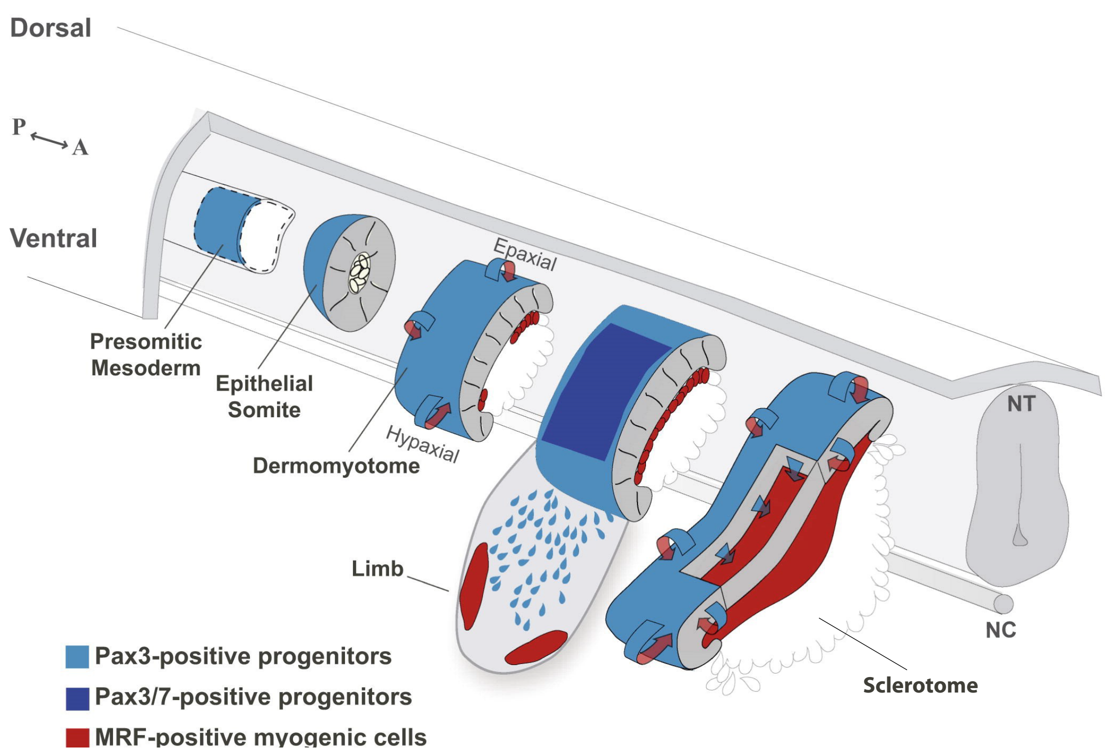


**Fig. 1.13. Dermomyotome development**. The dermomyotome arises from the dorsal-most region of the epithelial somite, which expresses *Pax3.* Cell proliferation within the dermomyotome leads to growth in the medio-lateral direction. Hence the dermomyotome can be subdivided into an epaxial (more medial and dorsal) domain, and an hypaxial (more lateral and ventral) domain. Delamination of cells from these dermomyotomal lips forms the underlying myotome, which expresses myogenic regulatory factors (MRF) including *MyoD* and *Myf5*. At limb levels, Pax3-positive muscle stem cells delaminate and migrate to the forming limb buds where they differentiate. Delamination eventually occurs from all the borders of the dermomyotome, and later the central *Pax7* expressing dermomyotome de-epithelializes to feed more muscle stem cells into the myotome. The dermomyotome also gives rise to other derivatives such as dermal, endothelial and brown fat cells. Adapted from Buckingham and Rigby, 2014.

and *Myf5*. This is the first step of the formation of the myotome (Buckingham and Relaix, 2007; Thorsteinsdóttir et al., 2011). Eventually, all the four borders of the dermomyotome form lips and contribute with cells to the underlying myotome (Fig. 1.13). Later, the central dermomyotome de-epithelializes through an EMT concomitant with an asymmetric cell division, in a way that the dorsal-most (basal) daughter cells contribute to the dermis, and the ventral (apical) daughter cells enter the myotome as proliferating Pax3- and/or Pax7-positive muscle stem cells (Buckingham and Relaix, 2007). This process also generates endothelial and smooth muscle cells. Eventually, all four lips of the dermomyotome de-epihelialize, which occurs at around embryonic day 7 in the chick (Ordahl et al., 2001; Scaal and Christ, 2004; Venters and Ordahl, 2002).

*1.5.2 Sclerotome*

The molecular specification of the sclerotome occurs in the epithelial somite, with *Pax1* expression being initiated in the ventral somite soon after the somite epithelializes (Borycki et al., 1997). However, the sclerotome soon becomes morphologically distinct from the dorsal dermomyotome by undergoing an EMT (Christ et al., 2004). Cells from the ventral somite decrease their expression of cell-adhesion molecules and increase their motility. This is accompanied by simultaneous production of Matrix Metalloproteinase 2 (MMP-2) and hyaluronate, resulting in increased extracellular space and decreased cellular attachment to both their neighbors and the ECM (Christ et al., 2004; Duong and Erickson, 2004; Solursh et al., 1979). The sclerotome then migrates medially to ensheath the notochord and neural tube and, at thoracic level, also laterally into the somatopleure. This early sclerotome has different compartments – the ventral sclerotome will give rise to the vertebral body, the central sclerotome will originate the pedicle, and the dorsal and lateral compartments will give rise to the neural arch and rib, respectively (Christ et al., 2004).

The sclerotome can further be divided in rostral and caudal compartments, and this rostro-caudal polarity results from processes occurring while cells are still in the PSM (see section 1.2.6, *Notch signaling and Mesp2 activation,* for more details). Before the morphological separation of the two halves of the sclerotome, these can first be distinguished molecularly, as hundreds of genes are specifically expressed in one region and excluded from the other (Hughes et al., 2009). Moreover, this molecular A-P pattern of the sclerotome

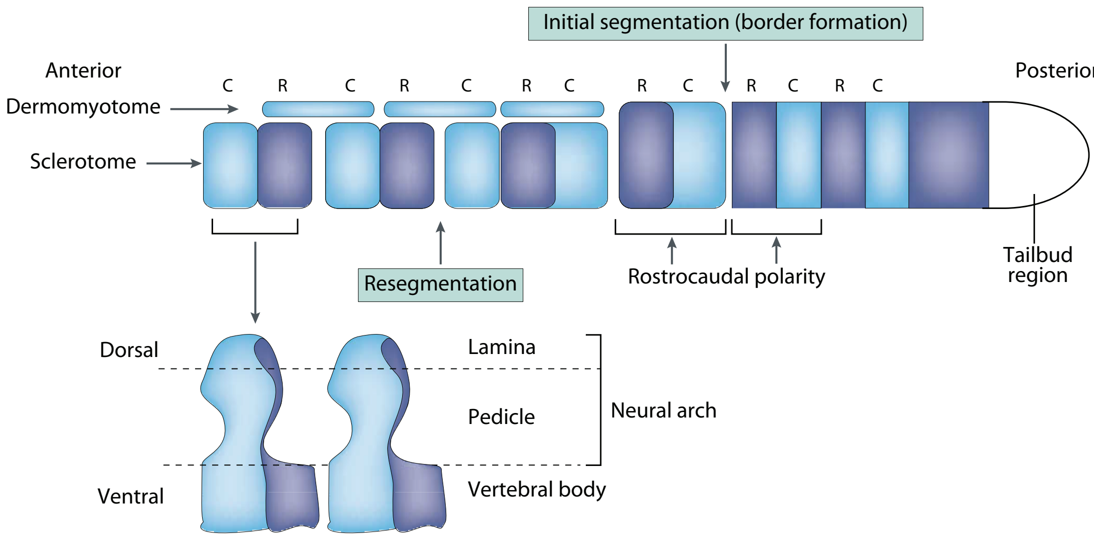


**Fig. 1.14. Resegmentation of the sclerotome**. Rostro-caudal polarity of somites is defined while cells are in the PSM. Later during somite development, the sclerotome (but not the dermomyotome and myotome) undergoes a resegmentation process, whereby its rostral and caudal halves segregate and reaggregate with neighboring halves from the adjacent sclerotome. Thus, one vertebrae will be composed of the rostral part of one sclerotome, and the caudal portion of the adjacent sclerotome. R – Rostral. C – Caudal. Adapted from Saga and Takeda, 2001.

imposes a segmented pattern on the peripheral nervous system, since the migration of neural crest cells and motor axons occur exclusively through the rostral part of the sclerotome, while the caudal half has a repellent effect on these cells (Fig. 1.14; Kuan et al., 2004). This rostro-caudal division of the sclerotome is maintained through the action of Tbx18, acting downstream of Mesp2 and in conjunction with Meox1 (Scaal, 2016). In terms of morphology, the rostral half of the sclerotome displays much lower cell density than the caudal region, and the two halves are later divided by the von Ebner's fissure, characterized by elongated sclerotomal cells which are oriented transversely to the axis (Keynes and Stern, 1984; Scaal, 2016).

The caudal and rostral halves of the same somite will give rise to different vertebrae through the process of re-segmentation (Fig. 1.14). Accordingly, the vertebral body is formed by the caudal half of one sclerotome and the rostral half of the posteriorly adjacent sclerotome (Aoyama and Asamoto, 2000; Christ et al., 2007; Scaal, 2016). Importantly, the dorsal dermomyotome and myotome retain their original segmentation and do not go through this re-segmentation process (Saga and Takeda, 2001; Scaal, 2016). This allows the segmented muscles to attach to two adjacent vertebrae through their tendons, allowing for movement of the vertebral column. This segmented muscle organization underlies the locomotion in fish, but is further modified to different extents during the development of terrestrial vertebrates (Fleming et al., 2015; Lauder, 1980).

## 2. The extracellular matrix

Every tissue and organ of a multicellular organism is surrounded by a particular, tissue-specific extracellular matrix (ECM). For decades, the ECM was viewed as just a "styrofoam packing material" (Rozario and DeSimone, 2010), filling the space between cells and tissues and providing a supportive structural scaffold (Frantz et al., 2010; Rozario and DeSimone, 2010). However, the genetic knock-out of several ECM components in mouse embryos proved to be embryonic lethal, while a wide range of syndromes in human was attributed to deficiencies in ECM components, thus establishing the ECM as crucial for both development and homeostasis (Iozzo and Gubbiotti, 2018; Rozario and DeSimone, 2010). In this section I will give a general overview of the components and functions of the ECM, the structure of its main receptors and signal transduction players, and its importance in both development and disease.

## 2.1. Overview of matrix components

There are two main types of ECMs: the interstitial matrix that surrounds mesenchymal cells and characterizes the connective tissue; and the basement membrane, which forms a sheet-like matrix underlying the basal side of epithelial and endothelial cells and surrounds fat, neural and muscle cells (Rozario and DeSimone, 2010; Thorsteinsdóttir et al., 2011). The ECM is highly dynamic, as several of its components undergo post-translational modifications and are constantly remodeled by proteolytic enzymes, mostly metalloproteinases (Frantz et al., 2010). The macromolecules that compose the ECM can also be divided into two groups: proteoglycans, which are highly hydrophilic and fill most of the interstitial space within tissues; and glycoproteins, which are glycosylated fibrous proteins (Frantz et al., 2010; Hynes and Naba, 2012; Mouw et al., 2014). About 300 mammalian ECM macromolecules have been identified to date, including more than 40 collagen subunits, 30 different proteoglycans and 200 glycoproteins, constituting around 1.5% of the mammalian proteome (Hynes and Naba, 2012).

Proteoglycans are composed of proteins covalently linked to glycosaminoglycans (GAGs), which are polymers of repeating disaccharides with added carboxyl and sulfate groups (Frantz et al., 2010; Hynes and Naba, 2012; Mouw et al., 2014). These include hyaluronic acid, keratan sulfate, chondroitin/dermatan sulfate, and heparan sulfate. GAGs are negatively charged and thus allow the proteoglycans to sequester divalent cations and water, providing space-filling and lubrication functions to these proteins. Conversely, the fibrous glycoproteins of the matrix confer other functions to the ECM, including the modulation of ECM assembly and cell-adhesion. Around 200 different glycoproteins have been described, but the major ECM components that comprise this group are the collagens, laminins and fibronectin (Hynes and Naba, 2012).

Collagens are the most abundant proteins of the ECM, making up to 30% of the protein content of adult human bodies (Ricard-Blum, 2011). These proteins are composed of 3 polypeptide α-chains that can assemble as homo- or heterotrimers in a triple helical structure, and the combination of 49 distinct α-chain subunits gives rise to 28 different collagen molecules. These assemble into networks with tissue-specific organization, distribution and density, and while there is commonly a mix of different collagens in the matrix of a given tissue, one type of collagen usually predominates. Collagens can be associated with either interstitial matrices or basement membranes, and they provide structural strength to tissues such as tendons, skin, cartilage and bone (Gordon and Hahn, 2010; Hynes and Naba, 2012; Mouw et al., 2014; Myllyharju and Kivirikko, 2004; Ricard-Blum, 2011).

Laminins are cross-shaped heterotrimers composed of one α, one β, and one γ chain, and are found in basement membranes (Durbeej, 2010; Yurchenco, 2011). In fact, all basement membranes contain at least one laminin isoform, and their assembly is dependent on the binding of laminins to their cellular receptors – in the absence of laminin in both cell culture and mammalian embryos, no other basement membrane components are assembled, not even collagen IV, which is one of its major constituents. Laminin nomenclature reflects their chain composition. For example, laminin 111 is composed of α1, β1 and γ1 chains, while laminin 221 is formed by α2, β2 and γ1. In vertebrates, different genes encode for five α, three β, and three γ chains, and distinct combination of these subunits gives rise to about 20 different laminin proteins. These have several distinct and tissue-specific functions, including physiological regulation of muscle, nerves, skin, kidney, lung and vasculature (Colognato and Yurchenco, 2000; Durbeej, 2010; Hynes and Naba, 2012; Mouw et al., 2014; Wickstrom et al., 2011; Yurchenco, 2011).

Finally, one of the most ubiquitous fibrous ECM protein during vertebrate development is fibronectin, responsible for functions from separating the early tissues of the embryo to organizing the interstitial ECM and is essential for cell attachment and migration. A detailed description of fibronectin structure, assembly and function is provided in section 3, *Fibronectin*.

## 2.2 More than a supportive scaffold: general functions of the ECM

The most fundamental function of the ECM is to provide a physical barrier between different tissues, which is critical for regulating tissue interactions and for maintaining tissue identity and integrity. The ECM simultaneously provides glue and barrier functions, avoiding the intermingling of different cell populations, while allowing their interactions and movement relative to each other (Brown, 2011; Rozario and DeSimone, 2010). Indeed, most cells in suspension do not survive, attesting for the importance of cell-substrate anchorage (Discher et al., 2005). However, as Richard O. Hynes emphasized, the ECM is “not just pretty fibrils” (Hynes, 2009). Each tissue has specialized and unique ECM organization and composition, reflecting tissue-specific functions. Moreover, the constant assembly and remodeling of the ECM affects ECM composition, its three-dimensional organization and its physical properties, which in turn has profound effects on cellular behavior, including their polarity, survival, proliferation, and even cell fate decisions (see section 2.5, *Importance in development and disease* for more details).

Another elemental function of the ECM is to provide a substrate for cell migration, on which it has a profound effect by regulating cellular polarity and adhesion. Importantly, different ECM components have different effects on cell migration. For example, cranial neural crest cells migrate faster when cultured on laminin matrices compared to trunk neural crest cells, while both cell types migrate at the same speed on fibronectin substrates (Strachan and Condic, 2003). In addition, cell migration is often dependent on integrins, which are cellular ECM receptors (Huttenlocher and Horwitz, 2011; see section 2.3, *Integrin ECM-receptors and focal adhesions* for more details)

Finally, the ECM also functions as a reservoir of morphogens, paracrine factors that diffuse from their secreting source to establish differential concentration gradients and regulate the function and activity of their target cells (Hynes and Naba, 2012; Wickstrom et al., 2011). The ECM interacts with morphogen gradients in several ways, including by limiting their diffusion, supporting morphogen presentation to their target cells and promoting their binding to specific cell-surface receptors (see section 2.4, *Interaction with growth factors* for more details).

Interaction between the ECM and its cellular receptors also modulates cell behavior directly, affecting proliferation, survival, apoptosis and differentiation. For example, integrin function is necessary for cell survival in both the chick retina and neural crest (Leu et al., 2004; Testaz et al., 2001). Conversely, modulation of integrin adhesions can also result in anoikis, which is of particular importance when cells contact with an ECM environment where they are not supposed to reside (Gilmore, 2005). In some contexts, particular ECM components actively direct apoptosis upon cellular engagement (Marastoni et al., 2008). In other contexts, integrin-mediated adhesion increases mitogenic signaling, allowing cells to progress in mitosis (Danen and Yamada, 2001), Finally, de-adhesion from the basement membrane in the mouse cerebellum and epidermis promotes cellular differentiation in an integrin-dependent manner (Blaess et al., 2004; Watt, 2002).

Thus, in addition to providing structural support to cells and tissues, the ECM and its binding to cellular receptors has a myriad of other crucial roles, which include providing tensile strength, promote or restrict cell movement, and regulate cellular proliferation, survival and differentiation.

## 2.3. Integrin ECM-receptors and focal adhesions

The major cellular receptors for ECM components are integrins, which are heterodimeric transmembrane glycoproteins, with one α chain non-covalently associated with a β chain. In mammals, the combination of 18 α and 8 β chains gives rise to 24 different integrin heterodimers, which have distinct distribution and ligand affinities, and partially overlapping substrate specificity. Thus, the group of ECM components to which a given cell can bind is determined by its integrin expression profile. Integrins sense and respond to different extracellular cues, including the chemical, physical and topographical characteristics of the ECM.

Integrins connect (and "integrate", hence their name) the extracellular and intracellular dimensions of cells (Tamkun et al., 1986). While an integrin binds to ECM ligands in the extracellular space, it anchors the ECM to the intracellular cytoskeleton, providing a mechanical link between the two structures (Campbell and Humphries, 2011). However, the cytoplasmic tails of integrins neither bind to the actomyosin network of the cytoskeleton directly nor have enzymatic activity. Thus, integrins promote intracellular signaling and couple the ECM to the cytoskeleton by recruiting an outstanding number of cytoplasmic interactors to its β subunit, which together constitute the integrin adhesion, or adhesome. All combined, the integrin receptors connected to the ECM, the cytoplasmic adhesome where chemical and mechanical signals are processed, and the cytoskeleton, form a complex supramolecular structure: the focal adhesion, the mechanotransduction center of the cell (Fig. 1.15; Ringer et al., 2017). The dynamics and functions of focal adhesions affect virtually all aspects of cell behavior and their formation is force-dependent (Barczyk et al., 2010; Ringer et al., 2017; Wickstrom et al., 2011; Wolfenson et al., 2013). The morphology and composition of the focal adhesions in a given cell are dependent on its integrin expression signature, which defines how chemical and mechanical signals are processed. Indeed, similar integrins binding to the same ECM ligand promote the formation of adhesions with different molecular composition and signaling characteristics, which may in turn synergize (Ringer et al., 2017). Moreover, although focal adhesions are stable structures, they are in constant turnover and can undergo radical and rapid alterations (Wolfenson et al., 2013).

Here I will focus on the different layers of focal adhesions, namely the structure and function of integrins, the cytoplasmic associated proteins that constitute the integrin adhesome, and their linkage and communication with the cytoskeleton.

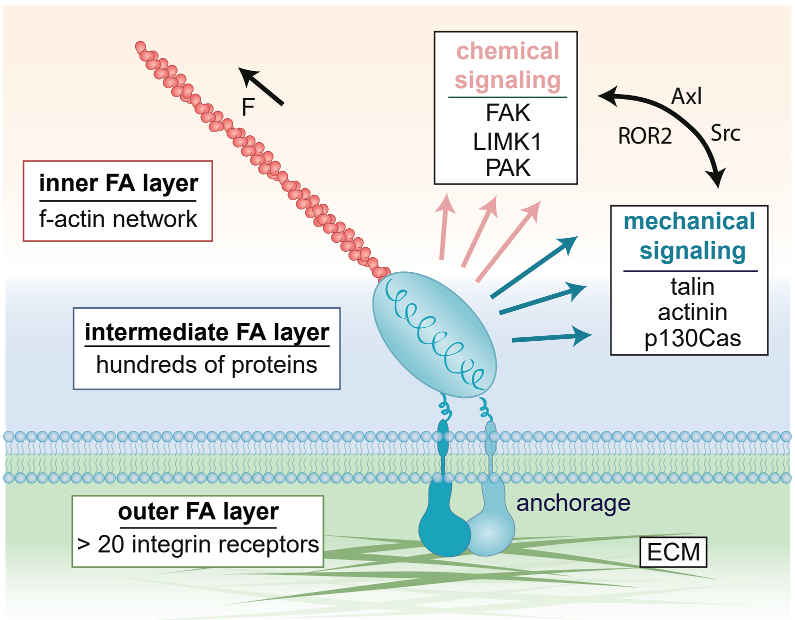


**Fig. 1.15. Structure of focal adhesions**. In the outer focal adhesion layer, integrins bind to components of the ECM. This recruits hundreds of adhesome proteins that compose the intermediate focal adhesion layer, where mechanical and chemical signals are transduced through the actions of proteins such as talin, α-actinin and p130Cas or FAK, LIMK1 or PAK, respectively. There is crosstalk between mechanical and chemical signaling in the focal adhesion, mediated through tyrosine kinases such as ROR2, Axl and Src. The inner-most layer of the focal adhesion is composed of the F-actin network, which also acts as a mechanosensitive module. FAK, focal adhesion kinase; LIMK – LIM kinase. PAK - p21-associated Kinase. Adapted from Ringer et al., 2017.

*2.3.1 Integrin structure*

Integrin subunits have short unstructured cytoplasmic tails of about 13-70 amino acids (except for β4) that connect to the cytoskeleton through multiple adaptor proteins; a single transmembrane helix domain of around 20 amino acids; and large 800-amino acid extracellular domains, which are responsible for binding to ECM ligands through specific peptide sequences or domains (Campbell and Humphries, 2011; Humphries et al., 2006; Hynes, 2002; Moser et al., 2009). Integrin subunits are only present on the cell surface when dimerized. The cell usually has an excess of β subunits in the cytoplasm, and the number of α subunits determines the total number of integrin dimers in the membrane, while the type of α subunits determines ligand specificity (Barczyk et al., 2010).

The extracellular portion of both α and β subunits have several distinct domains (Fig. 1.16 C). The α-chain contains seven-bladed β-propeller, a thigh, and two calf domains, which all support the integrin head (Barczyk et al., 2010; Campbell and Humphries, 2011; Moser et al., 2009). Some α subunits have a 200-amino acid I domain (or von Willebrand factor A domain), which, when present, is usually the ligand binding site of the integrin. Ligand binding is also allosterically affected by $Ca^{2+}$ binding to specific domains of the β-propeller (Barczyk et al., 2010). The ectodomain of the β subunits is composed of a plexin-sempahorin-integrin (PSI) domain, a hybrid domain, a βI domain and four cysteine-rich epidermal growth factor (EGF) repeats (Barczyk et al., 2010; Campbell and Humphries, 2011; Moser et al., 2009). In the absence of the I domain of the α-chain, the site for ligand binding is present in an intersection of the β-propeller of the α subunit and the βI domain of the β subunit.

Membrane-bound integrins occur in low, intermediate and high-affinity states. The low affinity, or inactive, state is characterized by a bent, closed conformation of the ectodomain (Fig. 1.16 A). This inactive conformation is maintained by the binding of the transmembrane and cytoplasmic portions of the α and β subunits. Indeed, mutations or deletions in the cytoplasmic or transmembrane domains of either subunit results in constitutive integrin activation. Upon binding of both talin and kindlin to the cytoplasmic tail of the β subunit, the association between α and β chains is lost and the ectodomain of the integrin shifts towards an extended, activated conformation, a process called inside-out activation or signalling (Fig. 1.16 B, C; Askari et al., 2009; Iwamoto and Calderwood, 2015; Wickstrom et al., 2011). Activation of integrins is required for their interaction with ECM components. Binding between activated integrins and their ligands increases the proximity of the ligands and leads to more integrin-ligand binding, which in turn promotes integrin clustering, enhancing the accumulation of integrin cytoplasmic associated molecules and downstream signal transduction. On the other hand, the binding of integrins to ECM components and their subsequent signal transduction is called outside-in signaling (Geiger et al., 2001; Miyamoto et al., 1996; Miyamoto et al., 1998).

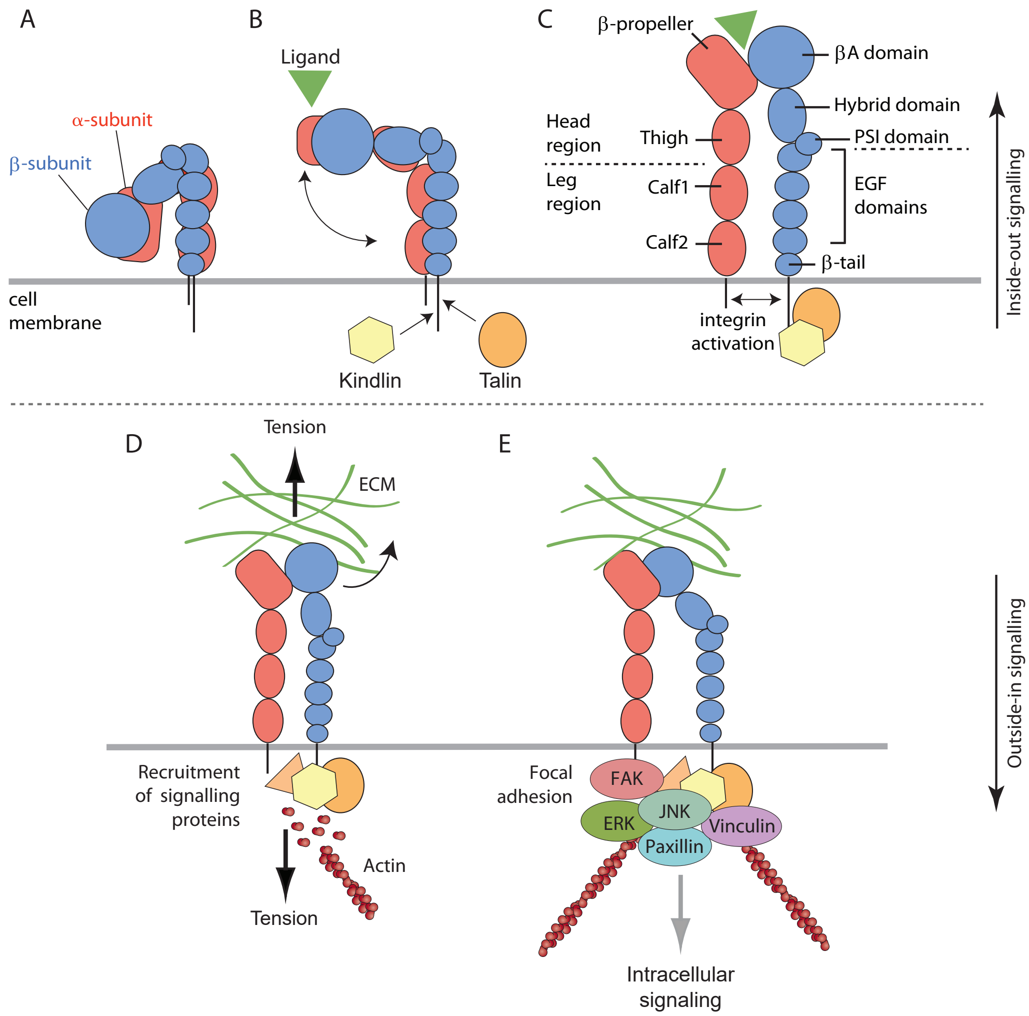


**Fig. 1.16. Integrin structure, activation and function. (A-C)** Inside-out signaling. (A) When inactive, integrins are in a bent conformation. (B) Upon talin and kindlin binding to the cytoplasmic tail of the β subunit, interaction with ligands in the extracellular space is permitted and the integrin shifts to a more extended conformation. (C) Further separation of the cytoplasmic tails of α and β subunits leads to full integrin extension and activation. **(D-E)** Outside-in signaling. (D) Binding of integrins to the ECM promotes the recruitment of adhesome proteins to the integrin cytoplasmic tails and polymerization of actin into f-actin. Both the ECM and the cytoskeleton exert tension to the integrin. (E) Further recruitment of adhesome components and binding of integrins to the cytoskeleton form the focal adhesion, which translates chemical and mechanical cues provided by the ECM intro intracellular signals. Adapted from Askari et al., 2009.

### *2.3.2 Integrin signaling and cytoplasmic associated molecules*

The integrin adhesion has two types of components, namely scaffolding molecules, which are adaptor and cytoskeletal proteins, and signaling or regulatory molecules, including kinases, phosphatases and GTPases, among others. Assembly of these multimolecular complexes is triggered upon outside-in signaling, when integrins bind to their extracellular ligands, which occurs after integrin activation (Fig. 1.16 D, E). This activates GTPases, actin nucleators and Non-muscle myosin II (NMMII), and further dissociates α and β transmembrane and intracellular domains, inducing conformational changes in the integrin ectodomain (Bharadwaj et al., 2017; Wolfenson et al., 2013). A remarkable number of components of integrin-mediated cell-ECM adhesions have been identified so far. To date, over 180 different proteins have been described, with more than 750 direct interactions reported (Wolfenson et al., 2013; Zaidel-Bar and Geiger, 2010). Each adhesome protein can interact on average with nine different partners, and distinct interactions affect both the structure and function of the adhesion site. Moreover, a given adhesome component may interact with different binding partners simultaneously, further increasing the complexity of the molecular interactions in integrin adhesions.

Despite the large number of molecules described to be associated with adhesomes, only a small subset of these proteins interacts directly with integrins (Wickstrom et al., 2011). Among these proteins, talin, kindlin and integrin linked kinase (ILK) are pivotal in regulating integrin signaling and their linkage to the cytoskeleton. Indeed, mouse embryos null for either one of these adhesome components fail to connect integrins to the actomyosin network, compromising integrin function and resulting in embryonic lethality (Monkley et al., 2000; Montanez et al., 2008; Sakai et al., 2003). Here I will provide a brief description of these key molecules and a few other important components of cell-ECM adhesions.

Talin and kindlin are cell-ECM adhesion components essential both for regulating integrin activation (inside-out signaling) and for intracellular signaling downstream of ECM-integrin binding (outside-in signaling; Wickstrom et al., 2011). In vertebrates, there are two and three isoforms of talin and kindlin, respectively. Talin occurs in the cytoplasm in a closed head-tail conformation, which is autoinhibitory. When activated, talin binds to the cytoplasmic NPxY motif of β integrin subunits via a structurally conserved phosphotyrosine binding (PTB) domain in its head region. This exposes cryptic domains in its tail responsible for binding actin and other scaffold proteins such as vinculin (Critchley and Gingras, 2008). It also breaks the covalent bond between α and β subunits, activating the integrin. Indeed, talin binding to the cytoplasmic domain of the β-chain is considered a final step in integrin activation (Ginsberg et al., 2005). However, the binding of kindlins to the distal NxxY motif of β integrin subunits is also pivotal for talin-mediated integrin activation (Moser et al., 2009), and the conformational shift between the inactivated to activated state of integrins does not occur in the absence of kindlins.

Kindlins also interact directly with ILK, which indirectly links kindlins to the cytoskeleton. ILK in turn binds to the β integrin cytoplasmic domain (Ginsberg et al., 2005; Moser et al., 2009) and has a role in promoting both inside-out and outside-in integrin signaling. Despite its name, ILK has no enzymatic activity, but is central to nucleate the PINCH-ILK-parvin (IPP) complex at integrin adhesion sites, which then recruits additional proteins and is implicated in the phosphorylation of many signaling pathway components, with effects in cell proliferation, survival and motility. In fact, in addition to binding directly to the β integrin subunit and the actin cytoskeleton, this complex interacts with many other molecules, including receptor tyrosine kinases, which are key components of the Akt

((Ak) Thymoma viral proto-oncogene), JNK (c-Jun N-terminal Kinase) and Wnt signaling pathways, thus modulating virtually all aspects of cellular function and behavior (Wickström et al., 2010; Wu, 2001).

Finally, another important component of the integrin adhesome is focal adhesion kinase (FAK), which is a scaffold protein that also directly interacts with β integrin subunits. FAK is a non-receptor tyrosine kinase frequently associated with other proteins of this family, namely Src. It is also a key regulator of the cytoskeleton and formation and turnover of integrin adhesions (Mitra et al., 2005; Schaller, 2010). Other important components of the adhesome are paxillin, which serves as a docking site for numerous cell-ECM adhesion components including FAK, ILK and regulators of the actin cytoskeleton; and vinculin, which is a cytoskeleton-associated molecule that binds to both talin and paxillin, further linking these adhesion components to the actin network.

In summary, an intracellular signal can induce integrin inside-out signaling, in which talin, kindlin, but also ILK and FAK participate in integrin activation and induce conformational changes in the protein. This promotes integrin-ligand binding in the extracellular space, leading to downstream integrin signaling, or outside-in signaling. This bidirectional signaling across the transmembrane domain of integrins induces and is dependent on the assembly of a high number of cytoplasmic effectors that associate with the β integrin subunit, each other, and the actomyosin cytoskeletal network. The outputs of integrin signaling are cell-specific and complex, and depend on the types of ECM ligands, integrin receptors, components of the integrin adhesion, and what other signaling pathways are active in the cell.

### *2.3.3 Focal adhesions and connection to the cytoskeleton*

The third component of focal adhesions is the actomyosin cytoskeleton, which links the cell membrane to the nucleus and is built from actin monomers that assemble into filamentous actin (F-actin) and from NMMII filaments, which, when activated, bind to F-actin (Eyckmans et al., 2011; Vicente-Manzanares et al., 2009). Upon outside-in integrin signaling, FAK, GTPases and others induce the remodeling of cytoskeletal components associated with focal adhesions, where actin is polymerized (Fig. 1.16; Dubash et al., 2009; Geiger and Yamada, 2011; Huveneers and Danen, 2009). Importantly, both the formation and function of focal adhesions are dependent on the activity of Rho-associated, coiled-coil containing protein kinases I and II (ROCKI/II) downstream of Rho GTPases, which phosphorylate the myosin light chain of NMMII, stimulating its contractility and, thus, promoting the contractility of the actomyosin network (Fig. 1.17, DeMali and Burridge, 2003; Huveneers and Danen, 2009; Kureishi et al., 1997; Yoneda et al., 2005). Myosin activity is further regulated by other kinases, including MLKC (myosin light chain kinase), MRCK (myotonic dystrophy kinase-related) and PAK (p21-associated kinase; Newell-Litwa et al., 2015).

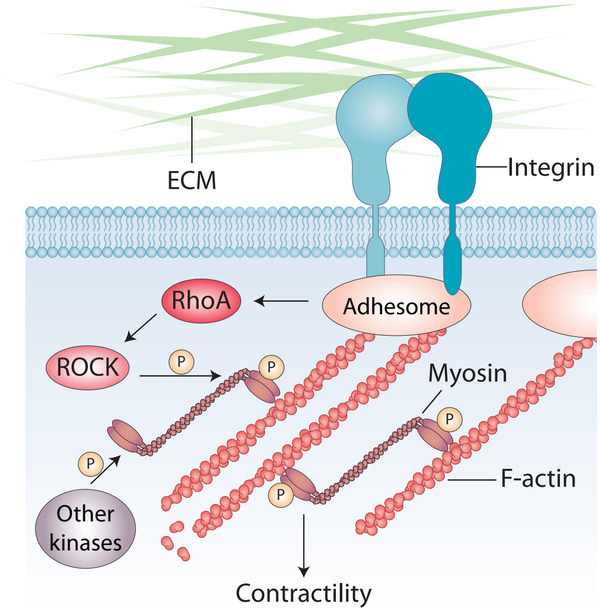


**Fig. 1.17. ROCK activity and actomyosin contractility.** Downstream of integrin signaling, effectors of RhoA GTPases ROCK I and II phosphorylate the myosin light chain of myosin, promoting its binding to filamentous actin and contractility of the actomyosin network.

As referred previously, the linkage of integrins to the actin cytoskeleton is accomplished by a subset of adhesome proteins. In addition to its role in mediating integrin activation, talin is a key player in establishing the integrin-cytoskeleton linkage, as it binds to F-actin both directly, and indirectly via interactions with vinculin (Schwartz, 2010). Linkage of integrins to the cytoskeleton is also mediated by other adhesome components, including filamin, which binds to the integrin β-chain and F-actin directly, and paxin, which binds to both paxillin and ILK (Zaidel-Bar and Geiger, 2010). Importantly, focal adhesion assembly occurs in a sequential manner, where certain proteins, namely talin, paxillin and vinculin, must first be present in the nascent adhesion for the recruitment of other proteins (Wolfenson et al., 2013).

The connection between the ECM and the cytoskeleton through integrins enables the focal adhesion to transduce mechanical signals (DuFort et al., 2011). Indeed, in addition to sensing the chemical properties of the ECM (i.e. composition), integrins are also sensitive to the physical properties of the ECM, such as stiffness, density, spacing and orientation. These in turn have profound effects on integrin adhesions, as adhesions associated with stiffer substrates are generally larger and more stable, and their composition, morphology and signaling are distinct from those formed on compliant substrates (Prager-Khoutorsky et al., 2011; Schlunck et al., 2008). This translates into changes in cytoskeletal organization and cell morphology, where cells contacting with stiffer environments are elongated and polarized, compared to cells attached to compliant surfaces which have a rounded morphology.

### *2.3.4 Transducing mechanical cues*

ECM-derived force promotes structural rearrangements of the ECM itself, force transmission through integrin adhesions and ultimately the remodeling of the cytoskeleton, affecting virtually every aspect of the intracellular structure (Eyckmans et al., 2011). However, the actomyosin network also enables the cell to exert force, with NMMII pulling on actin filaments to generate traction forces that in turn are transmitted to integrins and the ECM through the focal adhesions. Thus, integrins pulling the ECM and ECM signaling through integrins results in a mechanical feedback where both extracellular and intracellular derived forces are integrated by the focal-adhesion-ECM architecture (Eyckmans et al., 2011).

Mechanical cues promote many cellular events. Elevated tension through focal adhesions induces integrin clustering and conformational changes of adhesome proteins. In fact, talin, vinculin, and other integrin adhesion components are tension-sensitive molecules, and forces applied to these proteins expose additional cryptic binding sites, promoting the recruitment of more proteins to the adhesion site and stabilization of the focal adhesion structure. This strengthens integrin-ligand binding while also promoting specific phosphorylation events (Wolfenson et al., 2013).

Mechanotransduction pathways through integrins may also influence nuclear activity by phosphorylation of FAK, mitogen-activated protein kinase (MAPK) and extracellular signal-regulated kinase (ERK), resulting in the activation of signaling cascades that, among other effects, affect the activity of transcription factors and thus regulate gene expression (DuFort et al., 2011). Indeed, focal adhesions contain several signaling proteins, including FAK, MAPK, ERK and many more, which are involved in signaling pathways regulating virtually all aspects of cellular function, including proliferation, differentiation and migration. Thus, modulation of focal adhesions by mechanical and chemical cues, originating from both extracellular and intracellular sources, results in changes of multiple cellular responses. Activity of Rho GTPases, which modulate actin polymerization, is also stimulated by increased matrix stiffness, resulting in actin remodeling (Klein et al., 2009; Michael et al., 2009; Pasapera et al., 2010; Provenzano et al., 2009). These may also transmit mechanical signals to the nuclear lamin proteins, altering nuclear architecture and consequently modulating gene expression. Finally, a major consequence of mechanotransduction pathways at the cellular level is that cellular changes in mechanics can quickly spread from cells to tissues, organs or whole developing organisms (Harris et al., 1984).

## 2.4 Interaction with paracrine factors

In addition to receiving signals via chemical and mechanical cues provided by binding of integrins to the ECM, cells also receive instructive signals from soluble paracrine (or growth) factors, including those of Wnt, Hedgehog, Fgf and Transforming growth factor β

(Tgfβ) families. These morphogens are classically considered to have major instructive roles in regulating cell proliferation, specification and differentiation.

Importantly, while the ECM mediates cellular attachment and directly provides physical and chemical cues to cells, it also interacts with paracrine factors in diverse ways. It acts as a reservoir or sink for these factors, limiting their diffusion, restricting or promoting their presentation to target cells, or sequesters the morphogens for release at the appropriate time (Discher et al., 2009; Rozario and DeSimone, 2010). For example, heparan sulfate proteoglycans (HSPGs) are required for correct Fgf signaling during salivary gland branching in mammals (Makarenkova et al., 2009). The remodeling of the ECM by proteolytic enzymes such as MMPs (Matrix metalloproteases) or ADAM (A Disintegrin and Metalloproteinase) proteases promotes the release of ECM-bound paracrine factors. Alternatively, paracrine factors may be physically attached to specific ECM components which increases their affinity for their receptors and thus promotes signal transduction (Blaess et al., 2004; Brown, 2011; Rozario and DeSimone, 2010).

Conversely, ECM receptors may also directly interact with paracrine factor signaling. Syndecan, a non-integrin ECM receptor, binds to a variety of morphogens and may either increase ligand affinity of paracrine factor receptors or sequester the ligands near the membrane, increasing available ligand concentration (Carey, 1997; Oehrl and Panayotou, 2008). Similarly, αv-containing integrins have been shown to directly bind to, and activate, Tgfβ peptides *in vivo* (Aluwihare et al., 2009; Mu et al., 2002; Munger et al., 1999). Finally, integrins also feed into paracrine factor signaling pathways, because many kinases associated with the adhesome, such as MAPK and ERK, participate in numerous paracrine factor signaling cascades (Streuli, 2009).

Thus, either directly through attaching to cell surface receptors or indirectly by interacting with other factors, the ECM has many different roles and strongly influences cell function, therefore being a key regulator of cell physiology and homeostasis.

## 2.5 Importance in development and disease

Since the ECM and its downstream signaling through integrins has major impacts on cellular function and behavior, it is of no surprise that it plays pivotal roles during embryonic development. Indeed, development of Metazoans in general is dependent on integrins, as deficiencies in integrin subunits or function are embryonic lethal in flies, worms, zebrafish, frog, mouse, chick and sea urchins (Bouvard et al., 2001; Brown, 2000; Jülich et al., 2005; Marsden and Burke, 1998; Marsden and DeSimone, 2001; Rallis et al., 2010).

The production of ECM molecules and their assembly into matrices are both restricted and dynamic as development progresses, which contributes to anisotropies in the extracellular environment, allowing for cells to change shape, motility and polarity to generate all kinds of structures, from tubes, to cavities, to sheets and rods (Rozario and DeSimone, 2010).

Moreover, assembly and remodeling of the ECM often coincides with the initiation of a morphogenetic event, and accompanies the morphogenesis of emerging tissues, such as branched organs (Larsen et al., 2006). There are several reports on the importance of the ECM in embryo development. In the mammalian embryo, proteoglycans, GAGs, collagens and other ECM glycoproteins are crucial for normal development of for example mammary and salivary glands, gut, kidney and lung (Rozario and DeSimone, 2010). Collagen III, V, VII and XVII are all necessary for maintaining the integrity of the vasculature, eyes, connective tissue and skin (Andrikopoulos et al., 1995; Heinonen et al., 1999; Liu et al., 1997; Nishie et al., 2007). In *Xenopus*, syndecan-2 is involved in the specification of left-right asymmetry (Kramer and Yost, 2002).

Differentiation is also affected in several contexts when either integrin or ECM function are disrupted, including the differentiation of myoblasts into muscle (Menko and Boettiger, 1987), oligodendrocyte differentiation (Baron et al., 2005), and differentiation of mammary epithelial cells into milk-producing cells (Streuli et al., 1991). Altering the rigidity of the ECM also affects differentiation, with stiff matrices promoting osteogenic differentiation of mesenchymal stem cells, while soft matrices induce their differentiation into neurons (Engler et al., 2006). Migration is also perturbed in many contexts when integrin β1 activity is disrupted – neural crest cells derivatives such as Schwann cells are unable to migrate (Pietri et al., 2004), while primordial germ cells are specified correctly but fail to colonize the gonads (Anderson et al., 1999).

Many human diseases are caused by impaired cell-matrix interactions. This is particularly evident in tissues that are subjected to mechanical stress, such as skeletal muscle or skin. Causative mutations for either skin blistering diseases or some muscular dystrophies can occur at several levels of the integrin adhesion, including ECM components, integrin subunits, or cytoplasmic adhesion scaffold proteins associated with the adhesome. For example, different variants of epidermolysis bullosa, a skin blistering disease, are caused by mutations in at least 12 distinct genes, encoding basement membrane components and adhesion proteins (Wickstrom et al., 2011). Mutations in ECM components also underlie several different syndromes spanning all types of tissues and organs, such as atherosclerosis, osteoarthritis or myopia (Iozzo and Gubbiotti, 2018; Järveläinen, 2009). Finally, ECM remodulation is a crucial contributor to cancer progression. Many ECM components are known to promote tumor growth and vascularization, and in most cancers, a stiffer ECM resulting from increased ECM deposition results in more aggressive behaviors, including EMT and invasion (Frantz et al., 2010; Iozzo and Gubbiotti, 2018; Schwartz, 2010).

Thus, while the ECM has for decades been mostly regarded as a cellular packaging material with a largely passive role, new reports are constantly emerging proving the ECM to be a pivotal player in both embryo development and adult homeostasis.

# 3. Fibronectin

Fibronectin is a ubiquitous ECM glycoprotein exclusive to vertebrates, considered to have co-evolved together with the vertebrate cardiovascular system (Singh et al., 2010; Wickstrom et al., 2011). Fibronectin was first discovered in the 1940s (Edsall, 1978), isolated from blood at the time. This fibronectin form is soluble and is designated plasma fibronectin. A second major form, termed cellular fibronectin, assembles into insoluble fibrillar matrices in most tissues throughout all stages of life, from the earliest developmental stages to the adult organism (Singh et al., 2010). Cellular fibronectin is much more heterogenous than the plasma form, resulting from cell type- and species-specific splicing patterns of the single fibronectin-encoding gene, *Fn1* (Pankov and Yamada, 2002). Indeed, about 12 and 20 variants of the fibronectin protein have been discovered in mice and humans, respectively, all resulting from alternative splicing of the single ~8 kb mRNA (ffrench-Constant, 1995; Singh et al., 2010). Genome duplication in fish has resulted in the appearance of a second fibronectin gene, *fn1b* (Sun et al., 2005), but in the remaining vertebrate lineages, the *Fn1* gene appears to have remained functionally unchanged since it first appeared during vertebrate evolution, and it is essential for life (George et al., 1993; Hynes and Naba, 2012).

Research on fibronectin has mostly been conducted using cells *in vitro*, and although we already have decades worth of knowledge about its functions (as a reference, as of 2018, searching for “fibronectin review” in PubMed yields around 2600 results), many particularities of its *in vivo* roles remain elusive (Mao and Schwarzbauer, 2005; McDonald et al., 1987; Pankov and Yamada, 2002; Ruoslahti, 1988; Singh et al., 2010; Wierzbicka-Patynowski and Schwarzbauer, 2003). Accordingly, seminal findings about its biological relevance in several contexts, from development to disease, are still being accomplished to date (Zollinger and Smith, 2017). Here I will give an overview of cellular fibronectin structure, assembly and main functions, briefly addressing its many known roles during embryonic development, with a particular focus on somite formation.

## 3.1 Fibronectin structure

Fibronectin is a dimeric protein, with each subunit ranging from 230-270 kDa depending on the splice variant (Schwarzbauer and DeSimone, 2011). These subunits are connected through a pair of disulfide bonds at their C-termini and are composed of 3 different types of modules, types I, II and III (Fig. 1.18). Each fibronectin molecule includes 12 Type I repeats, which are about 40 amino acids long and have two disulfide bonds; 2 Type II repeats, comprising about 60 amino acids, also stabilized by two intrachain disulfide bonds; and 15 to 17 Type III repeats (Pankov and Yamada, 2002). These last repeats are composed of antiparallel β-sheets which have no disulfide bonds, allowing for conformational changes in response to chemical or mechanical stimuli (Schwarzbauer and DeSimone, 2011; Zollinger and Smith, 2017).

Of these Type III modules, two specific repeats encoded by single exons can be either included or excluded from the *Fn1* mRNA through alternative splicing (Fig. 1.18). These are the EIIIA, located between Types III11 and III12 repeats, and EIIIB, which is found between III7 and III8 repeats (Pankov and Yamada, 2002). These domains are usually absent from plasma fibronectin, while the cellular form may present none, one, or both (Schwarzbauer and DeSimone, 2011). Importantly, EIIIA and EIIIB are mostly included in cellular fibronectin during development, as their prevalence is low in adult tissues, and are also upregulated with injury, in tumors and in other pathologies (Schwarzbauer and DeSimone, 2011). Accordingly, double knockout of EIIIA and EIIIB results in embryonic lethality of mutant mice, which die from multiple vascular defects. While this suggests that EIIIA and EIIIB have a role during events of tissue remodeling, the specific *in vivo* functions of these domains are still unclear.

A third region located in a non-homologous stretch between III14 and III15, called V (variable in length), may also be subject to alternative splicing, being either completely or partially included (V+) or fully excluded (V0), depending on the tissue and the species considered. For example, humans have five different V variants resulting from total or partial inclusion or complete exclusion of this region; in contrast, in the chick, the V domain is never fully excluded, and fibronectin molecules have either a full-length V domain or a partial V domain restricted to its 5’ 44 amino acid segment, thus only generating two V variants (Pankov and Yamada, 2002; Schwarzbauer and DeSimone, 2011). This region is involved in fibronectin dimer secretion, as V0-V0 fibronectin homodimers are not secreted and are degraded intracellularly. The V region also binds to specific cell receptors, promoting cell adhesion (Schwarzbauer and DeSimone, 2011; Singh et al., 2010; see section 3.4, *Fibronectin interactions with integrins* for more details). While EIIIA and EIIIB are always absent from plasma fibronectin, most plasma fibronectin dimers are composed of one V0 subunit and one V+ subunit. Conversely, V0 subunits are generally absent from cellular fibronectin, most of which present either the full or partial V domain (Schwarzbauer and DeSimone, 2011).

Thus, alternative splicing of the single fibronectin-encoding gene produces a large amount of protein variants, which have different ligand-binding, solubility and cell-adhesive properties, and tissue-specificity.

Different domains on the fibronectin molecule are responsible for binding to a myriad of interactors, including cell-surface receptors, other ECM components such as collagens or heparin, and fibronectin itself (Fig. 1.18). This allows each fibronectin protein to simultaneously attach both to cells and the ECM (Singh et al., 2010).

There are two main regions of the fibronectin protein responsible for fibronectin self-association. There are several binding sites within the III15 domain, which interacts with the alternatively spliced domains and the amino-terminal domain. Here is the second and major fibronectin binding site, which includes the first 5 type I repeats (I1 to I5) and is essential for fibronectin matrix assembly. This domain also interacts with other ECM components, including heparin and tenascin (Schwarzbauer and DeSimone, 2011). Other

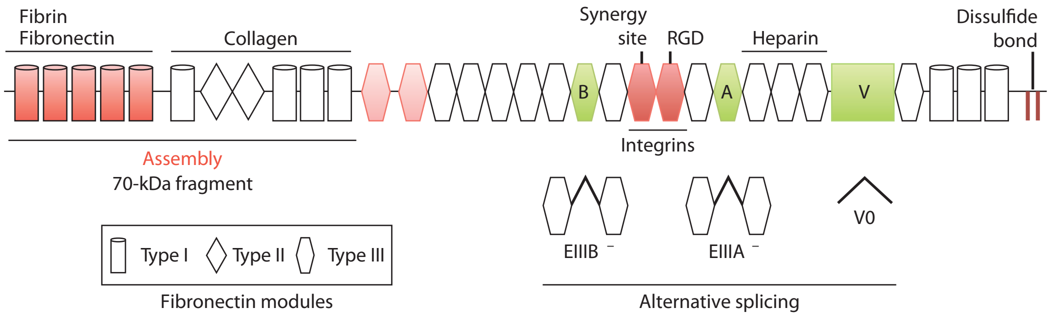


**Fig. 1.18. Structure of the fibronectin molecule**. Different types of repeats, alternatively spliced domains and different binding domains of the protein are represented. Adapted from Schwarzbauer and Desimone, 2011.

important fibronectin domains include the collagen-binding domain, which includes repeats I6-I9 and II1-II2, and a second heparin-binding domain that interacts with heparan sulfate proteoglycans, comprising III12-III14 (Pankov and Yamada, 2002). Fibronectin interacts with several cell-surface receptors through a myriad of domains (Pankov and Yamada, 2002). However, the major cell-binding domains are the Arginine-Glycine-Aspartic acid (RGD) sequence located in the III10 repeat and the adjacent synergy site on III9.

I will focus briefly on the N-terminal-most portion of the fibronectin molecule, which is the major domain responsible for fibril assembly, and the RGD sequence involved in cell binding, as they are common targets for disturbing the fibronectin ECM or its binding to integrins *in vivo*.

### *3.1.1 70kDa*

While the fibronectin molecule has several binding sites for fibronectin itself, the amino-terminal 70kDa domain comprising I1 to I9 and the two type II domains is essential for the assembly of the fibrillar matrix, also termed fibrillogenesis. When this portion is removed from the molecule, the resulting fibronectin lacking the 70kDa domain cannot co-assemble with full-length fibronectin fibrils (Ohashi et al., 2017; Schwarzbauer, 1991). Furthermore, when a fragment of the fibronectin molecule comprising this 70kDa N-terminal region is present in excess, it acts as a dominant negative, as it competes with the corresponding regions of the native fibrils and further assembly of the matrix is abolished (McKeown-Longo and Mosher, 1985). Fibronectin fibrillogenesis is also abrogated in the presence of just the first type I repeats of the fragment (I1 to I5, which correspond to the 27kDa N-terminal most domain of fibronectin), although to a lesser extent, suggesting that the full 70kDa N-terminal domain is needed for the correct building of fibronectin fibrils (McDonald et al., 1987; McKeown-Longo and Mosher, 1985). Importantly, the excess 70kDa fragment does not just inhibit *de novo* fibronectin matrix assembly, but also destabilizes already established fibronectin matrices around cells and in tissues (Sottile and Hocking, 2002).

*3.1.2. RGD*

The RGD sequence is present in many ECM components such as vitronectin and tenascin and is critical for their recognition and binding to about a third of the integrins described (Barczyk et al., 2010; Rozario and DeSimone, 2010). RGD binds to integrins through an interface between their two subunits, fitting into a cleft in the β-propeller of the α-chain and the βI-domain of the β-chain (Campbell and Humphries, 2011). Recognition of this sequence in ECM components depends on their 3D presentation, flanking residues and particular characteristics of the receptor (Pankov and Yamada, 2002).

In the fibronectin molecule, the RGD sequence in located within the III10 domain and is recognized by many different integrins, including α5β1, α3β1, α8β1, α9β1, all αv-containing integrins, and the platelet specific αIIβb3, suggesting that it has relevant roles across a broad range of different cell types (Campbell and Humphries, 2011; Zollinger and Smith, 2017). However, and although the fibronectin protein has many more domains recognized by cell-surface receptors, it only becomes prone to assemble into fibrils upon the interaction between its RGD sequence and α5β1 integrin (Aota et al., 1991; Aota et al., 1994; Pierschbacher et al., 1982). Importantly, this interaction is essential for development, as mouse embryos in which the RGD sequence of fibronectin was deleted die at mid-gestation (Takahashi et al., 2007). In a similar fashion to the action of excess 70kDa fragment in culture, the presence of excess RGD peptide in cell culture competes with the RGD-recognition pockets of integrin receptors, leading to impaired fibronectin fibrillogenesis (Pierschbacher and Ruoslahti, 1984).

## 3.2 Fibronectin matrix assembly

The fibronectin dimer is initially secreted in a folded, compact form (Potts and Campbell, 1994; Ruoslahti, 1988). However, the major functional form of fibronectin is in assembled multimeric fibrils. The assembly of this supramolecular structure is tightly regulated and depends on (1) the intracellular dimerization of fibronectin subunits, (2) localization of fibronectin to the cell-surface and binding to integrins, (3) cell-driven mechanical stretching of fibronectin through cytoskeleton-derived contractility (Ali and Hynes, 1977; Wu et al., 1995; Zollinger and Smith, 2017), and (4) interaction between different fibronectin molecules, which allow the association of dimers into fibrils (Mouw et al., 2014; Pankov and Yamada, 2002; Schwarzbauer and DeSimone, 2011; Singh et al., 2010).

The major integrin responsible for fibronectin matrix assembly is α5β1, which binds to the fibronectin protein through both the RGD sequence and the synergy site in the III9 domain (Singh et al., 2010). These two interactions are essential both for strong binding and fibril assembly (Friedland et al., 2009; Sechler et al., 1997). Binding to fibronectin promotes integrin activation and clustering, which in turn tethers fibronectin ligands to assembly initiation sites (Schwarzbauer and DeSimone, 2011). Integrin clustering also leads to the accumulation of cytoplasmic effectors, including FAK, paxillin and other adhesome components that activate actin polymerization into filaments and kinase-mediated signaling cascades (Geiger et al., 2001; Singh et al., 2010). FAK activity is of particular importance for fibronectin assembly, which does not occur in FAK-null mouse embryos (Ilić et al., 2004).

Once ligand-bound integrins are connected to the cytoskeleton, cytoskeletal contractility exerts force on the fibronectin dimer, which consequently unfolds and undergoes a conformational change from a compact soluble form towards an extended state (Fig. 1.19; Christopher et al., 1997; Dzamba et al., 1994; Gudzenko and Franz, 2015). This process is dependent on both ROCKI/II and NMMII activity and low Cdc42 levels (Kametaka et al., 2007; Torr et al., 2015). Extension of the fibronectin dimer exposes multiple cryptic fibronectin binding sites in the molecule (Baneyx et al., 2001; Lemmon and Weinberg, 2017; Zollinger and Smith, 2017) and stimulates the interaction between the 70kDa N-terminal domains of adjacent fibronectin dimers. These conformational changes and fibronectin-fibronectin contacts further promote the association of fibrils via non-covalent interactions (Chen and Mosher, 1996). With time, clustering of multiple fibronectin-bound integrins brings nascent fibronectin bundles together, which further interact and build a matrix

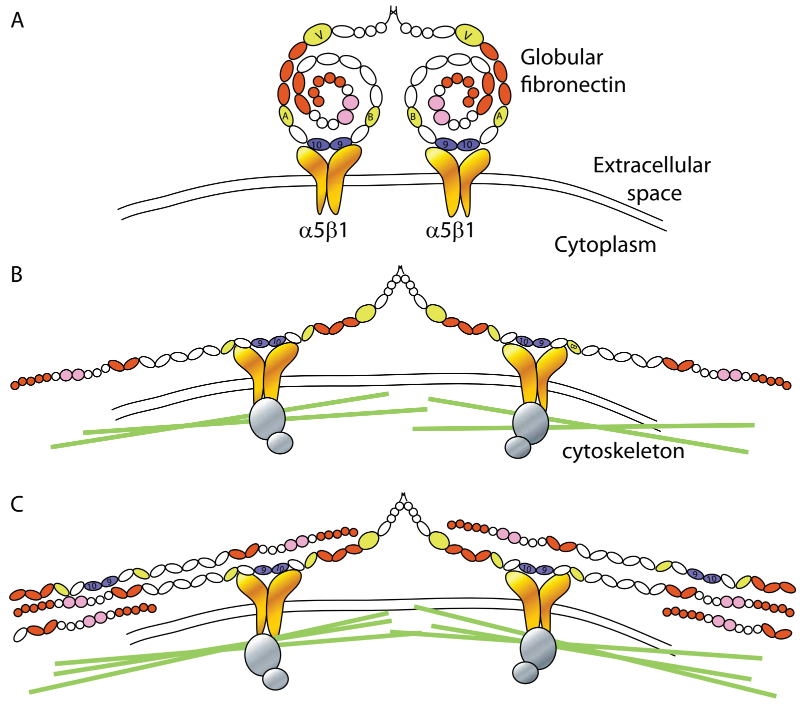


**Fig. 1.19. Fibronectin matrix assembly. (A-C)** Schematic representation of the steps of fibronectin matrix assembly. (A) The compact, globular fibronectin dimer is recognized by α5β1 integrin and binds to it. (B) This binding promotes integrin attachment to the cytoskeleton, which in turn exerts the traction force needed to extend the fibronectin dimer. (C) Extension of the fibronectin protein reveals cryptic binding sites for fibronectin self-association, promoting fibril assembly. Adapted from Mao and Schwarzbauer, 2005.

network that is irreversibly deoxycholate (DOC)-insoluble, a hallmark for mature fibronectin ECMs (McKeown-Longo and Mosher, 1983; Mouw et al., 2014). Further tension applied to fibronectin-α5β1 adhesions resulting both from cellular contractility and increase in ECM stiffness controls the maturation of these multiple integrin clusters, which coordinate cell shape and intracellular signaling with fibronectin ECM architecture (Schwarzbauer and DeSimone, 2011).

Importantly, this mature fibronectin ECM is not a static entity, as its integrity still depends on a basal level of assembly. Fibronectin-null cells are capable of assembling exogenous fibronectin into fibrils, but this matrix is lost both when cells are transferred to a fibronectin-deprived medium and when cultured in the presence of the 70kDa fragment (Sottile and Hocking, 2002; Wierzbicka-Patynowski and Schwarzbauer, 2003). Thus, fibronectin matrices are dynamic, being constantly remodeled and assembled.

Fibronectin fibrillogenesis is thus dependent on applied tension. While pulling on fibronectin dimers promotes the extension of the molecule and exposure of cryptic binding sites essential for matrix assembly, the rate of fibronectin fibrillogenesis is also influenced by matrix rigidity (Carraher and Schwarzbauer, 2013). Both the total number of α5β1-fibronectin adhesions and the number of tensioned α5β1-fibronectin bonds are increased on stiff substrates (Friedland et al., 2009). Stiff substrates also increase the rate of fibronectin assembly, which is delayed on soft substrates. Stiff substrates promote increased ability of cells to extend the fibronectin dimer, which can be stretched at least 5-6 fold (Carraher and Schwarzbauer, 2013; Little et al., 2008). This in turn exposes the cryptic binding sites of the molecule and stimulates the conversion of the fibronectin dimers into stable DOC-insoluble fibrils (Carraher and Schwarzbauer, 2013). High substrate stiffness also increases FAK downstream signaling (Carraher and Schwarzbauer, 2013). Hence, extension of the fibronectin protein in response to substrate stiffness levels may provide a mechanosensing mechanism that allows cells to probe the stiffness of their environment and adjust fibronectin assembly and cellular contractility accordingly (Carraher and Schwarzbauer, 2013). Indeed, high levels of mechanical strain applied to single fibronectin fibers promotes their extension and is sufficient to decrease both cell spreading and migration (Hubbard et al., 2016). Thus, outside-in signaling through fibronectin-α5β1 adhesions is regulated by matrix rigidity.

## 3.3 Fibronectin functions

Since it is one of the most ubiquitous components of the ECM, fibronectin is in place to mediate several cellular behaviors. Accordingly, fibronectin has been shown to be involved in cell-adhesion and migration (Frantz et al., 2010; Rozario and DeSimone, 2010), cellular growth and differentiation (Hynes, 1990), and has been implicated in cardiovascular diseases and in tumor metastasis, being an established marker of EMT in cancer (Frantz et al., 2010; Rozario and DeSimone, 2010).

Fibronectin directs the organization of the interstitial ECM (Frantz et al., 2010), particularly the deposition of collagen matrices (Sottile and Hocking, 2002; Zollinger and Smith, 2017), as collagens are not incorporated in the ECM in the absence of fibronectin. In fact, fibronectin fibrils act as a provisional scaffold that either potentiates and/or is required for subsequent deposition of many other ECM components, including for example tenascin, fibulin and fibrillin (Zollinger and Smith, 2017).

The fibronectin molecule also binds directly to a number of paracrine factors through its 12th–14th repeats, including several of the platelet-derived growth factor (PDGF)/vascular endothelial growth factor (VEGF) and Fgf families, and some members of the Tgfβ family (Zollinger and Smith, 2017). This results in enhanced growth factor activity, shown for example in VEGF-mediated differentiation and migration of endothelial progenitor cells, which are both increased in the presence of fibronectin (Wayner et al., 1989; Wijelath et al., 2004; Wijelath et al., 2006). Moreover, survival of cultured fibroblast is ensured by synergistic collaboration between fibronectin and fibronectin-bound Fgf. The latter must be in close proximity to the cell-binding domain of fibronectin, as presentation of both cell-binding and growth factor-binding domains to cell-surface receptors are essential for ensuring fibroblast survival (Lin et al., 2011).

Fibronectin is clearly crucial for embryogenesis, in particular for the formation of mesoderm, which is severely reduced in the *Fn1*-null embryo. Moreover, the fibronectin network has different topography, density and stiffness depending on the context, all of which influences cell function. Disentangling the intricacy of fibronectin functions in all its developmental contexts has thus been a challenge for researchers throughout the years, and new reports and methods are constantly emerging, slowly but steadily adding to our knowledge about this Jack-of-all-trades protein (see section 3.5, *Importance of fibronectin matrices in development*, for more details).

## 3.4 Fibronectin interaction with integrins

While integrin α5β1 is the major receptor for fibronectin, 11 other integrins bind to fibronectin in mammals, mostly by recognizing the RGD domain on III10, but other cell-binding domains can also be used (Pankov and Yamada, 2002). For example, EIIIA binds to α4- and α9-integrins, promoting cell adhesion (Liao et al., 2002). α4β1 is a non-RGD-binding integrin present in neural crest cells and cells of the cardiovascular and peripheral nervous system and interacts with fibronectin via its V region. This is also the case for α4β7, which is mainly present in hematopoietic cells. The distance between the RGD and the synergy site domains of fibronectin, which are altered upon conformational changes of the molecule, also define which integrins it can interact with (Zollinger and Smith, 2017). When fibronectin is still in a globular conformation, the RGD and synergy site are close, and both α5β1 and other RGD-recognizing integrins are able to bind to the molecule. Upon fibronectin extension, these two domains become further apart, and while α5β1-binding is reduced, other integrins such as αvβ3 that do not require the synergy site are still able to bind to fibronectin (Krammer et al., 2002).

Additional integrins other than α5β1 have also been shown to mediate fibronectin assembly *in vitro*, although appropriate external stimulation is usually required (Schwarzbauer and DeSimone, 2011; Wickstrom et al., 2011). These include integrins α4β1 (Sechler et al., 2000), αvβ1 (Yang and Hynes, 1996; Zhang et al., 1993), αvβ3 (Takahashi et al., 2007; Wennerberg et al., 1996; Wu et al., 1996), and αIIβb3 (Olorundare et al., 2001). However, only αv-containing integrins are able to assemble fibronectin fibrils in the absence of both α5β1 integrin and the RGD sequence of fibronectin *in vivo* (Singh et al., 2010; Takahashi et al., 2007). The topography and morphology of the resulting matrix is very different from that assembled by α5β1, with shorter and thicker, less profuse fibrils (Danen et al., 2002; Takahashi et al., 2007; Wennerberg et al., 1996). Intriguingly, a recent report showed that when both α5β1 and αv-class integrins are present, the latter outcompetes α5β1 and binds faster to fibronectin, preventing α5β1 from engaging with the molecule (Bharadwaj et al., 2017). Once engaged with fibronectin, αv integrins signal to α5β1 through RhoA/ROCK/NMMII to induce their clustering and promote additional adhesion sites to fibronectin, strengthening cellular adhesion. This is consistent with earlier reports showing that β1 integrins promote NMMII-independent formation of small peripheral adhesions, while αv integrins contribute to the formation of large focal adhesions (Schiller et al., 2013). Together, these two integrin classes cooperatively lead to full NMMII activation and enable cells to sense and respond to fibronectin rigidity, with α5β1 generating force on stiff fibronectin substrates and αv integrins mediating structural adaptations to these forces (Schiller et al., 2013).

Moreover, fibronectin binding to either α5β1 or αv-containing integrins transduces different signals. For example, upon attachment to fibronectin, RhoA activity decreases while that of Rac1 and Cdc42 increases, allowing for cell spreading. However, as soon as cells are spread, α5β1 (but not αv) bound to fibronectin increases RhoA activity and induces stress fiber formation, promoting the development of mature α5β1-fibronectin adhesion sites crucial for fibronectin assembly (Danen et al., 2002). This distinct signaling transduction by α5β1 versus αvβ3 engagement further influences cell behavior, promoting either proliferation or differentiation (García et al., 1999; Keselowsky et al., 2003; Keselowsky et al., 2005). Thus, α5β1 and αv-class integrins have distinct and cooperative roles in fibronectin assembly, adhesion and signal transduction.

Even though fibronectin binds to several integrins, α5β1 integrin remains the primary fibronectin receptor responsible for its assembly and signal transduction. In contrast to the other integrins, α5β1 recognizes and binds to the synergy site, which promotes downstream activation of FAK and is essential for assembly (Friedland et al., 2009; Ilić et al., 2004). Moreover, α5β1 affinity to the RGD sequence on fibronectin is much greater than any other integrin and α5β1 even binds efficiently to plasma fibronectin, which can be assembled into fibrils during for example wound healing (Huveneers et al., 2008).

## 3.5 Importance of fibronectin matrices in development

Fibronectin is widely expressed by multiple cell types during development, and its assembly is often concomitant with highly dynamic cell and tissue rearrangements. Many studies of the role of fibronectin matrices during developmental processes point to the importance of its correct assembly in both space and time, promoting tissue morphogenesis and differentiation (Schwarzbauer and DeSimone, 2011). Thus, it is of no surprise that the null mutation for *Fn1* is embryonic lethal (E10.5), with several striking mesodermal defects including deficient morphogenesis of the notochord, somites, heart and vasculature (George et al., 1993; Georges-Labouesse et al., 1996). α5-null mutation is also embryonic lethal, but it is milder and the embryo dies later (at around E9.5–E10; Yang et al., 1993). However, deleting both α5 or αv integrins results in increased embryonic defects at earlier stages, and earlier embryonic death (E7.5). Thus, both fibronectin and its major receptors are crucial for normal development (Yang et al., 1999).

The importance of fibronectin in development is apparent in events as early as gastrulation. Fibronectin is assembled between the epiblast and hypoblast in the chick (Krotoski et al., 1986) and along the *Xenopus* blastocoel roof (Lee et al., 1984) prior to gastrulation movements, which together with the mesodermal defects of *Fn1*-null mice suggest a role for fibronectin in providing the substrate for mesodermal migration during gastrulation. In the *Xenopus* embryo, fibronectin assembly is both coincident and required for all of the morphogenetic cellular movements during gastrulation, including epiboly, radial and mediolateral intercalation, convergent extension and mesendoderm migration (Davidson et al., 2004; Davidson et al., 2008). Similarly, during primitive streak formation in chick embryos, cell movements in the epiblast are coincident with extensive fibronectin fibril displacement (Czirok et al., 2006; Zamir et al., 2006). Additionally, fibronectin-integrin interactions are also required for the correct orientation of cellular divisions of blastocoel roof cells in the *Xenopus*, with the Wnt/Planar Cell Polarity (PCP) pathway controlling fibronectin assembly (Dzamba et al., 2009; Marsden and DeSimone, 2001).

In addition to mesodermal migration during gastrulation, fibronectin also directs the migration of the avian and amphibian neural crest (Duband and Thiery, 1982; Perris and Perissinotto, 2000; Rovasio et al., 1983), primordial germ cells in both frogs (Heasman et al., 1981) and mice (Ffrench-Constant et al., 1991), and the correct migration of cardiac precursors to the midline of chick and zebrafish embryos (Linask et al., 2005; Trinh and

Stainier, 2004). In the latter case, while cardiac precursors do not require fibronectin assembly for the migration process *per se*, it is crucial for their timely and directional migration to the midline and also for correct polarization and specification of the migrating myocardial precursors (Matsui et al., 2007; Trinh and Stainier, 2004). In the absence of fibronectin assembly in the midline, zebrafish embryos present a *cardia bifida* phenotype, which can be rescued by injecting exogenous fibronectin in the midline (Matsui et al., 2007). Proliferation of cardiac precursors and correct *Fgf8* expression are also compromised in *Fn1*-null mouse embryos (Mittal et al., 2013). Thus, fibronectin ECM is crucial for normal heart development, as it regulates proliferation, specification and migration of myocardial precursors in both mouse and zebrafish embryos.

Recent reports also implicate fibronectin- α5β1 interactions in the differentiation of neural crest cells into vascular smooth muscle cells. Fibronectin promotes their differentiation both through binding to α5β1 and interacting with Tgfβ. Importantly, Notch activation, which is required for differentiation of vascular smooth muscle cells, is only activated in cells expressing both fibronectin and α5β1 integrin, suggesting that fibronectin is important for inducing an autocrine signaling response by these cells (Turner et al., 2015; Vega and Schwarzbauer, 2016; Wang and Astrof, 2015).

Localized fibronectin assembly is also required during branching morphogenesis of several organs, including the lung, kidney and mammary and salivary glands (De Langhe et al., 2005; Fata et al., 2007; Larsen et al., 2006; Sakai et al., 2003). Blocking fibronectin assembly or synthesis abolishes cleft formation, while supplementation with exogenous fibronectin promotes branch formation.

## 3.6 Importance of fibronectin in somitogenesis

Another morphogenetic event where fibronectin plays a preponderant role is in somitogenesis. Almost 35 years ago, fibronectin was described to be present in the paraxial mesoderm of chick embryos, surrounding the PSM and somites (Duband et al., 1987; Krotoski et al., 1986; Lash et al., 1985; Newgreen and Thiery, 1980; Ostrovsky et al., 1983; Thiery et al., 1982). The *Fn1*-null mouse mutant confirmed its importance in somite formation, as these embryos form some paraxial mesoderm, but it does not segment (George et al., 1993; Georges-Labouesse et al., 1996). Importantly, this phenotype was also shared by FAK- (Furuta et al., 1995; Ilić et al., 1995) and Paxillin-null (Hagel et al., 2002) mouse embryos. However, while deletion of the gene encoding for α5 integrin subunit, *Itga5*, was also found to be an early embryonic lethal, these embryos still assembled fibronectin and formed the 7 most anterior somites (Goh et al., 1997; Yang et al., 1993). Conversely, double knockout of both *Itga5* and *Itgav*, which encodes for αv, completely abolished both fibronectin assembly and somite formation (Yang et al., 1999). Deficient fibronectin-integrin interactions in the PSM also leads to loss of somitic boundaries in zebrafish (Jülich et al., 2005; Koshida et al., 2005), and loss of function of either α5 or β1 integrin subunits disrupts somite formation in *Xenopus* embryos (Kragtorp and Miller, 2007; Marsden and DeSimone, 2001). Thus, fibronectin-integrin interactions are required for paraxial mesoderm segmentation in frogs, zebrafish and mouse embryos.

As described in section 1.3.1, *Boundary formation*, a feedback system between decreased N-cadherin mediated cell adhesion, Eph/Ephrin signaling and integrin α5β1 activation assures fibronectin assembly in the nascent somitic clefts, essential for cleft stabilization (Jülich et al., 2015; McMillen et al., 2016). That the fibronectin ECM is required in both the initiation and stabilization of somitic cleft morphogenesis was clearly shown in studies where chick PSMs were cultured *in vitro*. Indeed, cultured PSMs isolated from chick embryos still show segmented expression of *Hairy1*, *Dll1* and *Notch1* (Palmeirim et al., 1997; Palmeirim et al., 1998), but morphological somite formation was only possible in the presence of the ectoderm (Palmeirim et al., 1998). Rifes et al (2007) showed that the absence of ectoderm may be partially compensated for by supplementing isolated PSMs with exogenous fibronectin (Rifes et al., 2007). Moreover, PSMs isolated with an enzyme treatment that maintains its original fibronectin matrix can form morphologically distinct somites in the absence of the ectoderm. Thus, fibronectin protein provided by the overlying ectoderm is crucial not only for maintaining somitic boundaries as soon as they are formed, but also for mediating somite epithelialization. Indeed, mice null for α5 integrin exhibit a somitic phenotype that resembles that of Paraxis-null embryos, with distinctive (albeit deficient) somite borders but no epithelialized segments (Yang et al., 1999). In this context, the fibronectin assembled by the PSM, which does not produce its own fibronectin, is provided by the overlying, *Fn1*-expressing ectoderm (Rifes et al., 2007). The reception and building of fibronectin matrix by PSM cells is subsequently required for normal somite morphogenesis. This is reminiscent of what has been recently observed in the chick embryo, where fibronectin produced by the avian Wolffian duct (intermediate mesoderm) is transferred to the adjacent coelomic epithelium (lateral mesoderm), promoting its maturation (Yoshino et al., 2014). This raises the interesting possibility that the fibronectin protein provided by the ectoderm acts in a paracrine fashion to mediate PSM fibronectin assembly and subsequent cellular behaviors.

In addition, recent studies suggest that the fibronectin substrate may be doing more than just promoting somitic boundary morphogenesis and somite epithelialization. Interfering with β1-integrin in chick embryos though β1-targeting morpholinos leads to deficient Wnt and Notch signaling in the PSM, with consequences on normal positioning of *Meso1* (Rallis et al., 2010). In an additional report, isolated mouse PSM cells and PSM explants showed slower *Lnfg* oscillations when cultured on a fibronectin substrate compared to those cultured on BSA, concomitant with nuclear displacement of Yes-associated protein (YAP), a transcription factor implicated in mechanotransduction signaling (Hubaud et al., 2017).

These studies suggest that fibronectin may also be regulating segmentation clock dynamics, possibly through both chemical and mechanical cues, and may be a missing link in the coordination of segmentation clock oscillations and timely somite morphogenesis.

## II. Aims and Objectives

The above Introduction highlighted the complexity of paraxial mesoderm development, particularly the periodic formation of epithelial somites from the mesenchymal PSM. A considerable amount of knowledge about the mechanisms regulating this complex morphogenetic event has been unveiled since the first discovery of the segmentation clock (Palmeirim et al., 1997). However, much remains to be understood, including how segmentation clock oscillations are stabilized in the anterior PSM, and how the periodicity of these oscillations is translated into the periodic morphological formation of the segment boundaries. Furthermore, while fibronectin has long been implicated in the morphological aspects of somitogenesis, recent reports suggest that many intricacies of its role during somite formation, particularly regarding the control of its periodicity, still need to be dissected out. In addition, the role of fibronectin matrix mechanics *in vivo* is still mostly unknown, as studies are usually conducted *in vitro* with either absence or presence of the protein. This approach masks the effects of matrix topology, density and stiffness, mechanical cues that are as instructive as the presence of the molecule *per se* on cellular behavior. Thus, the aim of this thesis was to address the role of the fibronectin matrix during paraxial mesoderm development *in vivo*, with particular focus on its role in PSM maturation and subsequent somite morphogenesis.

In **Chapter 2**, we asked whether more contexts where fibronectin assembly is a paracrine event occur during early development of both chick and mouse embryos. We addressed which tissues express *Fn1* and thus produce the protein and which tissues assemble fibronectin intro a fibrillar matrix. We also assessed the mRNA expression and protein distribution of integrins α5 and αv from gastrulation (HH4 in the chick, E7.5 in the mouse) through organogenesis stages (E4 in the chick, E11.5 in the mouse). We found that during paraxial mesoderm development, fibronectin production and assembly is highly dynamic and correlates with exquisite morphogenetic events. Moreover, fibronectin matrix assembly can be autocrine, as in the case of paraxial mesoderm precursors within the primitive streak and the sclerotome undergoing EMT, while being paracrine in gastrulating PSM precursors and the developing PSM. Moreover, we put into evidence that a paracrine system of fibronectin matrix assembly is common in several other contexts during the stages under study, and stress that fibronectin assembly is a cell-cell communication event that can be as significant as morphogen signaling. The research presented in this chapter was published in *Developmental Dynamics* (2016) 245, 520–535.

In **Chapter 3**, we address the role of fibronectin during somite formation in chicken embryos, while also analyzing its potential role in regulating the segmentation clock. Our results show that both the binding of fibronectin to its receptors and an intact fibronectin matrix are required for correct segmentation clock dynamics and subsequent segment boundary morphogenesis. Our results further establish fibronectin as crucial player regulating somitogenesis and point to a novel role of this matrix in coupling segmentation clock oscillations with timely somite morphogenesis. In addition, we also implicate its mechanotransduction pathway in both segmentation clock dynamics and somite formation, adding to the increasing body of evidence arguing for a previously unappreciated instructive role of mechanical cues during somitogenesis. The work described in this chapter is included in a manuscript still in preparation.

In **Chapter 4**, we build on the knowledge that the epithelial somite is surrounded by a dense fibronectin matrix and ask whether this fibronectin matrix plays a role in somite maturation. We describe a previously unknown interaction between the fibronectin matrix assembled in the PSM and somites and the Shh signaling pathway. We found that an intact fibronectin matrix is required for correct Shh signaling in the ventral somite. Conversely, Shh negatively regulates *Fn1* expression in the ventral somite, possibly to maintain its production at lower levels before the correct timing for sclerotomal dispersal, when *Fn1* is strongly upregulated in this tissue (Chapter 2). Thus, the cross-regulation and cooperation of the fibronectin matrix and the Shh signaling pathway in the PSM and somites orchestrate timely somite patterning, morphogenesis and differentiation.

In the final chapter, **Chapter 5**, the main findings described in the previous chapters are discussed and integrated with the existing literature. We place a particular focus on the establishment of fibronectin as an active player regulating paraxial mesoderm development, and the recent advances in studying the role of mechanical cues during this process *in vivo*.

# III. References

**Abu-Abed, S., Dollé, P., Metzger, D., Beckett, B., Chambon, P. and Petkovich, M.** (2001). The retinoic acid-metabolizing enzyme, CYP26A1, is essential for normal hindbrain patterning, vertebral identity, and development of posterior structures. *Genes Dev.* **15**, 226–40.

**Alexander, T., Nolte, C. and Krumlauf, R.** (2009). Hox genes and segmentation of the hindbrain and axial skeleton. *Annu. Rev. Cell Dev. Biol.* **25**, 431–56.

**Ali, I. U. and Hynes, R. O.** (1977). Effects of cytochalasin B and colchicine on attachment of a major surface protein of fibroblasts. *Biochim. Biophys. Acta* **471**, 16–24.

**Aluwihare, P., Mu, Z., Zhao, Z., Yu, D., Weinreb, P. H., Horan, G. S., Violette, S. M. and Munger, J. S.** (2009). Mice that lack activity of alphavbeta6- and alphavbeta8-integrins reproduce the abnormalities of Tgfb1- and Tgfb3-null mice. *J. Cell Sci.* **122**, 227–32.

**Anderson, R., Fässler, R., Georges-Labouesse, E., Hynes, R. O., Bader, B. L., Kreidberg, J. A., Schaible, K., Heasman, J. and Wylie, C.** (1999). Mouse primordial germ cells lacking beta1 integrins enter the germline but fail to migrate normally to the gonads. *Development* **126**, 1655–64.

**Andrade, R. P., Palmeirim, I. and Bajanca, F.** (2007). Molecular clocks underlying vertebrate embryo segmentation: A 10-year-old hairy-go-round. *Birth Defects Res. Part C - Embryo Today Rev.* **81**, 65–83.

**Andrikopoulos, K., Liu, X., Keene, D. R., Jaenisch, R. and Ramirez, F.** (1995). Targeted mutation in the col5a2 gene reveals a regulatory role for type V collagen during matrix assembly. *Nat. Genet.* **9**, 31–6.

**Aota, S., Nagai, T. and Yamada, K. M.** (1991). Characterization of regions of fibronectin besides the arginine-glycine-aspartic acid sequence required for adhesive function of the cell-binding domain using site-directed mutagenesis. *J. Biol. Chem.* **266**, 15938–43.

**Aota, S., Nomizu, M. and Yamada, K. M.** (1994). The short amino acid sequence Pro-His-Ser-Arg-Asn in human fibronectin enhances cell-adhesive function. *J. Biol. Chem.* **269**, 24756–61.

**Aoyama, H. and Asamoto, K.** (1988). Determination of somite cells: independence of cell differentiation and morphogenesis. *Development* **104**, 15–28.

**Aoyama, H. and Asamoto, K.** (2000). The developmental fate of the rostral/caudal half of a somite for vertebra and rib formation: Experimental confirmation of the resegmentation theory using chick-quail chimeras. *Mech. Dev.* **99**, 71–82.

**Askari, J. a, Buckley, P. a, Mould, a P. and Humphries, M. J.** (2009). Linking integrin conformation to function. *J. Cell Sci.* **122**, 165–170.

**Aulehla, A. and Pourquié, O.** (2010). Signaling gradients during paraxial mesoderm development. *Cold Spring Harb. Perspect. Biol.* **2**, 1–17.

**Aulehla, A., Wehrle, C., Brand-Saberi, B., Kemler, R., Gossler, A., Kanzler, B. and Herrmann, B. G.** (2003). Wnt3a plays a major role in the segmentation clock controlling somitogenesis. *Dev. Cell* **4**, 395–406.

**Aulehla, A., Wiegraebe, W., Baubet, V., Wahl, M. B., Deng, C., Taketo, M., Lewandoski, M. and Pourquié, O.** (2008). A β-catenin gradient links the clock and wavefront systems in mouse embryo segmentation. *Nat. Cell Biol.* **10**, 186–193.

**Babiuk, R. P., Zhang, W., Clugston, R., Allan, D. W. and Greer, J. J.** (2003). Embryological origins and development of the rat diaphragm. *J. Comp. Neurol.* **455**, 477–87.

**Bailey, C. and Dale, K.** (2015). Somitogenesis in vertebrate development. In *eLS*, pp. 1–15. Chichester, UK: John Wiley & Sons, Ltd.

**Balling, R., Helwig, U., Nadeau, J., Neubüser, a, Schmahl, W. and Imai, K.** (1996). Pax genes and skeletal development. *Ann. N. Y. Acad. Sci.* **785**, 27–33.

**Baneyx, G., Baugh, L. and Vogel, V.** (2001). Coexisting conformations of fibronectin in cell culture imaged using fluorescence resonance energy transfer. *Proc. Natl. Acad. Sci. U. S. A.* **98**, 14464–8.

**Barczyk, M., Carracedo, S. and Gullberg, D.** (2010). Integrins. *Cell Tissue Res.* **339**, 269–280.

**Barnes, G. L., Alexander, P. G., Hsu, C. W., Mariani, B. D. and Tuan, R. S.** (1997). Cloning and characterization of chicken Paraxis: a regulator of paraxial mesoderm development and somite formation. *Dev. Biol.* **189**, 95–111.

**Baron, W., Colognato, H., Ffrench-Constant, C. and Ffrench-Constant, C.** (2005). Integrin-growth factor interactions as regulators of oligodendroglial development and function. *Glia* **49**, 467–79.

**Barrios, A., Poole, R. J., Durbin, L., Brennan, C., Holder, N. and Wilson, S. W.** (2003). Eph/Ephrin signaling regulates the mesenchymal-to-epithelial transition of the paraxial mesoderm during somite morphogenesis. *Curr. Biol.* **13**, 1571–82.

**Bénazéraf, B., Francois, P., Baker, R. E., Denans, N., Little, C. D. and Pourquié, O.** (2010). A random cell motility gradient downstream of FGF controls elongation of an amniote embryo. *Nature* **466**, 248–252.

**Bessho, Y., Sakata, R., Komatsu, S., Shiota, K., Yamada, S. and Kageyama, R.** (2001). Dynamic expression and essential functions of Hes7 in somite segmentation. *Genes Dev.* **15**, 2642–7.

**Bharadwaj, M., Strohmeyer, N., Colo, G. P., Helenius, J., Beerenwinkel, N., Schiller, H. B., Fässler, R. and Müller, D. J.** (2017). αV-class integrins exert dual roles on α5β1 integrins to strengthen adhesion to fibronectin. *Nat. Commun.* **8**, 14348.

**Blaess, S., Graus-Porta, D., Belvindrah, R., Radakovits, R., Pons, S., Littlewood-Evans, A., Senften, M., Guo, H., Li, Y., Miner, J. H., et al.** (2004). Beta1-integrins are critical for cerebellar granule cell precursor proliferation. *J. Neurosci.* **24**, 3402–3412.

**Borggrefe, T. and Oswald, F.** (2009). The Notch signaling pathway: Transcriptional regulation at Notch target genes. *Cell. Mol. Life Sci.* **66**, 1631–1646.

**Borycki, a G., Strunk, K. E., Savary, R. and Emerson, C. P.** (1997). Distinct signal/response mechanisms regulate pax1 and QmyoD activation in sclerotomal and myotomal lineages of quail somites. *Dev. Biol.* **185**, 185–200.

**Bothe, I., Ahmed, M. U., Winterbottom, F. L., von Scheven, G. and Dietrich, S.** (2007). Extrinsic versus intrinsic cues in avian paraxial mesoderm patterning and differentiation. *Dev. Dyn.* **236**, 2397–2409.

**Bouvard, D., Brakebusch, C., Gustafsson, E., Aszódi, A., Bengtsson, T., Berna, A. and Fässler, R.** (2001). Functional consequences of integrin gene mutations in mice. *Circ. Res.* **89**, 211–23.

**Brand-Saberi, B., Wilting, J., Ebensperger, C. and Christ, B.** (1996). The formation of somite compartments in the avian embryo. *Int. J. Dev. Biol.* **40**, 411–20.

**Brent, A. E., Schweitzer, R. and Tabin, C. J.** (2003). A somitic compartment of tendon progenitors. *Cell* **113**, 235–248.

**Brown, N. H.** (2000). Cell-cell adhesion via the ECM: integrin genetics in fly and worm. *Matrix Biol.* **19**, 191–201.

**Brown, N. H.** (2011). Extracellular matrix in development: insights from mechanisms conserved between invertebrates and vertebrates. *Cold Spring Harb. Perspect. Biol.* **3**, a005082–a005082.

**Buchberger, A., Seidl, K., Klein, C., Eberhardt, H. and Arnold, H. H.** (1998). cMeso-1, a novel bHLH transcription factor, is involved in somite formation in chicken embryos. *Dev. Biol.* **199**, 201–15.

**Buckingham, M. and Relaix, F.** (2007). The role of Pax genes in the development of tissues and organs: Pax3 and Pax7 regulate muscle progenitor cell functions. *Annu. Rev. Cell Dev. Biol.* **23**, 645–673.

**Buckingham, M. and Rigby, P. W. J.** (2014). Gene regulatory networks and transcriptional mechanisms that control myogenesis. *Dev. Cell* **28**, 225–238.

**Burgess, R., Rawls, A., Brown, D., Bradley, A. and Olson, E. N.** (1996). Requirement of the paraxis gene for somite formation and musculoskeletal patterning. *Nature* **384**, 570–573.

**Buttitta, L., Mo, R., Hui, C.-C. and Fan, C.-M.** (2003). Interplays of Gli2 and Gli3 and their requirement in mediating Shh-dependent sclerotome induction. *Development* **130**, 6233–6243.

**Cairns, D. M., Sato, M. E., Lee, P. G., Lassar, A. B. and Zeng, L.** (2008). A gradient of Shh establishes mutually repressing somitic cell fates induced by Nkx3.2 and Pax3. *Dev. Biol.* **323**, 152–65.

**Campbell, I. D. and Humphries, M. J.** (2011). Integrin structure, activation, and interactions. *Cold Spring Harb. Perspect. Biol.* **3**, a004994–a004994.

**Carey, D. J.** (1997). Syndecans: multifunctional cell-surface co-receptors. *Biochem. J.* **327 ( Pt 1**, 1–16.

**Carpio, R., Honoré, S. M., Araya, C. and Mayor, R.** (2004). Xenopus paraxis homologue shows novel domains of expression. *Dev. Dyn.* **231**, 609–613.

**Carraher, C. L. and Schwarzbauer, J. E.** (2013). Regulation of matrix assembly through rigidity-dependent fibronectin conformational changes. *J. Biol. Chem.* **288**, 14805–14814.

**Catala, M., Teillet, M.-A. and Le Douarin, N. M.** (1995). Organization and development of the tail bud analyzed with the quail-chick chimaera system. *Mech. Dev.* **51**, 51–65.

**Catala, M., Teillet, M. A., De Robertis, E. M. and Le Douarin, M. L.** (1996). A spinal cord fate map in the avian embryo: while regressing, Hensen's node lays down the notochord and floor plate thus joining the spinal cord lateral walls. *Development* **122**, 2599–610.

**Cayuso, J., Xu, Q. and Wilkinson, D. G.** (2015). Mechanisms of boundary formation by Eph receptor and ephrin signaling. *Dev. Biol.* **401**, 122–131.

**Chal, J., Guillot, C. and Pourquié, O.** (2017). PAPC couples the segmentation clock to somite morphogenesis by regulating N-cadherin-dependent adhesion. *Development* **144**, 664–676.

**Chapman, D. L. and Papaioannou, V. E.** (1998). Three neural tubes in mouse embryos with mutations in the T-box gene Tbx6. *Nature* **391**, 695–697.

**Chapman, D. L., Agulnik, I., Hancock, S., Silver, L. M. and Papaioannou, V. E.** (1996). Tbx6,a mouse T-Box gene implicated in paraxial mesoderm formation at gastrulation. *Dev. Biol.* **180**, 534–542.

**Chen, H. and Mosher, D. F.** (1996). Formation of sodium dodecyl sulfate-stable fibronectin multimers. Failure to detect products of thiol-disulfide exchange in cyanogen bromide or limited acid digests of stabilized matrix fibronectin. *J. Biol. Chem.* **271**, 9084–9.

**Chevallier, A., Kieny, M. and Mauger, A.** (1977). Limb-somite relationship: origin of the limb musculature. *J. Embryol. Exp. Morphol.* **41**, 245–58.

**Christ, B. and Ordahl, C. P.** (1995). Early stages of chick somite development. *Anat. Embryol. (Berl).* **191**, 381–396.

**Christ, B., Huang, R. and Scaal, M.** (2004). Formation and differentiation of the avian sclerotome. *Anat. Embryol. (Berl).* **208**, 411–24.

**Christ, B., Huang, R. and Scaal, M.** (2007). Amniote somite derivatives. *Dev. Dyn.* **236**, 2382–2396.

**Christopher, R. A., Kowalczyk, A. P. and McKeown-Longo, P. J.** (1997). Localization of fibronectin matrix assembly sites on fibroblasts and endothelial cells. *J. Cell Sci.* **110 ( Pt 5**, 569–81.

**Ciruna, B. and Rossant, J.** (2001). FGF signaling regulates mesoderm cell fate specification and morphogenetic movement at the primitive streak. *Dev. Cell* **1**, 37–49.

**Colognato, H. and Yurchenco, P. D.** (2000). Form and function: The laminin family of heterotrimers. *Dev. Dyn.* **218**, 213–234.

**Cooke, J. and Zeeman, E. C.** (1976). A clock and wavefront model for control of the number of repeated structures during animal morphogenesis. *J. Theor. Biol.* **58**, 455–76.

**Cordes, R., Schuster-Gossler, K., Serth, K. and Gossler, A.** (2004). Specification of vertebral identity is coupled to Notch signalling and the segmentation clock. *Development* **131**, 1221–33.

**Cotterell, J., Robert-Moreno, A. and Sharpe, J.** (2015). A local, self-organizing reaction-diffusion model can explain somite patterning in embryos. *Cell Syst.* **1**, 257–269.

**Critchley, D. R. and Gingras, A. R.** (2008). Talin at a glance. *J. Cell Sci.* **121**, 1345–1347.

**Cunningham, T. J., Brade, T., Sandell, L. L., Lewandoski, M., Trainor, P. A., Colas, A., Mercola, M. and Duester, G.** (2015). Retinoic acid activity in undifferentiated neural progenitors is sufficient to fulfill its role in restricting Fgf8 expression for somitogenesis. *PLoS One* **10**, e0137894.

**Czirok, A., Zamir, E. a., Filla, M. B., Little, C. D. and Rongish, B. J.** (2006). Extracellular matrix macroassembly dynamics in early vertebrate embryos. *Curr. Top. Dev. Biol.* **73**, 237–258.

**Dahmann, C., Oates, A. C. and Brand, M.** (2011). Boundary formation and maintenance in tissue development. *Nat. Rev. Genet.* **12**, 43–55.

**Dale, J. K., Maroto, M., Dequeant, M. L., Malapert, P., McGrew, M. and Pourquie, O.** (2003). Periodic Notch inhibition by lunatic fringe underlies the chick segmentation clock. *Nature* **421**, 275–278.

**Dale, J. K., Malapert, P., Chal, J., Vilhais-Neto, G., Maroto, M., Johnson, T., Jayasinghe, S., Trainor, P., Herrmann, B. and Pourquié, O.** (2006). Oscillations of the snail genes in the presomitic mesoderm coordinate segmental patterning and morphogenesis in vertebrate somitogenesis. *Dev. Cell* **10**, 355–366.

**Danen, E. H. and Yamada, K. M.** (2001). Fibronectin, integrins, and growth control. *J. Cell. Physiol.* **189**, 1–13.

**Danen, E. H. J., Sonneveld, P., Brakebusch, C., Fässler, R. and Sonnenberg, A.** (2002). The fibronectin-binding integrins α5β1 and αvβ3 differentially modulate RhoA-GTP loading, organization of cell matrix adhesions, and fibronectin fibrillogenesis. *J. Cell Biol.* **159**, 1071–1086.

**Davidson, L. a., Keller, R. and DeSimone, D. W.** (2004). Assembly and remodeling of the fibrillar fibronectin extracellular matrix during gastrulation and neurulation in Xenopus laevis. *Dev. Dyn.* **231**, 888–895.

**Davidson, L. A., Dzamba, B. D., Keller, R. and Desimone, D. W.** (2008). Live imaging of cell protrusive activity, and extracellular matrix assembly and remodeling during morphogenesis in the frog, Xenopus laevis. *Dev. Dyn.* **237**, 2684–2692.

**De Langhe, S. P., Sala, F. G., Del Moral, P. M., Fairbanks, T. J., Yamada, K. M., Warburton, D., Burns, R. C. and Bellusci, S.** (2005). Dickkopf-1 (DKK1) reveals that fibronectin is a major target of Wnt signaling in branching morphogenesis of the mouse embryonic lung. *Dev. Biol.* **277**, 316–331.

**Delaune, E. A., François, P., Shih, N. P. and Amacher, S. L.** (2012). Single-cell-resolution imaging of the impact of Notch signaling and mitosis on segmentation clock dynamics. *Dev. Cell* **23**, 995–1005.

**Delfini, M.-C., Dubrulle, J., Malapert, P., Chal, J. and Pourquie, O.** (2005). Control of the segmentation process by graded MAPK/ERK activation in the chick embryo. *Proc. Natl. Acad. Sci.* **102**, 11343–11348.

**DeMali, K. A. and Burridge, K.** (2003). Coupling membrane protrusion and cell adhesion. *J. Cell Sci.* **116**, 2389–97.

**Dequéant, M.-L., Glynn, E., Gaudenz, K., Wahl, M., Chen, J., Mushegian, A. and Pourquié, O.** (2006). A complex oscillating network of signaling genes underlies the mouse segmentation clock. *Science* **314**, 1595–8.

**Deries, M. and Thorsteinsdóttir, S.** (2016). Axial and limb muscle development: dialogue with the neighbourhood. *Cell. Mol. Life Sci.* **73**, 4415–4431.

**Deries, M., Schweitzer, R. and Duxson, M. J.** (2010). Developmental fate of the mammalian myotome. *Dev. Dyn.* **239**, 2898–2910.

**Dias, A. S., de Almeida, I., Belmonte, J. M., Glazier, J. A. and Stern, C. D.** (2014). Somites without a clock. *Science (80-. ).* **343**, 791–795.

**Dietrich, S., Schubert, F. R. and Lumsden, a** (1997). Control of dorsoventral pattern in the chick paraxial mesoderm. *Development* **124**, 3895–3908.

**Diez del Corral, R., Olivera-Martinez, I., Goriely, A., Gale, E., Maden, M. and Storey, K.** (2003). Opposing FGF and retinoid pathways control ventral neural pattern, neuronal differentiation, and segmentation during body axis extension. *Neuron* **40**, 65–79.

**Discher, D. E., Janmey, P. and Wang, Y.** (2005). Tissue cells feel and respond to the stiffness of their substrate. *Science* **310**, 1139–43.

**Discher, D. E., Mooney, D. J. and Zandstra, P. W.** (2009). Growth factors, matrices, and forces combine and control stem cells. *Science (80-. ).* **324**, 1673–1677.

**Duband, J. L. and Thiery, J. P.** (1982). Appearance and distribution of fibronectin during chick embryo gastrulation and neurulation. *Dev. Biol.* **94**, 337–50.

**Duband, J. L., Dufour, S., Hatta, K., Takeichi, M., Edelman, G. M. and Thiery, J. P.** (1987). Adhesion molecules during somitogenesis in the avian embryo. *J. Cell Biol.* **104**, 1361–74.

**Dubash, A. D., Menold, M. M., Samson, T., Boulter, E., García-Mata, R., Doughman, R. and Burridge, K.** (2009). Chapter 1. Focal Adhesions: New angles on an old structure.pp. 1–65.

**Dubrulle, J. and Pourquié, O.** (2004). Coupling segmentation to axis formation. 5783–5793.

**Dubrulle, J., McGrew, M. J. and Pourquié, O.** (2001). FGF signaling controls somite boundary position and regulates segmentation clock control of spatiotemporal Hox gene activation. *Cell* **106**, 219–232.

**DuFort, C. C., Paszek, M. J. and Weaver, V. M.** (2011). Balancing forces: architectural control of mechanotransduction. *Nat. Rev. Mol. Cell Biol.* **12**, 308–319.

**Duong, T. D. and Erickson, C. A.** (2004). MMP-2 plays an essential role in producing epithelial-mesenchymal transformations in the avian embryo. *Dev. Dyn.* **229**, 42–53.

**Durbeej, M.** (2010). Laminins. *Cell Tissue Res.* **339**, 259–268.

**Dzamba, B. J., Bultmann, H., Akiyama, S. K. and Peters, D. M.** (1994). Substrate-specific binding of the amino terminus of fibronectin to an integrin complex in focal adhesions. *J. Biol. Chem.* **269**, 19646–52.

**Dzamba, B. J., Jakab, K. R., Marsden, M., Schwartz, M. a. and DeSimone, D. W.** (2009). Cadherin adhesion, tissue tension, and noncanonical Wnt signaling regulate fibronectin matrix organization. *Dev. Cell* **16**, 421–32.

**Ebensperger, C., Wilting, J., Brand-Saberi, B., Mizutani, Y., Christ, B., Balling, R. and Koseki, H.** (1995). Pax-1, a regulator of sclerotome development is induced by notochord and floor plate signals in avian embryos. *Anat. Embryol. (Berl).* **191**, 297–310.

**Edsall, J. T.** (1978). Some early history of cold-insoluble globulin. *Ann. N. Y. Acad. Sci.* **312**, 1–10.

**Endo, T.** (2015). Molecular mechanisms of skeletal muscle development, regeneration, and osteogenic conversion. *Bone* **80**, 2–13.

**Engler, A. J., Sen, S., Sweeney, H. L. and Discher, D. E.** (2006). Matrix elasticity directs stem cell lineage specification. *Cell* **126**, 677–89.

**Evrard, Y. A., Lun, Y., Aulehla, A., Gan, L. and Johnson, R. L.** (1998). lunatic fringe is an essential mediator of somite segmentation and patterning. *Nature* **394**, 377–81.

**Eyckmans, J., Boudou, T., Yu, X. and Chen, C. S.** (2011). A Hitchhiker's Guide to Mechanobiology. *Dev. Cell* **21**, 35–47.

**Fan, C. M. and Tessier-Lavigne, M.** (1994). Patterning of mammalian somites by surface ectoderm and notochord: Evidence for sclerotome induction by a hedgehog homolog. *Cell* **79**, 1175–1186.

**Fan, C. M., Porter, J. a, Chiang, C., Chang, D. T., Beachy, P. a and Tessier-Lavigne, M.** (1995). Long-range sclerotome induction by sonic hedgehog: direct role of the amino-terminal cleavage product and modulation by the cyclic AMP signaling pathway. *Cell* **81**, 457–465.

**Fata, J. E., Mori, H., Ewald, A. J., Zhang, H., Yao, E., Werb, Z. and Bissell, M. J.** (2007). The MAPK(ERK-1,2) pathway integrates distinct and antagonistic signals from TGFalpha and FGF7 in morphogenesis of mouse mammary epithelium. *Dev. Biol.* **306**, 193–207.

**Feller, J., Schneider, A., Schuster-Gossler, K. and Gossler, A.** (2008). Noncyclic Notch activity in the presomitic mesoderm demonstrates uncoupling of somite compartmentalization and boundary formation. *Genes Dev.* **22**, 2166–2171.

**Ferjentsik, Z., Hayashi, S., Dale, J. K., Bessho, Y., Herreman, A., De Strooper, B., del Monte, G., de la Pompa, J. L. and Maroto, M.** (2009). Notch is a critical component of the mouse somitogenesis oscillator and is essential for the formation of the somites. *PLoS Genet.* **5**, e1000662.

**ffrench-Constant, C.** (1995). Alternative splicing of fibronectin - many different proteins but few different functions. *Exp. Cell Res.* **221**, 261–71.

**Ffrench-Constant, C., Hollingsworth, A., Heasman, J. and Wylie, C. C.** (1991). Response to fibronectin of mouse primordial germ cells before, during and after migration. *Development* **113**, 1365–73.

**Fleming, A., Kishida, M. G., Kimmel, C. B. and Keynes, R. J.** (2015). Building the backbone: the development and evolution of vertebral patterning. *Development* **142**, 1733–1744.

**Forsberg, H., Crozet, F. and Brown, N.** (1998). Waves of mouse Lunatic fringe expression, in four-hour cycles at two-hour intervals, precede somite boundary formation. *Curr Biol* **8**, 1027–1030.

**Frantz, C., Stewart, K. M. and Weaver, V. M.** (2010). The extracellular matrix at a glance. *J. Cell Sci.* **123**, 4195–4200.

**Freitas, C., Rodrigues, S., Charrier, J. B., Teillet, M. a and Palmeirim, I.** (2001). Evidence for medial/lateral specification and positional information within the presomitic mesoderm. *Development* **128**, 5139–47.

**Friedland, J. C., Lee, M. H. and Boettiger, D.** (2009). Mechanically activated integrin switch controls alpha5beta1 function. *Science* **323**, 642–4.

**Fujii, H.** (1997). Metabolic inactivation of retinoic acid by a novel P450 differentially expressed in developing mouse embryos. *EMBO J.* **16**, 4163–4173.

**Furuta, Y., Ilić, D., Kanazawa, S., Takeda, N., Yamamoto, T. and Aizawa, S.** (1995). Mesodermal defect in late phase of gastrulation by a targeted mutation of focal adhesion kinase, FAK. *Oncogene* **11**, 1989–95.

**García, A. J., Vega, M. D. and Boettiger, D.** (1999). Modulation of cell proliferation and differentiation through substrate-dependent changes in fibronectin conformation. *Mol. Biol. Cell* **10**, 785–98.

**Geiger, B. and Yamada, K. M.** (2011). Molecular architecture and function of matrix adhesions. *Cold Spring Harb. Perspect. Biol.* **3**, 1–21.

**Geiger, B., Bershadsky, A., Pankov, R. and Yamada, K. M.** (2001). Transmembrane crosstalk between the extracellular matrix-cytoskeleton crosstalk. *Nat. Rev. Mol. Cell Biol.* **2**, 793–805.

**George, E. L., Georges-labouesse, E. N., Patel-king, R. S., Rayburn, H. and Hynes, R. O.** (1993). Defects in mesoderm , neural tube and vascular development in mouse embryos lacking fibronectin. **1091**, 1079–1091.

**Georges-Labouesse, E. N., George, E. L., Rayburn, H. and Hynes, R. O.** (1996). Mesodermal development in mouse embryos mutant for fibronectin. *Dev. Dyn.* **207**, 145–56.

**Gilbert, S. F.** (2006). Developmental Biology. Sunderland (MA): Sinauer Associates.

**Gilmore, A. P.** (2005). Anoikis. *Cell Death Differ.* **12 Suppl 2**, 1473–7.

**Ginsberg, M. H., Partridge, A. and Shattil, S. J.** (2005). Integrin regulation. *Curr. Opin. Cell Biol.* **17**, 509–516.

**Goh, K. L., Yang, J. T. and Hynes, R. O.** (1997). Mesodermal defects and cranial neural crest apoptosis in alpha5 integrin-null embryos. *Development* **124**, 4309–4319.

**Gomez, C., Özbudak, E. M., Wunderlich, J., Baumann, D., Lewis, J. and Pourquié, O.** (2008). Control of segment number in vertebrate embryos. *Nature* **454**, 335–339.

**Gordon, M. K. and Hahn, R. A.** (2010). Collagens. *Cell Tissue Res.* **339**, 247–257.

**Gudzenko, T. and Franz, C. M.** (2015). Studying early stages of fibronectin fibrillogenesis in living cells by atomic force microscopy. *Mol. Biol. Cell* **26**, 3190–3204.

**Hagel, M., George, E. L., Kim, A., Tamimi, R., Opitz, S. L., Turner, C. E., Imamoto, A. and Thomas, S. M.** (2002). The adaptor protein paxillin is essential for normal development in the mouse and is a critical transducer of fibronectin signaling. *Mol. Cell. Biol.* **22**, 901–15.

**Hamburger, V. and Hamilton, H. L.** (1992). A series of normal stages in the development of the chick embryo. *Dev. Dyn.* **195**, 231–272.

**Harima, Y., Takashima, Y., Ueda, Y., Ohtsuka, T. and Kageyama, R.** (2013). Accelerating the tempo of the segmentation clock by reducing the number of introns in the Hes7 gene. *Cell Rep.* **3**, 1–7.

**Harima, Y., Imayoshi, I., Shimojo, H., Kobayashi, T. and Kageyama, R.** (2014). The roles and mechanism of ultradian oscillatory expression of the mouse Hes genes. *Semin. Cell Dev. Biol.* **34**, 85–90.

**Harris, a K., Stopak, D. and Warner, P.** (1984). Generation of spatially periodic patterns by a mechanical instability: a mechanical alternative to the Turing model. *J. Embryol. Exp. Morphol.* **80**, 1–20.

**Hatada, Y. and Stern, C. D.** (1994). A fate map of the epiblast of the early chick embryo. *Development* **120**, 2879–89.

**Heasman, J., Hynes, R. O., Swan, A. P., Thomas, V. and Wylie, C. C.** (1981). Primordial germ cells of Xenopus embryos: the role of fibronectin in their adhesion during migration. *Cell* **27**, 437–47.

**Heinonen, S., Männikkö, M., Klement, J. F., Whitaker-Menezes, D., Murphy, G. F. and Uitto, J.** (1999). Targeted inactivation of the type VII collagen gene (Col7a1) in mice results in severe blistering phenotype: a model for recessive dystrophic epidermolysis bullosa. *J. Cell Sci.* **112 ( Pt 2**, 3641–8.

**Herrgen, L., Ares, S., Morelli, L. G., Schröter, C., Jülicher, F. and Oates, A. C.** (2010). Intercellular coupling regulates the period of the segmentation clock. *Curr. Biol.* **20**, 1244–1253.

**Hirata, H., Bessho, Y., Kokubu, H., Masamizu, Y., Yamada, S., Lewis, J. and Kageyama, R.** (2004). Instability of Hes7 protein is crucial for the somite segmentation clock. *Nat. Genet.* **36**, 750–754.

**Horikawa, K., Radice, G., Takeichi, M. and Chisaka, O.** (1999). Adhesive subdivisions intrinsic to the epithelial somites. *Dev. Biol.* **215**, 182–9.

**Hrabě de Angelis, M., Mclntyre, J. and Gossler, A.** (1997). Maintenance of somite borders in mice requires the Delta homologue Dll1. *Nature* **386**, 717–721.

**Hubaud, A. and Pourquié, O.** (2014). Signalling dynamics in vertebrate segmentation. *Nat. Rev. Mol. Cell Biol.* **15**, 709–721.

**Hubaud, A., Regev, I., Mahadevan, L. and Pourquié, O.** (2017). Excitable dynamics and Yap-dependent mechanical cues drive the segmentation clock. *Cell* **171**, 668–682.e11.

**Hubbard, B., Buczek-Thomas, J. A., Nugent, M. A. and Smith, M. L.** (2016). Fibronectin fiber extension decreases cell spreading and migration. *J. Cell. Physiol.* **231**, 1728–36.

**Hughes, D. S., Keynes, R. J. and Tannahill, D.** (2009). Extensive molecular differences between anterior- and posterior-half-sclerotomes underlie somite polarity and spinal nerve segmentation. *BMC Dev. Biol.* **9**, 30.

**Humphries, J. D., Byron, A. and Humphries, M. J.** (2006). Integrin ligands at a glance. *J. Cell Sci.* **119**, 3901–3.

**Huppert, S. S., Ilagan, M. X. G., De Strooper, B. and Kopan, R.** (2005). Analysis of Notch function in presomitic mesoderm suggests a γ-secretase-independent role for presenilins in somite differentiation. *Dev. Cell* **8**, 677–688.

**Huttenlocher, A. and Horwitz, A. R.** (2011). Integrins in cell migration. *Cold Spring Harb. Perspect. Biol.* **3**, a005074.

**Huveneers, S. and Danen, E. H. J.** (2009). Adhesion signaling - crosstalk between integrins, Src and Rho. *J. Cell Sci.* **122**, 1059–1069.

**Huveneers, S., Truong, H., Fässler, R., Sonnenberg, A. and Danen, E. H. J.** (2008). Binding of soluble fibronectin to integrin alpha5 beta1 - link to focal adhesion redistribution and contractile shape. *J. Cell Sci.* **121**, 2452–62.

**Hynes, R. O.** (1990). *Fibronectins*. New York, NY: Springer New York.

**Hynes, R. O.** (2002). Integrins: Bidirectional, allosteric signaling machines. *Cell* **110**, 673–687.

**Hynes, R. O.** (2009). The Extracellular Matrix: Not just pretty fibrils. *Science (80-. ).* **326**, 1216–1219.

**Hynes, R. O. and Naba, A.** (2012). Overview of the Matrisome - An inventory of extracellular matrix constituents and functions. *Cold Spring Harb. Perspect. Biol.* **4**, a004903–a004903.

**Iimura, T. and Pourquié, O.** (2006). Collinear activation of Hoxb genes during gastrulation is linked to mesoderm cell ingression. *Nature* **442**, 568–571.

**Iimura, T., Yang, X., Weijer, C. J. and Pourquie, O.** (2007). Dual mode of paraxial mesoderm formation during chick gastrulation. *Proc. Natl. Acad. Sci.* **104**, 2744–2749.

**Ilić, D., Furuta, Y., Kanazawa, S., Takeda, N., Sobue, K., Nakatsuji, N., Nomura, S., Fujimoto, J., Okada, M. and Yamamoto, T.** (1995). Reduced cell motility and enhanced focal adhesion contact formation in cells from FAK-deficient mice. *Nature* **377**, 539–44.

**Ilić, D., Kovacic, B., Johkura, K., Schlaepfer, D. D., Tomasević, N., Han, Q., Kim, J., Howerton, K., Baumbusch, C., Ogiwara, N., et al.** (2004). FAK promotes organization of fibronectin matrix and fibrillar adhesions. *J. Cell Sci.* **117**, 177–87.

**Iozzo, R. V. and Gubbiotti, M. A.** (2018). Extracellular matrix: The driving force of mammalian diseases. *Matrix Biol.* **71–72**, 1–9.

**Ishimatsu, K., Takamatsu, A. and Takeda, H.** (2010). Emergence of traveling waves in the zebrafish segmentation clock. *Development* **137**, 1595–1599.

**Iwamoto, D. V. and Calderwood, D. A.** (2015). Regulation of integrin-mediated adhesions. *Curr. Opin. Cell Biol.* **36**, 41–47.

**Järveläinen, H.** (2009). Extracellular matrix molecules: potential targets in pharmacotherapy. *Pharmacol Rev.* **61**, 198–223.

**Jiang, Y.-J., Aerne, B. L., Smithers, L., Haddon, C., Ish-Horowicz, D. and Lewis, J.** (2000). Notch signalling and the synchronization of the somite segmentation clock. *Nature* **408**, 475–479.

**Johnson, J., Rhee, J., Parsons, S. M., Brown, D., Olson, E. N. and Rawls, A.** (2001). The Anterior/Posterior Polarity of Somites Is Disrupted in Paraxis-Deficient Mice. *Dev. Biol.* **229**, 176–187.

**Jouve, C., Palmeirim, I., Henrique, D., Beckers, J., Gossler, A., Ish-Horowicz, D. and Pourquié, O.** (2000). Notch signalling is required for cyclic expression of the hairy-like gene HES1 in the presomitic mesoderm. *Development* **127**, 1421–1429.

**Jouve, C., Iimura, T. and Pourquie, O.** (2002). Onset of the segmentation clock in the chick embryo: evidence for oscillations in the somite precursors in the primitive streak. *Development* **129**, 1107–17.

**Jülich, D., Geisler, R., Holley, S. a. and Tübingen 2000 Screen Consortium** (2005). Integrin alpha5 and delta/notch signaling have complementary spatiotemporal requirements during zebrafish somitogenesis. *Dev. Cell* **8**, 575–86.

**Jülich, D., Cobb, G., Melo, A. M., McMillen, P., Lawton, A. K., Mochrie, S. G. J., Rhoades, E. and Holley, S. A.** (2015). Cross-scale integrin regulation organizes ECM and tissue topology. *Dev. Cell* **34**, 33–44.

**Kageyama, R., Niwa, Y., Isomura, A., González, A. and Harima, Y.** (2012). Oscillatory gene expression and somitogenesis. *Wiley Interdiscip. Rev. Dev. Biol.* **1**, 629–641.

**Kageyama, R., Shimojo, H. and Isomura, A.** (2018). Oscillatory control of Notch signaling in development. In *Advances in experimental medicine and biology*, pp. 265–277.

**Kametaka, S., Moriyama, K., Burgos, P. V, Eisenberg, E., Greene, L. E., Mattera, R. and Bonifacino, J. S.** (2007). Canonical interaction of cyclin G associated kinase with adaptor protein 1 regulates lysosomal enzyme sorting. *Mol. Biol. Cell* **18**, 2991–3001.

**Kawakami, Y., Raya, A., Raya, R. M., Rodríguez-Esteban, C. and Izpisúa Belmonte, J. C.** (2005). Retinoic acid signalling links left-right asymmetric patterning and bilaterally symmetric somitogenesis in the zebrafish embryo. *Nature* **435**, 165–71.

**Keselowsky, B. G., Collard, D. M. and García, A. J.** (2003). Surface chemistry modulates fibronectin conformation and directs integrin binding and specificity to control cell adhesion. *J. Biomed. Mater. Res. A* **66**, 247–59.

**Keselowsky, B. G., Collard, D. M. and García, A. J.** (2005). Integrin binding specificity regulates biomaterial surface chemistry effects on cell differentiation. *Proc. Natl. Acad. Sci. U. S. A.* **102**, 5953–7.

**Keynes, R. J. and Stern, C. D.** (1984). Segmentation in the vertebrate nervous system. *Nature* **310**, 786–789.

**Kieny, M., Mauger, A. and Sengel, P.** (1972). Early regionalization of somitic mesoderm as studied by the development of axial skeleton of the chick embryo. *Dev. Biol.* **28**, 142–61.

**Klein, E. A., Yin, L., Kothapalli, D., Castagnino, P., Byfield, F. J., Xu, T., Levental, I., Hawthorne, E., Janmey, P. A. and Assoian, R. K.** (2009). Cell-cycle control by physiological matrix elasticity and in vivo tissue stiffening. *Curr. Biol.* **19**, 1511–1518.

**Knezevic, V., De Santo, R. and Mackem, S.** (1997). Two novel chick T-box genes related to mouse Brachyury are expressed in different, non-overlapping mesodermal domains during gastrulation. *Development* **124**, 411–9.

**Kondoh, H. and Takemoto, T.** (2012). Axial stem cells deriving both posterior neural and mesodermal tissues during gastrulation. *Curr. Opin. Genet. Dev.* **22**, 374–380.

**Koshida, S., Kishimoto, Y., Ustumi, H., Shimizu, T., Furutani-Seiki, M., Kondoh, H. and Takada, S.** (2005). Integrin alpha5-dependent fibronectin accumulation for maintenance of somite boundaries in zebrafish embryos. *Dev. Cell* **8**, 587–98.

**Kragtorp, K. a. and Miller, J. R.** (2007). Integrin alpha5 is required for somite rotation and boundary formation in Xenopus. *Dev. Dyn.* **236**, 2713–20.

**Kramer, K. L. and Yost, H. J.** (2002). Ectodermal syndecan-2 mediates left-right axis formation in migrating mesoderm as a cell-nonautonomous Vg1 cofactor. *Dev. Cell* **2**, 115–24.

**Krammer, A., Craig, D., Thomas, W. E., Schulten, K. and Vogel, V.** (2002). A structural model for force regulated integrin binding to fibronectin's RGD-synergy site. *Matrix Biol.* **21**, 139–47.

**Krol, A. J., Roellig, D., Dequeant, M.-L., Tassy, O., Glynn, E., Hattem, G., Mushegian, A., Oates, A. C. and Pourquie, O.** (2011). Evolutionary plasticity of segmentation clock networks. *Development* **138**, 2783–2792.

**Krotoski, D. M., Domingo, C. and Bronner-Fraser, M.** (1986). Distribution of a putative cell surface receptor for fibronectin and laminin in the avian embryo. *J. Cell Biol.* **103**, 1061–71.

**Kuan, C.-Y. K., Tannahill, D., Cook, G. M. W. and Keynes, R. J.** (2004). Somite polarity and segmental patterning of the peripheral nervous system. *Mech. Dev.* **121**, 1055–68.

**Kulesa, P. M. and Fraser, S. E.** (2002). Cell dynamics during somite boundary formation revealed by time-lapse analysis. *Science* **298**, 991–995.

**Kulesa, P. M., Schnell, S., Rudloff, S., Baker, R. E. and Maini, P. K.** (2007). From segment to somite: Segmentation to epithelialization analyzed within quantitative frameworks. *Dev. Dyn.* **236**, 1392–1402.

**Kumar, S. and Duester, G.** (2014). Retinoic acid controls body axis extension by directly repressing Fgf8 transcription. *Development* **141**, 2972–7.

**Kureishi, Y., Kobayashi, S., Amano, M., Kimura, K., Kanaide, H., Nakano, T., Kaibuchi, K. and Ito, M.** (1997). Rho-associated kinase directly induces smooth muscle contraction through myosin light chain phosphorylation. *J. Biol. Chem.* **272**, 12257–60.

**Kusumi, K., Sun, E., Kerrebrock, A. W., Bronson, R. T., Chi, D.-C., Bulotsky, M., Spencer, J. B., Birren, B. W., Frankel, W. N. and Lander, E. S.** (1998). The mouse pudgy mutation disrupts Delta homologue Dll3 and initiation of early somite boundaries. *Nat. Genet.* **19**, 274–278.

**Larsen, M., Artym, V. V., Green, J. A. and Yamada, K. M.** (2006). The matrix reorganized: extracellular matrix remodeling and integrin signaling. *Curr. Opin. Cell Biol.* **18**, 463–471.

**Lash, J. W., Ostrovsky, D., Mittal, B. and Sanger, J. W.** (1985). Alpha actinin distribution and extracellular matrix products during somitogenesis and neurulation in the chick embryo. *Cell Motil.* **5**, 491–506.

**Lauder, G. V** (1980). On the relationship of the myotome to the axial skeleton in vertebrate evolution. *Paleobiology* **6**, 51–56.

**Lee, G., Hynes, R. and Kirschner, M.** (1984). Temporal and spatial regulation of fibronectin in early Xenopus development. *Cell* **36**, 729–40.

**Leitges, M., Neidhardt, L., Haenig, B., Herrmann, B. G. and Kispert, A.** (2000). The paired homeobox gene Uncx4.1 specifies pedicles, transverse processes and proximal ribs of the vertebral column. *Development* **127**, 2259–67.

**Lemmon, C. A. and Weinberg, S. H.** (2017). Multiple cryptic binding sites are necessary for robust fibronectin assembly: An in silico study. *Sci. Rep.* **7**, 1–12.

**Leu, S. T., Jacques, S. A. L., Wingerd, K. L., Hikita, S. T., Tolhurst, E. C., Pring, J. L., Wiswell, D., Kinney, L., Goodman, N. L., Jackson, D. Y., et al.** (2004). Integrin alpha4beta1 function is required for cell survival in developing retina. *Dev. Biol.* **276**, 416–30.

**Lewis, J., Hanisch, A. and Holder, M.** (2009). Notch signaling, the segmentation clock, and the patterning of vertebrate somites. *J. Biol.* **8**, 44.

**Li, Y., Fenger, U., Niehrs, C. and Pollet, N.** (2003). Cyclic expression of esr9 gene in Xenopus presomitic mesoderm. *Differentiation.* **71**, 83–9.

**Liao, Y., Gotwals, P. J., Koteliansky, V. E., Sheppard, D. and Van De Water, L.** (2002). The EIIIA segment of fibronectin is a ligand for integrins alpha 9beta 1 and alpha 4beta 1 providing a novel mechanism for regulating cell adhesion by alternative splicing. *J. Biol. Chem.* **277**, 14467–74.

**Lin, F., Ren, X., Pan, Z., Macri, L., Zong, W., Tonnesen, M. G., Rafailovich, M., Bar-Sagi, D. and Clark, R. A. F.** (2011). Fibronectin growth factor-binding domains are required for fibroblast survival. *J. Invest. Dermatol.* **131**, 84–98.

**Linask, K. K., Ludwig, C., Han, M. D., Liu, X., Radice, G. L. and Knudsen, K. A.** (1998). N-cadherin/catenin-mediated morphoregulation of somite formation. *Dev. Biol.* **202**, 85–102.

**Linask, K. K., Manisastry, S. and Han, M.** (2005). Cross talk between cell-cell and cell-matrix adhesion signaling pathways during heart organogenesis: Implications for cardiac birth defects. *Microsc. Microanal.* **11**, 200–208.

**Little, W. C., Smith, M. L., Ebneter, U. and Vogel, V.** (2008). Assay to mechanically tune and optically probe fibrillar fibronectin conformations from fully relaxed to breakage. *Matrix Biol.* **27**, 451–461.

**Liu, X., Wu, H., Byrne, M., Krane, S. and Jaenisch, R.** (1997). Type III collagen is crucial for collagen I fibrillogenesis and for normal cardiovascular development. *Proc. Natl. Acad. Sci.* **94**, 1852–1856.

**Makarenkova, H. P., Hoffman, M. P., Beenken, A., Eliseenkova, A. V, Meech, R., Tsau, C., Patel, V. N., Lang, R. A. and Mohammadi, M.** (2009). Differential interactions of FGFs with Heparan Sulfate control gradient formation and branching morphogenesis. *Sci. Signal.* **2**, ra55-ra55.

**Mallo, M., Wellik, D. M. and Deschamps, J.** (2010). Hox genes and regional patterning of the vertebrate body plan. *Dev. Biol.* **344**, 7–15.

**Mansouri, A., Yokota, Y., Wehr, R., Copeland, N. G., Jenkins, N. A. and Gruss, P.** (1997). Paired-related murine homeobox gene expressed in the developing sclerotome, kidney, and nervous system. *Dev. Dyn.* **210**, 53–65.

**Mansouri, A., Voss, A. K., Thomas, T., Yokota, Y. and Gruss, P.** (2000). Uncx4.1 is required for the formation of the pedicles and proximal ribs and acts upstream of Pax9. *Development* **127**, 2251–8.

**Mao, Y. and Schwarzbauer, J. E.** (2005). Fibronectin fibrillogenesis, a cell-mediated matrix assembly process. *Matrix Biol.* **24**, 389–399.

**Marastoni, S., Ligresti, G., Lorenzon, E., Colombatti, A. and Mongiat, M.** (2008). Extracellular matrix: a matter of life and death. *Connect. Tissue Res.* **49**, 203–6.

**Marcelle, C., Stark, M. R. and Bronner-Fraser, M.** (1997). Coordinate actions of BMPs, Wnts, Shh and noggin mediate patterning of the dorsal somite. *Development* **124**, 3955–3963.

**Marsden, M. and Burke, R. D.** (1998). The βL integrin subunit is necessary for gastrulation in sea urchin embryos. *Dev. Biol.* **203**, 134–148.

**Marsden, M. and DeSimone, D. W.** (2001). Regulation of cell polarity, radial intercalation and epiboly in Xenopus: novel roles for integrin and fibronectin. *Development* **128**, 3635–3647.

**Martins, G. G., Rifes, P., Amândio, R., Rodrigues, G., Palmeirim, I. and Thorsteinsdóttir, S.** (2009). Dynamic 3D cell rearrangements guided by a fibronectin matrix underlie somitogenesis. *PLoS One* **4**, e7429.

**Masamizu, Y., Ohtsuka, T., Takashima, Y., Nagahara, H., Takenaka, Y., Yoshikawa, K., Okamura, H. and Kageyama, R.** (2006). Real-time imaging of the somite segmentation clock: Revelation of unstable oscillators in the individual presomitic mesoderm cells. *Proc. Natl. Acad. Sci.* **103**, 1313–1318.

**Matsui, T., Raya, A., Callol-Massot, C., Kawakami, Y., Oishi, I., Rodriguez-Esteban, C. and Izpisúa Belmonte, J. C.** (2007). miles-apart-Mediated regulation of cell-fibronectin interaction and myocardial migration in zebrafish. *Nat. Clin. Pract. Cardiovasc. Med.* **4 Suppl 1**, S77-82.

**McDonald, J. A., Quade, B. J., Broekelmann, T. J., LaChance, R., Forsman, K., Hasegawa, E. and Akiyama, S.** (1987). Fibronectin's cell-adhesive domain and an amino-terminal matrix assembly domain participate in its assembly into fibroblast pericellular matrix. *J. Biol. Chem.* **262**, 2957–67.

**McKeown-Longo, P. J. and Mosher, D. F.** (1983). Binding of plasma fibronectin to cell layers of human skin fibroblasts. *J. Cell Biol.* **97**, 466–472.

**McKeown-Longo, P. J. and Mosher, D. F.** (1985). Interaction of the 70,000-mol-wt amino-terminal fragment of fibronectin with the matrix-assembly receptor of fibroblasts. *J. Cell Biol.* **100**, 364–74.

**McMillen, P., Chatti, V., Jülich, D. and Holley, S. A.** (2016). A sawtooth pattern of Cadherin 2 stability mechanically regulates somite morphogenesis. *Curr. Biol.* **26**, 542–9.

**Menko, A. S. and Boettiger, D.** (1987). Occupation of the extracellular matrix receptor, integrin, is a control point for myogenic differentiation. *Cell* **51**, 51–7.

**Michael, K. E., Dumbauld, D. W., Burns, K. L., Hanks, S. K. and García, A. J.** (2009). Focal adhesion kinase modulates cell adhesion strengthening via integrin activation. *Mol. Biol. Cell* **20**, 2508–2519.

**Mitra, S. K., Hanson, D. A. and Schlaepfer, D. D.** (2005). Focal adhesion kinase: in command and control of cell motility. *Nat. Rev. Mol. Cell Biol.* **6**, 56–68.

**Mittal, A., Pulina, M., Hou, S. Y. and Astrof, S.** (2013). Fibronectin and integrin alpha 5 play requisite roles in cardiac morphogenesis. *Dev. Biol.* **381**, 73–82.

**Miyamoto, S., Teramoto, H., Gutkind, J. S. and Yamada, K. M.** (1996). Integrins can collaborate with growth factors for phosphorylation of receptor tyrosine kinases and MAP kinase activation: roles of integrin aggregation and occupancy of receptors. *J. Cell Biol.* **135**, 1633–42.

**Miyamoto, S., Katz, B. Z., Lafrenie, R. M. and Yamada, K. M.** (1998). Fibronectin and integrins in cell adhesion, signaling, and morphogenesis. *Ann. N. Y. Acad. Sci.* **857**, 119–29.

**Monkley, S. J., Zhou, X. H., Kinston, S. J., Giblett, S. M., Hemmings, L., Priddle, H., Brown, J. E., Pritchard, C. A., Critchley, D. R. and Fässler, R.** (2000). Disruption of the talin gene arrests mouse development at the gastrulation stage. *Dev. Dyn.* **219**, 560–74.

**Monsoro-Burq, A. H.** (2005). Sclerotome development and morphogenesis: When experimental embryology meets genetics. *Int. J. Dev. Biol.* **49**, 301–308.

**Montanez, E., Ussar, S., Schifferer, M., Bösl, M., Zent, R., Moser, M. and Fässler, R.** (2008). Kindlin-2 controls bidirectional signaling of integrins. *Genes Dev.* **22**, 1325–30.

**Morimoto, M., Takahashi, Y., Endo, M. and Saga, Y.** (2005). The Mesp2 transcription factor establishes segmental borders by suppressing Notch activity. *Nature* **435**, 354–359.

**Moser, M., Legate, K. R., Zent, R. and Fassler, R.** (2009). The tail of integrins, talins, and kindlins. *Science (80-. ).* **324**, 895–899.

**Mouw, J. K., Ou, G. and Weaver, V. M.** (2014). Extracellular matrix assembly: A multiscale deconstruction. *Nat. Rev. Mol. Cell Biol.* **15**, 771–785.

**Mu, D., Cambier, S., Fjellbirkeland, L., Baron, J. L., Munger, J. S., Kawakatsu, H., Sheppard, D., Broaddus, V. C. and Nishimura, S. L.** (2002). The integrin alpha(v) beta8 mediates epithelial homeostasis through MT1-MMP-dependent activation of TGF-beta1. *J. Cell Biol.* **157**, 493–507.

**Munger, J. S., Huang, X., Kawakatsu, H., Griffiths, M. J., Dalton, S. L., Wu, J., Pittet, J. F., Kaminski, N., Garat, C., Matthay, M. A., et al.** (1999). The integrin alpha v beta 6 binds and activates latent TGF beta 1: a mechanism for regulating pulmonary inflammation and fibrosis. *Cell* **96**, 319–28.

**Murphy, M. and Kardon, G.** (2011). Origin of vertebrate limb muscle: the role of progenitor and myoblast populations. *Curr. Top. Dev. Biol.* **96**, 1–32.

**Murray, P. J., Maini, P. K. and Baker, R. E.** (2011). The clock and wavefront model revisited. *J. Theor. Biol.* **283**, 227–238.

**Myllyharju, J. and Kivirikko, K. I.** (2004). Collagens, modifying enzymes and their mutations in humans, flies and worms. *Trends Genet.* **20**, 33–43.

**Naiche, L. A., Holder, N. and Lewandoski, M.** (2011). FGF4 and FGF8 comprise the wavefront activity that controls somitogenesis. *Proc. Natl. Acad. Sci.* **108**, 4018–4023.

**Nakaya, Y., Kuroda, S., Katagiri, Y. T., Kaibuchi, K. and Takahashi, Y.** (2004). Mesenchymal-epithelial transition during somitic segmentation is regulated by differential roles of Cdc42 and Rac1. *Dev. Cell* **7**, 425–438.

**Newell-Litwa, K. A., Horwitz, R. and Lamers, M. L.** (2015). Non-muscle myosin II in disease: mechanisms and therapeutic opportunities. *Dis. Model. Mech.* **8**, 1495–515.

**Newgreen, D. and Thiery, J. P.** (1980). Fibronectin in early avian embryos: synthesis and distribution along the migration pathways of neural crest cells. *Cell Tissue Res.* **211**, 269–91.

**Niederreither, K., McCaffery, P., Dräger, U. C., Chambon, P. and Dollé, P.** (1997). Restricted expression and retinoic acid-induced downregulation of the retinaldehyde dehydrogenase type 2 (RALDH-2) gene during mouse development. *Mech. Dev.* **62**, 67–78.

**Nishie, W., Sawamura, D., Goto, M., Ito, K., Shibaki, A., McMillan, J. R., Sakai, K., Nakamura, H., Olasz, E., Yancey, K. B., et al.** (2007). Humanization of autoantigen. *Nat. Med.* **13**, 378–383.

**Niwa, Y., Masamizu, Y., Liu, T., Nakayama, R., Deng, C.-X. and Kageyama, R.** (2007). The initiation and propagation of Hes7 oscillation are cooperatively regulated by Fgf and Notch signaling in the somite segmentation clock. *Dev. Cell* **13**, 298–304.

**Niwa, Y., Shimojo, H., Isomura, A., Gonzalez, A., Miyachi, H. and Kageyama, R.** (2011). Different types of oscillations in Notch and Fgf signaling regulate the spatiotemporal periodicity of somitogenesis. *Genes Dev.* **25**, 1115–1120.

**Novák, B. and Tyson, J. J.** (2008). Design principles of biochemical oscillators. *Nat. Rev. Mol. Cell Biol.* **9**, 981–991.

**Oates, A. C. and Ho, R. K.** (2002). Hairy/E(spl)-related (Her) genes are central components of the segmentation oscillator and display redundancy with the Delta/Notch signaling pathway in the formation of anterior segmental boundaries in the zebrafish. *Development* **129**, 2929–46.

**Oates, A. C., Morelli, L. G. and Ares, S.** (2012). Patterning embryos with oscillations: structure, function and dynamics of the vertebrate segmentation clock. *Development* **139**, 625–639.

**Oehrl, W. and Panayotou, G.** (2008). Modulation of growth factor action by the extracellular matrix. *Connect. Tissue Res.* **49**, 145–8.

**Oginuma, M., Takahashi, Y., Kitajima, S., Kiso, M., Kanno, J., Kimura, A. and Saga, Y.** (2010). The oscillation of Notch activation, but not its boundary, is required for somite border formation and rostral-caudal patterning within a somite. *Development* **137**, 1515–1522.

**Ohashi, T., Lemmon, C. A. and Erickson, H. P.** (2017). Fibronectin conformation and assembly: Analysis of fibronectin deletion mutants and fibronectin glomerulopathy (GFND) mutants. *Biochemistry* **56**, 4584–4591.

**Olorundare, O. E., Peyruchaud, O., Albrecht, R. M. and Mosher, D. F.** (2001). Assembly of a fibronectin matrix by adherent platelets stimulated by lysophosphatidic acid and other agonists. *Blood* **98**, 117–24.

**Ordahl, C. P. and Le Douarin, N. M.** (1992). Two myogenic lineages within the developing somite. *Development* **114**, 339–53.

**Ordahl, C. P., Berdougo, E., Venters, S. J. and Denetclaw, W. F.** (2001). The dermomyotome dorsomedial lip drives growth and morphogenesis of both the primary myotome and dermomyotome epithelium. *Development* **128**, 1731–44.

**Ostrovsky, D., Cheney, C. M., Seitz, A. W. and Lash, J. W.** (1983). Fibronectin distribution during somitogenesis in the chick embryo. *Cell Differ.* **13**, 217–23.

**Palmeirim, I., Henrique, D., Ish-Horowicz, D. and Pourquié, O.** (1997). Avian hairy gene expression identifies a molecular clock linked to vertebrate segmentation and somitogenesis. *Cell* **91**, 639–648.

**Palmeirim, I., Dubrulle, J., Henrique, D., Ish-Horowicz, D. and Pourquié, O.** (1998). Uncoupling segmentation and somitogenesis in the chick presomitic mesoderm. *Dev. Genet.* **23**, 77–85.

**Pankov, R. and Yamada, K. M.** (2002). Fibronectin at a glance. *J. Cell Sci.* **115**, 3861–3863.

**Pasapera, A. M., Schneider, I. C., Rericha, E., Schlaepfer, D. D. and Waterman, C. M.** (2010). Myosin II activity regulates vinculin recruitment to focal adhesions through FAK-mediated paxillin phosphorylation. *J. Cell Biol.* **188**, 877–890.

**Perris, R. and Perissinotto, D.** (2000). Role of the extracellular matrix during neural crest cell migration. *Mech. Dev.* **95**, 3–21.

**Pierschbacher, M. D. and Ruoslahti, E.** (1984). Cell attachment activity of fibronectin can be duplicated by small synthetic fragments of the molecule. *Nature* **309**, 30–3.

**Pierschbacher, M. D., Ruoslahti, E., Sundelin, J., Lind, P. and Peterson, P. A.** (1982). The cell attachment domain of fibronectin. Determination of the primary structure. *J. Biol. Chem.* **257**, 9593–7.

**Pietri, T., Eder, O., Breau, M. A., Topilko, P., Blanche, M., Brakebusch, C., Fässler, R., Thiery, J.-P. and Dufour, S.** (2004). Conditional beta1-integrin gene deletion in neural crest cells causes severe developmental alterations of the peripheral nervous system. *Development* **131**, 3871–83.

**Potts, J. R. and Campbell, I. D.** (1994). Fibronectin structure and assembly. *Curr. Opin. Cell Biol.* **6**, 648–55.

**Pourquié, O. and Tam, P. P. L.** (2001). A nomenclature for prospective somites and phases of cyclic gene expression in the presomitic mesoderm. *Dev. Cell* **1**, 619–20.

**Prager-Khoutorsky, M., Lichtenstein, A., Krishnan, R., Rajendran, K., Mayo, A., Kam, Z., Geiger, B. and Bershadsky, A. D.** (2011). Fibroblast polarization is a matrix-rigidity-dependent process controlled by focal adhesion mechanosensing. *Nat. Cell Biol.* **13**, 1457–1465.

**Provenzano, P. P., Inman, D. R., Eliceiri, K. W. and Keely, P. J.** (2009). Matrix density-induced mechanoregulation of breast cell phenotype, signaling and gene expression through a FAK-ERK linkage. *Oncogene* **28**, 4326–43.

**Psychoyos, D. and Stern, C. D.** (1996). Fates and migratory routes of primitive streak cells in the chick embryo. *Development* **122**, 1523–34.

**Radice, G. L., Rayburn, H., Matsunami, H., Knudsen, K. A., Takeichi, M. and Hynes, R. O.** (1997). Developmental defects in mouse embryos lacking N-cadherin. *Dev. Biol.* **181**, 64–78.

**Rallis, C., Pinchin, S. M. and Ish-Horowicz, D.** (2010). Cell-autonomous integrin control of Wnt and Notch signalling during somitogenesis. *Development* **137**, 3591–3601.

**Remak, R.** (1850). Untersuchungen uber die entwicklung der Wirbeltiere. Reimer, Berlin.

**Resende, T. P., Andrade, R. P. and Palmeirim, I.** (2014). Timing embryo segmentation: Dynamics and regulatory mechanisms of the vertebrate Segmentation Clock. *Biomed Res. Int.* **2014**, 1–12.

**Rhee, J., Takahashi, Y., Saga, Y., Wilson-Rawls, J. and Rawls, A.** (2003). The protocadherin papc is involved in the organization of the epithelium along the segmental border during mouse somitogenesis. *Dev. Biol.* **254**, 248–261.

**Ricard-Blum, S.** (2011). The Collagen Family. *Cold Spring Harb. Perspect. Biol.* **3**, 1–19.

**Riedel-Kruse, I. H., Muller, C. and Oates, A. C.** (2007). Synchrony dynamics during initiation, failure, and rescue of the Segmentation Clock. *Science (80-. ).* **317**, 1911–1915.

**Rifes, P. and Thorsteinsdóttir, S.** (2012). Extracellular matrix assembly and 3D organization during paraxial mesoderm development in the chick embryo. *Dev. Biol.* **368**, 370–381.

**Rifes, P., Carvalho, L., Lopes, C., Andrade, R. P., Rodrigues, G., Palmeirim, I. and Thorsteinsdóttir, S.** (2007). Redefining the role of ectoderm in somitogenesis: a player in the formation of the fibronectin matrix of presomitic mesoderm. *Development* **134**, 3155–3165.

**Ringer, P., Colo, G., Fässler, R. and Grashoff, C.** (2017). Sensing the mechano-chemical properties of the extracellular matrix. *Matrix Biol.* **64**, 6–16.

**Rovasio, R. A., Delouvee, A., Yamada, K. M., Timpl, R. and Thiery, J. P.** (1983). Neural crest cell migration: requirements for exogenous fibronectin and high cell density. *J. Cell Biol.* **96**, 462–73.

**Rowton, M., Ramos, P., Anderson, D. M., Rhee, J. M., Cunliffe, H. E. and Rawls, A.** (2013). Regulation of mesenchymal-to-epithelial transition by PARAXIS during somitogenesis. *Dev. Dyn.* **242**, 1332–1344.

**Rozario, T. and DeSimone, D. W.** (2010). The extracellular matrix in development and morphogenesis: A dynamic view. *Dev. Biol.* **341**, 126–140.

**Ruoslahti, E.** (1988). Fibronectin and its receptors. *Annu. Rev. Biochem.* **57**, 375–413.

**Saga, Y.** (2012). The mechanism of somite formation in mice. *Curr. Opin. Genet. Dev.* **22**, 331–338.

**Saga, Y. and Takeda, H.** (2001). The making of the somite: molecular events in vertebrate segmentation. *Nat. Rev. Genet.* **2**, 835–845.

**Saga, Y., Hata, N., Koseki, H. and Taketo, M. M.** (1997). Mesp2: a novel mouse gene expressed in the presegmented mesoderm and essential for segmentation initiation. *Genes Dev.* **11**, 1827–1839.

**Sakai, Y., Meno, C., Fujii, H., Nishino, J., Shiratori, H., Saijoh, Y., Rossant, J. and Hamada, H.** (2001). The retinoic acid-inactivating enzyme CYP26 is essential for establishing an uneven distribution of retinoic acid along the anterio-posterior axis within the mouse embryo. *Genes Dev.* **15**, 213–25.

**Sakai, T., Li, S., Docheva, D., Grashoff, C., Sakai, K., Kostka, G., Braun, A., Pfeifer, A., Yurchenco, P. D. and Fässler, R.** (2003). Integrin-linked kinase (ILK) is required for polarizing the epiblast, cell adhesion, and controlling actin accumulation. *Genes Dev.* **17**, 926–40.

**Sambasivan, R., Kuratani, S. and Tajbakhsh, S.** (2011). An eye on the head: the development and evolution of craniofacial muscles. *Development* **138**, 2401–15.

**Sato, Y., Yasuda, K. and Takahashi, Y.** (2002). Morphological boundary forms by a novel inductive event mediated by Lunatic fringe and Notch during somitic segmentation. *Development* **129**, 3633–44.

**Sawada, K. and Aoyama, H.** (1999). Fate maps of the primitive streak in chick and quail embryo: Ingression timing of progenitor cells of each rostro-caudal axial level of somites. *Int. J. Dev. Biol.* **43**, 809–815.

**Sawada, a, Fritz, a, Jiang, Y. J., Yamamoto, a, Yamasu, K., Kuroiwa, a, Saga, Y. and Takeda, H.** (2000). Zebrafish Mesp family genes, mesp-a and mesp-b are segmentally expressed in the presomitic mesoderm, and Mesp-b confers the anterior identity to the developing somites. *Development* **127**, 1691–1702.

**Sawada, A., Shinya, M., Jiang, Y. J., Kawakami, A., Kuroiwa, A. and Takeda, H.** (2001). Fgf/MAPK signalling is a crucial positional cue in somite boundary formation. *Development* **128**, 4873–80.

**Scaal, M.** (2016). Early development of the vertebral column. *Semin. Cell Dev. Biol.* **49**, 83–91.

**Scaal, M. and Christ, B.** (2004). Formation and differentiation of the avian dermomyotome. *Anat. Embryol. (Berl).* **208**, 411–424.

**Schaller, M. D.** (2010). Cellular functions of FAK kinases: insight into molecular mechanisms and novel functions. *J. Cell Sci.* **123**, 1007–13.

**Schambony, A., Kunz, M. and Gradl, D.** (2004). Cross-regulation of Wnt signaling and cell adhesion. *Differentiation* **72**, 307–318.

**Schiller, H. B., Hermann, M.-R., Polleux, J., Vignaud, T., Zanivan, S., Friedel, C. C., Sun, Z., Raducanu, A., Gottschalk, K.-E., Théry, M., et al.** (2013). β1- and αv-class integrins cooperate to regulate myosin II during rigidity sensing of fibronectin-based microenvironments. *Nat. Cell Biol.* **15**, 625–636.

**Schlunck, G., Han, H., Wecker, T., Kampik, D., Meyer-ter-Vehn, T. and Grehn, F.** (2008). Substrate rigidity modulates cell matrix interactions and protein expression in human trabecular meshwork cells. *Invest. Ophthalmol. Vis. Sci.* **49**, 262–9.

**Schoenwolf, G. C.** (1979). Observations on closure of the neuropores in the chick embryo. *Am. J. Anat.* **155**, 445–465.

**Schoenwolf, G. C., Garcia-Martinez, V. and Dias, M. S.** (1992). Mesoderm movement and fate during avian gastrulation and neurulation. *Dev. Dyn.* **193**, 235–248.

**Schrägle, J., Huang, R., Christ, B. and Pröls, F.** (2004). Control of the temporal and spatial Uncx4.1 expression in the paraxial mesoderm of avian embryos. *Anat. Embryol. (Berl).* **208**, 323–32.

**Schröter, C., Herrgen, L., Cardona, A., Brouhard, G. J., Feldman, B. and Oates, A. C.** (2008). Dynamics of zebrafish somitogenesis. *Dev. Dyn.* **237**, 545–53.

**Schröter, C., Ares, S., Morelli, L. G., Isakova, A., Hens, K., Soroldoni, D., Gajewski, M., Jülicher, F., Maerkl, S. J., Deplancke, B., et al.** (2012). Topology and dynamics of the Zebrafish Segmentation Clock core circuit. *PLoS Biol.* **10**, e1001364.

**Schwartz, M. A.** (2010). Integrins and extracellular matrix in mechanotransduction. *Cold Spring Harb. Perspect. Biol.* **2**, a005066–a005066.

**Schwarzbauer, J. E.** (1991). Alternative splicing of fibronectin: three variants, three functions. *Bioessays* **13**, 527–533.

**Schwarzbauer, J. E. and DeSimone, D. W.** (2011). Fibronectins, their fibrillogenesis, and in vivo functions. *Cold Spring Harb. Perspect. Biol.* **3**, 1–19.

**Sechler, J. L., Corbett, S. A. and Schwarzbauer, J. E.** (1997). Modulatory roles for integrin activation and the synergy site of fibronectin during matrix assembly. *Mol. Biol. Cell* **8**, 2563–73.

**Sechler, J. L., Cumiskey, a M., Gazzola, D. M. and Schwarzbauer, J. E.** (2000). A novel RGD-independent fibronectin assembly pathway initiated by alpha4beta1 integrin binding to the alternatively spliced V region. *J. Cell Sci.* **113 ( Pt 8**, 1491–1498.

**Shanmugalingam, S. and Wilson, S. W.** (1998). Isolation, expression and regulation of a zebrafish paraxis homologue. *Mech. Dev.* **78**, 85–9.

**Sheng, G., dos Reis, M. and Stern, C. D.** (2003). Churchill, a Zinc Finger transcriptional activator, regulates the transition between gastrulation and neurulation. *Cell* **115**, 603–613.

**Shih, N. P., François, P., Delaune, E. A. and Amacher, S. L.** (2015). Dynamics of the slowing segmentation clock reveal alternating two-segment periodicity. *Development* **142**, 1785–93.

**Singh, P., Carraher, C. and Schwarzbauer, J. E.** (2010). Assembly of fibronectin extracellular matrix. *Annu. Rev. Cell Dev. Biol.* **26**, 397–419.

**Solursh, M., Fisher, M., Meier, S. and Singley, C. T.** (1979). The role of extracellular matrix in the formation of the sclerotome. *J. Embryol. Exp. Morphol.* **54**, 75–98.

**Sonnen, K. F., Lauschke, V. M., Uraji, J., Falk, H. J., Petersen, Y., Funk, M. C., Beaupeux, M., François, P., Merten, C. A. and Aulehla, A.** (2018). Modulation of phase shift between Wnt and Notch signaling oscillations controls mesoderm segmentation. *Cell* **172**, 1079–1090.e12.

**Sottile, J. and Hocking, D. C.** (2002). Fibronectin polymerization regulates the composition and stability of extracellular matrix fibrils and cell-matrix adhesions. *Mol. Biol. Cell* **13**, 3546–59.

**Soza-Ried, C., Ozturk, E., Ish-Horowicz, D. and Lewis, J.** (2014). Pulses of Notch activation synchronise oscillating somite cells and entrain the zebrafish segmentation clock. *Development* **141**, 1780–1788.

**Stafford, D. a, Brunet, L. J., Khokha, M. K., Economides, A. N. and Harland, R. M.** (2011). Cooperative activity of noggin and gremlin 1 in axial skeleton development. *Development* **138**, 1005–1014.

**Stern, C. D.** (2004). Gastrulation in the chick. In Gastrulation: From cells to embryo. New York: Cold Spring Harbor Laboratory Press.

**Stern, C. D. and Keynes, R. J.** (1987). Interactions between somite cells: the formation and maintenance of segment boundaries in the chick embryo. *Development* **99**, 261–272.

**Stern, C. D., Fraser, S. E., Keynes, R. J. and Primmett, D. R.** (1988). A cell lineage analysis of segmentation in the chick embryo. *Development* **104 Suppl**, 231–44.

**Strachan, L. R. and Condic, M. L.** (2003). Neural crest motility and integrin regulation are distinct in cranial and trunk populations. *Dev. Biol.* **259**, 288–302.

**Streuli, C. H.** (2009). Integrins and cell-fate determination. *J. Cell Sci.* **122**, 171–177.

**Streuli, C. H., Bailey, N. and Bissell, M. J.** (1991). Control of mammary epithelial differentiation: basement membrane induces tissue-specific gene expression in the absence of cell-cell interaction and morphological polarity. *J. Cell Biol.* **115**, 1383–95.

**Sun, X., Meyers, E. N., Lewandoski, M. and Martin, G. R.** (1999). Targeted disruption of Fgf8 causes failure of cell migration in the gastrulating mouse embryo. *Genes Dev.* **13**, 1834–1846.

**Sun, L., Zou, Z., Collodi, P., Xu, F., Xu, X. and Zhao, Q.** (2005). Identification and characterization of a second fibronectin gene in zebrafish. *Matrix Biol.* **24**, 69–77.

**Swiatek, P. J., Lindsell, C. E., del Amo, F. F., Weinmaster, G. and Gridley, T.** (1994). Notch1 is essential for postimplantation development in mice. *Genes Dev.* **8**, 707–719.

**Takahashi, Y., Koizumi, K., Takagi, A., Kitajima, S., Inoue, T., Koseki, H. and Saga, Y.** (2000). Mesp2 initiates somite segmentation through the Notch signalling pathway. *Nat. Genet.* **25**, 390–6.

**Takahashi, Y., Inoue, T., Gossler, A. and Saga, Y.** (2003). Feedback loops comprising Dll1, Dll3 and Mesp2, and differential involvement of Psen1 are essential for rostrocaudal patterning of somites. *Development* **130**, 4259–68.

**Takahashi, Y., Sato, Y., Suetsugu, R. and Nakaya, Y.** (2005). Mesenchymal-to-epithelial transition during somitic segmentation: A novel approach to studying the roles of Rho family GTPases in morphogenesis. *Cells Tissues Organs* **179**, 36–42.

**Takahashi, S., Leiss, M., Moser, M., Ohashi, T., Kitao, T., Heckmann, D., Pfeifer, A., Kessler, H., Takagi, J., Erickson, H. P., et al.** (2007). The RGD motif in fibronectin is essential for development but dispensable for fibril assembly. *J. Cell Biol.* **178**, 167–178.

**Takashima, Y., Ohtsuka, T., Gonzalez, A., Miyachi, H. and Kageyama, R.** (2011). Intronic delay is essential for oscillatory expression in the segmentation clock. *Proc. Natl. Acad. Sci.* **108**, 3300–3305.

**Takemoto, T., Uchikawa, M., Yoshida, M., Bell, D. M., Lovell-Badge, R., Papaioannou, V. E. and Kondoh, H.** (2011). Tbx6-dependent Sox2 regulation determines neural or mesodermal fate in axial stem cells. *Nature* **470**, 394–398.

**Tam, P. P.** (1981). The control of somitogenesis in mouse embryos. *J. Embryol. Exp. Morphol.* **65 Suppl**, 103–28.

**Tamkun, J. W., DeSimone, D. W., Fonda, D., Patel, R. S., Buck, C., Horwitz, A. F. and Hynes, R. O.** (1986). Structure of integrin, a glycoprotein involved in the transmembrane linkage between fibronectin and actin. *Cell* **46**, 271–82.

**Tenin, G., Wright, D., Ferjentsik, Z., Bone, R., McGrew, M. J. and Maroto, M.** (2010). The chick somitogenesis oscillator is arrested before all paraxial mesoderm is segmented into somites. *BMC Dev. Biol.* **10**, 24.

**Testaz, S., Jarov,  a, Williams, K. P., Ling, L. E., Koteliansky, V. E., Fournier-Thibault, C. and Duband, J. L.** (2001). Sonic hedgehog restricts adhesion and migration of neural crest cells independently of the Patched- Smoothened-Gli signaling pathway. *Proc. Natl. Acad. Sci. U. S. A.* **98**, 12521–12526.

**Thiery, J. P., Duband, J. L., Rutishauser, U. and Edelman, G. M.** (1982). Cell adhesion molecules in early chicken embryogenesis. *Proc. Natl. Acad. Sci. U. S. A.* **79**, 6737–41.

**Thorsteinsdóttir, S., Deries, M., Cachaço, A. S. and Bajanca, F.** (2011). The extracellular matrix dimension of skeletal muscle development. *Dev. Biol.* **354**, 191–207.

**Torr, E. E., Ngam, C. R., Bernau, K., Tomasini-Johansson, B., Acton, B. and Sandbo, N.** (2015). Myofibroblasts exhibit enhanced fibronectin assembly that is intrinsic to their contractile phenotype. *J. Biol. Chem.* **290**, 6951–61.

**Totaro, A., Castellan, M., Di Biagio, D. and Piccolo, S.** (2018). Crosstalk between YAP/TAZ and Notch Signaling. *Trends Cell Biol.* **xx**, 1–14.

**Trinh, L. a. and Stainier, D. Y. R.** (2004). Fibronectin regulates epithelial organization during myocardial migration in zebrafish. *Dev. Cell* **6**, 371–382.

**Tseng, H.-T. and Jamrich, M.** (2004). Identification and developmental expression of Xenopus paraxis. *Int. J. Dev. Biol.* **48**, 1155–8.

**Turner, C. J., Badu-Nkansah, K., Crowley, D., van der Flier, A. and Hynes, R. O.** (2015). $\alpha$5 and $\alpha$v integrins cooperate to regulate vascular smooth muscle and neural crest functions in vivo. *Development* **142**, 797–808.

**Vega, M. E. and Schwarzbauer, J. E.** (2016). Collaboration of fibronectin matrix with other extracellular signals in morphogenesis and differentiation. *Curr. Opin. Cell Biol.* **42**, 1–6.

**Venters, S. J. and Ordahl, C. P.** (2002). Persistent myogenic capacity of the dermomyotome dorsomedial lip and restriction of myogenic competence. *Development* **129**, 3873–85.

**Vicente-Manzanares, M., Choi, C. K. and Horwitz, A. R.** (2009). Integrins in cell migration - the actin connection. *J. Cell Sci.* **122**, 1473–1473.

**Wahl, M. B., Deng, C., Lewandoski, M. and Pourquie, O.** (2007). FGF signaling acts upstream of the NOTCH and WNT signaling pathways to control segmentation clock oscillations in mouse somitogenesis. *Development* **134**, 4033–4041.

**Wang, X. and Astrof, S.** (2015). Neural crest cell-autonomous roles of fibronectin in cardiovascular development. *Development*.

**Watanabe, T., Sato, Y., Saito, D., Tadokoro, R. and Takahashi, Y.** (2009). EphrinB2 coordinates the formation of a morphological boundary and cell epithelialization during somite segmentation. *Proc. Natl. Acad. Sci.* **106**, 7467–7472.

**Watt, F. M.** (2002). Role of integrins in regulating epidermal adhesion, growth and differentiation. *EMBO J.* **21**, 3919–26.

**Wayner, E. A., Garcia-Pardo, A., Humphries, M. J., McDonald, J. A. and Carter, W. G.** (1989). Identification and characterization of the T lymphocyte adhesion receptor for an alternative cell attachment domain (CS-1) in plasma fibronectin. *J. Cell Biol.* **109**, 1321–30.

**Wennerberg, K., Lohikangas, L., Gullberg, D., Pfaff, M., Johansson, S. and Fässler, R.** (1996). Beta 1 integrin-dependent and -independent polymerization of fibronectin. *J. Cell Biol.* **132**, 227–38.

**Wickstrom, S. A., Radovanac, K. and Fassler, R.** (2011). Genetic analyses of integrin signaling. *Cold Spring Harb. Perspect. Biol.* **3**, a005116–a005116.

**Wickström, S. A., Lange, A., Montanez, E. and Fässler, R.** (2010). The ILK/PINCH/parvin complex: the kinase is dead, long live the pseudokinase! *EMBO J.* **29**, 281–91.

**Wierzbicka-Patynowski, I. and Schwarzbauer, J. E.** (2003). The ins and outs of fibronectin matrix assembly. *J. Cell Sci.* **116**, 3269–3276.

**Wijelath, E. S., Rahman, S., Murray, J., Patel, Y., Savidge, G. and Sobel, M.** (2004). Fibronectin promotes VEGF-induced CD34 cell differentiation into endothelial cells. *J. Vasc. Surg.* **39**, 655–60.

**Wijelath, E. S., Rahman, S., Namekata, M., Murray, J., Nishimura, T., Mostafavi-Pour, Z., Patel, Y., Suda, Y., Humphries, M. J. and Sobel, M.** (2006). Heparin-II domain of fibronectin is a vascular endothelial growth factor-binding domain: Enhancement of VEGF biological activity by a singular growth factor/matrix protein synergism. *Circ. Res.* **99**, 853–860.

**Wilkinson, D. G., Bhatt, S. and Herrmann, B. G.** (1990). Expression pattern of the mouse T gene and its role in mesoderm formation. *Nature* **343**, 657–659.

**Wilson, V., Manson, L., Skarnes, W. C. and Beddington, R. S. P.** (1995). The T gene is necessary for normal mesodermal morphogenetic cell movements during gastrulation. *Development* **121**, 877–86.

**Wolfenson, H., Lavelin, I. and Geiger, B.** (2013). Dynamic regulation of the structure and functions of integrin adhesions. *Dev. Cell* **24**, 447–58.

**Wong, P. C., Zheng, H., Chen, H., Becher, M. W., Sirinathsinghji, D. J. S., Trumbauer, M. E., Chen, H. Y., Price, D. L., Van der Ploeg, L. H. T. and Sisodia, S. S.** (1997). Presenilin 1 is required for Notch 1 and Dll1 expression in the paraxial mesoderm. *Nature* **387**, 288–292.

**Wu, C.** (2001). ILK interactions. *J. Cell Sci.* **114**, 2549–50.

**Wu, C., Keivens, V. M., O'Toole, T. E., McDonald, J. a and Ginsberg, M. H.** (1995). Integrin activation and cytoskeletal interaction are essential for the assembly of a fibronectin matrix. *Cell* **83**, 715–724.

**Wu, C., Hughes, P. E., Ginsberg, M. H. and McDonald, J. A.** (1996). Identification of a New Biological Function for the Integrin α v β 3 : Initiation of Fibronectin Matrix Assembly. *Cell Adhes. Commun.* **4**, 149–158.

**Yamaguchi, T. P., Takada, S., Yoshikawa, Y., Wu, N. and McMahon, A. P.** (1999). T (Brachyury) is a direct target of Wnt3a during paraxial mesoderm specification. *Genes Dev.* **13**, 3185–3190.

**Yang, J. T. and Hynes, R. O.** (1996). Fibronectin receptor functions in embryonic cells deficient in alpha 5 beta 1 integrin can be replaced by alpha V integrins. *Mol. Biol. Cell* **7**, 1737–1748.

**Yang, J. T., Rayburn, H. and Hynes, R. O.** (1993). Embryonic mesodermal defects in alpha 5 integrin-deficient mice. *Development* **119**, 1093–105.

**Yang, J. T., Bader, B. L., Kreidberg, J. a, Ullman-Culleré, M., Trevithick, J. E. and Hynes, R. O.** (1999). Overlapping and independent functions of fibronectin receptor integrins in early mesodermal development. *Dev. Biol.* **215**, 264–77.

**Yasuhiko, Y., Haraguchi, S., Kitajima, S., Takahashi, Y., Kanno, J. and Saga, Y.** (2006). Tbx6-mediated Notch signaling controls somite-specific Mesp2 expression. *Proc. Natl. Acad. Sci. U. S. A.* **103**, 3651–6.

**Yoneda, A., Multhaupt, H. A. B. and Couchman, J. R.** (2005). The Rho kinases I and II regulate different aspects of myosin II activity. *J. Cell Biol.* **170**, 443–453.

**Yoshino, T., Saito, D., Atsuta, Y., Uchiyama, C., Ueda, S., Sekiguchi, K. and Takahashi, Y.** (2014). Interepithelial signaling with nephric duct is required for the formation of overlying coelomic epithelial cell sheet. *Proc. Natl. Acad. Sci. U. S. A.* **111**, 6660–5.

**Yurchenco, P. D.** (2011). Basement membranes: Cell scaffoldings and signaling platforms. *Cold Spring Harb. Perspect. Biol.* **3**, 1–27.

**Zaidel-Bar, R. and Geiger, B.** (2010). The switchable integrin adhesome. *J. Cell Sci.* **123**, 1385–1388.

**Zákány, J., Kmita, M., Alarcon, P., de la Pompa, J. L. and Duboule, D.** (2001). Localized and transient transcription of Hox genes suggests a link between patterning and the segmentation clock. *Cell* **106**, 207–17.

**Zamir, E. a, Czirók, A., Cui, C., Little, C. D. and Rongish, B. J.** (2006). Mesodermal cell displacements during avian gastrulation are due to both individual cell-autonomous and convective tissue movements. *Proc. Natl. Acad. Sci. U. S. A.* **103**, 19806–19811.

**Zhang, N. and Gridley, T.** (1998). Defects in somite formation in lunatic fringe-deficient mice. *Nature* **394**, 374–377.

**Zhang, Z., Morla, A. O., Vuori, K., Bauer, J. S., Juliano, R. L. and Ruoslahti, E.**

(1993). The alpha v beta 1 integrin functions as a fibronectin receptor but does not support fibronectin matrix assembly and cell migration on fibronectin. *J. Cell Biol.* **122**, 235–42.

**Zhang, N., Norton, C. R. and Gridley, T.** (2002). Segmentation defects of Notch pathway mutants and absence of a synergistic phenotype in lunatic fringe/radical fringe double mutant mice. *genesis* **33**, 21–28.

**Zollinger, A. J. and Smith, M. L.** (2017). Fibronectin, the extracellular glue. *Matrix Biol.* **60–61**, 27–37.

# Chapter 2

## Fibronectin assembly during early embryo development: a versatile communication system between cells and tissues

*For an idea that does not first seem insane, there is no hope.*
— Albert Einstein

# Fibronectin assembly during early embryo development: a versatile communication system between cells and tissues.

Patrícia Gomes de Almeida, Gonçalo G. Pinheiro, Andreia M. Nunes*, André B. Gonçalves* and Sólveig Thorsteinsdóttir

*Developmental Dynamics* 245, 520–535, 2016

Centre for Ecology, Evolution and Environmental Change, Departamento de Biologia Animal, Faculdade de Ciências, Universidade de Lisboa, 1749-016 Lisboa, Portugal
* these authors contributed equally.

Contribution for the publication:

| | Experimental work depicted in Fig. | | | | | | | | Manuscript writing |
|---|---|---|---|---|---|---|---|---|---|
| | 1 | 2 | 3 | 4 | 5 | 6 | 7 | 8 | |
| Design and concept | III | III | III | III | III | III | III | III | III |
| Execution | II | III | III | III | III | III | III | III | |
| Analysis and interpretation | III | III | III | III | III | III | III | III | |

**Legend:**
- ...... non applicable
O ..... no intervention
I ....... minor contribution
II ...... moderate contribution
III .... major contribution/full execution

Note: this contribution does not exclude other contributions, similar or not, from the remaining authors

DEVELOPMENTAL DYNAMICS 245:520–535, 2016
DOI: 10.1002/DVDY.24391

PATTERNS & PHENOTYPES

# Fibronectin Assembly During Early Embryo Development: A Versatile Communication System Between Cells and Tissues

**Patrícia Gomes de Almeida, Gonçalo G. Pinheiro, Andreia M. Nunes, André B. Gonçalves, and Sólveig Thorsteinsdóttir***

Centre for Ecology, Evolution and Environmental Change (cE3c), Departamento de Biologia Animal, Faculdade de Ciências, Universidade de Lisboa, Lisboa, Portugal

**Background:** **Fibronectin extracellular matrix is essential for embryogenesis. Its assembly is a cell-mediated process where secreted fibronectin dimers bind to integrin receptors on receiving cells, which actively assemble fibronectin into a fibrillar matrix. During development, paracrine communication between tissues is crucial for coordinating morphogenesis, typically being mediated by growth factors and their receptors. Recent reports of situations where fibronectin is produced by one tissue and assembled by another, with implications on tissue morphogenesis, suggest that fibronectin assembly may also be a paracrine communication event in certain contexts.** **Results:** **Here we addressed which tissues express fibronectin (*Fn1*) while also localizing assembled fibronectin matrix and determining the mRNA expression and/or protein distribution pattern of integrins α5 and αV, α chains of the major fibronectin assembly receptors, during early chick and mouse development. We found evidence supporting a paracrine system in fibronectin matrix assembly in several tissues, including immature mesenchymal tissues, components of central and peripheral nervous system and developing muscle.** **Conclusions:** **Thus, similarly to growth factor signaling, fibronectin matrix assembly during early development can be both autocrine and paracrine. We therefore propose that it be considered a cell–cell communication event at the same level and significance as growth factor signaling during embryogenesis. *Developmental Dynamics 245:520–535, 2016*. © 2016 Wiley Periodicals, Inc.**

**Key words:** extracellular matrix; fibronectin; integrin alpha 5; paracrine signaling; autocrine signaling; embryogenesis

Submitted 8 July 2015; First Decision 20 January 2016; Accepted 25 January 2016; Published online 4 February 2016

## Introduction

The extracellular matrix (ECM) is a key regulator of vertebrate development. More than just providing mechanical support to cells and tissues, it also provides biochemical and biomechanical cues crucial for cell differentiation, tissue morphogenesis, and homeostasis (Frantz et al., 2010; Rozario and DeSimone, 2010). In addition, the ECM cooperates with other signaling pathways and controls gene expression, with effects in cell physiology, morphology, and differentiation (Goody and Henry, 2010; Rozario and DeSimone, 2010).

Fibronectin is a 230–270 kDa homodimeric glycoprotein, and is one of the most abundant ECM molecules during early vertebrate development (e.g., Wartiovaara et al., 1979; Duband and Thiery, 1982; Boucaut and Darribère, 1983). Each fibronectin dimer is composed of three types of repeating modules, types I, II, and III, which include binding domains for cell surface receptors, other ECM components, and other fibronectin molecules. In the chick and all mammals analyzed so far, fibronectin is produced from a single gene, *Fn1* (Singh et al., 2010). The transcripts can, however, undergo alternative splicing generating different fibronectin isoforms, which differ in the presence or absence of the alternatively spliced segments EIIIA, EIIIB, and V, but in the early chick embryo *Fn1* mRNA contains all three alternatively spliced segments (ffrench-Constant and Hynes, 1989).

After translation of the mRNA and the intracellular production of the fibronectin homodimer, it is secreted into the extracellular space in a soluble, compact conformation (Mao and Schwarzbauer, 2005). Integrins are heterodimeric transmembrane receptors composed of an α and a β subunit, which bind ECM molecules and connect them to the cytoskeleton and the associated signaling platforms (Barczyk et al., 2010). Integrins can exist in an active and inactive state, regulated by intracellular signals usually referred to as inside-out signaling, thus modulating their interaction with their extracellular ligands (Barczyk et al., 2010). Fibronectin matrix assembly starts when the compact fibronectin dimers bind to the active α5β1 integrin on the surface of cells through the RGD (Arg-Gly-Asp) and synergy sites which leads to

Grant sponsor: Fundação para a Ciência e a Tecnologia (FCT, Portugal); Grant numbers: PTDC/SAU-OBD/103771/2008, PTDC/SAU-BID/120130/2010, PTDC/SAU-ORG/118297/2010, PEst-OE/BIA/UI0329/2011, SFRH/BD/86980/2012, SFRH/BD/86985/2012, SFRH/BD/90827/2012.
A.M. Nunes and A.B. Gonçalves contributed equally to this work.
*Correspondence to: Sólveig Thorsteinsdóttir, Departamento de Biologia Animal, Faculdade de Ciências, Universidade de Lisboa 1749-016, Lisboa, Portugal. E-mail: solveig@fc.ul.pt

Article is online at: http://onlinelibrary.wiley.com/doi/10.1002/dvdy.24391/abstract

a conformational change that extends the dimer, exposes fibronectin–fibronectin interaction domains and allows fibril formation (Mao and Schwarzbauer, 2005; Singh et al., 2010). Notably, although α5β1 integrin is the major fibronectin receptor responsible for its assembly during development, αV integrins also play a role, because double-null mutants for both α5 and αV show reduced fibronectin assembly and have earlier and more severe defects than those of single mutants (Yang et al., 1993, 1999).

Fibronectin matrices have several important roles during embryonic development. When fibronectin–integrin interactions and matrix assembly are inhibited in *Xenopus laevis* embryos, epiboly and gastrulation movements fail to occur properly, the anterior–posterior axis is shortened and embryos lack heart and blood vessels (Marsden and DeSimone, 2001). Zebrafish embryos mutant for *fn1* have defects in the epithelial organization and migration of myocardial precursor cells, resulting in *cardia bifida* (Trinh and Stainier, 2004). Unlike amniotes, zebrafish has two fibronectin genes, *fn1* and *fn3* (now termed *fn1b*), and when both are absent, the body axis is truncated and somite formation and maturation is compromised (Jülich et al., 2005; Koshida et al., 2005; Snow et al., 2008). Similarly, mouse embryos null for *Fn1* also present a shortened anterior–posterior axis, cardiovascular defects and a general deficit in mesoderm, including impaired somite and notochord formation (George et al., 1993; Georges-Labouesse et al., 1996).

Our previous work has shown that fibronectin is crucial for somitogenesis in the chick embryo (Rifes et al., 2007). The presomitic mesoderm (PSM) expresses *Itga5*, the gene encoding the α chain of the α5β1 integrin, and is surrounded by a complex fibronectin matrix (Rifes et al., 2007; Rifes and Thorsteinsdóttir, 2012). However, *Fn1* mRNA is almost exclusively expressed by the overlying ectoderm (Rifes et al., 2007), suggesting that fibronectin acts like a paracrine factor in this context, with one tissue (the ectoderm) producing and the other (PSM) building the matrix. It is well known that cells are able to assemble exogenous fibronectin. For example, cells derived from *Fn1*-null mouse embryos and cultured in vitro are able to assemble a fibronectin matrix from human fibronectin added to the culture medium (Sottile and Hocking, 2002) and rat plasma fibronectin injected into the blastocoel of amphibian embryos is assembled into a matrix on the blastocoel roof (Darribère and Schwarzbauer, 2000).

More recently, examples of transfer of fibronectin molecules between neighboring cells or tissues in vivo have emerged. For example, analysis of mosaic zebrafish embryos where host cells are *fn1*- and *fn1b*-null and transplanted cells are *Itga5*-null shows that cells expressing *Itga5*, but not *fn1/fn1b*, are able to assemble fibronectin produced by the neighboring *itga5*-null cells (Jülich et al., 2009). In addition, fibronectin–green fluorescent protein (GFP) produced by the posterior tail bud of zebrafish embryos has been shown to be incorporated into the forming somite clefts in the anterior PSM (Jülich et al., 2015). Similarly, fibronectin-EGFP produced by the Wolffian duct was shown to be transferred to the adjacent coelomic epithelium promoting its maturation in a process termed interepithelial signaling (Yoshino et al., 2014).

These observations raise the interesting possibility that fibronectin matrix assembly is a versatile cell–cell communication event, where in addition to the traditional view that cells produce the fibronectin used to build their matrix (autocrine assembly), in certain contexts, the fibronectin protein used to build a matrix is produced by adjacent cells or tissues (paracrine assembly). To determine whether paracrine assembly is a widespread phenomenon during embryo development, we used in situ hybridization and immunohistochemistry in early chick and mouse embryos to address which tissues produce and which tissues assemble fibronectin. Our results indicate that, at the stages under study, a paracrine system of fibronectin matrix assembly is as common as the autocrine system, establishing fibronectin assembly as a paracrine cell–cell communication event in numerous contexts during development.

## Results

### At Early Stages of Chick Development *Fn1* is Primarily Expressed by Nonmesodermal Tissues

During early stages of chick embryo development (from Hamburger and Hamilton stage [HH] 4 to HH8), *Fn1* is expressed in the primitive streak and accompanies its regression (Fig. 1A–D, arrows). At stages HH4 and 5, *Fn1* is also strongly expressed in the lateral epiblast (Fig. 1A,B, white arrowheads). Sections through the streak at HH4 show that *Fn1* is expressed in the epiblast bordering the primitive streak as well as in the streak itself (Fig. 2A, arrow). A continuous fibronectin matrix lines the epiblast (Fig. 2D, arrowhead, G), but is broken up in the primitive streak (Fig. 2D, arrow, G). This is consistent with studies showing that degradation of the epiblast ECM is necessary for the ingression of the mesendoderm (Duband and Thiery, 1982; Krotoski et al., 1986; Nakaya et al., 2008).

Like *Fn1*, *Itga5* is also expressed in the primitive streak at all stages studied (Fig. 1E–H, arrows). At HH5, gastrulation is already under way and prechordal mesoderm, derived from the node, as well as mesoderm spreading laterally from the primitive streak, express *Itga5* (Fig. 1F, gray arrowheads), and this pattern is maintained at HH6–8 (Fig. 1G,H). While integrin α5 protein is detected in the membrane of cells both in the epiblast and the mesoderm (Fig. 2J,M), it is enriched in the midline (insert in Fig. 2J), where the fibronectin matrix is patchy (Fig. 2M, arrow). Integrin αV is present on epiblast cells (Fig. 2P,S), but appears to be downregulated upon their ingression to form the mesoderm (insert in Fig. 2P).

At HH6–8, *Fn1* continues to be expressed in the lateral as well as caudal epiblast (Fig. 1C,D, gray arrowheads) and is also strongly expressed in the nonneural ectoderm (Fig. 1C,D). Of interest, as the neural tube closes, the nonneural ectoderm is brought medially and *Fn1* expression thus becomes increasingly more medial, with a clear border of expression between the neuroepithelium, which does not express *Fn1* or expresses it only faintly, and the presumptive epidermis, which expresses *Fn1* strongly (white arrowheads in Fig. 1C,D). Sections of HH8 embryos confirm this observation (Fig. 2B,C, arrowheads) and show that the hypoblast/lateral endoderm also expresses *Fn1* at this stage (Fig. 2B,C).

Although the mesoderm is mostly negative for *Fn1* (Fig. 2B), immunolocalization of fibronectin at HH8 shows that a fibronectin matrix lines the mesoderm both dorsally and ventrally (Fig. 2E,F,H,I,N,T). The mesoderm expresses *Itga5* (Fig. 1H, gray arrowheads) and stains for integrin α5 (Fig. 2K,N) but not integrin αV (Fig. 2Q,T). Thus the mesoderm of the chick embryo is in a position to assemble the fibronectin synthesized by the nonneural ectoderm, as already suggested for later stages of chick embryo development (Rifes et al., 2007). It is important to note that the mesodermal fibronectin matrix is distinct from the ectodermal and

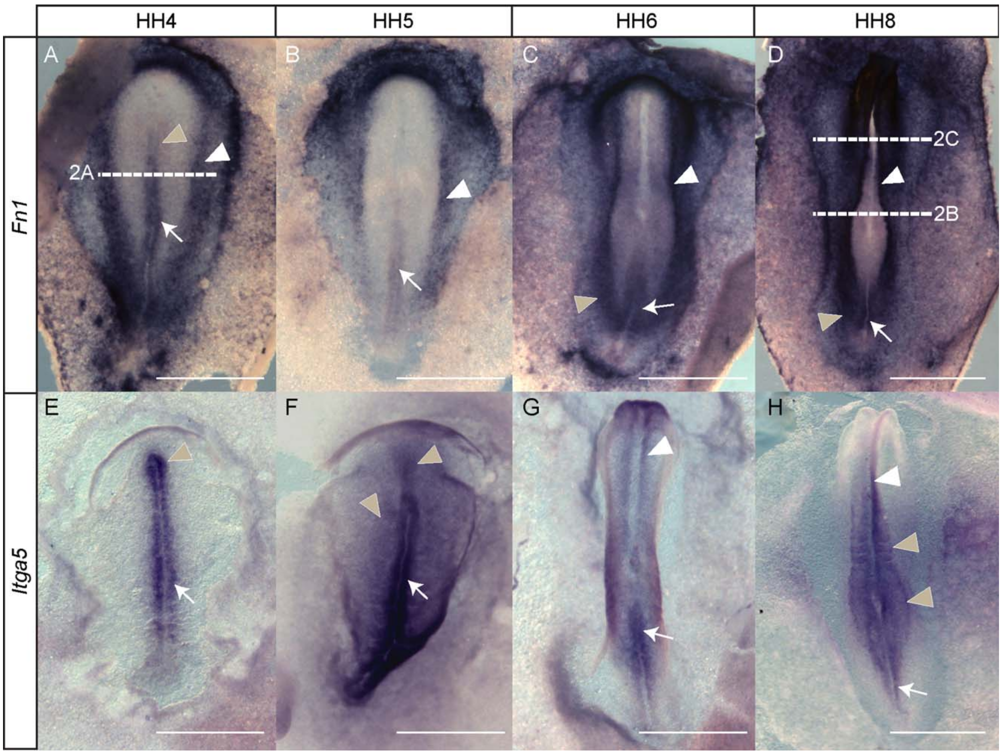


**Fig. 1.** **A–H**: During early chick embryo development, *Fn1* and *Itga5* mRNA expression patterns differ substantially. Expression patterns of the genes encoding for fibronectin, *Fn1* (A–D), and its receptor integrin α5, *Itga5* (E–H), from HH4 to HH8. *Fn1* is only weakly expressed in Hensen's node (A, gray arrowhead), while *Itga5* is strongly expressed in the node (E, gray arrowhead). *Fn1* and *Itga5* are both expressed in the primitive streak and accompany its regression (A–D,E–H, arrows). *Fn1* is strongly expressed by the lateral and caudal epiblast and the nonneural ectoderm at all stages (A–D, white arrowheads). As a consequence of neurulation, the presumptive epidermis moves medially and *Fn1* expression moves with it (C,D, white arrowheads). *Itga5* is strongly expressed in the forming mesoderm (F, gray arrowheads) and is also expressed in the neuroepithelium (G,H, white arrowheads). At HH8, *Itga5* expression is visible in the caudal mesoderm and somites (H, gray arrowheads). Transverse lines in A and D indicate level of sections in Fig. 2A-C. Scale bars = 500 μm.

endodermal matrices (see Fig. 2N, insert; Rifes and Thorsteinsdóttir, 2012). Finally, unlike the situation in the trunk where a fibronectin matrix is mostly restricted to tissue surfaces at these developmental stages (Fig. 2E,F,H,I,N,T), slightly more rostrally, fibronectin is present among the cells of the head mesenchyme (Fig. 2O,U), which are positive for integrin α5 (Fig. 2L,O), but negative for αV (Fig. 2R,U).

A fibronectin matrix progressively separates the notochord from the paraxial mesoderm (Fig. 2E,F, arrows), and both display enriched integrin α5 staining on their surfaces (Fig. 2K, arrowheads, N), indicating integrin clustering at these sites (e.g., Jülich et al., 2009). Fibronectin also surrounds developing blood vessels (Fig. 2E,F, orange arrowheads) which stain strongly for integrin α5, but not αV (data not shown; see Fig. 5D,F). Diffuse staining for integrin α5 is also present in the ectoderm and endoderm (Fig. 2K,L,N,O). Integrin αV is found in both ectoderm and endoderm, but is mostly absent from the mesoderm (Fig. 2Q,R,T,U). Furthermore, as observed in the mouse (Mittal et al., 2010; also see Fig. 3H), fibronectin immunoreactivity separates the dorsal neural folds from the adjacent nonneural ectoderm (Fig. 2F, gray arrowhead).

We conclude that during early stages of chick embryo development, some tissues appear to assemble a fibronectin matrix in a paracrine manner. The epiblast or nonneural ectoderm produce fibronectin, while the mesoderm and neuroepithelium, which appear to cluster α5β1 integrins, are in a position to build the matrix. In other cases, such as the primitive streak, there is co-expression of *Fn1* and *Itga5*, suggesting that gastrulating cells may produce fibronectin protein and assemble it. The fibronectin matrix lining the epiblast/nonneural ectoderm and endoderm also appears to be produced and assembled by these tissues.

### Pattern of Fibronectin Matrix Deposition in the Early Mouse Embryo is Analogous to the Chick, but the *Fn1* Expression Pattern is not Fully Conserved

To determine if this pattern of fibronectin assembly at primitive streak and early somite stages is conserved in the mouse,

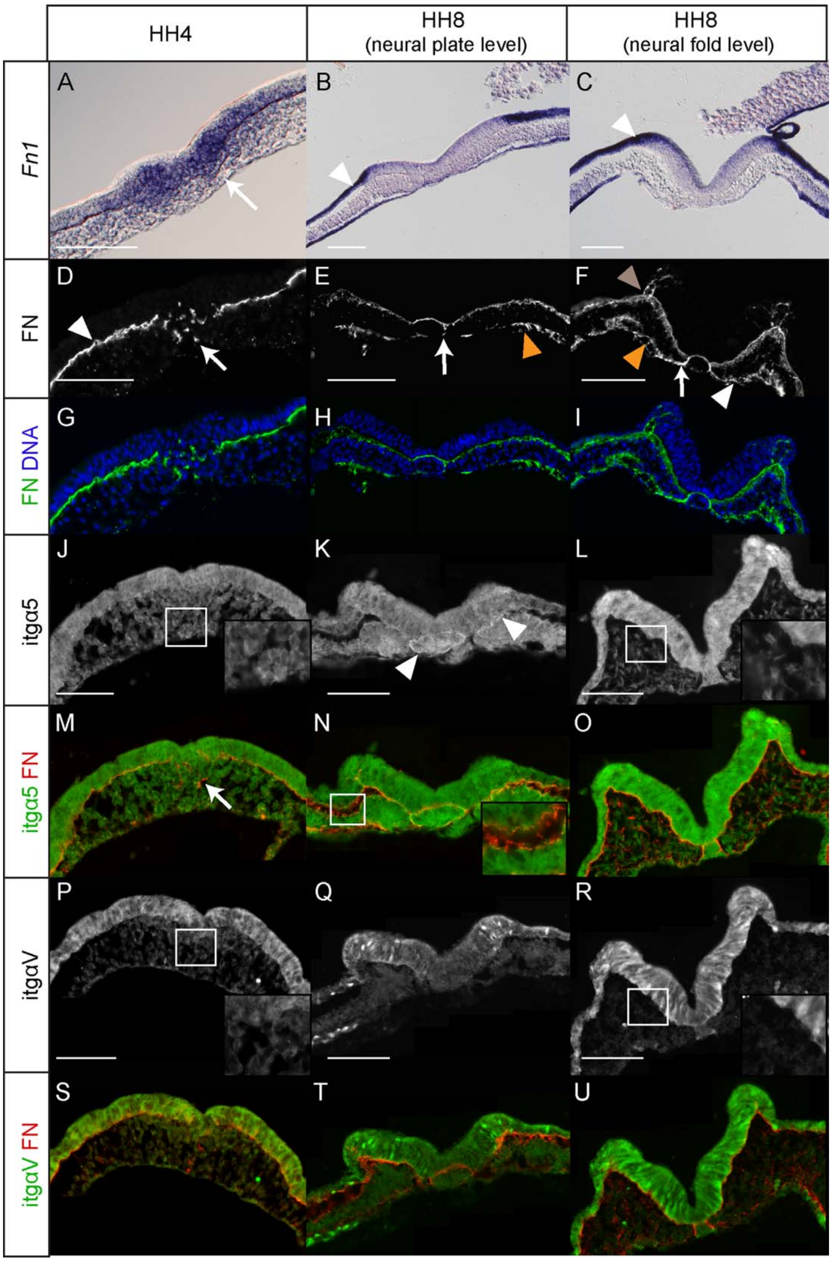


**Fig. 2.** **A–U**: During early chick embryo development, *Fn1* is most strongly expressed by epiblast/nonneural ectoderm and hypoblast/endoderm, while a fibronectin matrix lines all three germ layers. In situ hybridization for *Fn1* mRNA at HH4 (A) and HH8 (B,C). Immunohistochemistry for fibronectin (FN; D–I,M–O,S–U), integrin α5 (itgα5; J–O) and integrin αV (itgαV; P–U) at HH4 (first row) and HH8 (second and third row). At HH4, *Fn1* is expressed in the primitive streak (A, arrow) and the epiblast, and fibronectin lines the epiblast (D, arrowhead) but is patchy in the primitive streak (arrows in D,M). Integrin α5 staining is present both in the epiblast and mesenchyme (J), but is enriched in the midline (insert in J). Integrin αV is present in the epiblast (P), and appears to be down-regulated after ingression (insert in P). At HH8, *Fn1* is expressed by nonneural ectoderm (B,C, arrowheads) and the lateral endoderm/hypoblast (B,C), while fibronectin matrix lines the mesoderm (E,F, white arrowhead). Note that the mesodermal matrix is distinct from the ectodermal matrix (insert in N). Ectoderm, mesoderm and endoderm are positive for integrin α5, which is enriched in the peripheral notochord and on the surface of the mesoderm (K, arrowheads). Further rostrally, strong staining is seen in ectoderm and notochord, and fainter staining in the cephalic mesenchyme (L). The neuroepithelium, ectoderm and endoderm are positive for integrin αV, but staining is very weak or absent in the mesoderm at this stage (Q,R). Scale bars = 200 μm in A–C; 100 μm in D–U.

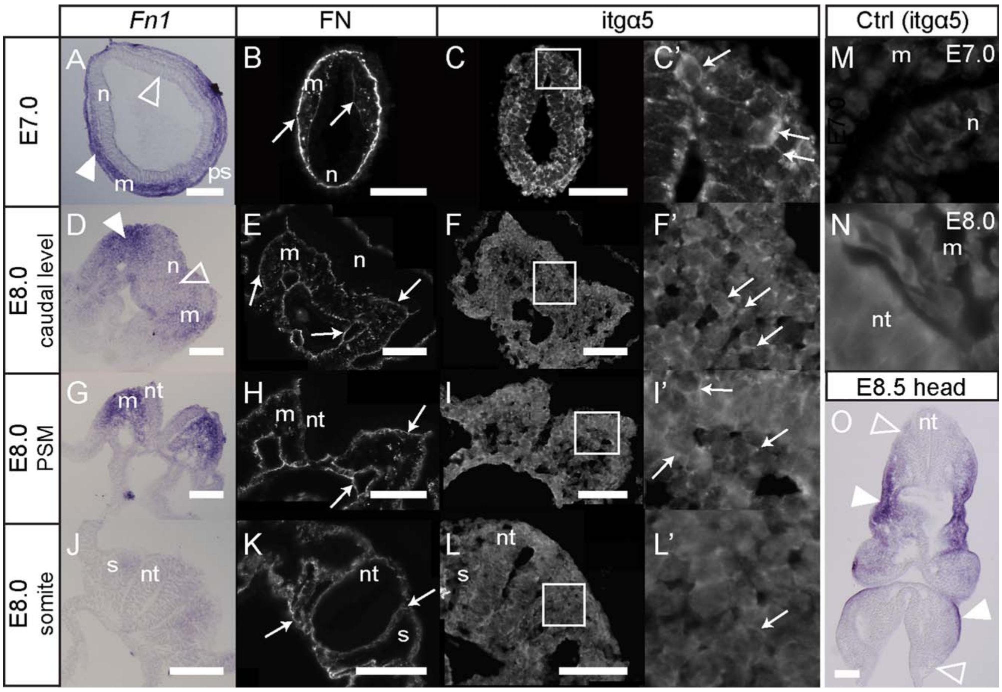


**Fig. 3.** **A–O**: *Fn1* is mostly produced by the mesoderm during early mouse development, while the matrix forms at all tissue boundaries. In situ hybridization for *Fn1* mRNA (first column, O) and immunohistochemistry for fibronectin (second column) and integrin α5 (third and fourth columns) on E7.0 (A–C′), E8.0 (D–L′) and E8.5 (O) mouse embryos. Negative controls for integrin antibody (M–N). At E7.0, *Fn1* expression is restricted to the mesoderm (A, arrowhead) and absent from the neuroepithelium (A, empty arrowhead). Fibronectin lines the endoderm/mesoderm and ectoderm/mesoderm interfaces (B, arrows). Integrin α5 is abundant in both the mesoderm and neuroepithelium (C,C′, arrows). At E8.0 *Fn1* is expressed by the nascent mesoderm (D, arrowhead) and the PSM (G). Weak expression is found in neuroepithelium (D, empty arrowhead, G), caudal and pharyngeal endoderm (D,O). Fibronectin lines tissue boundaries (E,H,K arrows) and is found within the early mesoderm (E,H). Weak staining for integrin α5 is detected on cells of all three germ layers (F,I) as shown for mesoderm (F′, arrows; compare with N) and mesoderm and neuroectoderm (I′, arrows; compare with N). At the somite level, *Fn1* expression is markedly reduced (J) but fibronectin (K) and integrin α5 (L,L′) distribution is maintained. Rostrally (O), *Fn1* is expressed by some (arrowheads), but not all (empty arrowheads), regions of the nonneural ectoderm. m, mesoderm; n, neuroepithelium; nt, neural tube; s, somite. Scale bars = 100 μm.

we analyzed *Fn1* expression and fibronectin protein deposition, as well as integrin localization in embryonic day (E) 7.0–E8.5 mouse embryos. At E7.0, *Fn1* is expressed in the primitive streak and by the mesoderm (Fig. 3A, white arrowhead). Thus, whereas in the chick *Fn1* expression in the streak is not maintained after cells colonize the mesoderm (Fig. 2A), in the mouse *Fn1* expression remains in the mesoderm (Fig. 3A,D,G). Moreover, a faint *Fn1* expression is detected in the caudal endoderm (Fig. 3D,O). *Fn1* is strongly expressed in the mesoderm up until the level of epithelial somites, where it becomes markedly reduced (Fig. 3J), a pattern that is maintained in the trunk at E8.5 and E9.5 (not shown; Mittal et al., 2010; Chen et al., 2015).

Despite these differences, a fibronectin matrix lines the endoderm/mesoderm and ectoderm/mesoderm interfaces (Fig. 3B, arrows) as well as other forming tissue boundaries (Fig. 3E,H,K, arrows), similarly to what is observed in the chick (Fig. 2D–I). Also, like observed in the chick, the neuroepithelium never expresses *Fn1* at the stages under study (Fig. 3A,D,G,J,O, empty arrowheads in A,D). Unlike in the chick, at these early stages of mouse development *Fn1* expression is mostly absent from the nonneural ectoderm (Fig. 3G,J,O). Rostrally *Fn1* is, however, expressed in certain regions of the nonneural ectoderm, for example in pharyngeal ectoderm and the optic eminence (Fig. 3O, arrowheads), as reported previously (Mittal et al., 2010). *Fn1* expression is also detected in pharyngeal endoderm and mesoderm (Fig. 3O, also see Mittal et al., 2010).

Integrin α5 and αV distribution is similar between the two models. Consistently with the results in the chick (Fig. 2J–K), ectodermal, mesodermal, and endodermal cells in the mouse show membrane staining for integrin α5 (Fig. 3C,F,I,L; compare with negative controls in Fig. 3M,N). A faint staining for integrin αV was observed in ectoderm and mesoderm at E7.0, but was absent from the mesoderm at E8.0 (data not shown).

We conclude that albeit having very similar patterns of fibronectin deposition and localization of its receptors, there are differences in the tissue source of fibronectin protein in these two amniote models: in the chick fibronectin protein is primarily produced by nonneural ectoderm and endoderm while in the mouse the main producer is the early mesoderm.

### Sclerotome and Dermomyotome/Dermis Express *Fn1* and Are in a Position to Provide Fibronectin to Neighboring Tissues

As evident from the results from HH4–8, apart from some expression in the primitive streak, *Fn1* is not expressed by the early mesoderm in the chick (also see Rifes et al., 2007). However, *Fn1* expression does come up in the intermediate mesoderm (Rifes et al., 2007; Yoshino et al., 2014) and in the caudal region of epithelialized somites (Rifes et al., 2007) concomitantly with de novo fibronectin matrix assembly within the newly formed somitic clefts (Rifes and Thorsteinsdóttir, 2012). Here we investigated the expression patterns of *Fn1*, *Itga5*, *ItgaV* as well as the pattern of fibronectin matrix accumulation and integrin localization during the stages of somite differentiation in E3–E4 chick embryos as well as *Fn1* expression and protein distribution in E10.5–E11.5 mouse embryos.

*Fn1* expression in the epidermal ectoderm in the chick is now much weaker (Fig. 4A,C,F,J) than at earlier stages (Fig. 2B,C) and the trunk ectoderm is also negative for *Fn1* in the mouse (Fig. 4Q,S). In both models, *Fn1* is expressed in the dermomyotome/dermis and in the sclerotome, but not in the myotome (Fig. 4A,C,F,G,J,K,Q,S).

*Fn1* expression in the sclerotome is not uniform. At both E3 and E4, *Fn1* expression in the central sclerotome (see Christ et al., 2004, for terminology) is stronger caudally than rostrally (Fig. 4A,C, arrowheads). However, immunohistochemistry for fibronectin on coronal sections shows that this enriched expression of *Fn1* is not accompanied by an enrichment of fibronectin matrix in the caudal part of the central sclerotome. Rather, immunoreactivity for fibronectin appears to be slightly increased in the rostral (Fig. 4B,D, arrows) compared with the caudal region. Neural crest cells migrate through the rostral sclerotome and some of them originate the dorsal root ganglia which express *Itga5* (Fig. 5A) and are surrounded by a fibronectin matrix (Fig. 4D, arrowheads). In the ventral sclerotome, which is closest to the notochord, *Fn1* expression is strong and continuous (arrows in Fig. 4 A,C,G,K).

Although *Itga5* mRNA is not detected in the sclerotome (Fig. 5A), integrin α5 protein is found on the cell surface of sclerotomal cells (Fig. 5D–D′,E–E′) and appears to be enriched in close proximity to fibronectin (Fig. 5E′, empty arrowhead). *ItgaV* expression is evident throughout the full extent of the sclerotome (Fig. 5B) and sclerotomal cells are also positive for integrin αV protein (Fig. 5F–F′,G–G′). Of interest, the notochord, which does not express *Fn1* (Fig. 4F,G,J,K), is surrounded by a prominent layer of fibronectin matrix (Fig. 4H,L, arrows), raising the possibility that fibronectin produced by the adjacent ventral sclerotome is incorporated into the matrix surrounding the notochord. Consistent with this hypothesis, the notochord expresses both *Itga5* and *ItgaV* (Fig. 5A,B arrows) and shows strong staining for both integrins α5 and αV (Fig. 5,D–E,D″–E″,F–G,F″–G″).

The myotome does not express *Fn1* in either chick or mouse (Fig. 4F,G,J,K,Q,R, empty arrowheads), but *Fn1* is expressed by the cells in the overlying dermomyotome/dermis and by the underlying central sclerotome (Fig. 4F,J,Q,S, white arrowheads). Nevertheless, a fibronectin matrix is found among the myotomal cells (Fig. 4H,L,R,T, empty arrowheads; also see inserts in L,T). The mouse myotome expresses *Itga5* (Bajanca et al., 2004) and stains positive for integrin αV (Hirsch et al., 1994; Deries et al., 2012), and we found this to be conserved in the chick both at the mRNA (Fig. 5A,B, arrowheads) and protein level (Fig. 5D′,F′, arrowhead). The three-dimensional (3D) reconstructions of fibronectin deposition in the chick myotome at E4 confirm that fibrillar fibronectin immunostaining is found inside the myotome (Fig. 4M,O, arrows), consistent with our results in the mouse (Deries et al., 2012).

These 3D reconstructions also reveal that a complex fibronectin matrix surrounds the dorsomedial lip of the dermomyotome like a "socket" (Fig. 4N,P, arrows), demonstrating that the dorsomedial lip retains an ECM longer than the rest of the dermomyotome as also observed in the mouse (Deries et al., 2012). Moreover, on the medial side of the myotome, in the middle of the segment, a ridge of fibronectin matrix can be identified between the myotome and the sclerotome (Fig. 4P, green arrow), which represents the border between the rostral and caudal sclerotome (Christ et al., 2004). From these results, we conclude that *Fn1* is expressed by the sclerotome and dermomyotome/dermis in both chick and mouse embryos while a fibronectin matrix can be found in or around all the axial tissues.

### During Early Stages of Limb Development, Ectoderm Expresses *Fn1* While a Fibronectin Matrix Fills the Limb Mesenchyme

Fibronectin is thought to play important roles in several aspects of limb bud development. For example, fibronectin has been implicated in the formation of precartilage condensations in the limb mesenchyme (Kulyk et al., 1989; Newman and Bhat, 2007) and as a substrate for the migration of myogenic precursor cells from the hypaxial dermomyotome lip to the forming limb muscle masses (Brand-Saberi et al., 1993). At the stages under study, *Fn1* is strongly expressed by the ectoderm (Fig. 6A–C), with the notable exception of the apical ectodermal ridge where it is either weakly expressed or absent (Fig. 6A–C, empty arrowheads in B,C).

Of interest, the ectoderm on the ventral side of the limb appears to express *Fn1* more strongly than the dorsal ectoderm (Fig. 6A–C, black arrows). In contrast, the limb mesenchyme shows no *Fn1* expression (Fig. 6A–C) except for the proximal-most mesenchyme at E4 which expresses some *Fn1* (Fig. 6C, white arrow) consistent with the onset of chondrogenesis in this region at this stage (Chimal-Monroy et al., 2003). Although the mesenchyme does not express *Fn1*, an extensive fibronectin matrix is found throughout the whole limb mesenchyme (Fig. 6F–H) and is particularly enriched around blood vessels (Fig. 6F–H, arrowheads), consistent with results in the mouse (Cachaço et al., 2005).

Indeed, as suggested by functional studies (Brand-Saberi et al., 1993), this fibronectin matrix may be important for the muscle progenitors that are colonizing the limb, which are surrounded by a fibrillar fibronectin staining (Fig. 6I, arrows in insert). The cells of the limb mesenchyme express *Itga5* mRNA (Fig. 6D, arrows) and integrin α5 protein (Fig. 6E, arrows), and both appear to be enriched in blood vessels (Fig. 6D,E arrowheads). Enlargement of the area of the distal mesenchyme demonstrates more clearly that limb mesenchymal cells are positive for integrin α5

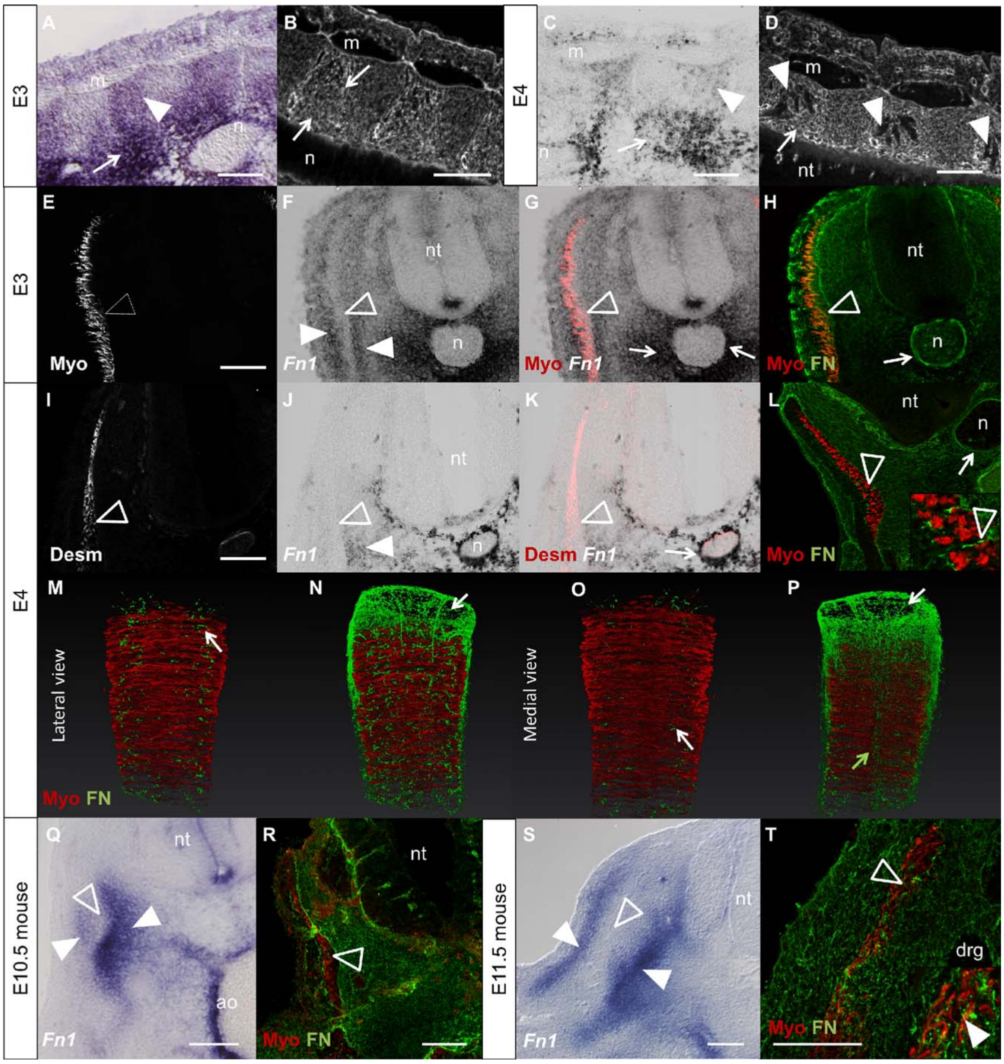


**Fig. 4.** **A–T**: *Fn1* is expressed in the sclerotome and dermomyotome/dermis while fibronectin matrices are much more widespread. *Fn1* expression (A,C) and immunostaining for fibronectin (B,D) on coronal sections of chick sclerotome at E3 (A,B) and E4 (C,D). Combined in situ hybridization for *Fn1* (F,G,J,K) and immunohistochemistry for myosin (E,G) or desmin (I,K) and fibronectin (H) on transverse sections of E3 (E–H) and E4 (I–K) embryos. Immunohistochemistry for myosin and fibronectin on transverse sections at E4 (L). 3D reconstruction of the fibronectin matrix within (M,O) and around (N,P) the myotome at E4. *Fn1* expression (Q,S) and fibronectin localization (R,T) on transverse sections of E10.5 (Q,R) and E11.5 (S,T) mouse embryos. *Fn1* expression is strong in caudal (A,C, arrowheads) and medial sclerotome (A,C, arrows). Fibronectin matrix is assembled throughout the sclerotome (B,D,H,L). The myotome does not express *Fn1* either in chick or mouse (F,G,J,K,Q,S empty arrowheads), but *Fn1* is expressed by dermomyotome and sclerotome in both species (F,J,Q,S, arrowheads). A fibronectin matrix lines the dermomyotome (arrows in N,P), can be found within the myotome (H,L,R,T, empty arrowheads; M,O, arrows) and lines the medial aspect of the myotome (P, green arrow). Myo, myosin heavy chain; Desm, desmin; nt, neural tube; n, notochord; m, myotome; ao, dorsal aorta. Scale bars = 100 μm.

protein (Fig. 6E′), which is consistent with results from the mouse (Bajanca and Thorsteinsdóttir, 2002). In contrast, integrin αV protein can only be detected in the ectoderm and a faint staining can be observed in the distal-most mesenchyme (Fig. 6J–J′). We conclude that the pattern observed in the early chick embryo limb, with *Fn1* being expressed by the ectoderm and assembled by the limb mesenchyme, which expresses integrin α5β1, is yet another example where fibronectin assembly is paracrine.

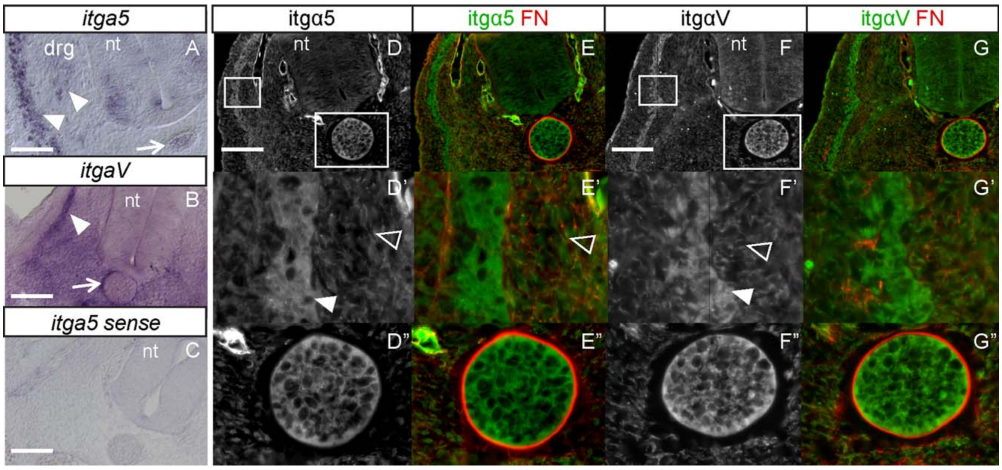


**Fig. 5.** **A–G″**: Integrin α5 and αV are both strongly expressed by myotome and notochord, while αV predominates in the sclerotome. In situ hybridization for *Itga5* (A), *ItgaV* (B) and with *Itga5* sense probe (C) in E3.5 chick embryos. Immunohistochemistry for integrin α5 (D–E″), integrin αV (F–G″) and fibronectin (E–E″,G–G″). The myotome shows strong expression of *Itga5* and *ItgaV* (A,B, arrowheads), and stains strongly for both proteins (D′, F′, arrowheads). The same occurs in the notochord (A,B, arrows, D″, F″). Although no *Itga5* was detected in the sclerotome at this stage (A) a faint staining for integrin α5 can be detected on sclerotomal cells (D′, empty arrowhead). mRNA for *ItgaV* can be detected in the sclerotome (B) and so can the protein (F′, empty arrowhead). nt, neural tube; drg, dorsal root ganglia. Scale bars = 100 μm.

### Endocardium and Epicardium Express *Fn1* While a Fibronectin Matrix is Also Found in the Myocardium During Early Stages of Cardiac Development

This duality of fibronectin expression vs. matrix assembly is also observed in the developing heart, another organ where fibronectin is essential for normal development (Linask and Lash, 1988; George et al., 1993; Trinh and Stainier, 2004; Mittal et al., 2013).

At E3 in the chick and at E10.5 in the mouse, an extensive fibronectin matrix is found in the myocardium of both atria and ventricles (Fig. 7A–C,F–H,K–M,P–R,N,O,T, arrows), which does not express *Fn1* (Fig. 7D,E,I,J,S, arrows). It has recently been shown that *Fn1* is strongly expressed by the endocardium in the mouse at E8.5–E9.5 (Mittal et al., 2010). Here we find that the endocardium, both in the atrium and the ventricle, of E3 chick embryos (Fig. 7D,E,I,J, arrowheads) and in E10.5 mouse embryos (Fig. 7S, arrowhead), strongly expresses *Fn1*. Immunolabeling of fibronectin on sections hybridized with the *Fn1* probe further demonstrate the mutually exclusive localization of mRNA and protein (Fig. 7E,J, arrows).

A strong *Fn1* expression is also seen in the endocardial cushions in the atrioventricular canal (Fig. 7D, asterisk, E) and outflow tract (not shown). As the epicardium covers the myocardium in both chick and mouse, it also strongly expresses *Fn1*, here shown for E3 chick embryo (Fig. 7I, green arrowhead, J), and it is lined with a fibronectin matrix (Fig. 7N,T). Myocardial cells stain for both integrin α5 and αV in the chick (Fig. 7K–M,P–R), which is consistent with studies in the mouse (Hirsch et al., 1994; Bajanca et al., 2004). Thus we conclude that the cells in the myocardium are in a position to assemble a fibronectin matrix from protein produced by the endocardium and/or the epicardium.

### Localized *Fn1* Expression and Widespread Fibronectin Matrix Assembly Characterizes Early Foregut Development

In the anterior region of the developing stomach, *Fn1* is strongly expressed in the dorsal mesenchyme (Fig. 8A, arrow), but this expression becomes progressively weaker in serial sections from anterior to posterior (Fig. 8A–F). Fibronectin protein is present throughout the mesenchyme of the stomach from anterior to posterior (Fig. 8J,K), thus not being restricted to the dorsoanterior mesenchyme strongly expressing *Fn1*. Cells in the mesenchyme are positive for integrin αV (Fig. 8N), while α5 localizes preferentially to blood vessels (Fig. 8L, arrowhead).

Weak *Fn1* expression can also be seen apically in the gut endoderm (Fig. 8A–I, open arrowheads in D,G), which is lined with a fibronectin matrix (Fig. 8J,K, arrowheads). Of interest, *Fn1* is strongly expressed by the endodermal diverticulum connecting the developing liver to the stomach (Fig. 8D–I, arrowhead in D,G), which is also lined with fibronectin before (not shown) and after fusion with gut endoderm (Fig. 8K, arrowhead). A clear border of *Fn1* expression is evident where the strongly expressing liver diverticulum (Fig. 8G, solid arrowhead) fuses with the faintly expressing endoderm of the stomach (Fig. 8G, open arrowhead). *Fn1* is also strongly expressed by the dorsal pancreatic bud (Fig. 8G,H, asterisks) including the region that connects to the endoderm of the stomach (Fig. 8I, asterisk).

Curiously, fibronectin protein staining is particularly strong near the liver diverticulum, raising the possibility that fibronectin protein produced by the liver diverticulum (and perhaps also the pancreatic bud) may actually enter the mesenchyme (Fig. 8K). Nevertheless, the liver diverticulum stains for both integrin α5 and αV (Fig. 8M,O, arrowheads), and is thus also in a position to

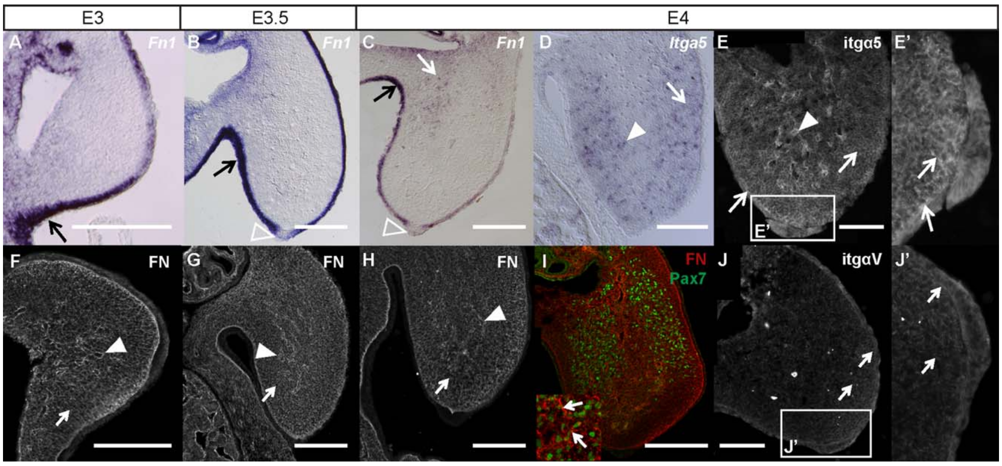


**Fig. 6.** **A-J′**: Limb ectoderm expresses *Fn1* while integrin α5 is found throughout the limb mesenchyme, which is filled with a fibronectin matrix. *Fn1* is strongly expressed by the ectoderm of the limb at all stages (shown here for the forelimb, A–C), with the exception of the apical ectodermal ridge, where *Fn1* expression is faint (A) or absent (B,C, arrowheads). Curiously, *Fn1* expression is particularly strong in the ventral ectoderm (A–C, black arrows). In contrast, *Fn1* is not expressed in mesenchyme (A–C), except for a weak expression in the proximal-most mesenchyme at E4 (C, white arrow). Immunohistochemistry for fibronectin shows the presence of a fibronectin matrix lining blood vessels (F–H, arrowheads), but a fibronectin matrix is also present among cells throughout the limb mesenchyme (F–H, arrows), including near Pax7-positive muscle progenitor cells (I, arrows in insert). The mesenchyme expresses *Itga5* in a patchy pattern (D, arrow) which appears to include, but not be restricted to blood vessels (D, arrowhead). Immunohistochemistry for integrin α5 confirms that the protein is present in the ectoderm and throughout the limb mesenchyme (E, E′, arrows), and is enriched on blood vessels (E, arrowhead). Integrin αV staining on the other hand, appears to be restricted to the ectoderm and more distal regions of the limb mesenchyme (J,J′,arrows). Scale bars = 200 μm in A–D,F–I; 100 μm in E,J.

assemble a fibronectin matrix. Finally, *Fn1* is also strongly expressed by the epithelial cells of the developing liver (Fig. 8P, arrow) while the fibronectin matrix is detected throughout the whole organ (Fig. 8Q). Integrin α5 protein seems to be present on all cells in the liver at this stage (Fig. 8R; compare with negative control in T), while αV staining is negative (Fig. 8S). We conclude that *Fn1* expression in the developing foregut is surprisingly localized, while a fibronectin matrix is found throughout the developing foregut and its associated organs.

## Discussion

Our results demonstrate that *Fn1*-expression is not restricted to certain cell types during development. In fact, at the stages under study *Fn1* is expressed by derivatives of all three germ layers: ectoderm (e.g., nonneural ectoderm), mesoderm (e.g., sclerotome, dermis) and endoderm (e.g., hepatic diverticulum). Moreover, *Fn1* is expressed by several epithelia as well as by certain populations of mesenchymal cells. Another striking feature of the *Fn1* expression pattern at the stages under study is that expression is frequently very strong and localized, as for example in the endocardium of the heart and in early hepatic and pancreatic diverticula in the foregut.

Through an analysis of *Fn1* expression, fibronectin matrix localization and the distribution of integrins capable of assembling fibronectin into a matrix (integrins α5 and αV), we conclude that, while *Fn1* expression is often localized, fibronectin matrices are widespread within or around the embryonic tissues studied. By comparing the *Fn1* expression patterns with integrin and fibronectin protein localization, we have identified (1) instances where a fibronectin matrix appears to be assembled by the tissue producing the protein (autocrine assembly); (2) situations where the tissue does not produce, but assembles, fibronectin, while neighboring tissues express *Fn1*, thus being likely providers of protein (paracrine assembly); and (3) cases where both mechanisms are likely to occur simultaneously (mixed assembly). These results are summarized in Table 1.

### Fibronectin Matrix Assembly in the Early Mesoderm is Mostly Autocrine in the Mouse Embryo but Paracrine in the Chick

Of interest, although the results for chick and mouse embryos are analogous for practically all stages studied, chick and mouse embryos differ in terms of *Fn1* expression during gastrulation. While the early mesoderm in the chick embryo does not express *Fn1*, the mouse mesoderm does. In this sense, the mouse embryo is more similar to zebrafish where *fn1/fn1b* are both expressed in the mesoderm (Trinh and Stainier, 2004). Thus fibronectin assembly by the early mesoderm appears to be autocrine in both mouse and zebrafish, but paracrine in the chick. The reason for this difference is not clear, but birds, which belong to a branch of the reptilian tree, are distant from the common amniote ancestor of reptiles and mammals; this may explain certain modifications in their early development (Sheng, 2015).

Nevertheless, the distribution of fibronectin and its receptors is conserved between chick and mouse embryos at all the stages studied. Moreover, at equivalent stages of *Xenopus* and zebrafish embryos fibronectin protein distribution follows a very similar pattern to that observed in amniote embryos (Davidson et al.,

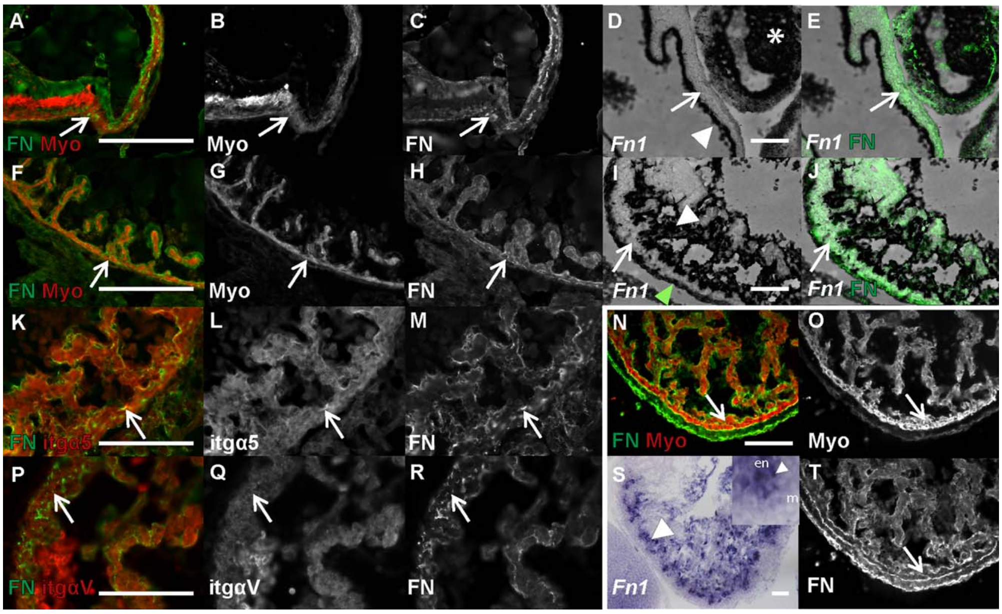


**Fig. 7.** **A–T**: *Fn1* is strongly expressed in the endocardium and epicardium while fibronectin protein is also found among myocardial cells. Transverse sections of the atrium (A–C) and ventricle (F–H,K–M,P–R) of an E3 chick embryo, processed for immunohistochemistry for fibronectin (first and third row), myosin (A,B,F,G), integrin α5 (K,L) and integrin αV (P,Q). Transverse sections of the atrium (D,E) and ventricle (I,J) of an E3 chick embryo processed for combined in situ hybridization for *Fn1* (D,E,I,J) followed by immunohistochemistry for fibronectin (E,J). Transverse sections of the ventricle of an E10.5 mouse embryo processed for double immunohistochemistry with anti-myosin (MF20) and anti-fibronectin antibodies (N,O,T) or for in situ hybridization for *Fn1* (S). The myocardium of both atrium and ventricle of E3 and E4 chick embryos show immunoreactivity for fibronectin (A,F,K,P, arrows), but do not express *Fn1* (D,I, arrows). Instead, strong *Fn1* expression is found in the endocardium (D,I, arrowheads) and in the endocardial-derived cardiac cushions in the atrioventricular canal (D, asterisk, E) and the epicardium (I, green arrowhead, J). The cells of the myocardium are also positive for integrin α5 (K,L, arrows) and integrin αV (P,Q, arrows). The pattern is the same in the mouse embryo, where the myocardium is positive for fibronectin (N, O, T, arrows), while the endocardium expresses the *Fn1* gene (S, arrowheads). myo, myosin heavy chain; FN, fibronectin; itgα5, integrin α5; itgαV, integrin αV; en, endocardium; m, myocardium. Scale bars = 100 μm.

2004; Trinh and Stainier, 2004; Latimer and Jessen, 2010). Indeed, a fibronectin matrix is crucial for gastrulation movements in *Xenopus*, zebrafish, and mouse (Yang et al., 1999; Marsden and DeSimone, 2001; Latimer and Jenssen, 2010) and is also needed for lateral mesoderm migration after ingression through the primitive streak in the chick (Harrison et al., 1993). Thus, regardless of the source of fibronectin, its assembly by integrins in the moving tissues is essential for the morphogenetic movements to occur (Zamir et al., 2008; Loganathan et al., 2014).

As gastrulation proceeds, the mesoderm regionalizes and the neural tube closes, a fibronectin matrix comes to line tissue borders, such as the different regions of the early mesoderm, somites, notochord, and neural tube (Duband et al., 1986; Ostrovsky et al., 1988; Davidson et al., 2004; Latimer and Jessen, 2010). The PSM also accumulates a fibronectin matrix at its periphery, even though it is mesenchymal and all its cells have the α5β1 on their surface. A recent study by Jülich et al. (2015) provides a possible explanation. It showed that close cell–cell apposition, reinforced by cell–cell adhesion by means of N-cadherin, keeps the α5β1 integrins of PSM cells physically associated, maintaining them in an inactive conformation. They therefore do not bind fibronectin and are unable to assemble a matrix. No apposing cells are present at tissue surfaces, and thus integrin α5β1 adopts an active conformation and subsequent fibronectin matrix assembly occurs freely on those surfaces (Jülich et al., 2015). Of interest, in the cephalic, limb, and hepatic mesenchymes, which also assemble fibronectin through a paracrine system (Table 1), a fibrillar fibronectin matrix forms among the α5β1-positive cells (see Figs. 2L,O, 6E–H, 8Q,R). Because cells in these mesenchymes are more dispersed than cells in the PSM are, α5β1 integrins may be active on all cells, allowing for the assembly of a matrix in between them.

### Fibronectin Matrix Assembly During Development is Surprisingly Versatile

Although it has been known for some time that cells in embryos or in culture are able to assemble exogenously added fibronectin (e.g., Darribère and Schwarzbauer, 2000; Sottile and Hocking, 2002), the concept that fibronectin matrix assembly is a versatile phenomenon, the nature of which is under strict developmental control, is not widespread.

Fibronectin is an important adhesion and migration substrate for cells (Pankov and Yamada, 2002). It is perhaps best known as an established marker of epithelial–mesenchymal transitions (EMTs) in both development and disease, where it is thought to

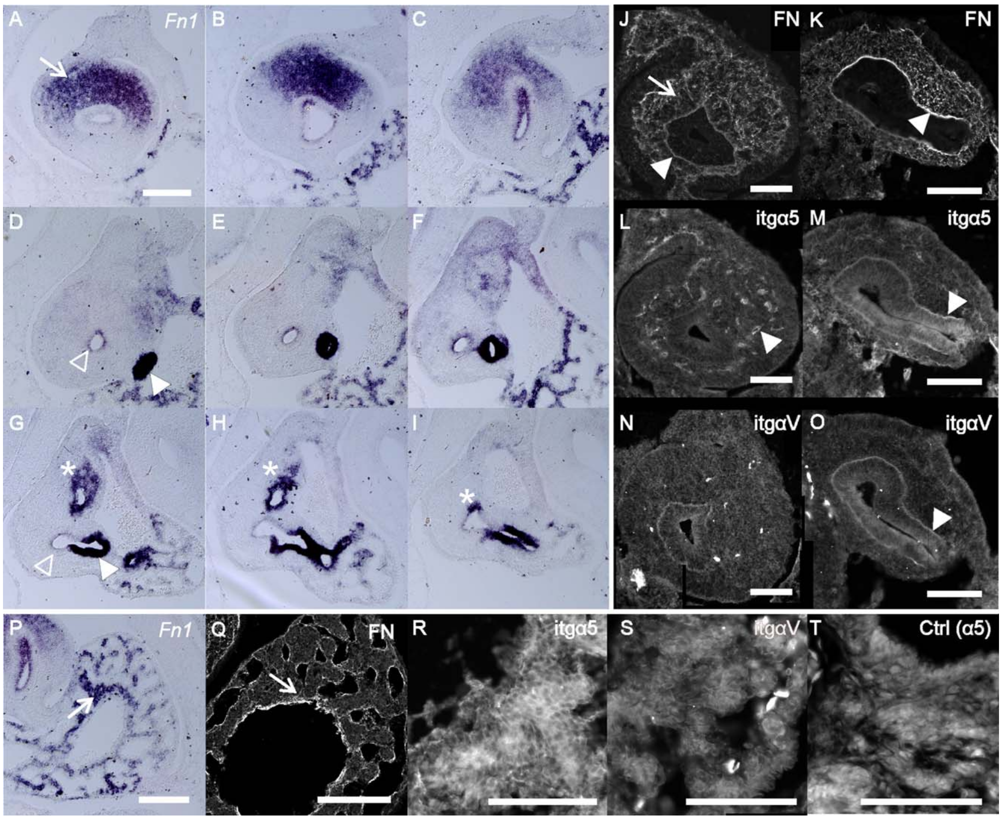


**Fig. 8.** **A–T**: Localized patterns of *Fn1* expression contrast with the generalized fibronectin matrix distribution in the foregut. In situ hybridization for *Fn1* in serial sections from anterior to posterior of the developing foregut shows that *Fn1* is strongly expressed in the dorsal mesenchyme of the anterior region of the stomach (A–C), is faintly expressed in the endodermal lining of the stomach (A–I, open arrowheads in D,G), is strongly expressed in the hepatic diverticulum (D–I, solid arrowhead in D,G) and in the dorsal pancreatic bud (asterisks in G–I). Immunohistochemistry for fibronectin protein shows that a fibronectin matrix is present in the mesenchyme (J, arrow) and lines the endoderm of the stomach (J,K, arrowheads). Immunohistochemistry for integrin α5 (L,M) and αV (N,O) shows that while αV is abundant in the mesenchyme and endoderm (N), α5 is mostly restricted to blood vessels (L, arrowhead). In posterior regions of the stomach, both αV and α5 protein are detected in the stomach endoderm and appear enriched in the endoderm of the hepatic diverticulum (M,O, arrowheads). *Fn1* is also strongly expressed in the endoderm of the developing liver (P, arrow). Fibronectin protein is detected in the whole organ (Q), and so are integrins α5 (R) and αV (S). T is negative control for integrin α5. Scale bars = 100 μm.

aid the dispersal and migration of cells after their deepithelialization (Thiery and Sleeman, 2006; Kalluri and Weinberg, 2009). In agreement with this established concept, we have found that in the stages under study, tissues undergoing EMTs, namely the primitive streak, sclerotome, dermis and endocardial cushions express *Fn1* and possess the receptors necessary to assemble their own matrix. Neural crest cells, another population undergoing EMT in the embryo, also express *Fn1* and are surrounded by a fibronectin matrix as they migrate (e.g., Duband et al., 1986; Mittal et al., 2010). Thus, upon activation of the EMT program, these tissues have an autocrine mode of fibronectin matrix assembly, which most likely aids their migration, stimulates their proliferation and protects them against apoptosis (Goh et al., 1997; Kalluri and Weinberg, 2009; Mittal et al., 2010). However, as we show here, promoting EMT through autocrine matrix assembly is only one of the many versatile roles of fibronectin during development.

In contrast, notochord, neuroepithelium, dorsal root ganglia, myotome, and myocardium do not express *Fn1* in either chick or mouse and are thus dependent on fibronectin produced by neighboring tissues to build their fibronectin matrices. These tissues require fibronectin for their normal development. In *Fn1*-null mice, the notochord fails to condense and the neural tube is deformed (George et al., 1993; George-Labouesse et al., 1996). The organization of the myocardium in these mice is also abnormal (George et al., 1997), a defect that may be due to impaired proliferation of cardiomyocyte precursors (Mittal et al., 2013). *Fn1*-null embryos have defects in neural crest cell proliferation (George et al., 1993; Mittal et al., 2010), but it is not clear whether fibronectin also plays a role in the organization and development

**TABLE 1. Classification of the Embryonic Tissues Analyzed in This Study According to Their System of Fibronectin Matrix Assembly**

| Fibronectin assembly system | Tissue | Figure | Stage | |
|---|---|---|---|---|
| | | | *Chick* | *Mouse* |
| Autocrine | | | | |
| Early mesoderm | Early mesoderm | 3 | | E7.0 |
| (mouse-specific) | PSM | 3 | | E8.0 |
| Epidermal ectoderm | Non-neural ectoderm | 1, 2 | HH4-8 | |
| | Limb ectoderm | 6 | E4 | |
| Endoderm | Endoderm | 2 | HH8 | E8.0 |
| | Hepatic/pancreatic diverticula | 8 | E4 | |
| Tissues undergoing EMTs | Primitive streak | 1-3 | HH4 | E7.0 |
| | Sclerotome | 3 | E4 | E10.5/11.5 |
| | Dermis | 3 | E4 | E10.5/11.5 |
| | Endocardial cushions | 7 | E3 | |
| Paracrine | | | | |
| Early mesoderm | Early mesoderm | 1, 2 | HH4-8 | |
| (chick-specific) | PSM | 1, 2 | HH4-8 | |
| Immature mesenchyme | Cephalic mesoderm | 2 | HH8 | |
| | Limb mesenchyme | 6 | E4 | |
| | Hepatic mesenchyme | 8 | E3.5 | |
| Nervous system | Early neuroepithelium | 1-3 | HH8 | E8.0 |
| | Neural tube | 2, 4 | HH8/E4 | E10.5/11.5 |
| | Dorsal root ganglia | 4, 5 | E4 | E10.5/11.5 |
| Striated muscle | Myotome | 4, 5 | E4 | E10.5/11.5 |
| | Myocardium | 7 | E4 | E10.5 |
| Notochord | Notochord | 2, 3, 4, 5 | HH8/E4 | E8.0 |
| Mixed | | | | |
| Gut | Foregut mesenchyme | 8 | E3.5 | |
| | Foregut endoderm | 8 | E3.5 | |

of the neural crest cell-derived dorsal root ganglia. Because *Fn1*-null embryos do not form somites (George et al., 1993), it is not possible to study the effect of fibronectin in myotome development in the mouse. However, in zebrafish, knockdown of *fn1* and *fn1b* leads to a perturbation of myocyte organization in the myotome (Snow et al., 2008). Our data indicate that these roles of fibronectin in the morphogenesis of notochord, neural tube, myocardium, and myotome are dependent on *Fn1* expression by neighboring tissues, revealing a new dimension of communication between tissues during development.

## Other ECM Components Assemble in a Paracrine Manner

Cooperation between different tissues in terms of matrix assembly is not specific to fibronectin. There are examples of paracrine assembly of other ECM components in several contexts. For example, collagen VII produced by dermal fibroblasts is essential for the maintenance of the basement membrane in the skin dermal–epidermal junction (Benny et al., 2015). Furthermore, nidogen produced by mesenchymal cells contributes to the basement membrane of the epithelial ureter buds in the developing kidney (Ekblom et al., 1994). The mesenchyme also produces laminins for the basement membrane at the epithelial–mesenchymal interface in kidney, lung, pancreas, mammary gland, and submandibular salivary gland (Nelson and Larsen, 2015). Importantly, although laminins are capable of self-polymerization, binding to their receptors and the resulting receptor clustering is essential for basement membrane organization and laminin signaling (Yurchenco, 2011). This suggests that, in addition to the situation observed here for fibronectin, the assembly of other ECMs may be considered a paracrine communication event in several contexts, thus being a more widespread phenomenon than generally appreciated.

## Does Fibronectin Matrix Assembly Follow the Modus Operandi of Growth Factor Signaling?

Cell–cell communication is a hallmark of vertebrate embryo development. While individual cells embark on a differentiation program through activation of particular transcription factors, they communicate with neighboring cells and neighboring tissues in a tightly choreographed crosstalk that ensures normal development. Growth factors, or paracrine factors, such as those of the fibroblast growth factor (Fgf), Wnt, Hedgehog, and transforming growth factor β (Tgfβ) families, play crucial roles in this crosstalk, as do their agonists and/or antagonists secreted into the extracellular space and their receptors on target cells that bind them and interpret their signals (e.g., Müller and Schier, 2011).

We have found that fibronectin assembly during early stages of chick and mouse development can be autocrine, paracrine or mixed, depending on the tissues or the developmental contexts (Table 1). Growth factors have analogous modes of action. They act primarily in a paracrine manner (e.g., Fgf8 from the apical ectodermal ridge acting on the underlying mesenchyme; Kawakami et al., 2003), but at other times they function in an autocrine manner (e.g., Fgf8 in the presomitic mesoderm; Dubrulle and Pourquié, 2004) or through a mixed autocrine-paracrine mechanism (e.g., Fgf8 expression in the myotome; Delfini et al., 2009).

We have also found that *Fn1*-expression is not restricted to certain cell types. The same situation is true for growth factors. Many of them are expressed by derivatives from all three germ layers. For example, *Shh* is expressed by ectoderm (e.g., ectoderm of forming hair follicles; Morgan et al., 1998), mesoderm (e.g., notochord, zone of polarizing activity in the limb buds; Riddle et al., 1993), and endoderm (e.g., gut endoderm; Roberts et al., 1995) and is expressed both by epithelial (e.g., endoderm) and mesenchymal (e.g., zone of polarizing activity) cells.

A striking feature of the *Fn1* expression pattern at the stages under study is that expression is frequently very strong and localized. Paracrine growth factors, are, in certain stages and contexts, strongly expressed by localized signaling centers, such as for example Wnt1/Wnt3a in the dorsal neural tube (Ikeya et al., 1997) and Wnt7a in the dorsal limb ectoderm (Parr and McMahon, 1995), with effects in the patterning of neighboring tissues. There are several lines of evidence to suggest that fibronectin can travel from one tissue to the next. For example, Sanders (1986) describes fibronectin-positive "dense bodies" appearing to come from the nonneural ectoderm and spread over the mesoderm, an observation that has been confirmed using 3D reconstruction of confocal images of embryos labeled for fibronectin (Rifes and Thorsteinsdóttir, 2012). More recently, elegant experiments performed in the early chick embryo unequivocally showed that GFP-labeled fibronectin produced by the Wolffian duct travels to the basal side of the coelomic epithelium, where it is assembled into a matrix (Yoshino et al., 2014).

### Conclusion

Here, we report that fibronectin matrix assembly during early development can, depending on the tissue or developmental context, be either autocrine or paracrine in an analogous mode of action to that described for paracrine growth factors. We, therefore, propose that fibronectin matrix assembly be considered a cell–cell communication system at the same level and significance as growth factor signaling during embryo patterning and morphogenesis.

## Experimental Procedures

### Embryos

Fertilized chicken (*Gallus gallus*) eggs obtained from commercial sources (Sociedade Agrícola Quinta da Freiria, Portugal) were incubated at 37.5°C in a humidified atmosphere for up to 4 days. Embryos were collected and staged according to Hamburger and Hamilton (1992). Mouse embryos were obtained from crossings of outbred Hsd:ICR (CD-1) mice (Harlan Interfauna Iberica, SA, Spain). The day of the vaginal plug was considered E0.5 and embryos were collected at E7.0–E11.5.

### Cryosectioning

Both chick and mouse embryos were fixed in either 0.2% or 4% paraformaldehyde (PFA) in phosphate buffer saline (PBS; 137 mM NaCl, 2.68 mM KCl, 8.1 mM $Na_2HPO_4$, 1.47 mM $KH_2PO_4$) overnight at 4°C and processed for cryoembedding as described previously (Bajanca et al., 2004). Twelve- to 30-μm cryosections were obtained in a Bright Clinicut 3020 cryostat and processed for in situ hybridization and/or immunohistochemistry.

### In Situ Hybridization

For whole-mount in situ hybridization, embryos were collected in PBS and fixed overnight at 4°C in 4% formaldehyde with 2 mM ethylene glycol-bis (β-amino-ethyl ether) tetra acetic acid (EGTA) in PBS for chicken embryos, or 4% PFA in PBS for mouse embryos. Embryos were then rinsed in PBT (PBS, 0.1% Tween 20), dehydrated in a gradient of methanol and stored at -20°C until use (Bajanca et al., 2004; Rifes et al., 2007). In situ hybridization was performed as described previously (Henrique et al., 1995). For chicken embryos up to HH15, proteinase (proteinase K, Roche, 10 μg/ml) digestion was from 4 min (HH4) to 15 min (HH15), and for 3 (HH18–21) and 3.5–4 (HH22–24) -day-old embryos, we used 30 and 35 min of proteinase digestion, respectively. For mouse embryos, proteinase digestion time was 5 min for E7.0 and 10 min for E8.0–E8.5.

Plasmids with fragments of chicken *Fn1, ItgaV*, and *Itga5* cDNA were produced previously (Rifes et al. 2007). Reverse transcription PCRs were used to generate cDNA fragments of mouse *Fn1* using the sense oligo 5′-CCATTGAAGGTTTGCAACCCAC-3′ and the antisense oligo 5′-TGTGGTGGTCAGGAACCGCA-3′. The resulting fragments were cloned into the pCRII-TOPO vector (Invitrogen), plasmid DNA was isolated and the constructs were sequenced to confirm that the inserts were correct. Digoxigenin (DIG)-labeled RNA probes were produced according to standard procedures adapted from Sambrook et al. (1989). Sense probes were also produced and used as controls for the in situ hybridizations and did not display any signal above background (see Fig. 5C for an example).

For in situ hybridization on sections, fresh cryostat sections of chicken or mouse embryos were dried for 1 hr at room temperature and washed in PBS, followed by incubation with 10 μg/ml proteinase K in PBS for 5 min. Sections were post-fixed in 4% PFA in PBS for 30 min, washed in PBS, and then incubated in hybridization buffer (Henrique et al., 1995) for 30 min at 65°C. Probes were diluted 1 μg/ml in hybridization buffer and hybridization was done overnight at 65°C. Sections were thoroughly washed in 100 mM maleic acid buffer with 0.1% Tween 20 (MABT) or Tris-Buffered Saline with 0.1% Tween 20 (TBST) and incubated for 1 hr 30 min with 2% Blocking reagent (Roche) and 20% Sheep serum (Sigma-Aldrich) in MABT or TBST (MABT-BS or TBST-BS). Incubation with an alkaline phosphatase-conjugated anti-DIG antibody (1:2,000 in MABT-BS or TBST-BS; Roche) was done overnight at 4°C. After a full day of MABT/TBST washes and a 1 hr 30 min wash in NTMT (0.1 M NaCl, 0.1M Tris-HCl, 0.05 M $MgCl_2$ with 1% Tween-20, pH 9.5), sections were exposed to NBT/BCIP (Roche, 450 μg/ml NBT, 175 μg/ml BCIP) in NTMT until the reaction was well visible.

### Immunohistochemistry

Immunohistochemistry on cryostat sections was performed as described previously (Bajanca et al., 2004) with minor modifications. In chick embryos, blocking was done with 5% bovine serum albumin in PBS, incubations in primary antibodies were overnight at 4°C, incubations in secondary antibodies were for 1 hr at room temperature, and slides were mounted in 5 mg/ml propyl gallate in glycerol/PBS (9:1) with 0.01% azide. For mouse embryos, blocking was done with the Mouse-On-Mouse (MOM) kit (Vector Laboratories). Whole-mount immunohistochemistry was performed as described previously (Rifes and Thorsteinsdóttir, 2012).

Primary antibodies used were rabbit polyclonal anti-fibronectin antibody (Sigma, 1:400), mouse monoclonal anti-cellular fibronectin (Sigma, 1:100), mouse monoclonal anti-light meromyosin region of myosin heavy chain (MF20, DSHB, 1:50), mouse monoclonal anti-desmin (D3, DSHB, 1:50), mouse monoclonal anti-chick α5 integrin (D71E2, DSHB, 1:20), rabbit polyclonal anti-mouse α5 integrin (Chemicon, 1:100), rabbit polyclonal anti-αV integrin (CD51, Enzo, 1:100), and mouse monoclonal anti-Pax7 (PAX7, DSHB, 1:50). All antibodies were diluted in PBS with 1% BSA. Negative controls were run in each experiment. They were normal rabbit serum (NRS, Sigma) at the same dilution as the primary antibody (for the Chemicon and Enzo polyclonal antibodies, which are neat sera) or PBS with 1% BSA for the remaining antibodies (affinity purified polyclonal antibodies and monoclonal antibodies).

Secondary antibodies used were Alexa Fluor 488- or 568-conjugated goat anti mouse IgG F(ab′)$_2$ fragments (Molecular Probes, 1:1,000) and Alexa Fluor 488- or 568-conjugated goat anti rabbit IgG F(ab′)$_2$ fragments (Molecular probes, 1:1,000), all diluted in PBS with 1% BSA. Exceptions to this standard procedure were the following: (1) when integrin antibodies were used in mouse cryosections (and respective controls), because of high background staining, we used the MOM kit, and the appropriate kit solutions for blocking and antibody dilutions; (2) Sections of both chick and mouse stained for the respective integrin α5 antibodies were processed for antigen retrieval before blocking. In these cases, sections were immersed in 10 mM Tris Base, 1 mM EDTA solution, 0.05% Tween 20, pH 9.0 at 95°C for 10–20 min depending on the embryo stage. DNA was visualized with To-Pro 3 (Invitrogen, 1:800 with ribonuclease A, Sigma, 10 mg/ml) or 4,6-Diamidino-2-phenylindole (DAPI, 5 μg/ml, Sigma).

### Combined In Situ Hybridization and Immunohistochemistry on Sections

Sections were processed for in situ hybridization as described above. After exposure of the alkaline phosphatase reaction, sections were thoroughly washed in PBS and processed for immunohistochemistry as described above.

### Image Acquisition and Analysis

Whole-mount in situ hybridizations were photographed with an ImagingSource DFK 23U274 camera coupled to a Zeiss Lumar V12 stereomicroscope. In situ hybridization on sections were photographed with an Olympus DP50 camera coupled to an Olympus BX51 microscope while combined in situ hybridization and immunohistochemistry images were acquired on a Leica SPE confocal microscope. Immunofluorescence images were acquired on the Leica SPE confocal microscope or on a Hamamatsu Orca R2 camera coupled to an Olympus BX60 microscope. Images were analyzed and processed for brightness and contrast adjustments in Fiji v. 1.49. When applicable, the pairwise stitching Fiji plugin was used in contiguous images of the same sample to generate a single image (Preibisch et al., 2009). Z-stacks of whole-mount immunohistochemistry and pairwise stitched immunofluorescence images were analyzed and processed in Amira v.5.3.3 (Visage Imaging Inc.) software as described previously (Rifes and Thorsteinsdóttir, 2012).

## Acknowledgments

We thank the members of our group Gabriela Rodrigues, Luís Marques, Marianne Deries, and Manuel Koch (University of Cologne, Germany) who spent a sabbatical leave with us for helpful discussions, Marta Palma for excellent technical support, Marianne Deries for critically reading the manuscript, and Raquel P. Andrade for designing the mouse *Fn1* probe. The MF20, D3, and Pax7 antibodies were developed by D.A. Fischman (MF20, D3) and A. Kawakami (Pax7) and were obtained from the Developmental Studies Hybridoma Bank, developed under the auspices of the NICHD and maintained by The University of Iowa, Department of Biology (Iowa City, IA). P.G.A., A.M.N., and A.B.G. are funded by Fundação para a Ciência e a Tecnologia (FCT, Portugal).

## References

Bajanca F, Thorsteinsdóttir S. 2002. Integrin expression patterns during early limb muscle development in the mouse. Mech Dev 119S:131–134.
Bajanca F, Luz M, Duxson MJ, Thorsteinsdóttir S. 2004. Integrins in the mouse myotome: developmental changes and differences between the epaxial and hypaxial lineage. Dev Dyn 231:402–415.
Barczyk M, Carracedo S, Gullberg D. 2010. Integrins. Cell Tissue Res 339:269–280.
Benny P, Badowski C, Lane EB, Raghunath M. 2015. Making more matrix: enhancing the deposition of dermal–epidermal junction components in vitro and accelerating organotypic skin culture development, using macromolecular crowding. Tissue Eng Part A 21:183–192.
Boucaut JC, Darribère T. 1983. Presence of fibronectin during early embryogenesis in amphibian *Pleurodeles waltlii*. Cell Differ 12: 77–83.
Brand-Saberi B, Krenn V, Grim M, Christ B. 1993. Differences in the fibronectin-dependence of migrating cell populations. Anat Embryol (Berl) 187:17–26.
Cachaço AS, Pereira CS, Pardal RG, Bajanca F, Thorsteinsdóttir S. 2005. Integrin repertoire on myogenic cells changes during the course of primary myogenesis in the mouse. Dev Dyn 232:1069–1078.
Chen D, Wang X, Liang D, Gordon J, Mittal A, Manley N, Degenhardt K, Astrof S. 2015. Fibronectin signals through integrin α5β1 to regulate cardiovascular development in a cell type-specific manner. Dev Biol 407:195–210.
Chimal-Monroy J, Rodríguez-León J, Montero JA, Gañan Y, Macias D, Merino R, Hurle JM. 2003. Analysis of the molecular cascade responsible for mesodermal limb chondrogenesis: Sox genes and BMP signaling. Dev Biol 257:292–301.
Christ B, Huang R, Scaal M. 2004. Formation and differentiation of the avian dermomyotome. Anat Embryol (Berl) 208:333–350.
Darribère T, Schwarzbauer JE. 2000. Fibronectin matrix composition and organization can regulate cell migration during amphibian development. Mech Dev 92:239–250.
Davidson LA, Keller R, DeSimone DW. 2004. Assembly and remodeling of the fibrillar fibronectin extracellular matrix during gastrulation and neurulation in *Xenopus laevis*. Dev Dyn 231:888–895.
Delfini MC, De La Celle M, Gros J, Serralbo O, Marics I, Seux M, Scaal M, Marcelle C. 2009. The timing of emergence of muscle progenitors is controlled by an FGF/ERK/SNAIL1 pathway. Dev Biol 333:229–237.
Deries M, Gonçalves AB, Vaz R, Martins GG, Rodrigues G, Thorsteinsdóttir S. 2012. Extracellular matrix remodeling accompanies axial muscle development and morphogenesis in the mouse. Dev Dyn 241:350–364.
Duband JL, Thiery JP. 1982. Appearance and distribution of fibronectin during chick embryo gastrulation and neurulation. Dev Biol 94:337–350.

DEVELOPMENTAL DYNAMICS

Duband JL, Rocher S, Chen WT, Yamada KM, Thiery JP. 1986. Cell adhesion and migration in the early vertebrate embryo: location and possible role of the putative fibronectin receptor complex. J Cell Biol 102:160–178.
Dubrulle J, Pourquié O. 2004. fgf8 mRNA decay establishes a gradient that couples axial elongation to patterning in the vertebrate embryo. Nature 427:419–422.
Ekblom P, Ekblom M, Fecker L, Klein G, Zhang HY, Kadoya Y, Chu ML, Mayer U, Timpl R. 1994. Role of mesenchymal nidogen for epithelial morphogenesis in vitro. Development 120:2003–2014.
ffrench-Constant C, Hynes RO. 1989. Alternative splicing of fibronectin is temporally and spatially regulated in the chicken embryo. Development 106:375–388.
Frantz C, Stewart KM, Weaver VM. 2010. The extracellular matrix at a glance. J Cell Sci 123:4195–200.
George EL, Georges-Labouesse EN, Patel-King RS, Rayburn H, Hynes RO. 1993. Defects in mesoderm, neural tube and vascular development in mouse embryos lacking fibronectin. Development 119:1079–1091.
George EL, Baldwin HS, Hynes RO. 1997. Fibronectins are essential for heart and blood vessel morphogenesis but are dispensable for initial specification of precursor cells. Blood 90:3073–3081.
Georges-Labouesse EN, George EL, Rayburn H, Hynes RO. 1996. Mesodermal development in mouse embryos mutant for fibronectin. Dev Dyn 207:145–156.
Goh KL, Yang JT, Hynes RO. 1997. Mesodermal defects and cranial neural crest apoptosis in $\alpha$5 integrin-null embryos. Development 124:4309–4319.
Goody MF, Henry CA. 2010. Dynamic interactions between cells and their extracellular matrix mediate embryonic development. Mol Reprod Dev 77:475–488.
Hamburger V, Hamilton HL. 1992. A series of normal stages in the development of the chick embryo. 1951. Dev Dyn 195:231–272.
Harrisson F, Van Nassauw L, Van Hoof J, Foidart JM. 1993. Microinjection of anti-fibronectin antibodies in the chicken blastoderm: inhibition of mesoblast cell migration but not of cell ingression at the primitive streak. Anat Rec 236:685–696.
Henrique D, Adam J, Myat A, Chitnis A, Lewis J, Ish-Horowicz D. 1995. Expression of a Delta homologue in prospective neurons in the chick. Nature 375:787–790.
Hirsch E, Gullberg D, Balzac F, Altruda F, Silengo L, Tarone G. 1994. $\alpha$v integrin subunit is predominantly located in nervous tissue and skeletal muscle during mouse development. Dev Dyn 201:108–120.
Ikeya M, Lee SM, Johnson JE, McMahon AP, Takada S. 1997. Wnt signalling required for expansion of neural crest and CNS progenitors. Nature 389:966–970.
Jülich D, Geisler R, Holley SA. 2005. Integrin$\alpha$5 and Delta/Notch signaling have complementary spatiotemporal requirements during zebrafish somitogenesis. Dev Cell 8:575–586.
Jülich D, Mould AP, Koper E, Holley SA. 2009. Control of extracellular matrix assembly along tissue boundaries via Integrin and Eph/Ephrin signaling. Development 136:2913–2921.
Jülich D, Cobb G, Melo AM, McMillen P, Lawton AK, Mochrie SG, Rhoades E, Holley SA. 2015. Cross-scale integrin regulation organizes ECM and tissue topology. Dev Cell 34:33–44.
Kawakami Y, Rodríguez-León J, Koth CM, Büscher D, Itoh T, Raya A, Ng JK, Esteban CR, Takahashi S, Henrique D, Schwarz MF, Asahara H, Izpisúa Belmonte JC. 2003. MKP3 mediates the cellular response to FGF8 signalling in the vertebrate limb. Nat Cell Biol 5:513–519.
Kalluri R, Weinberg RA. 2009. The basics of epithelial-mesenchymal transition. J Clin Invest 119:1420–1428.
Koshida S, Kishimoto Y, Ustumi H, Shimizu T, Furutani-Seiki M, Kondoh H, Takada S. 2005. Integrin$\alpha$5-dependent fibronectin accumulation for maintenance of somite boundaries in zebrafish embryos. Dev Cell 8:587–598.
Krotoski DM, Domingo C, Bronner-Fraser M. 1986. Distribution of a putative cell surface receptor for fibronectin and laminin in the avian embryo. J Cell Biol 103:1061–1071.
Kulyk WM, Rodgers BJ, Greer K, Kosher RA. 1989. Promotion of embryonic chick limb cartilage differentiation by transforming growth factor-$\beta$. Dev Biol 135:424–430.
Latimer A, Jessen JR. 2010. Extracellular matrix assembly and organization during zebrafish gastrulation. Matrix Biol 29:89–96.
Linask KK, Lash JW. 1988. A role for fibronectin in the migration of avian precardiac cells. II. Rotation of the heart-forming region during different stages and its effects. Dev Biol 129:324–329.
Loganathan R, Little CD, Joshi P, Filla M, Cheuvront T, Lansford R, Rongish BJ. 2014. Identification of emergent motion compartments in the amniote embryo. Organogenesis 10:350–364.
Mao Y, Schwarzbauer JE. 2005. Fibronectin fibrillogenesis, a cell-mediated matrix assembly process. Matrix Biol 24:389–399.
Marsden M, DeSimone DW. 2001. Regulation of cell polarity, radial intercalation and epiboly in *Xenopus*: novel roles for integrin and fibronectin. Development 128:3635–3647.
Mittal A, Pulina M, Hou SY, Astrof S. 2010. Fibronectin and integrin alpha 5 play essential roles in the development of the cardiac neural crest. Mech Dev 127:472–484.
Mittal A, Pulina M, Hou S-Y, Astrof S. 2013. Fibronectin and integrin alpha 5 play requisite roles in cardiac morphogenesis. Dev Biol 381:73–82.
Morgan BA, Orkin RW, Noramly S, Perez A. 1998. Stage-specific effects of sonic hedgehog expression in the epidermis. Dev Biol 201:1–12.
Müller P, Schier AF. 2011. Extracellular movement of signaling molecules. Dev Cell 21:145–158.
Nakaya Y, Sukowati EW, Wu Y, Sheng G. 2008. RhoA and microtubule dynamics control cell–basement membrane interaction in EMT during gastrulation. Nat Cell Biol 10:765–775.
Nelson DA, Larsen M. 2015. Heterotypic control of basement membrane dynamics during branching morphogenesis. Dev Biol 401:103–109.
Newman SA, Bhat R. 2007. Activator-inhibitor dynamics of vertebrate limb pattern formation. Birth Defects Res C Embryo Today Rev 81:305–319.
Ostrovsky D, Sanger JW, Lash JW. 1988. Somitogenesis in the mouse embryo. Cell Differ 23:17–25.
Pankov R, Yamada KM. 2002. Fibronectin at a glance. J Cell Sci 115:3861–3863.
Parr BA, McMahon AP. 1995. Dorsalizing signal Wnt-7a required for normal polarity of D-V and A-P axes of mouse limb. Nature 374:350–353.
Preibisch S, Saalfeld S, Tomancak P. 2009. Globally optimal stitching of tiled 3D microscopic image acquisitions. Bioinformatics 25:1463–1465.
Riddle RD, Johnson RL, Laufer E, Tabin C. 1993. Sonic hedgehog mediates the polarizing activity of the ZPA. Cell 75:1401–1416.
Rifes P, Carvalho L, Lopes C, Andrade RP, Rodrigues G, Palmeirim I, Thorsteinsdóttir S. 2007. Redefining the role of ectoderm in somitogenesis: a player in the formation of the fibronectin matrix of presomitic mesoderm. Development 134:3155–3165.
Rifes P, Thorsteinsdóttir S. 2012. Extracellular matrix assembly and 3D organization during paraxial mesoderm development in the chick embryo. Dev Biol 368:370–381.
Roberts DJ, Johnson RL, Burke AC, Nelson CE, Morgan BA, Tabin C. 1995. Sonic hedgehog is an endodermal signal inducing Bmp-4 and Hox genes during induction and regionalization of the chick hindgut. Development 121:3163–3174.
Rozario T, DeSimone DW. 2010. The extracellular matrix in development and morphogenesis: a dynamic view. Dev Biol 341:126–140.
Sambrook SK, Fritsch EF, Maniatis T. 1989. Molecular cloning: a laboratory manual. Cold Spring Harbor, NY: Cold Spring Harbor Laboratory Press.
Sanders EJ. 1986. Mesoderm migration in the early chick embryo. In: Browder LW editor. Developmental biology. A comprehensive synthesis. New York: Plenum Press. p 449–480.
Sheng G. 2015. Epiblast morphogenesis before gastrulation. Dev Biol 401:17–24.
Singh P, Carraher C, Schwarzbauer JE. 2010. Assembly of fibronectin extracellular matrix. Annu Rev Cell Dev Biol 26:397–419.
Snow CJ, Peterson MT, Khalil A, Henry CA. 2008. Muscle development is disrupted in zebrafish embryos deficient for fibronectin. Dev Dyn 237:2542–2553.
Sottile J, Hocking DC. 2002. Fibronectin polymerization regulates the composition and stability of extracellular matrix fibrils and cell-matrix adhesions. Mol Biol Cell 13:3546–3559.

Thiery JP, Sleeman JP. 2006. Complex networks orchestrate epithelial-mesenchymal transitions. Nat Rev Mol Cell Biol 7:131–142.
Trinh LA, Stainier DYR. 2004. Fibronectin regulates epithelial organization during myocardial migration in zebrafish. Dev Cell 6: 371–382.
Wartiovaara J, Leivo I, Vaheri A. 1979. Expression of the cell surface-associated glycoprotein, fibronectin, in the early mouse embryo. Dev Biol 69:247–257.
Yang JT, Rayburn H, Hynes RO. 1993. Embryonic mesodermal defects in $\alpha5$ integrin-deficient mice. Development 119:1093–1105.
Yang JT, Bader BL, Kreidberg JA, Ullman-Culleré M, Trevithick JE, Hynes RO. 1999. Overlapping and independent functions of fibronectin receptor integrins in early mesodermal development. Dev Biol 215:264–277.
Yoshino T, Saito D, Atsuta Y, Uchiyama C, Ueda S, Sekiguchi K, Takahashi Y. 2014. Interepithelial signaling with nephric duct is required for the formation of overlying coelomic epithelial cell sheet. Proc Natl Acad Sci U S A 111:6660–6665.
Yurchenco PD. 2011. Basement membranes: cell scaffoldings and signaling platforms. Cold Spring Harb Perspect Biol 3: 1–27.
Zamir EA, Rongish BJ, Little CD, 2008. The ECM moves during primitive streak formation—computation of ECM versus cellular motion. PLoS Biol 6:e247.

# Chapter 3

## A fibronectin-dependent mechanotransduction pathway in control of the chick embryo segmentation clock

*Somewhere, something incredible is waiting to be known.*
— Carl Sagan

# A fibronectin-dependent mechanotransduction pathway in control of the chick embryo segmentation clock

Patrícia Gomes de Almeida[1,2], Pedro Rifes[3], Ana Patrícia Jesus[2], Raquel P. Andrade[2] and Sólveig Thorsteinsdóttir[1]

[1] Centre for Ecology, Evolution and Environmental Change, Faculdade de Ciências, Universidade de Lisboa, Lisbon, Portugal;
[2] Centre for Biomedical Research, Universidade do Algarve, Faro, Portugal;
[3] Center for Stem Cell and Developmental Biology (DanStem), University of Copenhagen, Denmark

Contribution for the publication:

| | Experimental work depicted in Fig. | | | | | | | | | | Manuscript writing |
|---|---|---|---|---|---|---|---|---|---|---|---|
| | 1 | 2 | 3 | 4 | 5 | 6 | 7 | 8 | 9 | 10 | |
| Design and concept | III | III | II | III | III | III | III | III | III | - | III |
| Execution | III | III | II | III | III | III | III | III | III | - | |
| Analysis and interpretation | III | III | II | III | III | III | III | III | III | - | |

| | Experimental work depicted in Sup. Fig. | | | | | | | |
|---|---|---|---|---|---|---|---|---|
| | S1 | S2 | S3 | S4 | S5 | S6 | S7 | S8 |
| Design and concept | III | II | O | O | I | III | III | III |
| Execution | II | O | O | O | II | III | III | III |
| Analysis and interpretation | III | II | O | O | II | III | III | III |

**Legend:**
- ...... non applicable
O ..... no intervention
I ....... minor contribution
II ...... moderate contribution
III .... major contribution/full execution

Note: this contribution does not exclude other contributions, similar or not, from the remaining authors

## Abstract

Somite formation is a complex morphogenetic event, where cyclic waves of expression of segmentation clock genes travel along the presomitic mesoderm (PSM), concomitantly with the periodic epithelialization of its anterior end to form a new somite pair. Fibronectin is essential for somite formation in all vertebrate model embryos studied, but whether the assembly state of the matrix (i.e. stiffness, density, etc.) or its signaling through integrins have an active role in regulating the genetic and morphological intricacies of somitogenesis remains elusive. Here we address whether a fibronectin matrix-dependent mechanotransduction pathway is involved in regulating segmentation clock oscillations and boundary morphogenesis. We perturbed the fibronectin-integrin-actomyosin axis in the chick PSM *in vivo* by interfering with (1) the contractility of the actomyosin cytoskeleton, (2) Rho associated kinase function, (3) integrin-RGD binding and (4) fibronectin matrix assembly. We found that each of these players is required for correct segmentation clock oscillations and *Meso1* positioning. Furthermore, changes in segmentation clock dynamics were always accompanied by defects in the morphogenesis of somite boundaries. Our results strongly suggest that the mechanosensitive signaling pathway downstream of integrin-fibronectin interactions is an active player in regulating the mechanism by which cyclic waves of gene expression in the PSM are translated into periodic somite individualization. Our study also provides a novel example where the mechanotransduction machinery of the cell is required for a key developmental event *in vivo*.

**Keywords**: fibronectin, segmentation clock, boundary formation, somitogenesis, mechanotransduction

## Introduction

In developing tissues, cells are constantly receiving and integrating instructive information, including mechanical signals generated through adhesion to neighboring cells and/or the surrounding extracellular matrix (ECM). While morphogens have been extensively studied and long recognized as major chemical regulators of cellular processes (Marek and Kubícek, 1981; Slack, 1987; Tiedemann, 1976), the importance of mechanical forces in development have only recently started to be fully appreciated (Chan et al., 2017; Merle and Farge, 2018). In fact, the ability of cells to sense and respond to mechanical signals has been found to regulate critical processes underlying embryo development, including cell proliferation, migration and differentiation (Barriga et al., 2018; Cosgrove et al., 2016; Smutny et al., 2017; Wolfenson et al., 2016).

The ECM is a major transmitter of mechanical signals. Cells bind to the ECM mostly through integrins, which are primarily linked to the actomyosin cytoskeleton through adaptor proteins (Barczyk et al., 2010; Geiger and Yamada, 2011; Wolfenson et al., 2013). These multimolecular complexes (i.e. focal adhesions) act as mechanotransduction centers allowing cells to perceive the chemical and physical properties of the ECM, such as its molecular composition, density and stiffness, which in turn have profound effects on cell behavior. In fact, loss-of-function of several ECM components leads to embryonic lethality, highlighting the crucial role of the ECM in vertebrate development, where the coordination of forces within cells, between cells and with their surroundings is essential to generate a supracellular architecture (Lecuit and Lenne, 2007; Quintin et al., 2008; Rozario and DeSimone, 2010). Although our knowledge about the mechanical biology of vertebrate embryogenesis has increased significantly in recent years, much is still to be learned (Eyckmans et al., 2011; Heisenberg and Bellaïche, 2013; Merle and Farge, 2018).

One of the most conspicuous morphogenetic events during early vertebrate embryogenesis is the formation of somites, the source of the precursors of the axial skeleton and skeletal muscles of body and limbs (Christ et al., 2007). Somites are transient spheres of epithelioid cells that form rhythmically from the anterior portion of the mesenchymal presomitic mesoderm (PSM), located on each side of the axial structures (Bailey and Dale, 2015). Cyclic waves of expression of the so-called segmentation clock genes (Dequéant et al., 2006; Masamizu et al., 2006; Palmeirim et al., 1997) travel along the PSM in a posterior to anterior direction under the influence of fibroblast growth factor (Fgf)/Wnt and opposing retinoic acid (RA) gradients within the tissue (Aulehla and Pourquié, 2010; Mallo, 2016). Cell-autonomous gene expression oscillations in adjacent PSM cells are kept in synchrony under the control of the Notch signaling pathway (Ozbudak and Lewis, 2008). When this wave of expression reaches the anterior PSM at the end of each cycle, oscillations first slow down and then arrest (Morimoto et al., 2005; Shih et al., 2015). The transcription factor Mesp2/Meso1 is upregulated downstream of the segmentation clock in the anterior PSM, leading to Eph/Ephrin signaling which mediates somitic boundary formation (Barrios et al., 2003; Nakajima et al., 2006; Saga, 2012; Watanabe et al., 2009) followed by the progressive rearrangement of anterior PSM cells into a somite (Morimoto et al., 2005; Shih et al., 2015).

The PSM of all vertebrate model embryos is surrounded by a fibronectin-rich ECM, and both fibronectin and its integrin receptors are required for somite formation (George et al., 1993; Georges-Labouesse et al., 1996; Goh et al., 1997; Jülich et al., 2005; Koshida et al., 2005; Kragtorp and Miller, 2007; Rifes et al., 2007; Takahashi et al., 2007; Yang et al., 1993; Yang et al., 1999). Moreover, substituting the RGD binding site in fibronectin with an RGE sequence (*Fn1*$^{RGE/RGE}$) in mouse embryos, thus only perturbing its binding to the integrin receptors using this motif, also leads to dramatic defects in somitogenesis (Girós et al., 2011). Gene inactivation experiments do not, however, provide information about how the qualitative characteristics of this ECM affect somite formation since the ECM state (i.e. stiffness, elasticity, etc.) is not addressed. We have previously shown that the fibronectin matrix assembled around the chick PSM becomes progressively denser and more complex as the PSM matures (Rifes and Thorsteinsdóttir, 2012). Indeed, fibronectin has been shown to provide structural support for cells to attach to, polarize and change their shape and position, culminating in the cellular rearrangements needed for somite epithelialization (Martins et al., 2009). We have hypothesized that this posterior to anterior gradient of fibronectin matrix complexity culminates in a matrix assembly state that supports somite epithelialization in the anterior end of the PSM (Rifes and Thorsteinsdóttir, 2012; Rifes et al., 2007). Interestingly, adhesion to a fibronectin substrate was noted as a regulator of the oscillations of *Lfng*, a segmentation clock gene, in cultured mouse tailbud cells (Hubaud et al., 2017; Lauschke et al., 2013; Morimoto et al., 2005). Cell adhesion to fibronectin was linked to dampening and eventual arrest of *Lnfg* oscillations (Hubaud et al., 2017), reminiscent of what is observed in the anterior PSM prior to somite epithelialization. However, how PSM cells sense and respond to the fibronectin-dependent ECM gradient, and what is its role in segmentation clock oscillations *in vivo* remains unknown.

In this study, we address the involvement of fibronectin ECM and its downstream mechanotransduction pathway in the regulation of both segmentation clock dynamics and subsequent somite formation *in vivo*, using the chick embryo as a model. We perturbed (1) the intracellular mechanotransduction machinery of the cell by chemically blocking Non-Muscle Myosin II (NMMII) activity directly with Blebbistatin or indirectly by targeting Rho-associated protein kinases I and II (ROCK-I/II) (2) the ECM-cell interface, competitively inhibiting integrin binding to the RGD site of fibronectin and (3) extracellular fibronectin matrix assembly. All of these treatments resulted in abnormal segmentation clock oscillations, a mis-positioning of *Meso1* expression in the rostral PSM and perturbations in somite morphogenesis. These results strongly suggest that the tissue tension generated by the fibronectin matrix surrounding the PSM is coupling timely segmentation clock oscillations to morphological somite formation.

## Materials and Methods

*Embryos*

Fertile eggs were obtained from commercial sources (Sociedade Agrícola Quinta da Freiria or Pintobar Exploração Avícola, Lda, Portugal) and incubated for up to 48 hours at 37.5ºC in a humidified chamber until the desired HH stage (Hamburger and Hamilton, 1992).

For HH11-14 embryos, somite staging was performed according to Pourquié and Tam, 2001, where the forming somite (rostral end of the PSM) is termed somite 0 (S0). Somites progressively more rostral to S0 are termed SI, SII, SIII etc., and the terminology S-I ("S minus 1"), S-II, S-III, etc., is used for progressively more caudal somite-length portions of the PSM (Pourquié and Tam, 2001).

*Embryo explant culture and experimental treatments*

Explant tissues of HH11-14 embryos were collected and cultured as previously described (Palmeirim et al., 1997; Rifes et al., 2007). Embryos were bisected along the midline and then cut transversally rostral to somites IV and Hensen's node. The two contralateral halves thus retained half of the neural tube and notochord as well as the first four somites and the PSM, with all remaining neighboring tissues intact. Explants were placed on top of a polycarbonate filter floating on M199 medium supplemented with 10% chick serum, 5% fetal calf serum and 100 U/ml of penicillin and streptomycin (Palmeirim et al., 1997). Explants were then cultured at 37ºC with 5% $CO_2$ from 6 to 12 hours.

InSolution™Blebbistatin (Calbiochem) and RockOut (Calbiochem) diluted in DMSO were used at a final concentration of 50 μM in culture medium. Equal volumes of DMSO (Sigma-Aldrich) were used as control for both drugs. The RGD peptide (Sigma) was diluted in culture medium and used at 0.9 mM, while control explants were cultured in medium only. We first confirmed the inhibitory effect of the RGD peptide through a cell adhesion assay. C2C12 cells cultured in control medium (i.e. in the absence of RGD) attached and spread normally to gelatin-coated dishes, while cells cultured in RGD-containing medium were rounded and completely detached from the substrate and other cells, in agreement with the extensive literature on this effect (Danen et al., 2002; Pierschbacher and Ruoslahti, 1984; Singh et al., 2010; Takahashi et al., 2007).

*Embryo electroporation and* ex ovo *culture*

HH4-5 embryos were electroporated on one (randomly selected) side in the presumptive PSM and/or ectoderm following a previously described methodology (Voiculescu et al., 2008) and cultured *ex ovo* using the Early Chick culture method (Chapman et al., 2001). The electroporation mixture contained plasmid DNA at 0.5-1 μg/μl mixed with 0.4% Fast

Green for visualization. Embryos were submerged in an electroporation chamber filled with Tyrode's saline and three pulses of 6-9 V, 50 ms each, at 350 ms intervals were applied. Embryos were then cultured at 37.5ºC in a humidified chamber for about 26 hours.

Control embryos were electroporated with pCAGGs containing a GFP reporter (pCAGGs-GFP; hereafter abbreviated GFP). pCAGGs-70kDa qFN1 was kindly provided by Yuki Sato (Sato et al., 2017) and was co-electroporated with the pCAGGs-GFP plasmid in experimental embryos (hereafter abbreviated 70kDa+GFP).

*Cryosectioning and immunohistochemistry*

Cryosectioning was performed on whole embryos and embryo explants fixed in 4% paraformaldehyde in 0.12 M phosphate buffer containing 4% sucrose and processed for cryoembedding as previously described (Bajanca et al., 2004). Briefly, fixed samples were embedded in 7.5% gelatin in 0.12 M phosphate buffer containing 15% sucrose, frozen on dry ice-chilled isopentane and stored at -80ºC until sectioning. Cryostat sections (10-30 µm) were processed for immunofluorescence as previously described (Gomes de Almeida et al., 2016). Permeabilization of sections was performed with 0.2% Triton-X100 in phosphate buffered saline (PBS). 5% bovine serum albumen (BSA) or a combination of 1% BSA and 10% Normal Goat Serum (NGS) in PBS were used for blocking depending on the presence or absence of anti-fibronectin antibodies, respectively. Primary and secondary antibodies were diluted in 1% BSA in PBS. Sections were incubated with primary antibodies overnight at 4ºC and with secondary antibodies for 1 hour at room temperature.

For whole-mount immunodetection, explants were fixed in 4% paraformaldehyde in PBS and processed as previously described (Martins et al., 2009; Rifes and Thorsteinsdóttir, 2012). 1% Triton-X100 in PBS was used for permeabilization and 1% BSA in PBS was used for blocking and antibody dilution. Antibody incubation was performed overnight at 4ºC.

The following primary antibodies were used: anti-ZO-1 (Zymed, 1:100 or Invitrogen, 1:100); anti-N-cadherin (BD Biosciences, 1:100); anti-fibronectin (Sigma, 1:400), anti-activated caspase3 (Cell Signaling, 1:1000) and anti-GFP (Invitrogen, 1:100). For F-actin staining we used Alexa 488-conjugated phalloidin (Invitrogen, 1:40) and for staining DNA we used ToPro3 (Invitrogen, 1:500) in conjunction with ribonuclease A (Sigma, 10 µg/ml), 4% Methyl Green (Sigma, diluted 1:250; Prieto et al., 2015) or 4′,6-diamidino-2-phenylindole (DAPI, 5µg/ml in PBS with 0.1% Triton-X100). For detection of the primary antibodies we used the adequate secondary goat anti-mouse and anti-rabbit Alexa 488-, Alexa 568- or Alexa 546-conjugated F'ab fragments from Invitrogen (dillution 1:1000).

In situ *hybridization*

*In situ* hybridization using DIG-labeled RNA probes was performed as described previously (Henrique et al., 1995) with minor alterations (Gomes de Almeida et al., 2016; Rifes et al., 2007). RNA probes were synthetized from linearized plasmids, which have previously been described: *Dll1* (Henrique et al., 1995), *Meso1* (Buchberger et al., 1998), *Hairy1* (Palmeirim et al., 1997) and *Hairy2* (Jouve et al., 2000).

*Statistical analysis*

Paired Student's t-tests were performed to assess for differences in the number of somites formed in Blebbistatin-, RockOut- and RGD-treated explants relative to the respective controls, and in embryos electroporated with GFP only and GFP+70kDa. Differences in the frequency of morphological and gene expression phenotypes found in 70kDa-electroporated embryos compared to GFP-electroporated control embryos was tested through a Chi-square test. Differences in somite size and cell number of 70kDa-electroporated embryos compared to GFP-electroporated control embryos was tested through a nested ANOVA. Statistical significance was set at $p<0.05$. Statistical analyses were performed in Statistica 10 and Graphpad Prism 5.

*Sample preparation and imaging*

Whole mount explants were gradually dehydrated in methanol and cleared in methylsalicylate (Sigma-Aldrich) as described previously (Martins et al., 2009; Rifes and Thorsteinsdóttir, 2012), except for phalloidin-labelled embryos and explants, where a shorter series of ethanol dehydration series was used. Cryostat sections were mounted in Vectashield (Vector Laboratories) or in 5mg/ml propyl gallate in glycerol/PBS (9:1) with 0.01% azide.

Immunofluorescence images were taken on a confocal Leica SPE microscope, following imaging acquisition steps described previously (Rifes and Thorsteinsdóttir, 2012). Imaging of electroporated embryos and explants processed for *in situ* hybridization was performed using a Zeiss LUMAR V12 Stereoscope coupled to a Zeiss Axiocam 503 color 3MP camera.

Image analysis was performed using Fiji v. 1.49 and Amira V.5.3.3 (Visage Imaging Inc.) software. Image histogram corrections were performed in Fiji and exported as TIFF files. When applicable, we generated a single image from contiguous images of the same sample using the pairwise stitching Fiji plugin (Preibisch et al., 2009). For the analysis of *in situ* hybridization patterns along the PSM of explants, the Fiji plugin Straighten (Kocsis et al., 1991) was used.

## Results

***The intracellular mechanosensitive machinery of PSM cells is required to tune segmentation clock oscillations and for boundary positioning***

In the chick embryo, a new pair of somites buds off from the anterior PSM every 90 min, which is the period of segmentation clock oscillations (Fig. 3.1 A). To investigate the potential involvement of mechanical cues in regulating genetic oscillations in the PSM, we first perturbed the integrity and function of the actomyosin cytoskeleton, required for cells to sense and transduce tensional cues and exert force. Chicken embryo half explants (Fig. 3.1 B) were cultured in the presence of either Blebbistatin, which inhibits NMMII and consequently disrupts the actomyosin network, or RockOut, a chemical inhibitor of ROCK-I and -II enzymes, downstream effectors of RhoA, involved in regulating actomyosin contractility (Fig. 3.1 C; Ringer et al., 2017; Straight et al., 2003; Yarrow et al., 2005). The contralateral control sides were cultured in the presence of DMSO (Fig. 3.1 B). Cell death in cultured explants was assessed through immunostaining for activated Caspase3, and no significant apoptosis was found in any of the explant types (Supplementary Fig. 3.1 A-D). DMSO-treated explants formed the expected number of somites, an average of 3.6 somites in 6 hours (n=177, Fig. 3.1 D). Conversely, contralateral RockOut-treated halves formed an average of 3.1 somite-like structures during the same culture period (n=91, Fig. 3.1 D). Importantly, these structures were harder to distinguish upon macroscopic observation compared to those formed in the DMSO-treated control, as they appeared more diffuse. Culturing with Blebbistatin had a stronger effect on somitogenesis, since these explants formed on average only 1.5 new somites (n=19, Fig. 3.1 D) in 6 hours, which is consistent with previous studies (Chuai et al., 2006; Wei et al., 2001). RockOut-treated explants consistently maintained a difference of 0.5 somites relative to their contralateral controls even after 10.5h of culture (n=10; Fig. 3.1 D). In contrast, Blebbistatin-treated embryos did not form any additional somites when cultured for periods longer than 6 hours (n=10), suggesting that such explants are unable to form more than 1 or 2 somites (Fig. 3.1 D).

We then analyzed the expression of *Hairy1*, a segmentation clock gene expressed in the PSM (Palmeirim et al., 1997). *Hairy1* expression patterns in control and Blebbistatin- or RockOut-treated contralateral halves were different in 80% (n=7/9 and 8/10, respectively; Fig. 3.2 A-C, arrowheads) of the explants analyzed. *Hairy1* expression was either absent or in a different phase of the cycle relative to the contralateral controls. These results indicate that Blebbistatin and RockOut treatments lead to a dysregulation of the cycles of expression of segmentation clock genes along the PSM, supporting a role for the generation and transduction of tensional cues mediated by NMMII and ROCKI/II activity in temporal regulation of *Hairy1* oscillations.

In the anterior PSM, oscillations of Notch signaling activity are required for the correct

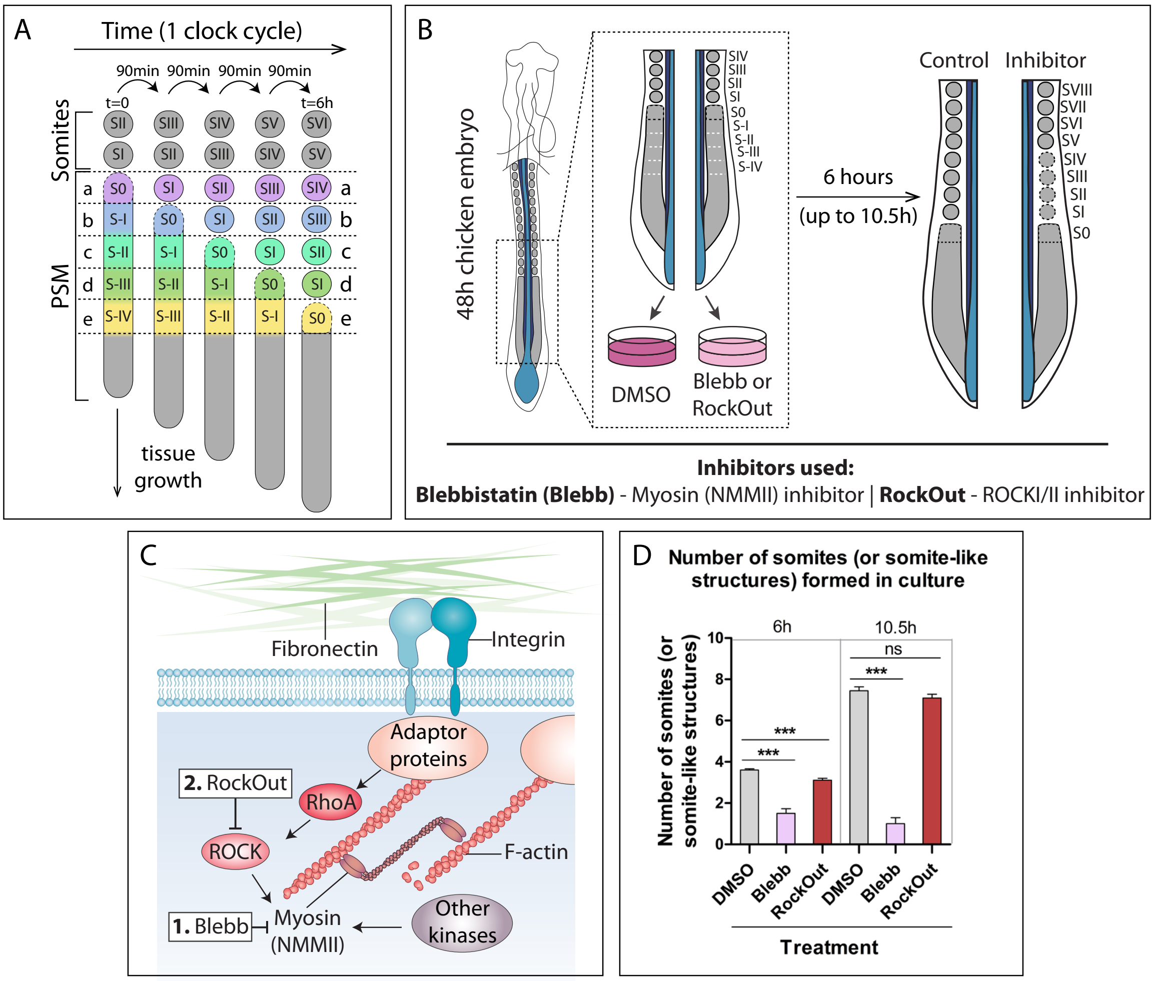


**Fig. 3.1. Inhibition of Non-Muscle Myosin II (NMMII) and ROCKI/II activity *in vivo*.** (**A**) Schematic representation of chick PSM maturation and somite formation over time. A new pair of somites buds off from the anterior PSM every 90 min. This is also the period of segmentation clock oscillations in the chick embryo. With each new cycle a pair of somites form and somites anterior to it mature (SI becomes SII, SII becomes SIII, etc). In our culture system, for example, S0 at the beginning of culture (i.e. the somite which is the process of forming from the anterior PSM at t=0) will have become SIV after 6 hours (i.e., 4 cycles) of culture (region a in A). Similarly, the tissue at S-IV at t=0 will have become S0 after 6 hours of culture (region e in A). (**B**) Schematic representation of our culture system. Posterior explants of 48h chick embryos were bisected along the midline and cultured for 6 or 10.5 hours. One side of the explant was cultured with either Blebbistatin (Blebb) or RockOut, while the contra-lateral half was cultured with equal volume of DMSO. (**C**) Schematic representation of the action of Blebbistatin (1) and RockOut (2) on NMMII activity. Blebbistatin inhibits Non-muscle myosin II (NMMII) ATPase activity directly. RockOut inhibits ROCKI/II which normally promotes phosphorylation of myosin light chain leading to increased ATPase activity of NMMII. (**D**) Number of somites or somite-like structures formed in culture in the presence of DMSO, RockOut and Blebbistatin at 6 and 10.5 hours of culture. Explants cultured with DMSO formed sharp somite boundaries and clearly individualized somites. RockOut treated explants formed distinguishable somite-like structures, but their boundaries were diffuse. Blebbistatin-treated explants formed only 1 or 2 somites. ns – not significant, *** – p<0.01.

spatial and temporal upregulation of *Mesp2* (Niwa et al., 2011; Saga and Takeda, 2001; Sato et al., 2002), which activates downstream targets involved in the formation of the future somitic cleft (Saga, 2012). Since we found that inhibition of NMMII and ROCKI/II activity leads to a dysregulation in *Hairy1* expression cycles, indicating altered Notch signaling dynamics in the PSM, we asked whether this is accompanied by deficient *Mesp2*

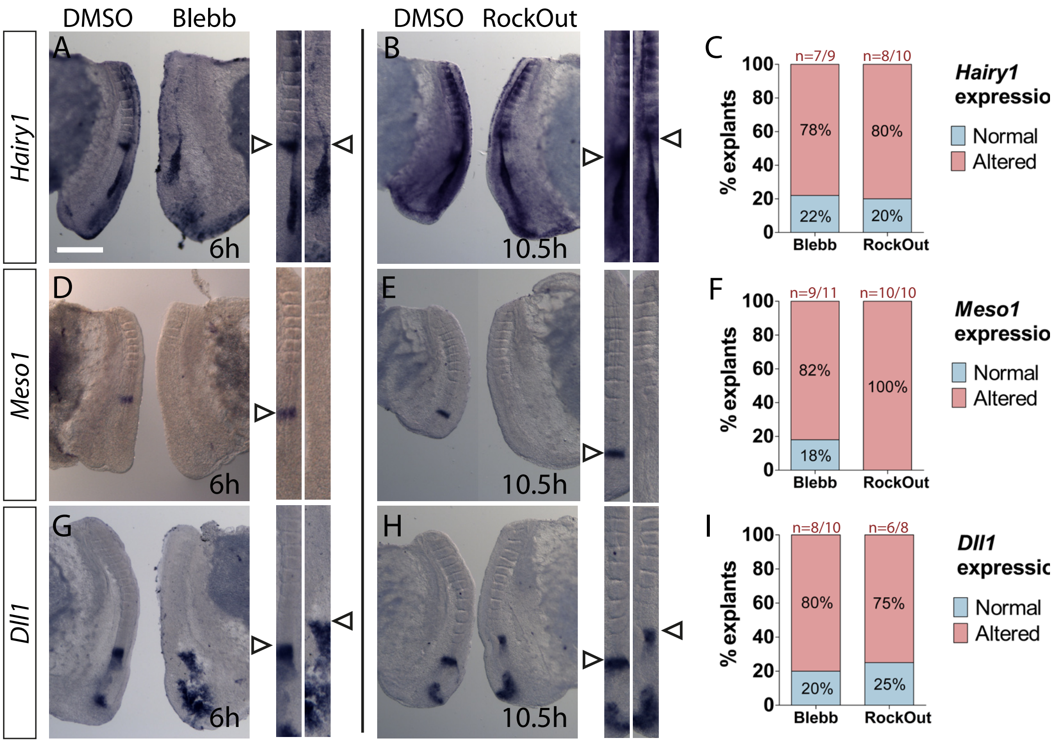


**Fig. 3.2**. **Inhibiting either NMMII or ROCKI/II activity results in altered segmentation clock oscillations, *Meso1* positioning and *Dll1* downregulation.** (**A-I**) Expression of *Hairy1* (A-C) and *Meso1* (D-F) at 6 hours of culture, and *Dll1* (G-I) at 10.5 hours of culture, of Blebbistatin- (A, D, G) and RockOut-treated explants (C, E, H) is altered compared to the respective contralateral controls, suggesting that the molecular machinery responsible for sensing and responding to tension is needed for maintaining the correct pace of segmentation clock oscillations. Straightened images of respective explant pairs to the right, aligned by SIV. Rostral is on top. Scale bar (shown in A): 500 µm. (**C, F, I**) Percentage of Blebbistatin- and RockOut-treated explants with altered *Hairy1* (C), *Meso1* (F) and *Dll1* (I) expression compared to the contralateral controls. Blebb – Blebbistatin.

expression. Thus, we analyzed the expression of the chick *Mesp2* homolog, *Meso1*, under our experimental conditions. *Meso1* expression was altered in the vast majority of either Blebbistatin- (n=9/11) or RockOut-treated explants (n=10/10) relative to the contralateral controls (Fig. 3.2 D-F). Importantly, Blebbistatin- and RockOut-treated explants exhibited altered *Meso1* expression compared to contralateral controls already after 3 hours of culture (n=8/9 and 5/5, respectively; Supplementary Fig. 3.2 A-B). This means that the molecular program in control of future boundary positioning is already affected 2 cycles after the addition of the inhibitors. We observed explant pairs where *Meso1* expression was located more rostrally in NMMII- and ROCKI/II-inhibited explants than in the control side. We also observed differences in the number of bands of *Meso1* expression, clearly indicating that the normal cycle of activation and suppression of *Meso1* in the rostral PSM was altered by either treatment. These results strongly suggest that NMMII- and ROCKI/II- activity are necessary for correct *Meso1* expression in space and time.

The expression of *Mesp2* at the S-I position in the mouse leads to the repression of Notch signaling (Takahashi et al., 2003) that underlies the caudal restriction of *Dll1* expression in S0 (Saga, 2012). In chicken embryos, *Meso1* is upregulated in S-II, stays expressed until S-I (Fig. 3.1 A, Supplementary Fig. 3.2 C) and is then downregulated and upregulated again in S-II (Buchberger et al., 1998). Moreover, *Dll1* expression in chicken embryos is only caudally restricted in the most recently formed somite (SI; Supplementary Fig. 3.2 D-E), indicating that up to 3 somite cycles, i.e. 270 minutes, take place from the time *Meso1* is upregulated in S-II until *Dll1* is downregulated in SI (Fig. 3.1 A). We thus analyzed *Dll1* expression in Blebbistatin- and RockOut-treated explants after 10.5h of culture (i.e. three cycles after *Meso1* expression is dysregulated). As expected, timely downregulation of *Dll1* expression in the anterior PSM did not occur in either Blebbistatin- (80%, n=8/10) or RockOut-treated (75%, n=6/8) explants compared to the respective contralateral controls (Fig. 3.2 G-I).

Altogether, interfering with the intracellular mechanotransduction machinery through inhibition of NMMII or ROCKI/II activity perturbs *Hairy1* oscillations along the PSM (Fig. 3.2 A-C), with an effect on *Meso1* expression (Fig. 3.2 D-F) and *Dll1* downregulation later on (Fig. 3.2 G-I). Our data reveal a surprising and previously unknown role of NMMII and ROCKI/II activity in regulating the segmentation clock and its downstream targets in the anterior PSM.

***Non-muscle myosin II is required for cleft formation and cell polarization, and its action on cell polarization is independent of ROCKI/II***

In addition to the changes in segmentation clock dynamics, we also found a difference in the number of somites formed when NMMII and ROCKI/II activity is impaired (Fig. 3.1 D). Somite formation requires both the formation of a cleft and a mesenchyme-to-epithelium transition of border cells anterior to this cleft (Martins et al., 2009; Saga, 2012). To determine if there is an impairment in this process when NMMII and ROCKI/II activity is blocked, we performed a detailed analysis of the morphology of S0 - SIII after culture (regions e, d, c and b in Fig. 3.1 A) in these explants.

We first investigated nuclear alignment and the distribution patterns of F-actin and the *zonula occludens* protein 1 (ZO-1), in untreated embryos. As previously described, peripheral cells in S0 polarize F-actin and their nuclei align (first stage of epithelialization; Martins et al., 2009); Supplementary Fig. 3.3 A, C, D). Then, as they transition from S0 to SI, their polarization gets more pronounced (second stage of epithelialization; Martins et al., 2009) concomitantly with their apico-basal elongation and acquisition of an aster-like arrangement (Supplementary Fig. 3.3 E, G, H), a process that is only completed by SII (Martins et al., 2009). Moreover, we found that while ZO-1 was clearly present at the apical extremity of the peripheral epithelioid cells of somite SI (Supplementary Fig. 3.3 F), no ZO-1 labeling is found in an early stage S0 (Supplementary Fig. 3.3 B). Thus, this ZO-1 rich apical adhesion ring (in fact, a ball in the spherical 3D somite) is a marker for the transition between S0 and SI, or in other words, the transition between PSM and somite.

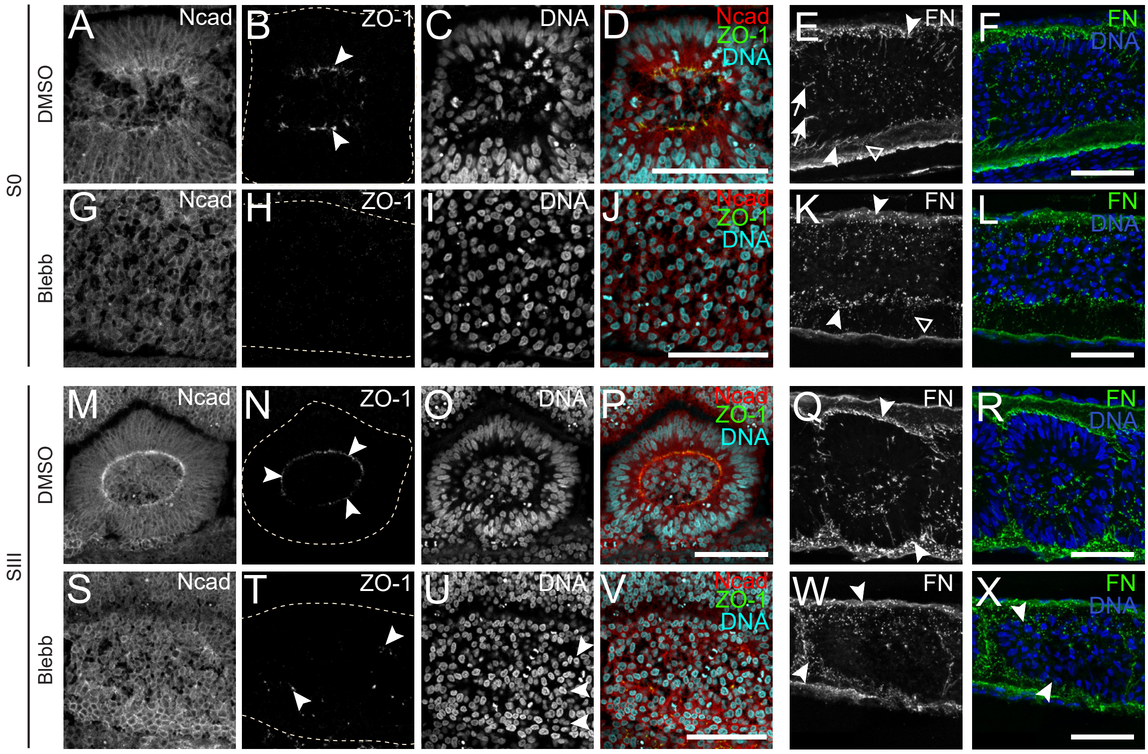


**Fig. 3.3. NMMII inhibition fully abolishes N-cadherin and ZO-1 polarization and impairs fibronectin fibrillogenesis.** Sagittal views of explants cultured in control (DMSO) medium (A-F, M-R) and their contralateral Blebbistatin-treated halves (G-L, S-X) at the S0 (A-L) and SIII (M-X) levels, immunostained for N-cadherin (first column), ZO-1 (second column) and fibronectin (fifth column) and stained for DNA (third and fifth column). Explants were cultured for 6 hours (somite levels are at t=6h). S0 of DMSO-treated explants show apically enriched N-cadherin and ZO-1 (A, B, arrowheads) and an aster-like nuclear arrangement (C, D), while the equivalent axial level of the contralateral Blebbistatin-treated explant shows no signs of polarized cell-cell adhesions (G, H) or nuclear alignment (I, J). SIII cells of DMSO-treated explants are also apically polarized in terms of N-cadherin and ZO-1 staining (M, N, arrowheads), but no N-cadherin, ZO-1 or nuclear polarization are observed at the same axial level of contralateral Blebbistatin-treated halves (S-U, arrowheads in T). Only an incipient nuclear alignment is present (U, arrowhead). Fibronectin assembly around somites is also deficient in Blebbistatin-treated explants (K, W, arrowheads) compared to the contralateral controls (E, Q, arrowheads). Empty arrowheads in E and K – Fibronectin pillars connecting the endoderm and somites. Arrows in E – Fibronectin assembly in the nascent somitic cleft. Rostral to the left and dorsal on top. Dashed lines mark borders of S0 (B,H) and somite (N, T). FN – fibronectin. Ncad – N-cadherin. Blebb – Blebbistatin. Scale bars: 50 µm.

We then compared the morphology of S0 and recently formed somites of embryo half explants after culture in Blebbistatin vs their contralateral controls. Cells in S0 and SI at the end of 6 hours of culture were in stage S-IV and S-III, respectively, when the inhibitors were added (regions e and d in Figure 3.1 A). These regions in the control explants underwent somite formation normally. In a late S0 stage, N-cadherin is apically polarized (Fig. 3.3 A, D) and some ZO-1 accumulation can already be observed apically (Fig. 3.3 B, D, arrowheads). Peripheral cell alignment is also normal (Fig. 3.3 C, D) and fibronectin matrix accumulation can be observed in the nascent somitic clefts (Fig. 3.3 E, F; arrows in E). In contrast, the contralateral explant half cultured with Blebbistatin does not show any signs of peripheral cell alignment (Fig. 3.3 I, J), apical enrichment of N-cadherin (Fig. 3.3 G, J), ZO-1 immunostaining (Fig. 3 H, J) or fibronectin matrix accumulation within the tissue

(Fig. 3.3 K, L). Moreover, while the rostral PSM and somites of the DMSO-treated explants are surrounded by a continuous and dense fibronectin matrix (Fig. 3.3 E, arrowheads), this network is disrupted and dot-like in contralateral Blebbistatin-treated explants (compare Fig. 3.3 E and K, arrowheads). DMSO-treated explants show a typical apical enrichment of F-actin in SI (Supplementary Fig. 3.4 A, C), but F-actin labeling in the contralateral Blebbistatin-treated halves appears dispersed, with no signs of any apical enrichment (Supplementary Fig. 3.4 D, F). Indeed, in the area where SI should have formed, no sign of somitic boundaries is detectable, neither by nuclear alignment (compare Supplementary Fig. 3.4 B and E) nor through apical enrichment of F-actin (compare Supplementary Fig. 3.4 A and D). We conclude that when PSM regions e and c (Fig. 3.1 A) are exposed to Blebbistatin, they are unable to form individualized somites 6 hours later.

We next turned our attention to somites at stages SII and SIII at the end of 6 hours of culture. These were in stage S-II and S-I (regions c and b in Figure 3.1 A) and had thus upregulated *Meso1* before the inhibitors were added (Buchberger et al., 1998). Again, control explants showed that normal, clearly individualized and polarized somites formed from these regions (Figure 3.3 M-P). In contrast, on the Blebbistatin-treated side apical enrichment of N-cadherin fails to occur (Fig. 3.3 S, V), ZO-1 is only detected in small foci (Fig. 3.3 T, V) and the fibronectin matrix, although present, appears less dense (Fig. 3.3 W, X). Interestingly, an incipient nuclear alignment is present in a position where the caudal border of SIII should be and is the only morphological indication of a somitic segment (Fig. 3.3 U, X, arrowheads; Supplementary Fig. 3.4 K, arrowheads). Moreover, NMMII-inhibited explants showed numerous F-actin-enriched foci dispersed throughout the paraxial tissue (Supplementary Fig. 3.4 J), indicating that cells were unable to polarize their F-actin into the apically enriched adhesion belts (compare Supplementary Fig. 3.4 G-I with J-L). Epithelial tissues other than somites (e.g. ectoderm and neural tube) did not show an altered morphology after incubation with Blebbistatin under the conditions used. These epithelial cells displayed ZO-1 labeling in the form of apical tight junction belts, in a similar pattern as observed in control explants (Supplementary Fig. 3.5 A-N). Altogether these results demonstrate that NMMII activity is required for the acquisition of the aster-like epithelioid morphology of somitic cells. However, PSM regions that had already upregulated *Meso1* before the addition of Blebbistatin form incipient clefts.

RockOut-treated explants also show strong perturbations in segmentation clock dynamics (Fig. 3.2 C, F, I) and somite formation was impaired, although to a lesser extent than observed for Blebbistatin-treated explants (Fig. 3.1 D). To better understand this difference in capacity to form somites between these two treatments, we also performed a detailed analysis of the morphology of RockOut-treated explants, again focusing on S0 and recently formed somites (regions e, d, c and b in Fig. 3.1 A). We found that control half explants undergo normal somite formation, with normal alignment of nuclei (Fig. 3.4 C, Supplementary Fig. 3.6 B, arrowheads) and both N-cadherin (Supplementary Fig. 3.6 A, arrowheads) and ZO-1

(Fig. 3.4 A, arrowheads) accumulate in the apical side of the cells. In the RockOut-treated contralateral side, formation of the somitic clefts is deficient and S0 shares the somitocoel with SI (Supplementary Fig. 3.6 D-F, arrows) and sometimes also SII (Fig 3.4 E-H, arrows). In fact, while the control half explant showed normal accumulation of fibronectin in the nascent clefts (Fig. 3.4 B, arrows), no fibronectin is observed in the incomplete somitic clefts in RockOut-treated explants (Fig. 3.4 F, arrows). In both control and RockOut-treated halves, somite SIII (stage S-I before culture and region b in Fig. 3.1 A) which had upregulated *Meso1* before addition of the drug, shows normal accumulation of ZO-1 (Fig. 3.4 I, M, arrowhead) and N-cadherin (Supplementary Fig. 3.6, G, J), nuclear alignment (Fig. 3.4, K, O, Supplementary Fig. 3.6, H, L) and a complete cleft containing a fibronectin matrix (Fig. 3.4 J, N). We conclude that ROCKI/II inhibition does not significantly perturb somitic cell polarization, but S0, SI and sometimes SII (i.e. regions e, d and sometimes c in Fig. 3.1A) fail to form a normal cleft and to detach into discrete individual somites.

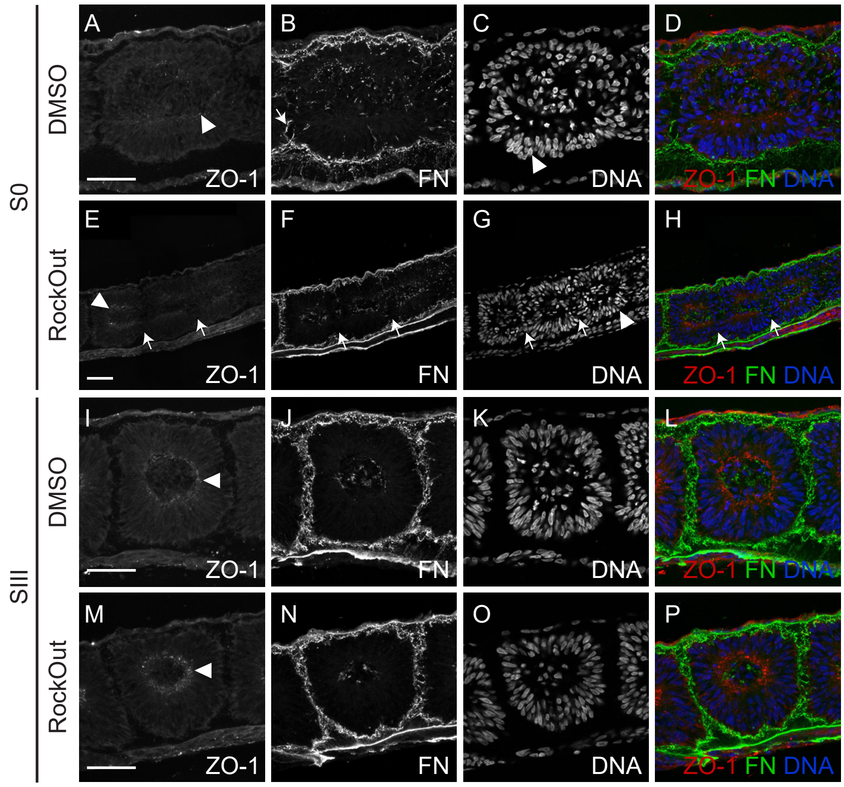


**Fig. 3.4. ROCKI/II inhibition impairs morphological somite formation, leading to deficient ZO-1 polarization and fibronectin assembly.** Sagittal views of explants cultured in control (DMSO) medium (A-D, I-L) and their contralateral RockOut-treated halves (E-H, M-P) at the s0 (A-H) and SII (I-P) levels, immunostained for ZO-1 (first column), fibronectin (second column) and stained for DNA (Methyl green; third column). Fourth column shows the respective merge of all stainings. Explants were cultured for 6 hours (somite levels are at t=6h). Rostral to the left, dorsal to the top. FN – fibronectin. Somites formed during culture in control explants show normal accumulation of ZO-1 (A, arrowhead), fibronectin assembly in the nascent cleft (B, arrow) and nuclear alignment (C, arrowhead). In contrast, somites formed in contralateral RockOut-treated explants fail to form a clear cleft (E-H, arrows), although ZO-1 is partially polarized (E, arrowhead) and nuclei are aligned (G, arrowhead). Both explants show normal ZO-1 polarization (I, M, arrowheads), fibronectin assembly (J, N) and nuclear alignment (K, O) at SII level. Rostral on the left and dorsal on top. Scale bars: 50 µm

Our results demonstrate that segmentation clock dynamics, *Meso1* expression and cleft formation, but not the polarization of somitic cells, are dependent on ROCKI/II activity. In contrast, NMMII activity is required for all these processes, including the capacity of rostral PSM cells to acquire their polarized, elongated morphology, suggesting that perturbing NMMII activity leads to an almost complete failure in somite formation. Taken together, these results indicate that the PSM cell mechanosensitive machinery plays a crucial role in regulating the translation of segmentation clock dynamics into periodic cleft formation.

*Integrin-RGD binding is necessary for the fine-tuning of clock oscillations and for defining the position and morphogenesis of the somitic cleft*

The α5β1 integrin binds to the RGD site on fibronectin and this binding plays a crucial role during somitogenesis (Takahashi et al., 2007). Moreover, strong α5β1-fibronectin binding (Friedland et al., 2009; Pierschbacher and Ruoslahti, 1984) modulates cell tension, allowing for cell spreading and subsequent strong adherence to the substrate in culture (Danen et al., 2002; Geiger et al., 2009; Huveneers and Danen, 2009).

Thus, we asked whether fibronectin-integrin interactions via RGD are mediating the effects of the mechanosensitive pathway on segmentation clock oscillations and, consequently, somite formation. To this end, we cultured embryo half explants in the presence of an RGD peptide (Fig. 3.5 A), which competes with available integrin RGD-binding pockets (Fig. 3.5 B), while the contralateral half was cultured in control medium. RGD-treated explants did not show increased cell death compared to contralateral controls, as shown by immunostaining for activated Caspase3 (Supplementary Fig. 3.1 E-F). After a 6-hour culture period with RGD, explants showed a consistent, albeit small, difference in the number of somites formed when compared to the contralateral control ($p<0.01$, 3.9 somites for control explants, n=112; 3.7 somites for RGD-treated explants, n=67). This difference was maintained during longer culture periods (Fig. 3.5 C). We then assessed the expression of *Hairy1, Meso1* and *Dll1* in RGD-treated explants. We found that control and RGD-treated contralateral explants displayed different *Hairy1* expression patterns (Fig. 3.5 D-F) in 60% (n=6/10) of the cases at 6 hours of culture, 29% (n=4/14) at 7.5 hours, 64% (n=9/14) at 9 hours and 13% (n=1/8) at 10.5 hours (Fig. 3.5 F). *Meso1* positioning was altered in 40% (n=4/10) of the cases studied at 6 hours of culture, 44% (n=4/9) at 9 hours and in 71% (n=5/7) at 12 hours (Fig. 3.5 G-I). Finally, *Dll1* expression was also altered in RGD-treated halves relative to the contralateral control sides from 9 hours onwards (Fig. 3.5 J-L, n=4/9 at 9 hours, n=9/13 at 10.5 hours and n=8/12 at 12 hours). We conclude that integrin-RGD interactions are needed to maintain the normal pattern of *Hairy1* oscillations, *Meso1* positioning and timely downregulation of *Dll1* in the anterior PSM. This suggests that the binding of α5β1 to the RGD site on fibronectin acts on the segmentation clock and its downstream target genes in the rostral PSM.

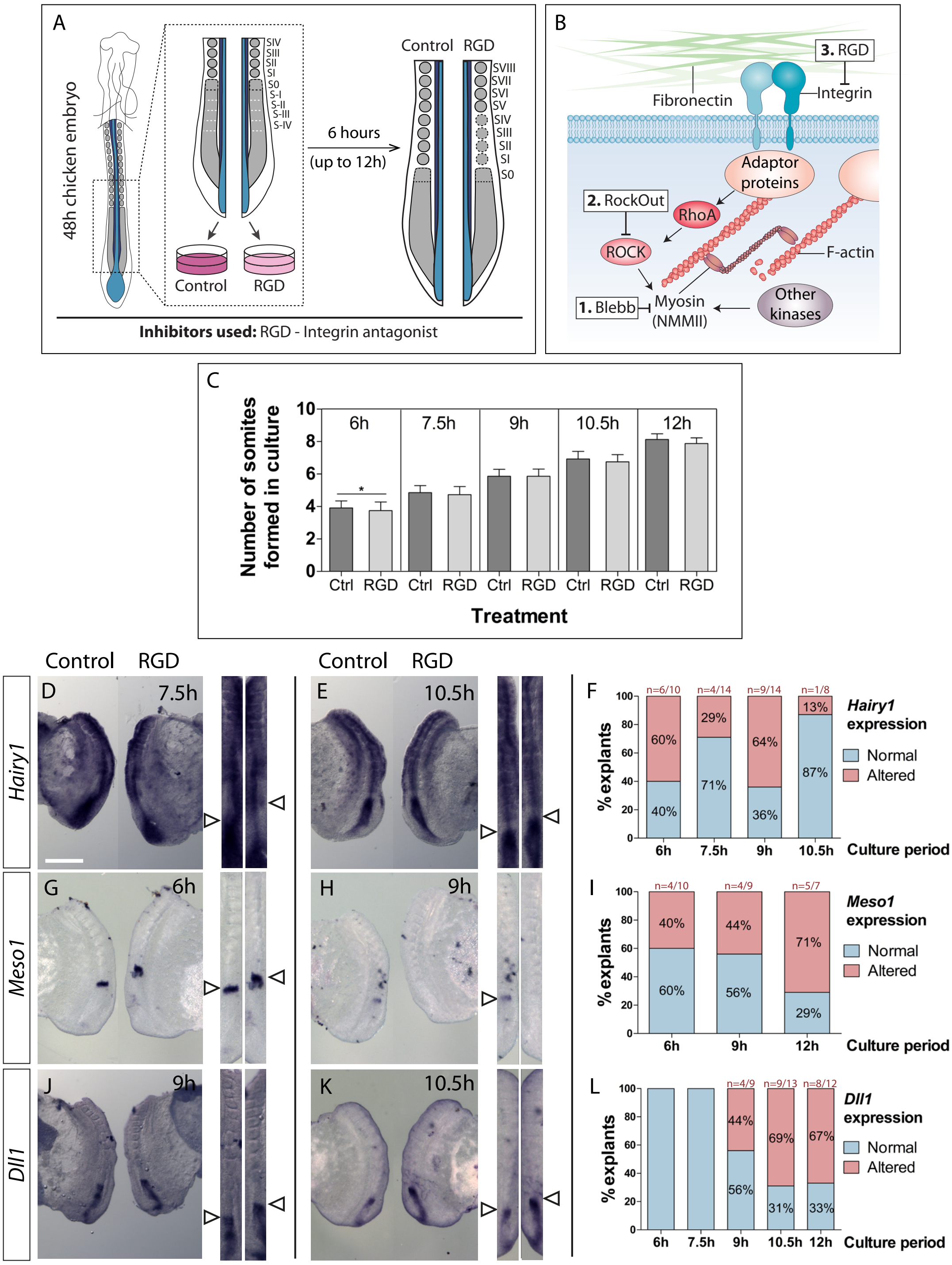


**Fig. 3.5. Integrin-RGD binding is needed for the correct pace of segmentation clock oscillations. (A)** Schematic representation of our culture system. Posterior explants of 48h chick embryos were bisected along the midline and cultured for 6 to 12h hours. One side of the explant was cultured with RGD, while the contra-lateral half was cultured in control medium. **(B)** Schematic representation of the action of RGD (3). RGD competes with the RGD-binding pockets of integrins, interfering with their binding to the ECM. **(C)** Number of somites formed in culture in Control and RGD-treated explants at 6, 7.5, 9, 10.5 and 12 hours of culture. * – $p<0.05$. **(D-L)** Expression of *Hairy1* (D, E), *Meso1* (G, H) and *Dll1* (J, K) in RGD-treated explants and contralateral controls at representative timepoints of culture. Straightened images of respective explant pairs to the right, aligned by SIV. Rostral is on top. Scale bars: 500 µm. (F, I, L) Percentage of RGD-treated explants with altered *Hairy1* (F), *Meso1* (I) and *Dll1* (L) expression compared to the contralateral controls. Impairing integrin-RGD binding alters *Hairy1* and *Meso1* expression relative to contralateral controls from 6 hours of culture onwards (D-H, arrowheads, F, I). *Dll1* expression also becomes misaligned at 9 hours of culture (J-K, arrowheads, L).

To determine if altered segmentation clock dynamics translate into hindered somite morphogenesis when integrin-fibronectin interactions are impaired, we analyzed the morphology of S0 and recently formed somites of RGD-treated explants vs their contralateral controls after 6 hours of incubation. Indeed, the S0 of RGD-treated explants (region e in Fig. 3.1 A) shows deficient nuclear alignment (Fig. 3.6 B, E, H, K, arrowheads) and N-cadherin polarization (Fig. 3.6 A, G, arrowheads) when compared to contralateral controls. This is also accompanied by deficient fibronectin assembly in the nascent cleft (Fig. 3.6 D, F, J, L arrowheads). At the level of SII (region c in Fig. 3.1 A), complete somite individualization seems to be impaired in RGD-treated explants compared to controls (Fig. 3.6 N, Q, T, W, arrowheads) and although N-cadherin polarization appears normal (Fig. 3.6 M, S, arrowheads), cleft formation and fibronectin assembly between adjacent somites is deficient (Fig. 3.6 P, V, arrowheads).

Our results show that α5β1-fibronectin binding via RGD regulates the positioning of the future segmental border by perturbing the normal *Hairy1* expression pattern and the correct positioning of *Meso1* expression in the anterior PSM, the same effect as observed in Blebbistatin- and Rock-Out-treated explants. Moreover, the three treatments also result

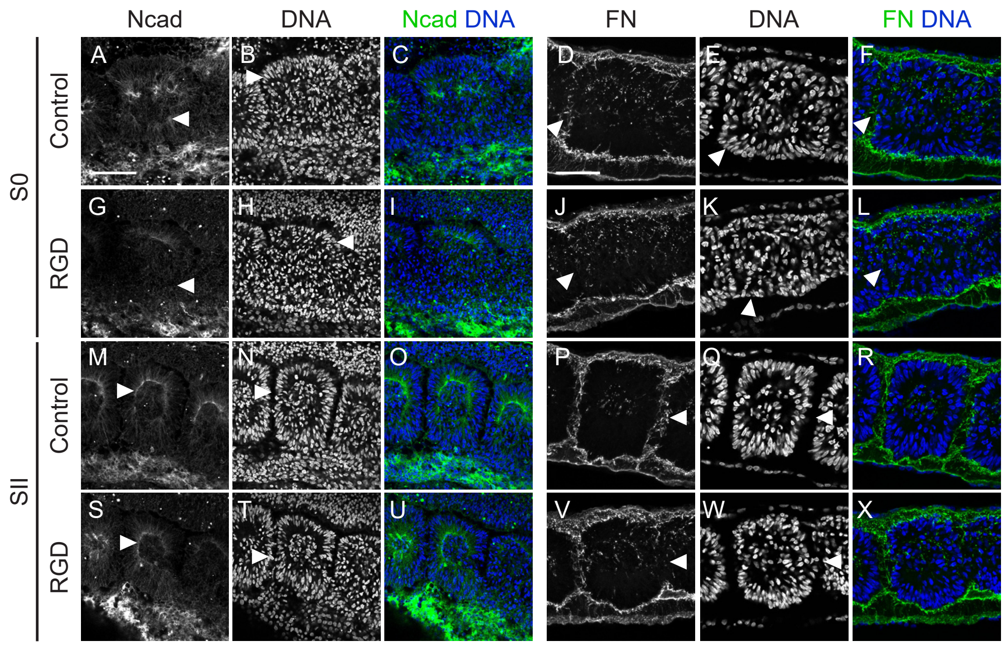


**Fig. 3.6. Formation of somitic clefs is impaired when integrin-RGD binding is inhibited.** (A-X) Longitudinal (left) and sagittal (right) views of explants cultured in control medium (A-F, M-R) and their contralateral RGD-treated halves (G-L, S-X) at S0 (A-L) and SII (M-X) levels, immunostained for N-cadherin (Ncad, first column), fibronectin (FN, fourth column) and DNA (second and fifth columns). Third and sixth columns show the respective merge of all stainings. Explants were cultured for 6 hours (somite levels are at t=6h). Both control and RGD-treated explants show normal accumulation of N-cadherin in the apical side of peripheral somitic cells (first column, arrowheads) and nuclear alignment (second and fifth column, arrowheads). Fibronectin assembly is also similar in contralateral explants (fourth column). Arrowheads in the first column point to N-cadherin polarization; in the second and fifth column point to nuclei alignment; and in the fourth and sixth column to fibronectin assembly in somitic clefts. Rostral to the left, midline to the top in longitudinal sections (left columns) and dorsal to the top in sagittal sections. Scale bars: 50 µm.

in the persistence of *Dll1* expression in the rostral PSM. We also show that incubation with RGD, like Blebbistatin and Rock-Out treatments, leads to deficient morphogenesis of the segment boundary, with incomplete separation of somites and impaired fibronectin assembly in nascent clefts.

***Correct fibronectin matrix assembly is a requirement for normal somite morphogenesis***

To study the effects of inhibiting α5β1-fibronectin signaling in segmentation clock dynamics and subsequent somite formation using a different approach, we interfered directly with fibronectin matrix assembly in the PSM and somites.

To this end, we electroporated primitive streak stage chick embryos (Fig. 3.7 A) with a construct expressing the 70kDa fibronectin fragment, which acts as a dominant-negative inhibitor of fibronectin assembly (Fig. 3.7 B; McKeown-Longo and Mosher, 1985; Sato et al., 2017). These embryos were co-electroporated with a construct expressing GFP to follow electroporated cells, while control embryos were electroporated with GFP only. Both types of embryos were then cultured for 26 hours (see Materials and Methods for more detail, Fig. 3.7 A). No significant differences in cell death between GFP- and 70kDa-electroporated embryos was detected (Supplementary Fig. 3.1, G-H). Defects in fibronectin matrix assembly in 70kDa-electroporated embryos are clearly visible when compared with GFP-electroporated embryos (compare Fig. 3.7 E with I, and L with M, arrows). While the somites of control embryos are surrounded by a continuous and dense fibronectin matrix (Fig 3.7 E), somites of 70kDa-electroporated embryos show a disrupted fibronectin matrix composed of fibrils that appear thinner than those of controls (Fig. 3.7 I). This disruption of the fibronectin matrix is accompanied by several morphological defects of 70kDa-electroporated embryos relative to control embryos (Fig. 3.7 C). While GFP-electroporated embryos show normal axial elongation (Fig. 3.7 D), 70kDa embryos often showed a shortened anterior-posterior axis (Fig. 3.7 C, H) and a kinked neural tube (Fig. 3.7 C, Supplementary Fig. 3.7 D-D''), consistent with the phenotype of *Fn1*-null and $Fn1^{RGE/RGE}$ mouse embryos (George et al., 1993; Girós et al., 2011). Moreover, paraxial mesoderm was frequently detached from the neural tube (Fig. 3.7 C, H-K, Supplementary Fig. 3.7 C, arrow), which is reminiscent of the results obtained when β1 integrin blocking antibodies were applied to chick embryos (Drake and Little, 1991; Drake et al., 1992).

The average number of somites formed in 70kDa-electroporated embryos is not different from the average number of somites formed in embryos electroporated with GFP only (14.5 somites for control embryos, n=154; 14.3 somites for 70kDa-electroporated embryos, n=144). However, the somites formed in the presence of the 70 kDa fragment have several morphological defects which were detectable macroscopically, including fused or crammed somites and diffuse segmental borders (Fig. 3.7 C, L-M, Supplementary Fig. 3.7 A-F''). At the cellular level, peripheral cells of nascent somites of 70kDa-electroporated embryos

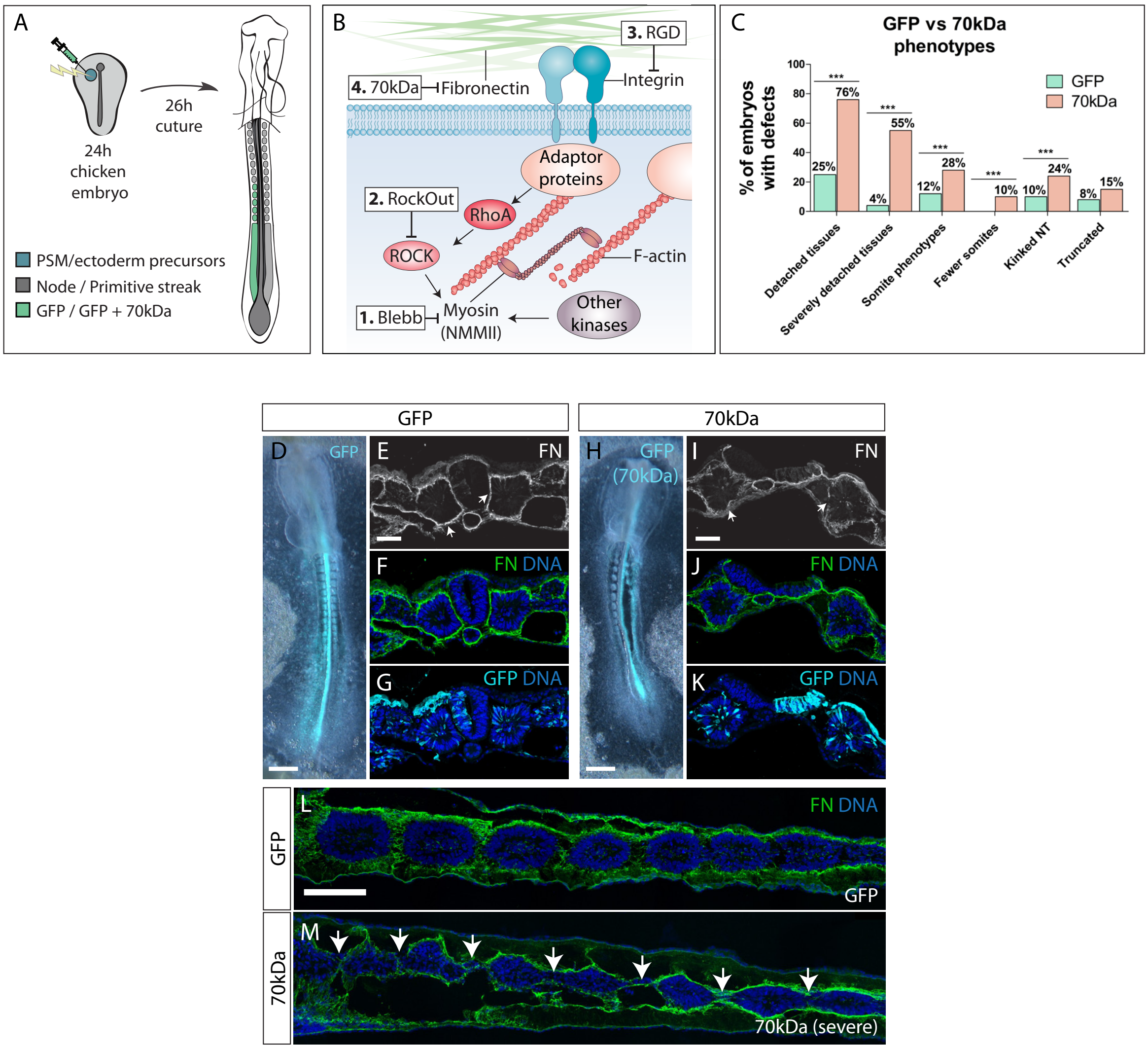


**Fig. 3.7. Electroporation with a 70kDa expressing vector impairs fibronectin assembly, which is accompanied by various morphological defects.** (**A**) Schematic representation of our electroporation setup. PSM/ectoderm precursors of primitive-streak stage embryos were electroporated with either a GFP-expressing vector (GFP) alone, or co-electroporated with a 70kDa-expressing vector (70kDa) and were incubated for about 26 hours. **(B)** Schematic representation of the action of 70kDa (4). 70kDa disrupts the assembly of fibronectin matrix by competitively binding to the N-terminal self-assembly domains on the protein, impairing fibronectin fibril formation. (**C**) Percentage of electroporated embryos with morphological defects, including detached (and severely detached) tissues, kinked neutral tube, truncated A-P axis, abnormal somite morphology, and fewer somites in the electroporated side compared to the control non-electroporated side. (**D-M**) Representative morphology of embryos electroporated with either GFP (C, L) or 70kDa (M). (D-K) Transverse sections of GFP- (E-G) and 70kDa-electroporared embryos (I-K) immunostained for fibronectin (FN; E-F, I-J), GFP (G, K) and with DAPI staining (F-G, J-K). Detachment of tissues is clearly visible in 70kDa-electroporated embryos (H), which is accompanied by a severe disruption in the fibronectin matrix (compare I-J with E-F, arrows). (L-M) Sagittal sections of embryos electroporated with GFP (L) and (M) 70kDa, the latter with a severe phenotype. Arrows point to deficient somitic clefts. Ventral view and rostral on top in D, H. Dorsal on top in E-G, I-K. Rostral to the left and dorsal on top in L, M. Scale bars: (C, G) 500 µm, (D-F, H-J) 50 µm, (L-M) 500 µm.

accumulate ZO-1 apically (Fig. 3.8 A, E, I), which is maintained as the somite matures (Fig. 3.8 M, Q, U). However, somites in 70kDa-treated embryos are abnormal in shape and appear smaller in the severely affected embryos (Fig. 3.8 I-L, U-X). Quantification of the number of cells per somite and the size of somites in sections of 70kDa-electroporated embryos (n=5), compared to somites from control embryos (n=2), shows that they tend to have fewer cells and be smaller in size, although these differences do not reach statistical significance (Supplementary Fig. 3.8 A-C). However, measurements of the width and length of somites SI and SV in images of whole mount embryos shows that somites of 70kDa-electroporated embryos (n=143), although not significantly different in length, are significantly shorter in width than those of GFP electroporated embryos (n=151; Supplementary Fig. 3.8 E-K).

In addition to defects in somite morphology, the ectoderm and endoderm are separated from the paraxial mesoderm in 70kDa-electroporated embryos, indicating that the fibronectin matrix present is not sufficient for holding these tissues together (brackets in Fig. 3.8 C, G, K, O, S, W). In fact, GFP-electroporated embryos show a dense fibronectin matrix connecting the somite to the ectoderm and endoderm (Fig. 3.8 C, empty arrowheads), while in 70kDa-electroporated embryos, this matrix appears disrupted (Fig. 3.8 F, J, empty arrowheads) in a way that is very similar to what was observed when NMMII activity is inhibited (Fig. 3.3 E, K, empty arrowheads). Moreover, somitic clefts of 70kDa-electroporated embryos with more severe phenotypes were incomplete (Fig. 3.7 L-M, Fig. 8 K, W, arrows). Thus, impaired fibronectin matrix assembly results in defective morphogenesis of somites and a deficient cohesion between embryonic tissues.

***Impaired fibronectin assembly leads to dysregulation of embryonic clock oscillations, incorrect Meso1 positioning and segment boundary defects***

To investigate whether our results showing a dysregulation of *Hairy1, Meso1* and *Dll1* expression when the interaction between integrin α5β1 and fibronectin is impaired were reproduced when fibronectin matrix assembly is perturbed, we electroporated embryos with 70kDa (co-electroporated with GFP, See Materials and Methods for more detail; Fig. 3.7 A) only selecting for analysis embryos in which the GFP signal was restricted to one side of the embryo. This allows the detection of shifts in the positioning of the expression of these genes in electroporated vs non-electroporated sides of the same embryo. Controls were electroporated on one side with GFP only. We also analyzed the expression of *Hairy2*, another segmentation clock gene. We found a high frequency of different expression patterns of *Hairy1* in contralateral PSMs of embryos expressing 70kDa on one side when compared to controls electroporated with GFP only (82% different patterns in 70kDa-electroporated embryos, n=9/11 vs 40% in embryos electroporated with GFP construct, n=4/10; $p<0.01$; Fig. 3.9 A-C). We also found a high incidence of asymmetric *Hairy2* expression patterns in embryos electroporated with 70kDa compared to control embryos (62%, n=8/13 versus

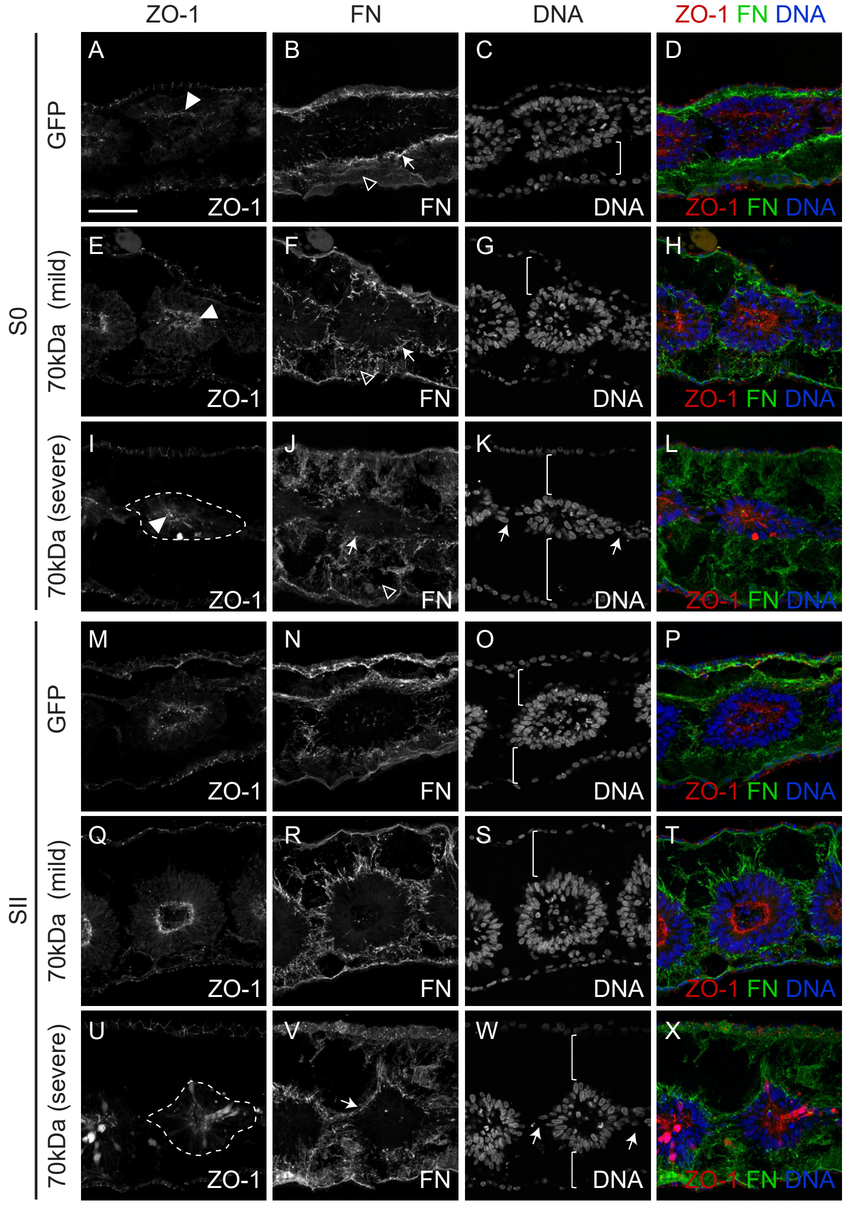


**Fig. 3.8. Somite morphology of 70kDa-electroporated embryos is severely compromised.** Sagittal views of embryos electroporated with GFP (A-D, M-P) and 70kDa (E-L, Q-X) with either mild (E-H, Q-T) or severe (I-L, U-X) phenotypes, at S0 (A-L) and SII (M-X) levels, immunostained for ZO-1 (first column) and fibronectin (second column) and stained for DNA (third column). Fourth column shows the merge of the respective channels. GFP- and 70kDa-electroporated embryos all polarize ZO-1 normally (A, E, I, arrowheads) but the fibronectin matrix surrounding the somites of 70kDa-treated embryos is disrupted compared to GFP-electroporated embryos (E, F, J, arrows). Somites of 70kDa-electroporated embryos are also severely detached from both the ectoderm and endoderm compared to embryos electroporated only with GFP (second column, brackets), and the fibronectin matrix connecting the endoderm to the somites is severely compromised (A, F, J, empty arrowheads). Somites of embryos electroporated with 70kDa with more severe defects also fail to fully detach from their neighbors (K, W, arrows). Rostral to the left and dorsal to the top. Dashed lines indicate altered somite morphology. Scale bars: 50 µm.

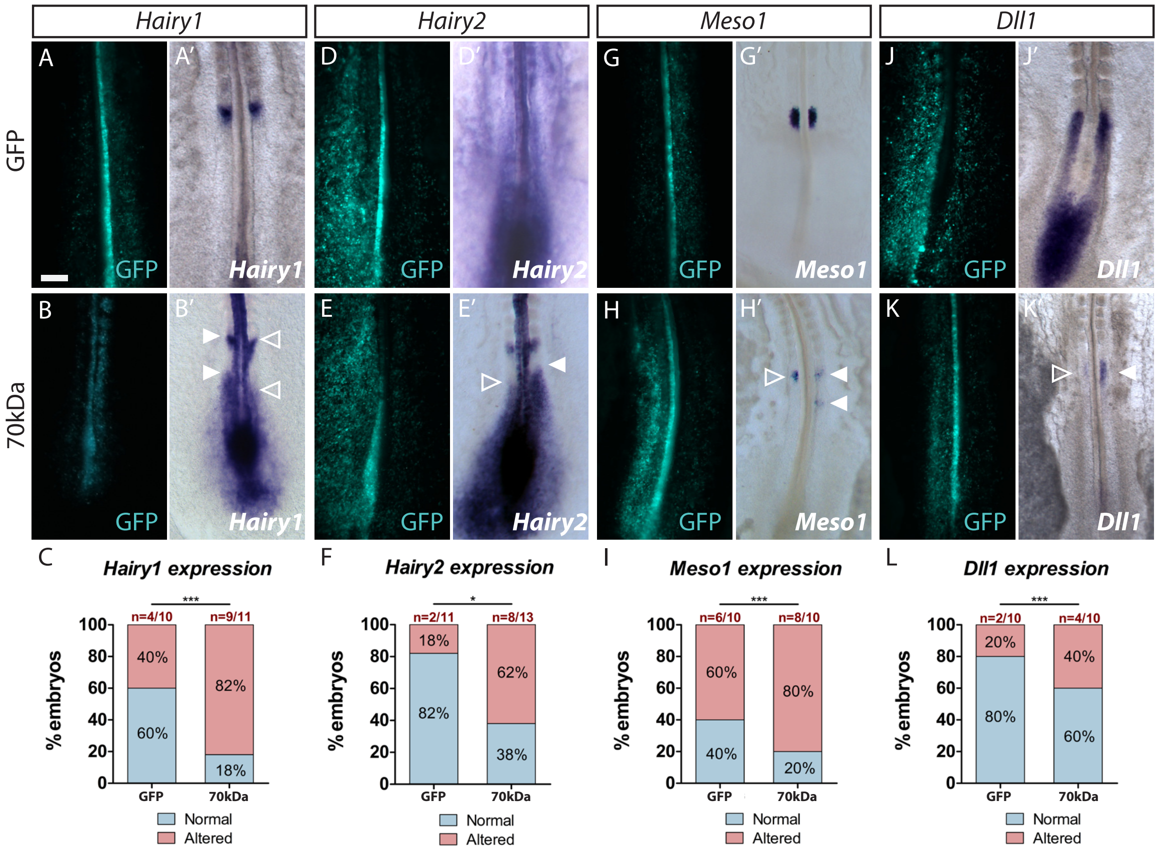


**Fig. 3.9. Segmentation clock oscillations require normal fibronectin assembly in the PSM.** Expression of segmentation clock genes in GFP- (top row) and 70kDa -electroporated embryos (middle row). (Bottom row) Percentage of GPF- and 70kDa-electroporated embryos with asymmetric expression between the electroporated PSM and the contralateral non-electroporated control PSM. Expression of *Hairy1* (A-C), *Hairy2* (D-F), *Meso1* (G-I) and *Dll1* (J-L). Perturbing the assembly of fibronectin on one side of the PSM alters the pace of both *Hairy1* (B', arrowheads) and *Hairy2* (E', arrowheads) oscillations relative to the non-electroporated PSM in most embryos studied (C, F). Correct *Meso1* positioning is compromised (H', arrowheads) and *Dll1* expression is also asymmetric (K', arrowheads). * $p<0.05$, *** $p<0.01$. Rostral is on top in A-K'. Scale bars: 200 µm.

18%, n=2/11, respectively; $p<0.05$; Fig. 3.9 D-F). We next tested whether *Meso1* positioning was also different between the two sides in embryos expressing 70kDa on one side. Although many control embryos show different *Meso1* expression in the two contralateral PSMs, the effect is much more pronounced and statistically significant in 70kDa-electroporated embryos (80%, n=8/10 vs 60%, 6/10 different patterns, $p<0.01$; Fig. 3.9 G-I). Finally, 40% (n=4/10) of 70kDa-electroporated embryos also show alterations in *Dll1* expression compared to 20% (n=2/10) in the controls ($p<0.01$, Fig. 3.9 J-L).

Taken together, our results show that a fibronectin-α5β1 mechanotransduction pathway has a significant and novel role in the fine tuning of segmentation clock oscillations and positioning of future segment boundary, with consequences on normal somite morphogenesis.

## Discussion

*Fibronectin matrix and its downstream mechanotransduction pathway coordinate segmentation clock dynamics and segment boundary formation*

We have identified a mechanotransduction pathway involving a fibronectin-integrin-NMMII axis, which regulates the dynamic expression of segmentation clock genes in the chick embryo. Four treatments interfering with different players in this pathway (covering extracellular matrix assembly, cell surface integrin-fibronectin binding and the intracellular mechanotransduction pathway) all lead to altered segmentation clock dynamics, dysregulated *Meso1* expression, impaired or deficient cleft formation and alterations in somite morphology (Fig. 3.10 A). These results demonstrate that the fibronectin matrix surrounding the PSM is not just providing structural support for the morphogenetic events leading to somite epithelialization. Rather, the mechanosensitive pathway downstream of integrin-fibronectin interactions appears to be a major player in regulating the mechanism by which cyclic waves of expression in the PSM are translated into the periodic epithelialization of somites.

The similarity of the phenotypes obtained in experiments blocking ROCK-I/II and impairing normal cell-fibronectin interactions (RGD and 70kDa) suggest that the fibronectin matrix is transducing mechanical signals via integrin α5β1 and ROCK and that these signals regulate segmentations clock oscillations. Indeed, a fibronectin-α5β1-RhoA-ROCK-NMMII axis in believed to play key roles in cellular force generation in a variety of cell types (Bharadwaj et al., 2017; Daley et al., 2011; Kametaka et al., 2007; Schiller et al., 2013; Torr et al., 2015). Our data show that blocking different elements of this axis leads to asymmetric patterns of *Hairy1* expression on the experimental versus the control sides, as well as incorrect *Meso1* positioning. In agreement with our data, chicken embryos electroporated with RNAi constructs against the integrin β1 chain, part of the α5β1 fibronectin receptor, show dampened and/or asymmetric expression of *Hairy2* and *Lfng* in the PSM and fail to express *Meso1* (Rallis et al., 2010). Moreover, mouse embryos expressing a fibronectin where the RGD sequence has been substituted with RGE (*Fn1*$^{RGE/RGE}$ embryos) show asymmetric and/or dampened expression of *Lnfg* and *Hes7* segmentation clock genes in the PSM and *EphA4*, a direct target of Mesp2 in the anterior PSM (Nakajima et al., 2006), is either diffusely expressed or absent (Girós et al., 2011). Altogether this strongly indicates that impairing the fibronectin-α5β1-RhoA-ROCK-NMMII axis, leads to a dysregulation of segmentation clock oscillations and the mispositioning of the segmental border.

An *in vitro* system for studying PSM cell oscillations has recently been established, where tailbud PSM explants from mouse embryos with a *Lfng*-Venus reporter are plated on fibronectin *in vitro* and allowed to grow out in a circular direction (Lauschke et al., 2013). These two-dimensional PSMs show oscillatory expression of *Lfng* and undergo 12-15 oscillatory cycles before upregulating Mesp2, just like in the PSM *in vivo* (Lauschke et al.,

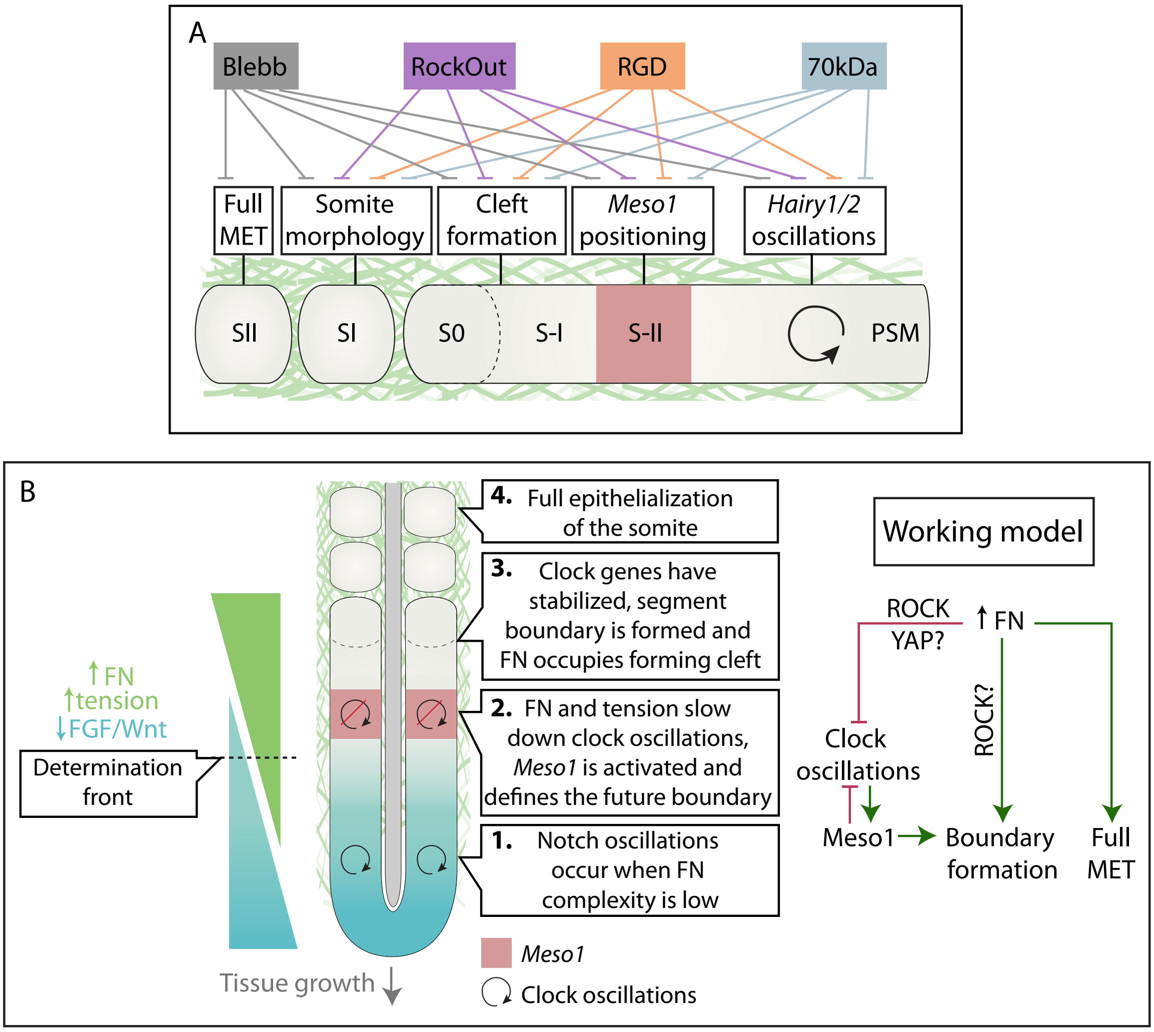


**Fig. 3.10 – Summary of the results and Working model. (A)** Schematic representation of the effects of all the treatments used in the different phases of somite formation. Interfering with fibronectin matrix assembly (70kDa), integrin-RGD binding (RGD) and ROCKI/II (RockOut) and NMMII (Blebb) activity, all result in altered segmentation clock dynamics, dysregulated *Meso1* expression, impaired or deficient boundary formation and alterations in somite morphology. Interfering directly with NMMII also disrupts the second stage of somite epithelialization, i.e. full epithelialization of the segment. **(B)** Our findings suggest that the mechanotransduction pathway downstream of integrin-fibronectin binding is a key player regulating both segmentation clock dynamics and correct somite formation. We thus propose a model in which the fibronectin matrix complexity gradient is integrated in the current view of the clock and wavefront model for somitogenesis (Cooke and Zeeman, 1976, Pais de Azevedo et al., 2018). The progressive increase of fibronectin assembly from posterior to anterior in the PSM is translated into a tensional gradient, with anterior PSM cells contacting with a stiffer environment. This is concomitant with the decrease in Fgf/Wnt levels. Thus upon passing the determination front, cells sense both a stiffer environment and decreasing Fgf/Wnt signaling. Increased fibronectin binding to integrins stimulates ROCK and possibly YAP activity (Hubaud et al. 2017), which in turn promote the slowdown of clock oscillations and *Meso1* expression at the S-II/S-I region, that eventually stabilizes Notch signaling in the anterior PSM. Increased fibronectin-derived tension thus culminates in the cessation of the cyclic expression of clock genes in the anterior PSM and promotes the cellular rearrangements underlying somite epithelialization. A fibronectin-integrin-actomyosin axis is thus a strong candidate for mediating the translation of the cycling gene expression in the PSM into the correct temporal and spatial somite formation.

2013). Interestingly, Hubaud and collaborators demonstrated that these oscillations can be prolonged for longer (>20 cycles) when ROCK inhibitor (Y-27632) is added to the medium (Hubaud et al., 2017) suggesting that ROCK activity normally stops segmentation clock oscillations in this system.

ROCK acts downstream of integrins and phosphorylates the NMMII regulatory light chains while simultaneously inhibiting myosin light chain phosphatase. This increases the ATPase activity of NMMII and promotes its binding to F-actin, thus increasing cell contractility (Newell-Litwa et al., 2015). Together with the increased cell tension of the actomyosin cytoskeleton, ROCK activity is known to promote the nuclear localization of the Yes-associated protein (YAP), an intracellular sensor of cell mechanics, in several cell types (Piccolo et al., 2014). Remarkably, YAP-null mouse mutants (Morin-Kensicki et al., 2006) have a phenotype very similar to that of integrin α5-null mutants (Yang et al., 1993) and *Fn1*$^{RGE/RGE}$ embryos (Girós et al., 2011), suggesting that they contribute to the same processes during early embryo development. Indeed, isolated mouse PSM cells cultured on fibronectin display nuclear localization of YAP and YAP-dependent inhibition of clock oscillations, independently of Notch activity (Hubaud et al., 2017). Moreover, electroporating the PSM of chick embryos with constitutively active YAP results in the loss of the oscillatory pattern of *Lnfg* expression. Since cells on compliant matrices tend to have YAP in the cytoplasm and cells on stiffer substrates have nuclear YAP (Piccolo et al., 2014), these results are consistent with the hypothesis that a certain mechanical environment promotes segmentation clock oscillations and when this environment stiffens beyond a particular point, oscillations dampen and come to a halt, leading to the upregulation of *Meso1* and the definition of the next boundary.

*Morphological somite formation occurs in two steps, which appear to have different mechanical requirements*

Mesp2/Meso1 activity is the first step in morphological boundary formation in both mouse and chick (Saga, 2012). It has been demonstrated in the mouse that Mesp2 is activated in the rostral PSM by the travelling wave of Notch signaling and its rostral border of expression is defined by the rostral limit of Tbx6 expression (Oginuma et al., 2010). Mesp2 transcription factor upregulates Ripply expression, which downregulates *Mesp2* transcription and Tbx6 in preparation for the positioning of the next band of *Mesp2/Meso1* expression (Takahashi et al., 2010). Mesp2/Meso1 also activates the expression of EphA4, which interacts with ephrinB2 in cells rostral to the Mesp2/Meso1 expression domain causing cell-cell repulsion and the formation of an incipient cleft (Nakajima et al., 2006; Watanabe et al., 2009). As soon as the cleft forms, fibronectin matrix assembly occurs in the cleft (Jülich et al., 2015; Rifes and Thorsteinsdóttir, 2012), thus stabilizing it. Moreover, the deposition of fibronectin within this cleft is thought to promote the epithelialization of cells rostral to the cleft (Martins et al., 2009). Thus, the formation of the cleft and the epithelialization of the cells rostral to the nascent boundary can be defined as the first step of morphological somite formation, i.e. beginning of stage S0. The second step is defined as the epithelialization of the remaining cells in S0 until cells have acquired a spindle-like shape and organized into a rosette, pinching off from the PSM as SI (Martins et al., 2009).

The phenotype of RockOut, RGD and 70kDa treated embryos is very similar (Fig. 3.10 A). All show perturbations in expression of *Hairy1* (and *Hairy2*, when assessed), an abnormal positioning of *Meso1* and defects in somite boundary development. Although somite morphology is also perturbed in these explants, the acquisition of the spindle-shape cell morphology of cells which occurs as S0 develops into SI does not appear to be significantly perturbed. Thus, the first step of morphological somite formation is affected but the second step is not. In contrast, Blebbistatin-treated explants not only have the defects listed above, but cells that had already upregulated *Meso1* before the addition of the drug and formed an incipient cleft during culture, were completely unable to epithelialize. In fact, Blebbistatin-treated explants formed only 1 or 2 somites in culture, and cells in the somites formed did not acquire the elongated, spindle-shape typical of SI somites. In fact, somites that formed just before the addition of Blebbistatin even lost their spindle-shape morphology and acquired a more cuboidal shape (data not shown). These results demonstrate that Blebbistatin affects both steps of morphological somite formation.

RockOut targets NMMII activity indirectly by inhibiting ROCKI/II, one of the kinases that activate NMMII (Newell-Litwa et al., 2015). In contrast, Blebbistatin targets the NMMII ATPase directly and thus has the same effect as inhibiting all kinases able to activate NMMII. Our results thus raise the possibility that segmentation clock oscillations, *Meso1* positioning and boundary formation are dependent on a fibronectin-integrin-ROCK-NMMII axis, while the acquisition of the spindle-shaped morphology of cells is dependent on another NMMII activator. Interestingly, $Ca^{++}$/calmodulin signaling can activate NMMII and inhibiting calmodulin was shown to block the acquisition of this morphology during chick somitogenesis (Chernoff and Hilfer, 1982). This issue warrants further investigation.

*Interplay between Notch signaling and fibronectin-integrin signaling during somite formation*

Notch signaling is essential for the synchrony, period and pattern of segmentation clock oscillations. When all Notch activity is lost in mouse embryos (as in *Psen1/Psen2*-null embryos) both cyclic expression of clock genes and somite formation is lost (Ferjentsik et al., 2009). Notch signaling is necessary for the synchronization of neighboring cultured PSM cells (Tsiairis and Aulehla, 2016), and increasing the number of DeltaD copies in zebrafish embryos leads to changes in the wave patterns and shorter periods of oscillations (Liao et al., 2016). The fact that interfering with fibronectin assembly, integrin-RGD binding and mechanotransduction players results in altered segmentation clock dynamics suggests that albeit crucial, Notch is not the only player regulating the pace of clock oscillations. In fact, the Notch signaling pathway and the fibronectin-integrin-mechanotransduction pathway are highly likely to crosstalk in this context. Integrins are prime candidates to mediate this cross talk. For example, Notch signaling was shown to activate α5β1 integrin and to increase adhesion to fibronectin in myeloid cell lines (Hodkinson et al., 2007). Conversely, β1 integrins are needed for correct Notch signaling in neural progenitors (Campos et al., 2006). In the zebrafish, combined roles of integrin α5β1 and Notch are needed for normal somitogenesis (Jülich et al., 2005). Finally, in the chick PSM, β1 integrin signaling via integrin linked-kinase (ILK) enhances Notch signaling and cooperation between β1 integrin and Notch is needed for correct *Meso1* expression in this context (Rallis et al., 2010). As mentioned above, adhesion of cultured PSM cells to fibronectin also modulates Notch signaling in these cells, in a YAP-dependent manner (Hubaud et al., 2017). Remarkably, YAP directly interacts with the Notch signaling pathway in neural crest cells (Manderfield et al., 2015) and cultured epidermal stem cells (Totaro et al., 2017). Interestingly, we observed that the intercellular space between PSM cells greatly increases when NMMII is inhibited in our cultured explants, and cells become loose and detached from their neighbors (Supplementary Fig. 3.5, O-P). This will likely reduce cell-cell contacts and affect Notch signaling, since the direct contact of the receptors and ligands of adjacent PSM cells will probably be impaired. Altogether, these findings suggest that in the PSM, interaction between the Notch pathway and the mechanotransduction pathway receiving cues from the fibronectin matrix assembly state allows for coordinated cyclic expression of segmentation clock genes with the correct period.

*Fibronectin matrix complexity gradient as a player in the wavefront*

While the waves of Notch activity travel through the entire length of the PSM, this is only translated into segment formation in the anterior-most region of the tissue. Opposing gradients of Fgf/Wnt and RA in the PSM are thought to define the so called determination front, which defines the region where PSM cells become competent for somite formation (Hubaud and Pourquié, 2014). This maturation program includes slowing down segmentation clock oscillations until they reach a halt when cells become part of a somite. Comparatively high concentrations of Fgf/Wnt in the posterior PSM are thought to maintain PSM cells in a mesenchymal uncommitted state, while anterior PSM cells receive lower doses of Fgf/Wnt and high concentrations of RA synthesized by the epithelial somites, which is thought to counteract Fgf activity (Aulehla and Pourquié, 2010; Bajard et al., 2014; Diez del Corral et al., 2003; Dunty et al., 2007; Naiche et al., 2011). However, the actual functional role of these gradients has recently been challenged. While Wnt signaling has a clear role in boundary positioning and shows wavefront activity, Fgf seems more important for the expansion and viability of the axial progenitors before they enter the PSM (Aulehla et al., 2003; Bajard et al., 2014; Boulet and Capecchi, 2012; Mallo, 2016). Moreover, the role of RA in opposing the effects of Fgf is also unclear, since the Fgf gradient is a result of progressive mRNA degradation as PSM cells are displaced more anteriorly in the PSM, and RA has no described role in regulating mRNA stability, acting only at the transcriptional level (Cunningham and Duester, 2015; Dubrulle and Pourquié, 2004).

The mechanical cues provided by the increasing complexity of the fibronectin matrix in the anterior PSM may provide at least as much information to PSM cells as these diffusing factors (Mammoto and Ingber, 2010; Schwarz and Safran, 2013). Thus, based on our data, we propose that the posterior to anterior gradient of fibronectin matrix density and complexity, combined with the gradient of cell density that exists from posterior to anterior (Bellairs et al., 1978; Bellairs et al., 1980; Bénazéraf et al., 2010; Jülich et al., 2015; McMillen et al., 2016), can be interpreted by the PSM cells as an increasing tensional gradient which would be a contributor to the wavefront. Hence, the anterior end of the PSM would receive and integrate a combination of chemical and mechanical signals, namely decreased Fgf/Wnt levels and increased RA levels (Aulehla and Pourquié, 2010) and, simultaneously, an increase in fibronectin matrix complexity and stiffness. The fibronectin matrix and its downstream mechanotransduction pathways may thus be an underappreciated part of the complex network of players known to regulate the robust segmentation clock oscillations and correct spatiotemporal somite formation.

## Acknowledgements

We thank Dr. Yuki Sato for generously sharing the pCAGGs-q70kDa construct. This work was supported by Fundação para a Ciência e a Tecnologia (FCT, Portugal) projects PTDC/SAU-OBD/103771/2008, PTDC/BEXBID/5410/2014, UID/BIA/00329/2013, UID/BIM/04773/2013 and PPBI-POCI-01-0145-FEDER-022122, and FCT scholarships SFRH/BD/86980/2012 (PGA) and SFRH/BD/37423/2007 (PR). We also thank all members of our laboratories for helpful discussions.

## References

**Aulehla, A. and Pourquié, O.** (2010). Signaling gradients during paraxial mesoderm development. *Cold Spring Harb. Perspect. Biol.* **2**, 1–17.

**Aulehla, A., Wehrle, C., Brand-Saberi, B., Kemler, R., Gossler, A., Kanzler, B. and Herrmann, B. G.** (2003). Wnt3a plays a major role in the segmentation clock controlling somitogenesis. *Dev. Cell* **4**, 395–406.

**Bailey, C. and Dale, K.** (2015). Somitogenesis in vertebrate development. In *eLS*, pp. 1–15. Chichester, UK: John Wiley & Sons, Ltd.

**Bajanca, F., Luz, M., Duxson, M. J. and Thorsteinsdóttir, S.** (2004). Integrins in the mouse myotome: Developmental changes and differences between the epaxial and hypaxial lineage. *Dev. Dyn.* **231**, 402–415.

**Bajard, L., Morelli, L. G., Ares, S., Pecreaux, J., Julicher, F. and Oates, A. C.** (2014). Wnt-regulated dynamics of positional information in zebrafish somitogenesis. *Development* **141**, 1381–1391.

**Barczyk, M., Carracedo, S. and Gullberg, D.** (2010). Integrins. *Cell Tissue Res.* **339**, 269–280.

**Barriga, E. H., Franze, K., Charras, G. and Mayor, R.** (2018). Tissue stiffening coordinates morphogenesis by triggering collective cell migration in vivo. *Nature* **554**, 523–527.

**Barrios, A., Poole, R. J., Durbin, L., Brennan, C., Holder, N. and Wilson, S. W.** (2003). Eph/Ephrin signaling regulates the mesenchymal-to-epithelial transition of the paraxial mesoderm during somite morphogenesis. *Curr. Biol.* **13**, 1571–82.

**Bellairs, R., Curtis, A. S. and Sanders, E. J.** (1978). Cell adhesiveness and embryonic differentiation. *J. Embryol. Exp. Morphol.* **46**, 207–13.

**Bellairs, R., Sanders, E. J. and Portch, P. A.** (1980). Behavioural properties of chick somitic mesoderm and lateral plate when explanted in vitro. *J. Embryol. Exp. Morphol.* **56**, 41–58.

**Bénazéraf, B., Francois, P., Baker, R. E., Denans, N., Little, C. D. and Pourquié, O.** (2010). A random cell motility gradient downstream of FGF controls elongation of an amniote embryo. *Nature* **466**, 248–252.

**Bharadwaj, M., Strohmeyer, N., Colo, G. P., Helenius, J., Beerenwinkel, N., Schiller, H. B., Fässler, R. and Müller, D. J.** (2017). αV-class integrins exert dual roles on α5β1 integrins to strengthen adhesion to fibronectin. *Nat. Commun.* **8**, 14348.

**Boulet, A. M. and Capecchi, M. R.** (2012). Signaling by FGF4 and FGF8 is required for axial elongation of the mouse embryo. *Dev. Biol.* **371**, 235–245.

**Buchberger, A., Seidl, K., Klein, C., Eberhardt, H. and Arnold, H. H.** (1998). cMeso-1, a novel bHLH transcription factor, is involved in somite formation in chicken embryos. *Dev. Biol.* **199**, 201–15.

**Campos, L. S., Decker, L., Taylor, V. and Skarnes, W.** (2006). Notch, epidermal growth factor receptor, and beta1-integrin pathways are coordinated in neural stem cells. *J. Biol. Chem.* **281**, 5300–9.

**Chan, C. J., Heisenberg, C.-P. and Hiiragi, T.** (2017). Coordination of morphogenesis and cell-fate specification in development. *Curr. Biol.* **27**, R1024–R1035.

**Chapman, S. C., Collignon, J., Schoenwolf, G. C. and Lumsden, A.** (2001). Improved method for chick whole-embryo culture using a filter paper carrier. *Dev. Dyn.* **220**, 284–9.

**Chernoff, E. A. and Hilfer, S. R.** (1982). Calcium dependence and contraction in somite formation. *Tissue Cell* **14**, 435–49.

**Christ, B., Huang, R. and Scaal, M.** (2007). Amniote somite derivatives. *Dev. Dyn.* **236**, 2382–2396.

**Chuai, M., Zeng, W., Yang, X., Boychenko, V., Glazier, J. A. and Weijer, C. J.** (2006). Cell movement during chick primitive streak formation. *Dev. Biol.* **296**, 137–49.

**Cosgrove, B. D., Mui, K. L., Driscoll, T. P., Caliari, S. R., Mehta, K. D., Assoian, R. K., Burdick, J. A. and Mauck, R. L.** (2016). N-cadherin adhesive interactions modulate matrix mechanosensing and fate commitment of mesenchymal stem cells. *Nat. Mater.* **15**, 1297–1306.

**Cunningham, T. J. and Duester, G.** (2015). Mechanisms of retinoic acid signalling and its roles in organ and limb development. *Nat. Rev. Mol. Cell Biol.* **16**, 110–123.

**Daley, W. P., Kohn, J. M. and Larsen, M.** (2011). A focal adhesion protein-based mechanochemical checkpoint regulates cleft progression during branching morphogenesis. *Dev. Dyn.* **240**, 2069–2083.

**Danen, E. H. J., Sonneveld, P., Brakebusch, C., Fässler, R. and Sonnenberg, A.** (2002). The fibronectin-binding integrins α5β1 and αvβ3 differentially modulate RhoA-GTP loading, organization of cell matrix adhesions, and fibronectin fibrillogenesis. *J. Cell Biol.* **159**, 1071–1086.

**Dequéant, M.-L., Glynn, E., Gaudenz, K., Wahl, M., Chen, J., Mushegian, A. and Pourquié, O.** (2006). A complex oscillating network of signaling genes underlies the mouse segmentation clock. *Science* **314**, 1595–8.

**Diez del Corral, R., Olivera-Martinez, I., Goriely, A., Gale, E., Maden, M. and Storey, K.** (2003). Opposing FGF and retinoid pathways control ventral neural pattern, neuronal differentiation, and segmentation during body axis extension. *Neuron* **40**, 65–79.

**Drake, C. J. and Little, C. D.** (1991). Integrins play an essential role in somite adhesion to the embryonic axis. *Dev. Biol.* **143**, 418–21.

**Drake, C. J., Davis, L. A., Hungerford, J. E. and Little, C. D.** (1992). Perturbation of beta 1 integrin-mediated adhesions results in altered somite cell shape and behavior. *Dev. Biol.* **149**, 327–38.

**Dubrulle, J. and Pourquié, O.** (2004). fgf8 mRNA decay establishes a gradient that couples axial elongation to patterning in the vertebrate embryo. *Nature* **427**, 419–422.

**Dunty, W. C., Biris, K. K., Chalamalasetty, R. B., Taketo, M. M., Lewandoski, M. and Yamaguchi, T. P.** (2007). Wnt3a/ -catenin signaling controls posterior body development by coordinating mesoderm formation and segmentation. *Development* **135**, 85–94.

**Eyckmans, J., Boudou, T., Yu, X. and Chen, C. S.** (2011). A hitchhiker's guide to mechanobiology. *Dev. Cell* **21**, 35–47.

**Ferjentsik, Z., Hayashi, S., Dale, J. K., Bessho, Y., Herreman, A., De Strooper, B., del Monte, G., de la Pompa, J. L. and Maroto, M.** (2009). Notch is a critical component of the mouse somitogenesis oscillator and is essential for the formation of the somites. *PLoS Genet.* **5**, e1000662.

**Friedland, J. C., Lee, M. H. and Boettiger, D.** (2009). Mechanically activated integrin switch controls alpha5beta1 function. *Science* **323**, 642–4.

**Geiger, B. and Yamada, K. M.** (2011). Molecular architecture and function of matrix adhesions. *Cold Spring Harb. Perspect. Biol.* **3**, 1–21.

**Geiger, B., Spatz, J. P. and Bershadsky, A. D.** (2009). Environmental sensing through focal adhesions. *Nat. Rev. Mol. Cell Biol.* **10**, 21–33.

**George, E. L., Georges-Labouesse, E. N., Patel-King, R. S., Rayburn, H. and Hynes, R. O.** (1993). Defects in mesoderm, neural tube and vascular development in mouse embryos lacking fibronectin. *Development* **119**, 1079–1091.

**Georges-Labouesse, E. N., George, E. L., Rayburn, H. and Hynes, R. O.** (1996). Mesodermal development in mouse embryos mutant for fibronectin. *Dev. Dyn.* **207**, 145–56.

**Girós, A., Grgur, K., Gossler, A. and Costell, M.** (2011). α5β1 integrin-mediated adhesion to fibronectin is required for axis elongation and somitogenesis in mice. *PLoS One* **6**, e22002.

**Goh, K. L., Yang, J. T. and Hynes, R. O.** (1997). Mesodermal defects and cranial neural crest apoptosis in alpha5 integrin-null embryos. *Development* **124**, 4309–4319.

**Gomes de Almeida, P., Pinheiro, G. G., Nunes, A. M., Gonçalves, A. B. and Thorsteinsdóttir, S.** (2016). Fibronectin assembly during early embryo development: A versatile communication system between cells and tissues. *Dev. Dyn.* **245**, 520–35.

**Hamburger, V. and Hamilton, H. L.** (1992). A series of normal stages in the development of the chick embryo. *Dev. Dyn.* **195**, 231–272.

**Heisenberg, C. and Bellaïche, Y.** (2013). Forces in tissue morphogenesis and patterning. *Cell* **153**, 948–62.

**Henrique, D., Adam, J., Myat, A., Chitnis, A., Lewis, J. and Ish-Horowicz, D.** (1995). Expression of a Delta homologue in prospective neurons in the chick. *Nature* **375**, 787–790.

**Hodkinson, P. S., Elliott, P. A., Lad, Y., McHugh, B. J., MacKinnon, A. C., Haslett, C. and Sethi, T.** (2007). Mammalian NOTCH-1 activates β1 integrins via the small GTPase R-Ras. *J. Biol. Chem.* **282**, 28991–29001.

**Hubaud, A. and Pourquié, O.** (2014). Signalling dynamics in vertebrate segmentation. *Nat. Rev. Mol. Cell Biol.* **15**, 709–721.

**Hubaud, A., Regev, I., Mahadevan, L. and Pourquié, O.** (2017). Excitable dynamics and Yap-dependent mechanical cues drive the segmentation clock. *Cell* **171**, 668–682.e11.

**Huveneers, S. and Danen, E. H. J.** (2009). Adhesion signaling - crosstalk between integrins, Src and Rho. *J. Cell Sci.* **122**, 1059–1069.

**Jouve, C., Palmeirim, I., Henrique, D., Beckers, J., Gossler, A., Ish-Horowicz, D. and Pourquié, O.** (2000). Notch signalling is required for cyclic expression of the hairy-like gene HES1 in the presomitic mesoderm. *Development* **127**, 1421–1429.

**Jülich, D., Geisler, R., Holley, S. a. and Tübingen 2000 Screen Consortium** (2005). Integrin alpha5 and delta/notch signaling have complementary spatiotemporal requirements during zebrafish somitogenesis. *Dev. Cell* **8**, 575–86.

**Jülich, D., Cobb, G., Melo, A. M., McMillen, P., Lawton, A. K., Mochrie, S. G. J., Rhoades, E. and Holley, S. A.** (2015). Cross-Scale Integrin Regulation Organizes ECM and Tissue Topology. *Dev. Cell* **34**, 33–44.

**Kametaka, S., Moriyama, K., Burgos, P. V, Eisenberg, E., Greene, L. E., Mattera, R. and Bonifacino, J. S.** (2007). Canonical interaction of cyclin G associated kinase with adaptor protein 1 regulates lysosomal enzyme sorting. *Mol. Biol. Cell* **18**, 2991–3001.

**Kocsis, E., Trus, B. L., Steer, C. J., Bisher, M. E. and Steven, A. C.** (1991). Image averaging of flexible fibrous macromolecules: the clathrin triskelion has an elastic proximal segment. *J. Struct. Biol.* **107**, 6–14.

**Koshida, S., Kishimoto, Y., Ustumi, H., Shimizu, T., Furutani-Seiki, M., Kondoh, H. and Takada, S.** (2005). Integrin alpha5-dependent fibronectin accumulation for maintenance of somite boundaries in zebrafish embryos. *Dev. Cell* **8**, 587–98.

**Kragtorp, K. a. and Miller, J. R.** (2007). Integrin alpha5 is required for somite rotation and boundary formation in Xenopus. *Dev. Dyn.* **236**, 2713–20.

**Lauschke, V. M., Tsiairis, C. D., François, P. and Aulehla, A.** (2013). Scaling of embryonic patterning based on phase-gradient encoding. *Nature* **493**, 101–105.

**Lecuit, T. and Lenne, P.-F.** (2007). Cell surface mechanics and the control of cell shape, tissue patterns and morphogenesis. *Nat. Rev. Mol. Cell Biol.* **8**, 633–44.

**Liao, B. K., Jörg, D. J. and Oates, A. C.** (2016). Faster embryonic segmentation through elevated Delta-Notch signalling. *Nat. Commun.* **7**, 1–12.

**Mallo, M.** (2016). Revisiting the involvement of signaling gradients in somitogenesis. *FEBS J.* **283**, 1430–1437.

**Mammoto, T. and Ingber, D. E.** (2010). Mechanical control of tissue and organ development. *Development* **137**, 1407–1420.

**Manderfield, L. J., Aghajanian, H., Engleka, K. A., Lim, L. Y., Liu, F., Jain, R., Li, L., Olson, E. N. and Epstein, J. A.** (2015). Hippo signaling is required for Notch-dependent smooth muscle differentiation of neural crest. *Development* **142**, 2962–2971.

**Marek, M. and Kubícek, M.** (1981). Morphogen pattern formation and development in growth. *Bull. Math. Biol.* **43**, 259–70.

**Martins, G. G., Rifes, P., Amândio, R., Rodrigues, G., Palmeirim, I. and Thorsteinsdóttir, S.** (2009). Dynamic 3D cell rearrangements guided by a fibronectin matrix underlie somitogenesis. *PLoS One* **4**, e7429.

**Masamizu, Y., Ohtsuka, T., Takashima, Y., Nagahara, H., Takenaka, Y., Yoshikawa, K., Okamura, H. and Kageyama, R.** (2006). Real-time imaging of the somite segmentation clock: Revelation of unstable oscillators in the individual presomitic mesoderm cells. *Proc. Natl. Acad. Sci.* **103**, 1313–1318.

**McKeown-Longo, P. J. and Mosher, D. F.** (1985). Interaction of the 70,000-mol-wt amino-terminal fragment of fibronectin with the matrix-assembly receptor of fibroblasts. *J. Cell Biol.* **100**, 364–74.

**McMillen, P., Chatti, V., Jülich, D. and Holley, S. A.** (2016). A sawtooth pattern of Cadherin 2 stability mechanically regulates somite morphogenesis. *Curr. Biol.* **26**, 542–9.

**Merle, T. and Farge, E.** (2018). Trans-scale mechanotransductive cascade of biochemical and biomechanical patterning in embryonic development: the light side of the force. *Curr. Opin. Cell Biol.* **55**, 111–118.

**Morimoto, M., Takahashi, Y., Endo, M. and Saga, Y.** (2005). The Mesp2 transcription factor establishes segmental borders by suppressing Notch activity. *Nature* **435**, 354–359.

**Morin-Kensicki, E. M., Boone, B. N., Howell, M., Stonebraker, J. R., Teed, J., Alb, J. G., Magnuson, T. R., O'Neal, W. and Milgram, S. L.** (2006). Defects in yolk sac vasculogenesis, chorioallantoic fusion, and embryonic axis elongation in mice with targeted disruption of Yap65. *Mol. Cell. Biol.* **26**, 77–87.

**Naiche, L. A., Holder, N. and Lewandoski, M.** (2011). FGF4 and FGF8 comprise the wavefront activity that controls somitogenesis. *Proc. Natl. Acad. Sci.* **108**, 4018–4023.

**Nakajima, Y., Morimoto, M., Takahashi, Y., Koseki, H. and Saga, Y.** (2006). Identification of Epha4 enhancer required for segmental expression and the regulation by Mesp2. *Development* **133**, 2517–25.

**Newell-Litwa, K. A., Horwitz, R. and Lamers, M. L.** (2015). Non-muscle myosin II in disease: mechanisms and therapeutic opportunities. *Dis. Model. Mech.* **8**, 1495–515.

**Niwa, Y., Shimojo, H., Isomura, A., Gonzalez, A., Miyachi, H. and Kageyama, R.** (2011). Different types of oscillations in Notch and Fgf signaling regulate the spatiotemporal periodicity of somitogenesis. *Genes Dev.* **25**, 1115–1120.

**Oginuma, M., Takahashi, Y., Kitajima, S., Kiso, M., Kanno, J., Kimura, A. and Saga, Y.** (2010). The oscillation of Notch activation, but not its boundary, is required for somite border formation and rostral-caudal patterning within a somite. *Development* **137**, 1515–1522.

**Ozbudak, E. M. and Lewis, J.** (2008). Notch signalling synchronizes the zebrafish segmentation clock but is not needed to create somite boundaries. *PLoS Genet.* **4**, e15.

**Palmeirim, I., Henrique, D., Ish-Horowicz, D. and Pourquié, O.** (1997). Avian hairy gene expression identifies a molecular clock linked to vertebrate segmentation and somitogenesis. *Cell* **91**, 639–648.

**Piccolo, S., Dupont, S. and Cordenonsi, M.** (2014). The Biology of YAP/TAZ: Hippo Signaling and Beyond. *Physiol. Rev.* **94**, 1287–1312.

**Pierschbacher, M. D. and Ruoslahti, E.** (1984). Cell attachment activity of fibronectin can be duplicated by small synthetic fragments of the molecule. *Nature* **309**, 30–3.

**Pourquié, O. and Tam, P. P. L.** (2001). A nomenclature for prospective somites and phases of cyclic gene expression in the presomitic mesoderm. *Dev. Cell* **1**, 619–20.

**Preibisch, S., Saalfeld, S. and Tomancak, P.** (2009). Globally optimal stitching of tiled 3D microscopic image acquisitions. *Bioinformatics* **25**, 1463–1465.

**Prieto, D., Aparicio, G., Machado, M. and Zolessi, F. R.** (2015). Application of the DNA-specific stain methyl green in the fluorescent labeling of embryos. *J. Vis. Exp.* e52769.

**Quintin, S., Gally, C. and Labouesse, M.** (2008). Epithelial morphogenesis in embryos: asymmetries, motors and brakes. *Trends Genet.* **24**, 221–30.

**Rallis, C., Pinchin, S. M. and Ish-Horowicz, D.** (2010). Cell-autonomous integrin control of Wnt and Notch signalling during somitogenesis. *Development* **137**, 3591–3601.

**Rifes, P. and Thorsteinsdóttir, S.** (2012). Extracellular matrix assembly and 3D organization during paraxial mesoderm development in the chick embryo. *Dev. Biol.* **368**, 370–381.

**Rifes, P., Carvalho, L., Lopes, C., Andrade, R. P., Rodrigues, G., Palmeirim, I. and Thorsteinsdóttir, S.** (2007). Redefining the role of ectoderm in somitogenesis: a player in the formation of the fibronectin matrix of presomitic mesoderm. *Development* **134**, 3155–3165.

**Ringer, P., Colo, G., Fässler, R. and Grashoff, C.** (2017). Sensing the mechano-chemical properties of the extracellular matrix. *Matrix Biol.* **64**, 6–16.

**Rozario, T. and DeSimone, D. W.** (2010). The extracellular matrix in development and morphogenesis: A dynamic view. *Dev. Biol.* **341**, 126–140.

**Saga, Y.** (2012). The mechanism of somite formation in mice. *Curr. Opin. Genet. Dev.* **22**, 331–338.

**Saga, Y. and Takeda, H.** (2001). The making of the somite: molecular events in vertebrate segmentation. *Nat. Rev. Genet.* **2**, 835–845.

**Sato, Y., Yasuda, K. and Takahashi, Y.** (2002). Morphological boundary forms by a novel inductive event mediated by Lunatic fringe and Notch during somitic segmentation. *Development* **129**, 3633–44.

**Sato, Y., Nagatoshi, K., Hamano, A., Imamura, Y., Huss, D., Uchida, S. and Lansford, R.** (2017). Basal filopodia and vascular mechanical stress organize fibronectin into pillars bridging the mesoderm-endoderm gap. *Development* **144**, 281–291.

**Schiller, H. B., Hermann, M.-R., Polleux, J., Vignaud, T., Zanivan, S., Friedel,**

**C. C., Sun, Z., Raducanu, A., Gottschalk, K.-E., Théry, M., et al.** (2013). β1- and αv-class integrins cooperate to regulate myosin II during rigidity sensing of fibronectin-based microenvironments. *Nat. Cell Biol.* **15**, 625–636.

**Schwarz, U. S. and Safran, S. A.** (2013). Physics of adherent cells. *Rev. Mod. Phys.* **85**, 1327–1381.

**Shih, N. P., François, P., Delaune, E. A. and Amacher, S. L.** (2015). Dynamics of the slowing segmentation clock reveal alternating two-segment periodicity. *Development* **142**, 1785–93.

**Singh, P., Carraher, C. and Schwarzbauer, J. E.** (2010). Assembly of fibronectin extracellular matrix. *Annu. Rev. Cell Dev. Biol.* **26**, 397–419.

**Slack, J. M. W.** (1987). We have a morphogen! *Nature* **327**, 553–554.

**Smutny, M., Ákos, Z., Grigolon, S., Shamipour, S., Ruprecht, V., Čapek, D., Behrndt, M., Papusheva, E., Tada, M., Hof, B., et al.** (2017). Friction forces position the neural anlage. *Nat. Cell Biol.* **19**, 306–317.

**Straight, A. F., Cheung, A., Limouze, J., Chen, I., Westwood, N. J., Sellers, J. R. and Mitchison, T. J.** (2003). Dissecting temporal and spatial control of cytokinesis with a myosin II Inhibitor. *Science* **299**, 1743–7.

**Takahashi, Y., Inoue, T., Gossler, A. and Saga, Y.** (2003). Feedback loops comprising Dll1, Dll3 and Mesp2, and differential involvement of Psen1 are essential for rostrocaudal patterning of somites. *Development* **130**, 4259–68.

**Takahashi, S., Leiss, M., Moser, M., Ohashi, T., Kitao, T., Heckmann, D., Pfeifer, A., Kessler, H., Takagi, J., Erickson, H. P., et al.** (2007). The RGD motif in fibronectin is essential for development but dispensable for fibril assembly. *J. Cell Biol.* **178**, 167–178.

**Takahashi, J., Ohbayashi, A., Oginuma, M., Saito, D., Mochizuki, A., Saga, Y. and Takada, S.** (2010). Analysis of Ripply1/2-deficient mouse embryos reveals a mechanism underlying the rostro-caudal patterning within a somite. *Dev. Biol.* **342**, 134–45.

**Tiedemann, H.** (1976). Pattern formation in early developmental stages of amphibian embryos. *J. Embryol. Exp. Morphol.* **35**, 437–44.

**Torr, E. E., Ngam, C. R., Bernau, K., Tomasini-Johansson, B., Acton, B. and Sandbo, N.** (2015). Myofibroblasts exhibit enhanced fibronectin assembly that is intrinsic to their contractile phenotype. *J. Biol. Chem.* **290**, 6951–61.

**Totaro, A., Castellan, M., Battilana, G., Zanconato, F., Azzolin, L., Giulitti, S., Cordenonsi, M. and Piccolo, S.** (2017). YAP/TAZ link cell mechanics to Notch signalling to control epidermal stem cell fate. *Nat. Commun.* **8**, 15206.

**Tsiairis, C. D. and Aulehla, A.** (2016). Self-organization of embryonic genetic oscillators into spatiotemporal wave patterns. *Cell* **164**, 656–67.

**Voiculescu, O., Papanayotou, C. and Stern, C. D.** (2008). Spatially and temporally controlled electroporation of early chick embryos. *Nat. Protoc.* **3**, 419–426.

**Watanabe, T., Sato, Y., Saito, D., Tadokoro, R. and Takahashi, Y.** (2009). EphrinB2 coordinates the formation of a morphological boundary and cell epithelialization during somite segmentation. *Proc. Natl. Acad. Sci.* **106**, 7467–7472.

**Wei, L., Roberts, W., Wang, L., Yamada, M., Zhang, S., Zhao, Z., Rivkees, S. A., Schwartz, R. J. and Imanaka-Yoshida, K.** (2001). Rho kinases play an obligatory role in vertebrate embryonic organogenesis. *Development* **128**, 2953–62.

**Wolfenson, H., Lavelin, I. and Geiger, B.** (2013). Dynamic regulation of the structure and functions of integrin adhesions. *Dev. Cell* **24**, 447–58.

**Wolfenson, H., Meacci, G., Liu, S., Stachowiak, M. R., Iskratsch, T., Ghassemi, S., Roca-Cusachs, P., O'Shaughnessy, B., Hone, J. and Sheetz, M. P.** (2016). Tropomyosin controls sarcomere-like contractions for rigidity sensing and suppressing growth on soft matrices. *Nat. Cell Biol.* **18**, 33–42.

**Yang, J. T., Rayburn, H. and Hynes, R. O.** (1993). Embryonic mesodermal defects in alpha 5 integrin-deficient mice. *Development* **119**, 1093–1105.

**Yang, J. T., Bader, B. L., Kreidberg, J. a, Ullman-Culleré, M., Trevithick, J. E. and Hynes, R. O.** (1999). Overlapping and independent functions of fibronectin receptor integrins in early mesodermal development. *Dev. Biol.* **215**, 264–77.

**Yarrow, J. C., Totsukawa, G., Charras, G. T. and Mitchison, T. J.** (2005). Screening for cell migration inhibitors via automated microscopy reveals a Rho-kinase inhibitor. *Chem. Biol.* **12**, 385–95.

## Supplementary figures

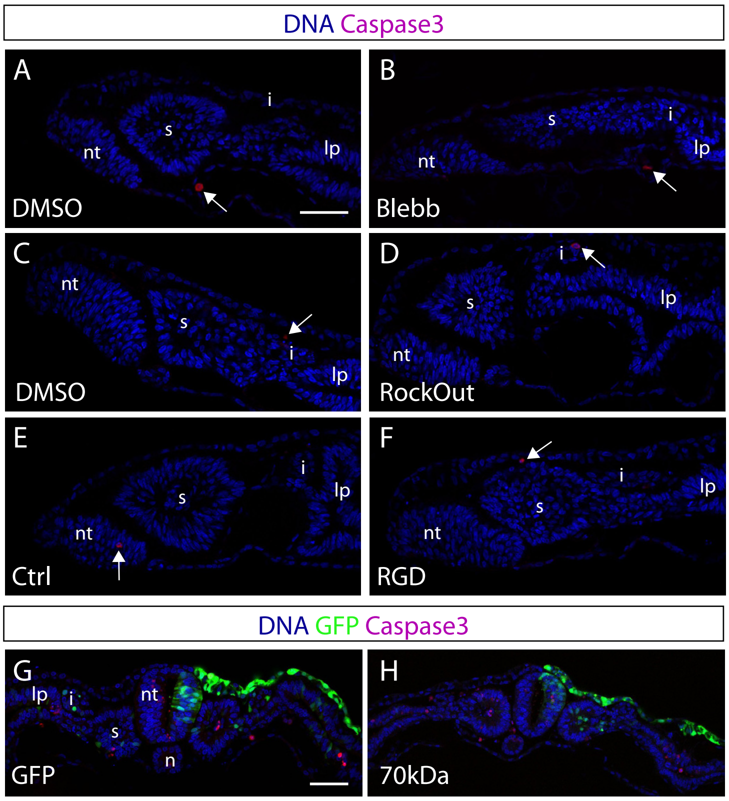


**Supplementary Fig. 3.1.** (A-E) Transverse sections of DMSO- and contralateral Blebbistatin-treated explants (A, B), DMSO- and contralateral RockOut-treated explants (C, D), Control and contralateral RGD-treated explants (E, F), GFP-electroporated embryo (G) and 70kDa- electroporated embryo (H) stained for DNA (blue), activated Caspase3 (magenta) and GFP (green, G, H). Arrows point to activated Caspase3-positive cells. Blebb – Blebbistatin; nt – neural tube; s – somite; i – intermediate mesoderm; lp – lateral plate mesoderm. Dorsal is on top. Scale bars: 50 µm.

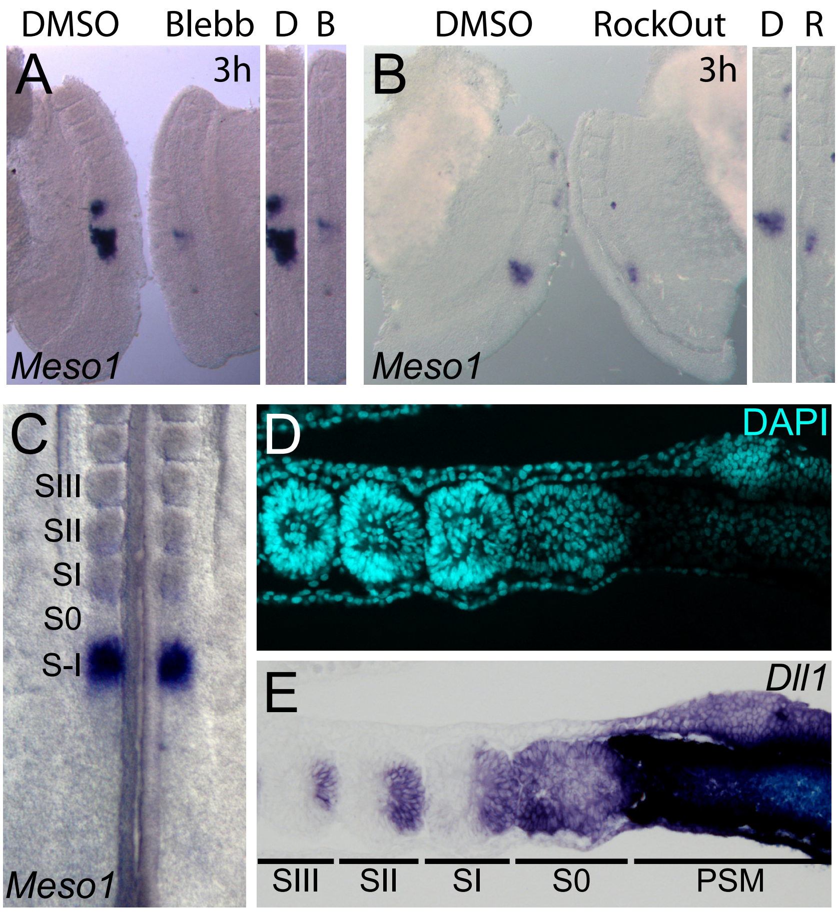


**Supplementary Fig. 3.2.** (**A-B**) *Meso1* expression in a Blebbistatin-treated (A), RockOut-treated (B) explant and respective contralateral controls at 3 hours of culture, showing misaligned expression. (**C**) *Meso1* expression in a noncultured intact 48h chick embryo, at the level of S-I. (**D-E**) Sagittal views of nuclear staining (D) and *Dll1* expression (E) in the rostral PSM and somites. *Dll1* expression is restricted to the caudal halves of formed somites (SI, SII, SIII), but in the forming somite (S0) it is expressed in the whole segment. Rostral is on top in A-C. Rostral to the left and dorsal on top in D and E.

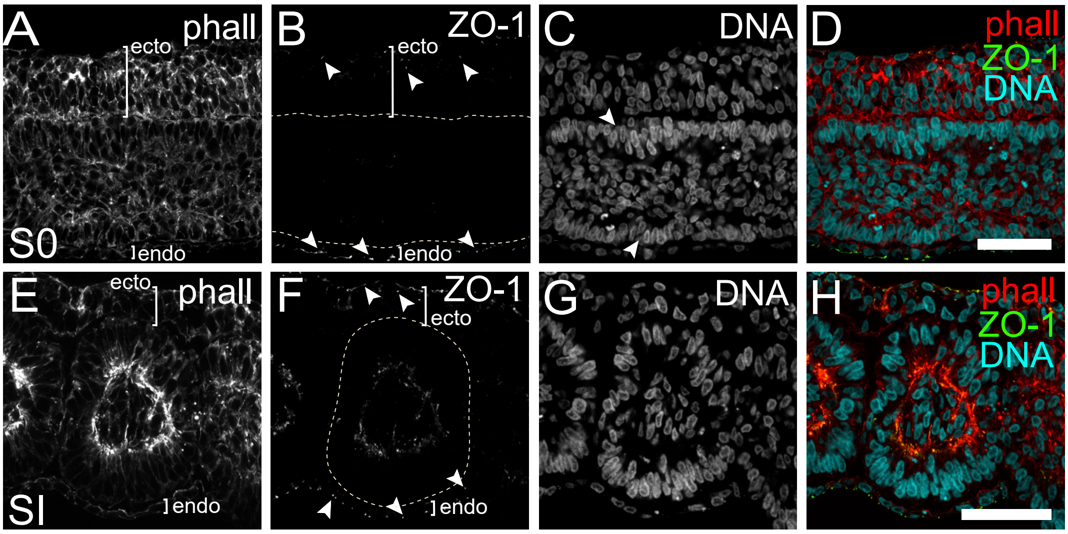


**Supplementary Fig. 3.3.** Sagittal views of F-actin and ZO-1 localization during PSM epithelialization and somite formation. Peripheral cells in the early S0 stage (A-D) show signs of an epithelioid organization, with elongated actin cytoskeleton (A) and aligned nuclei (C, arrowheads). However apically localized ZO -1 staining is not yet present in the PSM (B, dashed line), contrasting with the clearly visible ZO-1 staining in the form of strong apical dots (arrowheads in B) in the apposed endoderm and ectoderm (brackets in A and B). The most recently formed somite, SI (E-H), reveals a clear ZO-1 labeling, restricted to the apical end of the peripheral epithelial layer (F). Concordantly, F-actin staining (E) is also strongly enriched apically, and the peripheral nuclei are aligned and distinct from the ones in the somitocoel (G, H). Rostral to the left and dorsal on top. Dashed lines mark borders of S0 (B) and SI (F). Phall: phalloidin F-actin staining; DNA: ToPro-3 nuclear staining; endo: endoderm; ecto: ectoderm. Scale bars: 50 µm.

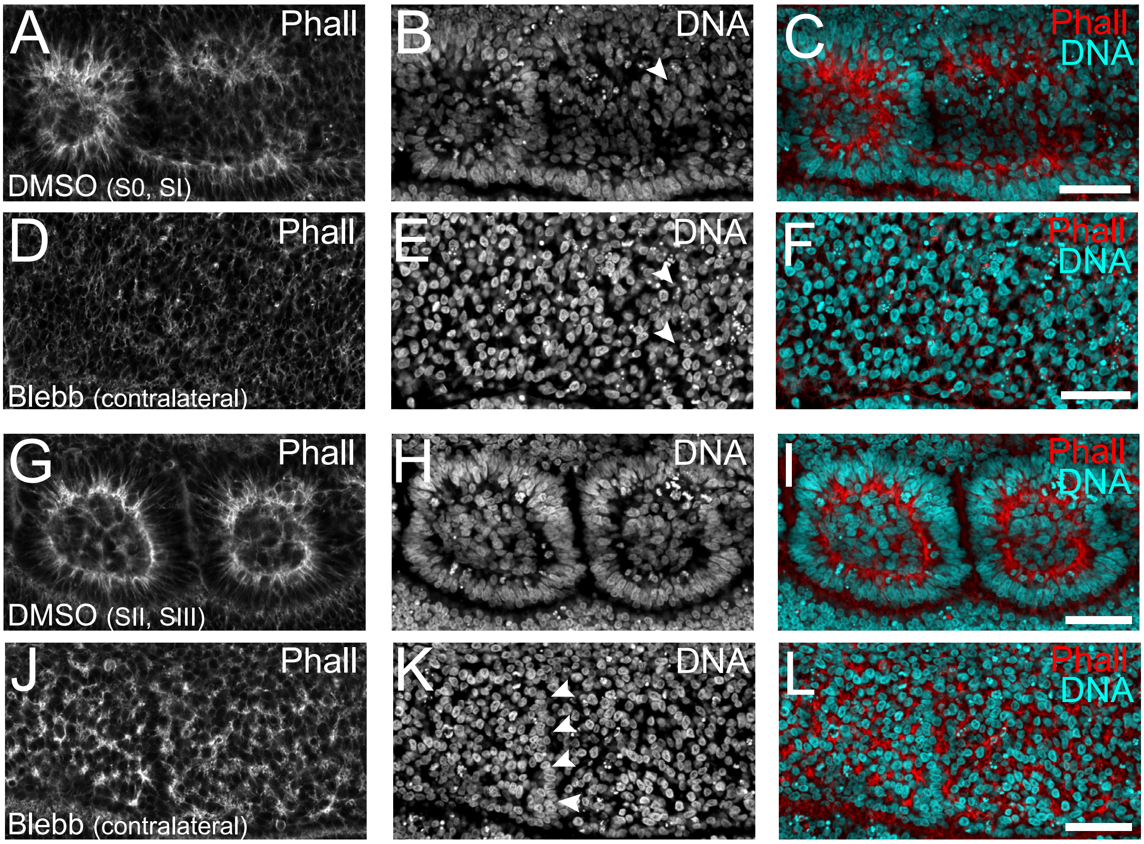


**Supplementary Fig. 3.4.** Sagittal sections of DMSO-treated explants (A-C, G-I) and contralateral Blebbistatin-treated explants (D-F, J-L) stained for F-actin and DNA. Rostral PSM epithelialization of DMSO-treated explants occurs normally, with F-actin apical enrichment (A) and nuclear alignment (B) in S0 and SI. At the same axial level in the contralateral Blebbistatin-treated explant (D-F), no signs of an epithelial arrangement or of the somitic segment are present, with only dispersed F-actin staining (D) and nonaligned nuclear organization (E). Further rostrally, somites formed during culture in DMSO-treated explants are markedly epithelial (G-I), composed of an outer cell layer with aligned nuclei (H) and elongated cells with apically enriched F-actin (G). At the equivalent axial level in the Blebbistatin-treated explant (J-L), the somitic segments were severely affected, but are still noticeable, with nuclei lining up at the prospective inter-somitic border (K, arrowheads). On the other hand, F-actin congregates into separate foci (J), with no particular arrangement (L). Rostral to the left and dorsal on top. Blebb: Blebbistatin; Phall: phalloidin F-actin staining; DNA: ToPro-3 nuclear staining. Scale bars: 50 µm.

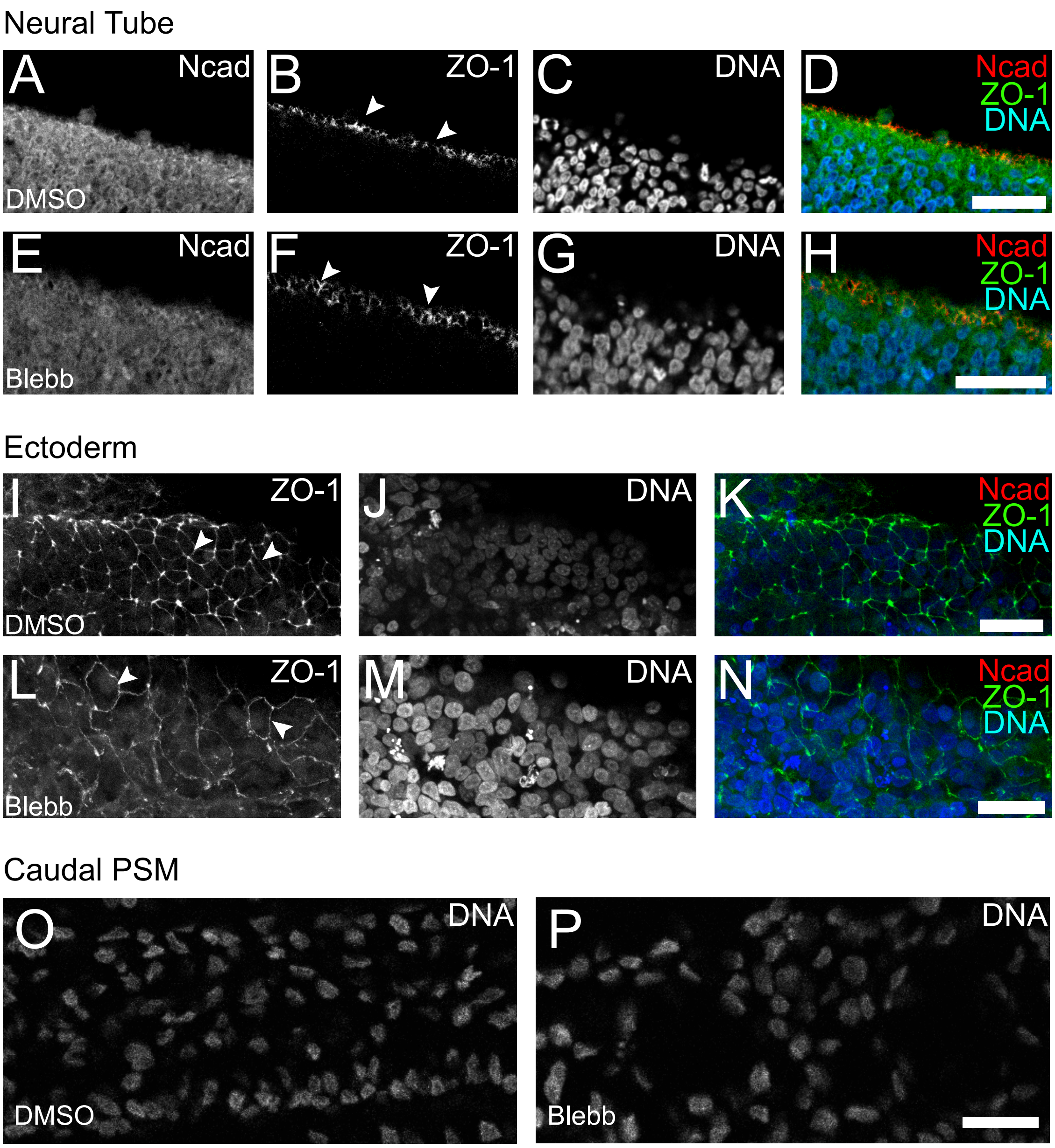


**Supplementary Fig. 3.5. (A-N)** Absence of significant effect of NMMII inhibition with Blebbistatin on neural tube and ectoderm. Explants cultured in the presence of DMSO vehicle (A-D and I-K) showed strong apically located ZO-1 labeling (B, I) both in the neural tube (A-D) and in the overlying ectoderm (I-K). In the presence of Blebbistatin (E-H, L-N), ZO-1 labeling was also restricted to the apical end of neural tube cells (F) and in the ectoderm (L). Dorsal view of the ectoderm clearly depicts the ZO-1-rich apical adhesion belt characteristic of epithelial cells in both DMSO-treated (arrowheads in I) and Blebbistatin-treated explants (arrowheads in L). Interestingly, inhibition of cell derived tension by Blebbistatin appeared to result in wider ectoderm cells (compare K and N). **(O-P)** Sagittal sections of caudal PSMs of DMSO-treated (O) and contralateral Blebbistatin-treated (P) explants, stained for DNA. Blebbistatin-treated explants show lower nuclear density compared to contralateral controls (O-P). Neural tube images (A-H) are transverse single optical confocal slices of cultured explants. Ectoderm images (I-N) result from 10-12 µm z-projections of longitudinal optical confocal slices. Rostral on the left and dorsal on top (O-P). Blebb: Blebbistatin; Ncad: N-cadherin. DNA: ToPro3 or Methyl green. Arrowheads point to ZO-1 labeling. Scale bars: 20 µm.

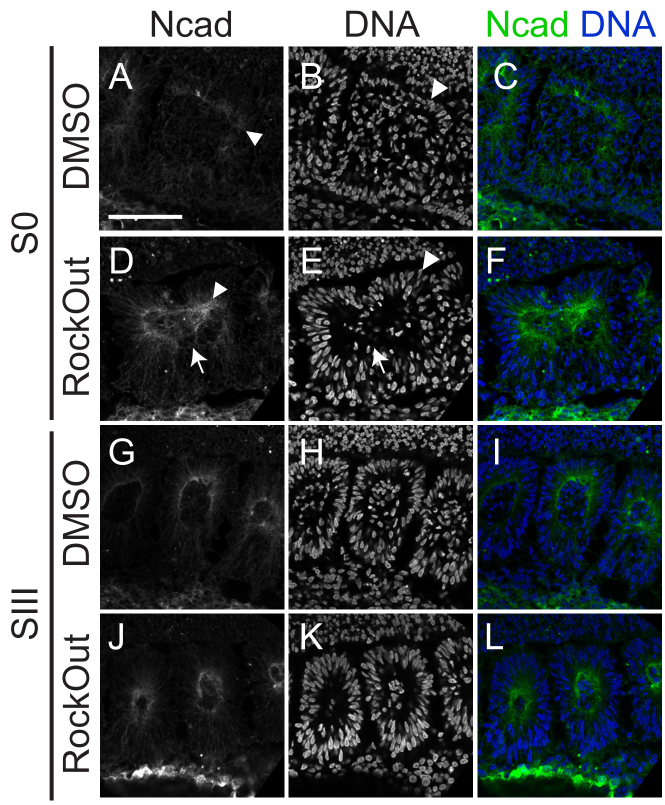


**Supplementary Fig. 3.6.** Longitudinal views of explants cultured in control (DMSO) medium (A-C, G-I) and their contralateral RockOut-treated halves (D-F, J-M) at S0 (A-F) and SII (G-M) levels, immunostained for N-cadherin (first column) and stained for DNA (second column). Third column shows the respective merge of all stainings. Explants were cultured for 6 hours (somite levels are at t=6h). Somites formed during culture in control explants show normal accumulation of N-cadherin (A, arrowhead) and nuclear alignment (B, arrowhead). In contrast, somites formed in contralateral RockOut-treated explants fail to form a clear cleft (D-F, arrows), although N-cadherin is partially polarized (D, arrowhead) and nuclei are aligned (E, arrowhead). Both explants show normal N-cadherin polarization (G, J) and nuclear alignment (H, L) at SII level. Rostral on the left and midline on top. Ncad - N-cadherin. Scale bars: 50 µm.

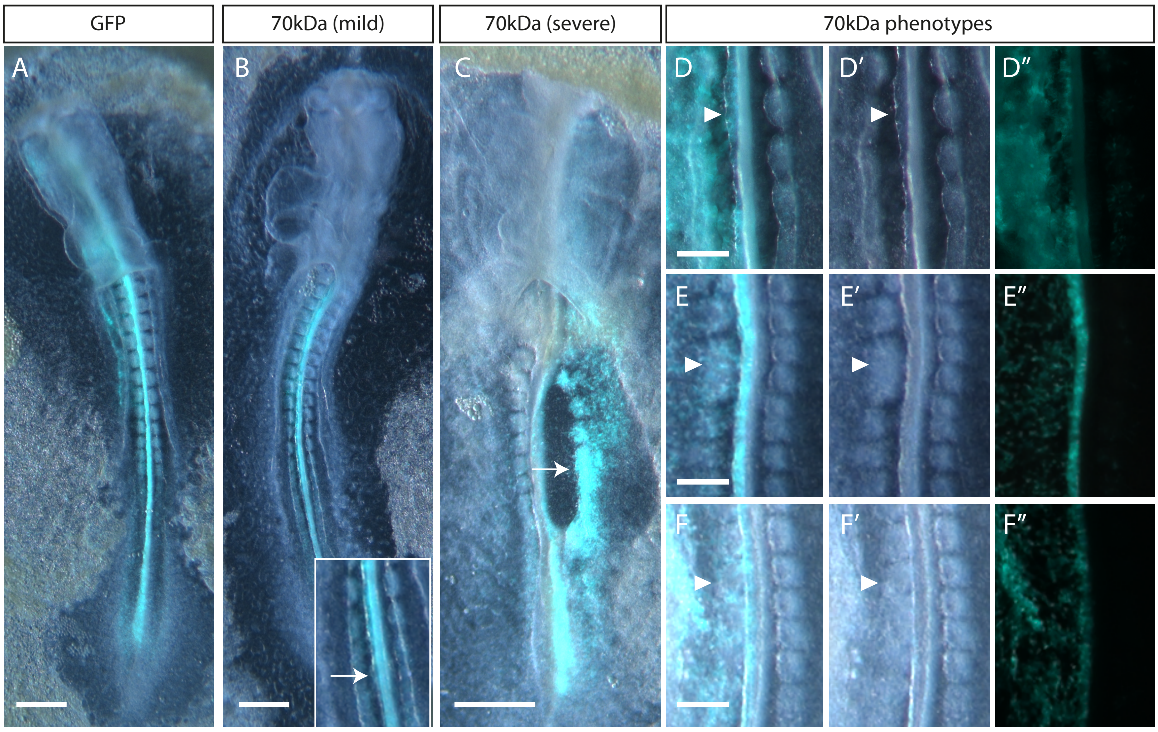


**Supplementary Fig. 3.7.** Morphology of electroporated embryos. (A) Embryo electroporated with GFP only. (B, C) Embryos co-electroporated with 70kDa, showing mild (B) and severe (C) phenotypes. Embryos with mild phenotypes mostly had the PSM and somites detaching from the surrounding tissues (B, arrow), while severe phenotypes included severely detached tissues (C, arrow) and a shortened A-P axis (C). (D-F'') Close up of embryos electroporated with 70kDa showing kinked neural tube (D-D'', arrowheads), fused somites (E-E'', arrowheads) and fewer somites in the electroporated side (F-F'', arrowheads). Ventral view and rostral on top. Green is GFP. Scale bars: (A-C) 500 µm, (D-F'') 200 µm.

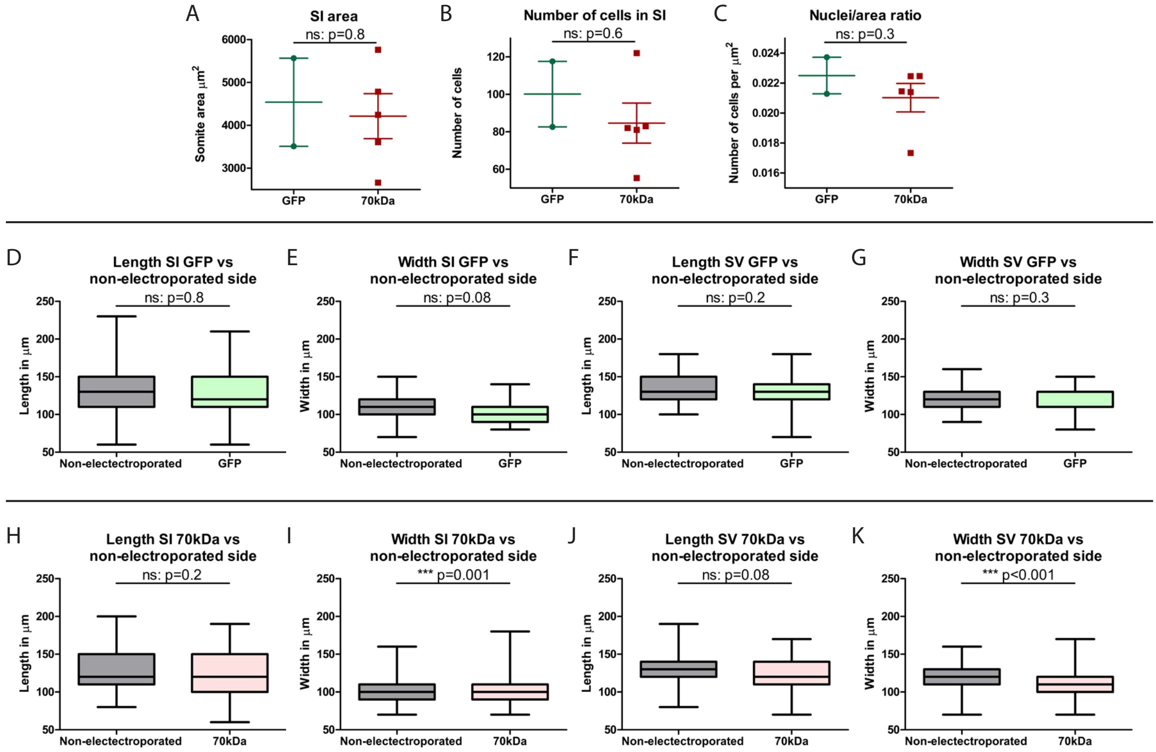


**Supplementary Fig. 3.8**. **Number of cells, area and size of somites of GFP- and 70kDa-electroporated embryos**. (A-C) Mean area (A), number of cells (B) and cell number per area ratio (C) of SI of GFP- (n=2) and 70kDa-electroporated (n=5) embryos. Up to 4 different sagittal sections per embryo were used for each measurement and the average is displayed. (D-K) Comparison between the length (D, H, F, J) and width (E, I, G, K) of SI (D-E, H-I) and SV (F-G, J-K) from GPF- (D-G) and 70kDa-electroporated embryos (H-K) of the electroporated side vs the control non-electroporated side. The measurements were made on images from whole mount embryos. Somites from GFP-electroporated embryos do not show a significant difference in either length or width between electroporated vs non-electroporated sides (n=151), but the widths of SI and SV of the electroporated side of 70kDa-treated embryos are significantly smaller than that of the contralateral non-electroporated control side (n=143). ns – not significant; *** p<0.001.

# Chapter 4

## Crosstalk between Sonic hedgehog signaling and Fibronectin matrix during somite morphogenesis

*You need the dark in order to show the light.*
— Bob Ross

# Crosstalk between Sonic hedgehog signaling and Fibronectin matrix during somite morphogenesis

Patrícia Gomes de Almeida[1,2] , Raquel P. Andrade[2] and Sólveig Thorsteinsdóttir[1]

[1] Centre for Ecology, Evolution and Environmental Change, Faculdade de Ciências, Universidade de Lisboa, Lisbon, Portugal;
[2] Centre for Biomedical Research, Universidade do Algarve, Faro, Portugal.

Contribution for the publication:

| | Experimental work depicted in Fig. | | | | | | | Manuscript writing |
|---|---|---|---|---|---|---|---|---|
| | 1 | 2 | 3 | 4 | 5 | 6 | S1 | |
| Design and concept | III | III | III | III | III | III | III | |
| Execution | III | III | III | III | III | III | III | III |
| Analysis and interpretation | III | III | III | III | III | III | III | |

**Legend:**
- ...... non applicable
O ..... no intervention
I ....... minor contribution
II ...... moderate contribution
III .... major contribution/full execution

Note: this contribution does not exclude other contributions, similar or not, from the remaining authors

## Abstract

Sonic hedgehog (Shh) is a key regulator of paraxial mesoderm development, controlling the timing of somite formation and specifying its ventral domain which gives rise to the sclerotome, precursor of vertebrae and ribs. The fibronectin extracellular matrix surrounding the paraxial mesoderm of vertebrate embryos is also essential for its correct development. In the absence of the fibronectin-encoding gene *Fn1*, axis extension is impaired and the mouse presomitic mesoderm that forms, fails to form epithelial somites. Moreover, interfering with fibronectin assembly or binding to its specific receptors in vertebrate embryos all result in somitogenesis defects. Here we describe a previously unidentified crosstalk between the fibronectin matrix and Shh signaling during paraxial mesoderm development. The fibronectin matrix surrounding the chick presomitic mesoderm and somites is essential for correct Shh signaling in these tissues. Furthermore, once active in the ventral somite, Shh signaling negatively modulates *Fn1* expression, possibly ensuring fibronectin production by the ventral somite is at lower levels until the correct timing for sclerotomal dispersal. Our results further establish the fibronectin extracellular matrix as an active player in regulating the development of the paraxial mesoderm, cooperating with the Shh signaling pathway to orchestrate correct somite patterning and morphogenesis.

**Keywords:** Fibronectin, extracellular matrix, Sonic hedgehog, somite, notochord

## Introduction

The extracellular matrix (ECM) has diverse roles during vertebrate embryogenesis, providing mechanical support, polarizing cells, supporting cell migration and maintaining tissue boundaries. Moreover, through binding to integrins, the ECM controls gene expression directly or through cooperating with other signaling pathways (Frantz et al., 2010; Rozario and DeSimone, 2010), and changes in ECM stiffness and density can direct cell fate decisions (Engler et al., 2006; Trappmann et al., 2012). Thus, the ECM is a pivotal regulator of vertebrate development.

One of the most ubiquitous ECM molecules during early development is fibronectin. Mice null for *Fn1*, the gene encoding fibronectin, display multiple defects from E8.0 onwards and die before E10.5, highlighting the importance of this ECM component in development (George et al., 1993; Georges-Labouesse et al., 1996). The presomitic mesoderm (PSM) of vertebrate embryos is surrounded by a fibronectin-rich ECM (Duband et al., 1987; Koshida et al., 2005; Rifes et al., 2007), which increases in complexity and density as the PSM matures (Rifes and Thorsteinsdóttir, 2012). Strikingly, in the absence of fibronectin, the PSM of all vertebrate embryos studied fails to form somites, precursors of the axial skeleton and muscle which form periodically from the anterior end of the PSM (George et al., 1993; Georges-Labouesse et al., 1996; Yang et al., 1993; Yang et al., 1999). Accordingly, its specific cell surface receptors are also required for this process (George et al., 1993; Georges-Labouesse et al., 1996; Goh et al., 1997; Jülich et al., 2005; Koshida et al., 2005; Kragtorp and Miller, 2007; Rifes et al., 2007; Watanabe et al., 2007; Yang et al., 1993) . Thus, it has been proposed that a fibronectin matrix of a certain complexity and density is required to support the cellular rearrangements fundamental to the formation of somites (Martins et al., 2009). Moreover, this fibronectin matrix becomes progressively thicker and more compact as the epithelial somites mature (Rifes and Thorsteinsdóttir, 2012). However, whereas the role of fibronectin in somitogenesis has long been appreciated, its role in the epithelial somite remains elusive. Work from our lab identified a dynamic regulation of *Fn1* expression during sclerotome development, suggesting a possible role of fibronectin in the patterning and morphogenesis of the ventral somite (Gomes de Almeida et al., 2016).

One of the key players regulating somite development is Sonic hedgehog (Shh), a morphogen crucial for numerous processes during vertebrate embryogenesis. Shh produced by the notochord and floor plate of the neural tube ensures survival of somitic cells and somite dorso-ventral patterning, specifying the ventral somite to give rise to the sclerotome, precursor of vertebrae and ribs (Marcelle et al., 1999). Moreover, Shh was also shown to influence the pace of the segmentation clock underlying the periodic segmentation of the PSM, and subsequent somite formation (Resende et al., 2010). Shh interacts with ECM molecules in various contexts during development, including proteoglycans, vitronectin and laminin in the developing mouse brain (Blaess et al., 2004; Chan et al., 2009; Pons and

Martí, 2000) and it directly inactivates β1 integrins during neural tube morphogenesis in the chick (Fournier-Thibault et al., 2009). It also modulates the production of chondroitin sulfate proteoglycans in the developing enteric nervous system (Nagy et al., 2016) and fibronectin expression in cultured renal fibroblasts (Ding et al., 2012). *Fn1* is expressed in the ventral epithelial somite (Rifes et al., 2007) raising the possibility that its expression may be regulated by Shh in somites.

Here, we address whether the fibronectin matrix surrounding the PSM and somites has role in regulating Shh signaling in these tissues and, conversely, if Shh influences *Fn1* expression in the somites. We found that an intact fibronectin matrix is required for correct Shh signaling in the PSM and somites of chick embryos, and that Shh signaling, together with other notochord-derived factors, in turn negatively modulates *Fn1* expression in the ventral somite. Our results thus point to a Shh and fibronectin crosstalk during paraxial mesoderm development – the fibronectin matrix surrounding the PSM and somites assures correct Shh signaling in these tissues, thus allowing for the correct *tempo* of somite formation and their subsequent dorso-ventral patterning; Shh in turn regulates fibronectin production in the developing sclerotome, maintaining fibronectin production at intermediate levels before sclerotome dispersal. These results further implicate fibronectin as an active player during paraxial mesoderm development, cooperating with other signaling pathways to orchestrate somite morphogenesis and differentiation.

## Materials and methods

### *Embryos*

Fertilized chicken eggs (*Gallus gallus*) from commercial sources (Sociedade Agrícola Quinta da Freiria and Pintobar Exploração Avícola, Lda, Portugal) were incubated at 37.5ºC in a humidified chamber until stages HH4-14 (Hamburger and Hamilton, 1992).

### *Embryo explant culture*

HH11-14 embryos were collected and cut transversally rostral to somites IV or X (Pourquié and Tam, 2001) and Hensen’s node. Embryo explants were placed on top of an Isopore Membrane Filter (Merck) floating on Chick Explant medium, composed of M199 culture medium (Gibco) supplemented with 10% Chick serum (Sigma), 5% fetal bovine serum (Gibco) and 100 U/ml of penicillin and streptomycin (Invitrogen) and cultured at 37ºC and 5% $CO_2$ from 6 to 12 hours (Palmeirim et al., 1997).

In one set of experiments whole posterior explants (see Fig. 1 A) were cultured in Chick Explant medium supplemented with either (1) 100 µg/ml of 70kDa fibronectin N-terminal fragment (hereafter referred to as 70kDa; McKeown-Longo and Mosher, 1985; Sigma, F0287), (2) 100 µg/ml of recombinant 70kDa (r70kDa, see below), (3) 200 µg/ml of 70kDa (Sigma, F0287) which had been dialyzed (d70kDa) against M199 medium in a D-Tube Dialyzer (MWCO 6-8; Merck Millipore), (4) 0.9 mM RGD (Sigma, G4391) or (5) 6 mM sucrose. Control explants were cultured in medium only or with 100 µg/ml of Bovine Serum Albumen (BSA).

In a second set of experiments, explants were bisected along the midline, but maintaining the notochord on one side only, thus generating a notochord-containing explant (No+) and a notochord-ablated contralateral explant (No-; see Fig. 4 A and Fig. 5 A). In some experimental cases, the lateral plate mesoderm of No- explants was also removed (No-Lat-). Explants were then cultured in Chick Explant medium as described above. A subset of No+ explant halves were cultured with 10µg/ml of Cyclopamine (Merck, 239803), and a subset of No- explants were supplemented with 4µg/ml of Shh (Citomed, 464-SH-025). Appropriate volumes of DMSO were used for contralateral control explants.

*Embryo electroporation and culture*

Primitive streak stage (HH4-5) chick embryos were electroporated on one side in the area containing PSM and ectoderm precursors following previously described methodologies (Voiculescu et al., 2008; Fig 1J) and then cultured *ex-ovo* using Chapman's Early Chick culture method (EC culture, Chapman et al., 2001). Embryos were attached to a filter paper carrier and placed in an electroporation chamber filled with Tyrode's saline, where three 50 ms pulses of 6-9 V separated by 350 ms intervals were applied. DNA plasmids were used at 0.5-1 µg/µl and mixed with 0.3 µl 0.4% Fast Green in water for visualization. Following electroporation, embryos were cultured in a humidified chamber at 37.5ºC for 24 hours.

Control embryos were electroporated with a modified pCAGGs vector driving GFP expression to facilitate the identification of electroporated cells (pCAGGs-GFP). Experimental embryos were electroporated either with (1) a pCAGGs-GFP vector into which the sequence of chick 70kDa with an N-terminal myc-tag (myc:70kDa) had been cloned, (2) co-electroporated with pCAGGs-GFP and 100ng/µl of double stranded RNAi against *Fn1* (Fn1-RNAi, see below), (3) co-electroporated with pCAGGs-GFP and a pCAGGs vector containing the quail 70kDa (q70kDa) or (4) electroporated with a pCAGGs vector containing the full-length quail *Fn1* gene, in which EGFP was inserted between the third and fourth type III domains of the fibronectin protein (qFN-EGFP). The q70kDa and qFN-EGFP constructs were kindly provided by Yuki Sato (Sato et al., 2017).

*Cell culture*

C2C12 cells (ATCC, CRL 1772) were cultured in DMEM GlutaMAX (Gibco) supplemented with 10% fetal bovine serum (Invitrogen) and 100 U/ml of streptomycin and penicillin (Invitrogen). Glass coverslips were coated with 0.1% gelatin for 1 hour at 37ºC before seeding C2C12 cells. HEK293 cells (ATCC, CRL 1573) were cultured in DMEM/F12

GlutaMax (Gibco) supplemented with 10% fetal bovine serum and 3% puromycin. Cultured cells were maintained at 37ºC in a humified atmosphere with 5% $CO_2$.

Fibronectin matrix assembly was perturbed by adding 200 μg/ml of the d70kDa fragment to the culture medium of C2C12 cells for 6 hours, while cells supplemented with 200 μg/ml bovine serum albumen (BSA, Sigma B3311) served as a control.

*Expression and purification of recombinant 70kDa peptide*

The 70kDa N-terminal region of fibronectin was cloned into a modified pCEP vector containing an N-terminal double Strep II tag. HEK293 cells were stably transfected and screened for high levels of protein expression (see below). The recombinant 70kDa peptide (r70kDa) was purified from the culture medium by Strep-Tactin Sepharose (IBA) kit and dialyzed as described above.

*Western blot analysis*

r70kDa in conditioned medium from HEK293 transfected cells was quantified by Strep tag detection. Samples were run in duplicates on a 10% SDS-PAGE gel and blotted onto a nitrocellulose membrane for 1 hour. The membrane was blocked with 0.5% Tween-20 in Phosphate Buffer Saline (PBS) supplemented with 3% BSA for 1 hour, following incubation with an Strep-Tactin-HRP solution for Strep II Tag detection (Strep-Tactin-HRP conjugate kit, IBA) for 1 hour. The membrane was then washed and developed using an Immun-Star HRP Substrate kit (BioRad).

*RNAi synthesis*

To generate double stranded RNAi against *Fn1* (Fn1-RNAi), sense and antisense single stranded RNAs were synthesized from linearized plasmids as described previously (Rifes et al., 2007) and double stranded RNAi was subsequently generated using BLOCK-iT RNAi TOPO Transcription Kit (Thermofisher).

*RNA extraction and RT-qPCR*

The electroporated and non-electroporated sides of both pCAGGs-GFP and *Fn1*-RNAi electroporated embryos were dissected out and processed for RNA extraction using the RNAqueous-Micro Total RNA Isolation Kit (Ambion). RNA quality was confirmed using Experion RNA analysis kits (BioRad) and cDNA synthesis from 100ng of each RNA sample was performed in triplicates using an iScript cDNA Synthesis Kit (BioRad). Real-time qPCR reactions were performed in each of the triplicates with SsoFast EvaGreen Supermix (BioRad) and 2 ng of cDNA. Transcript levels were normalized against the expression of three reference genes (*ActB*, *GusB* and *LMNA*) and results were analyzed in CFX 3.0 BioRad Manager software. Primers used to amplify *Fn1* were the following: forward primer 5'-AGACGGCAGCCACCAAATGTA-3' and reverse primer 5'-GTCGTTGCGTCTGGGCTCA-3'.

In situ *hybridization and cryoembedding*

*In situ* hybridization was performed as previously described (Henrique et al., 1995) with minor modifications (Gomes de Almeida et al., 2016; Rifes et al., 2007). Antisense digoxigenin-labeled RNA probes were synthetized as previously described: *Fn1* (Rifes et al., 2007), *Shh* (Riddle et al., 1993) and *Patched2* (Pearse et al., 2001).

Cryoembedding was performed in whole embryos, electroporated embryos and cultured explants fixed in 4% paraformaldehyde in 0.12 M phosphate buffer with 4% sucrose. After fixation, samples were washed in 0.12 M phosphate buffer with 4%, followed by 15% sucrose, embedded in 7.5% gelatin in 0.12 M phosphate with 15% sucrose and frozen in dry-iced chilled isopentane (Bajanca et al., 2004). Samples were stored at -80ºC until sectioning.

*Imunocytochemistry and immunohistochemistry*

Immunocytochemistry on C2C12 cells was performed as previously described (Vaz et al., 2012). Briefly, cells seeded on coverslips were fixed in 1% PFA in PBS for 30 minutes and permeabilized with 0.5% Triton X-100 in PBS for 5 minutes. Blocking was performed with 2% bovine serum albumen (BSA) in PBS and antibodies were diluted in this solution. Primary antibody incubation was performed overnight at 4ºC, while incubation with secondary antibodies was performed for 30 minutes at room temperature.

Embryos and explants fixed in 4% paraformaldehyde in 0.12 M phosphate buffer with 4% sucrose were cryoembedded as described above. 10-30 µm cryostat (Leica CM1860) sections were processed for immunohistochemistry as described previously (Gomes de Almeida et al., 2016). Sections were permeabilized with 0.2% Triton-X100 in PBS and blocked with 5% BSA in PBS. Primary and secondary antibodies were diluted in 1% BSA in PBS.

Whole-mount immunohistochemistry was performed in explants fixed in 4% paraformaldehyde in PBS, which were then processed as previously described (Martins et al., 2009; Rifes and Thorsteinsdóttir, 2012). Briefly, a solution of 1% Triton-X100 and 1% BSA in PBS was used for permeabilization, blocking, and antibody dilution. Antibody incubation was performed at 4ºC overnight. After post-fixation with 2% PFA for 1-2 hours, whole mount explants were slowly dehydrated through a methanol series and cleared in methylsalicylate (Sigma-Aldrich) as previously described (Martins et al., 2009; Rifes and Thorsteinsdóttir, 2012).

Primary antibodies were against Fibronectin (Sigma F-3648, 1:400) and c-Myc (Santa Cruz 9E10, 1:100). F-actin was visualized with Alexa Fluor 568-conjugated phalloidin

(Molecular Probes A-12380, 1:40). DNA staining was performed with either ToPro3 (Invitrogen T3605, 1:500) together with ribonuclease A (Sigma, 10 µg/ml), 4% Methyl Green (Sigma 67060, diluted 1:250; (Prieto et al., 2015) or 4′,6-diamidino-2-phenylindole (DAPI, Sigma, 5µg/ml in PBS with 0.1% Triton-X100). Goat anti-mouse or anti-rabbit Alexa 488- or Alexa 568-conjugated secondary antibody F'ab fragments (Invitrogen) were used for detection of primary antibodies.

*Sample preparation, image acquisition and analysis*

Both C2C12-containing coverslips and cryostat sections were mounted in 5mg/ml propyl gallate in glycerol/PBS (9:1) with 0.01% sodium azide. Explants processed for whole mount immunohistochemistry were mounted in methylsalicilate (Martins et al., 2009).

Immunofluorescence images were obtained on a confocal Leica SPE microscope or a BX60 Olympus microscope coupled to an Hamamatsu Orca R2 camera. Imaging of whole mount *in situ* hybridization samples and electroporated embryos was performed using a Zeiss LUMAR V12 Stereoscope coupled to a Zeiss Axiocam 503 color 3MP camera. Images of sections from embryos and explants processed for *in situ* hybridization were acquired with an Olympus DP50 camera coupled to a BX51 Olympus microscope. Fiji v. 1.49 and Amira V.5.3.3 (Visage Imaging Inc.) softwares were used for image analysis and histogram corrections. When applicable, single images were generated from contiguous images of one sample by using the pairwise stitching Fiji plugin (Preibisch et al., 2009).

## Results

### ***The fibronectin extracellular matrix is essential for Shh signaling in the PSM and newly formed somites***

To determine if the fibronectin matrix is involved in regulating Shh signaling in the PSM and somites, posterior chick explants were cultured for 6 hours in the presence of a 70kDa fibronectin fragment (hereafter referred to as 70kDa). This fragment corresponds to the N-terminal region of the fibronectin protein that connects extended fibronectin dimers to each other, leading to fibril assembly (Mao and Schwarzbauer, 2005). The 70kDa protein acts as a dominant negative form of fibronectin that binds to the matching N-terminal regions of fibronectin molecules already assembled in the matrix, disrupting the existing matrix, and also blocks binding of new molecules to this matrix (Fig. 4.1 A; Mao and Schwarzbauer, 2005; McKeown-Longo and Mosher, 1985).

We first analyzed the expression of the Shh signaling target gene *Patched2*, a readout for Shh signaling, in these explants. We found that when fibronectin fibrillogenesis is disrupted, *Patched2* expression in the PSM and somites SI - SX is strongly downregulated compared to control explants, indicating a decrease of Shh signaling in these tissues (compare Fig 4.1 B-E to Fig. 4.1 F-I, n=6). Indeed, while the three anterior-most somites of 70kDa-treated explants retain normal *Patched2* expression (Fig. 4.1 C,G), the PSM and remaining somites have either reduced or no *Patched2* expression (compare Fig. 4.1 B, D-C with Fig 4.1 F, G-H). These results suggest that the fibronectin matrix surrounding the PSM and newly formed somites is essential for Shh to reach or to induce *Patched2* in these tissues. The anterior-most somites were already at stages SVIII-SX before culture and had therefore already assembled a dense fibronectin matrix before the addition of the 70kDa fragment (Rifes and Thorsteinsdóttir, 2012). These matrices would probably be less affected by the action of the 70kDa fragment compared to the more immature fibronectin matrices of the PSM and SI.

During the course of our experiments, we discovered that the commercial 70kDa fragment we were using was combined with sucrose for cryoprotection, which following reconstitution in our culture medium resulted in a final concentration of 6mM sucrose. To exclude the possibility that our previous results were a consequence of this high sucrose content, we cultured posterior explants in Explant Culture medium with 6 mM sucrose, thus mimicking the amount of sucrose content in our 70kDa culture medium. Under these conditions, *Patched2* expression in the PSM and somites is normal (Fig. 4.1 J, n=5/5), confirming that the defects we encountered in 70kDa-treated explants result from its action and are not due to the sucrose present in the commercial product.

To further confirm our results, we aimed to interfere with the fibronectin matrix through additional approaches. First, we produced the 70kDa protein using a eukaryotic expression system (courtesy of Manuel Koch, University of Köln, Germany). We cultured HEK293 cells transfected with a modified pCEP vector which constitutively drives the production of a recombinant 70kDa protein (hereafter referred to as r70kDa, see Materials and Methods for more details). After confirming r70kDa production through Western blot analysis (Sup. Fig. 4.1 A), the protein was purified from the HEK293 cell culture medium, dialyzed and used in our explant culture system. Surprisingly, explants cultured in the presence of r70kDa protein for 6 hours showed normal *Patched2* expression relative to control explants (Fig. 4.1 K-L, n=11/11), suggesting that Shh signaling in these tissues is unperturbed. The reason for this contradictory result is presently unclear, but the r70kDa protein has an N-terminal Strep-II tag which may possibly interfere with its binding to native fibronectin, thus perturbing (or abolishing) its dominant negative action on matrix assembly.

We next interfered with fibronectin binding to its integrin receptors by culturing posterior chick explants in the presence of an RGD peptide. In cell culture, excess RGD inhibits cell-matrix adhesion (Barczyk et al., 2010; Harburger and Calderwood, 2009; Pierschbacher and Ruoslahti, 1984; Yamada and Kennedy, 1984). This excess RGD binds to the RGD-binding pockets of α5β1 and other RGD-binding integrins, disrupting further binding of cells to RGD-containing ECM components, particularly fibronectin. RGD-treated explants showed

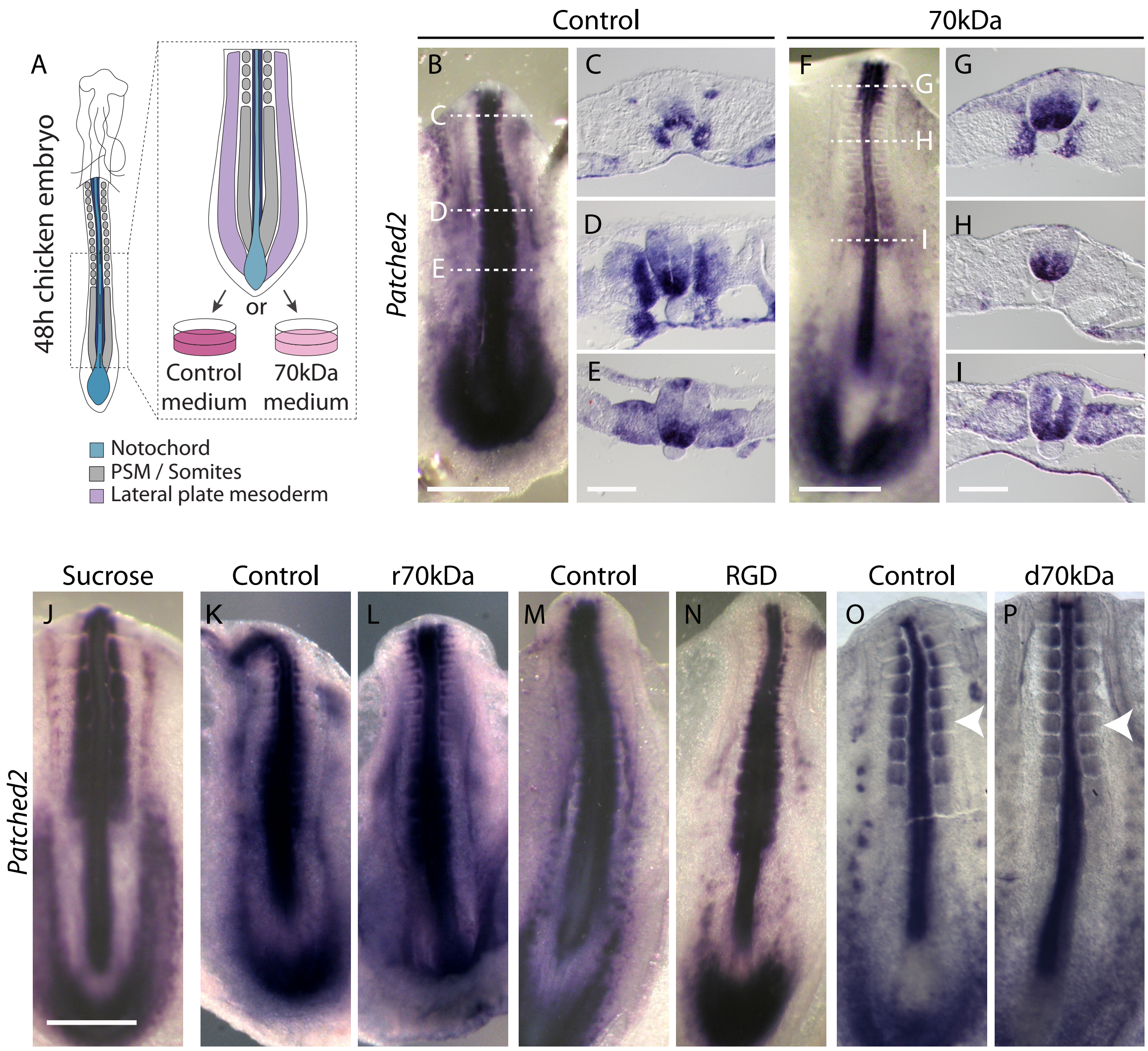


**Fig. 4.1. The fibronectin extracellular matrix is essential for Shh signaling in the PSM and somites. (A)** Schematic representation of the chick explant culture system. Whole posterior explants containing the 10 most recent somites and the PSM were cultured in the presence of 100 µg/ml 70kDa fibronectin fragment in Chick Explant medium for 6 hours. This peptide binds to the fibronectin-binding domains of fibrils already present in the matrix, disrupting their assembly. Whole control explants were cultured with 100 µg/ml BSA in Chick Explant medium. **(B-I)** *In situ* hybridization for *Patched2* in control (B-E) and 70kDa-treated explants (F-I) cultured for 6 hours. **(J)** *In situ* hybridization for *Patched2* in an explant cultured with 6mM sucrose for 6 hours. **(K-L)** *In situ* hybridization for *Patched2* in explants cultured for 6 hours in control medium (K) or in the presence of the r70kDa (L). **(M-N)** - *In situ* hybridization for *Patched2* in explants cultured for 7.5 hours in control (M) vs RGD-containing culture medium (N). **(O-P)** - *In situ* hybridization for *Patched2* in explants cultured in control (O) or d70kDa-containing medium (P). Arrowheads point to *Patched2* expression in the somites. **Scale bars:** (B, F, J-P) 500 µm; (C-E, G-H) 50 µm.

normal *Patched2* expression compared to control explants at 6 hours of culture, suggesting that Shh signaling is normal in these conditions (Fig. 4.1 M-N). Thus, both r70kDa and RGD were ineffective in reproducing our previous results with the commercial 70kDa.

We then dialyzed the commercial 70kDa fragment and tested its efficiency in C2C12 cells cultured for 48 hours, which had thus assembled a complex fibronectin matrix. While the fibronectin matrix of cells treated with the d70kDa for 6 hours was similar to that of control cells and seemed unperturbed by the action of the fragment (Sup. Fig. 4.1, B, C), the morphology and cytoskeletal arrangement of d70kDa-treated cells was altered (Sup. Fig. 4.1 D, E), suggesting that the d70kDa interfered with the geometry and/or density of the fibronectin matrix. We then cultured posterior chick explants in the presence of the d70kDa fragment for 6 hours and assessed *Patched2* expression in these conditions. In d70kDa-treated explants, *Patched2* expression in newly formed somites is more diffuse and less intense when compared to control explants (n=2/2), suggesting a decrease in Shh signaling (Fig. 4.1 O, P, arrowheads).

We next designed a double stranded RNAi against *Fn1* to disrupt its expression in the overlying ectoderm and somites. To this end, HH4 embryos were electroporated in PSM and ectoderm precursors on one side of the embryo (Fig. 4.2 A) with either a pCAGGs vector expressing GFP (control, pCAGGs-GFP; Sup. Fig. 4.1 F) or co-electroporated with both pCAGGs-GFP and *Fn1*-RNAi (Sup. Fig. 4.1 G). Embryos were then cultured in EC culture for 24 hours, and *Fn1* expression levels were assessed through RT-qPCR in the electroporated vs non-electroporated sides of control and RNAi-treated embryos (n=4 for each experimental condition). While *Fn1* expression levels were variable between different individuals, it was generally similar on the electroporated side compared to the contralateral non-electroporated side in control embryos (Sup. Fig. 4.1 I). In 3 out of 4 RNAi treated embryos there is a slight, but non-significant reduction of *Fn1* expression on the electroporated side (Sup. Fig. 4.1 I). We conclude that our RNAi against *Fn1* either does not efficiently block *Fn1* expression or an insufficient number of surface ectoderm cells (which are the major producers of fibronectin at PSM-levels; Rifes et al., 2007) receive the *Fn1*-RNAi and, thus, the total *Fn1* expression level on the electroporated side is not significantly affected.

We then designed a pCAGGS-GFP vector expressing the 70kDa protein with a myc-tag in its N-terminal region (myc:70kDa) and electroporated HH4 embryos either with myc:70kDa or pCAGGs-GFP for control (Sup. Fig. 4.1 H). Immunohistochemistry for myc detection did not show any myc protein neither in the fibronectin matrix nor the cytoplasm of myc:70kDa electroporated cells, suggesting that the 70kDa protein is not successfully produced (Sup. Fig. 4.1 J-K).

Finally, we co-electroporated HH4 embryos with pCAGGs-GFP and a pCAGGs vector expressing the quail 70kDa (q70kDa; Sato et al., 2017). As before, control embryos were electroporated with pCAGGs-GFP only. The fibronectin matrix of these embryos is clearly disrupted compared to control embryos, indicating that the q70kDa peptide is both produced and efficiently interferes with *in vivo* fibronectin matrix assembly in our experimental setup (compare Fig. 4.2 B and E. arrows). Moreover, these embryos showed clear morphological defects compared to control embryos (Fig. 4.2 B-G), including detachment of PSM and somites from the surrounding tissues (Fig. 4.2 G, bracket) and abnormal somite shape (Fig. 4.2 E-G). We next addressed *Patched2* expression in pCAGGs-GFP- and q70kDa-electroporated embryos. Surprisingly, *Patched2* in the somites of these embryos appeared very similar (n=10 and n=11, respectively; Fig. 4.2 H-K), contrasting with the phenotype

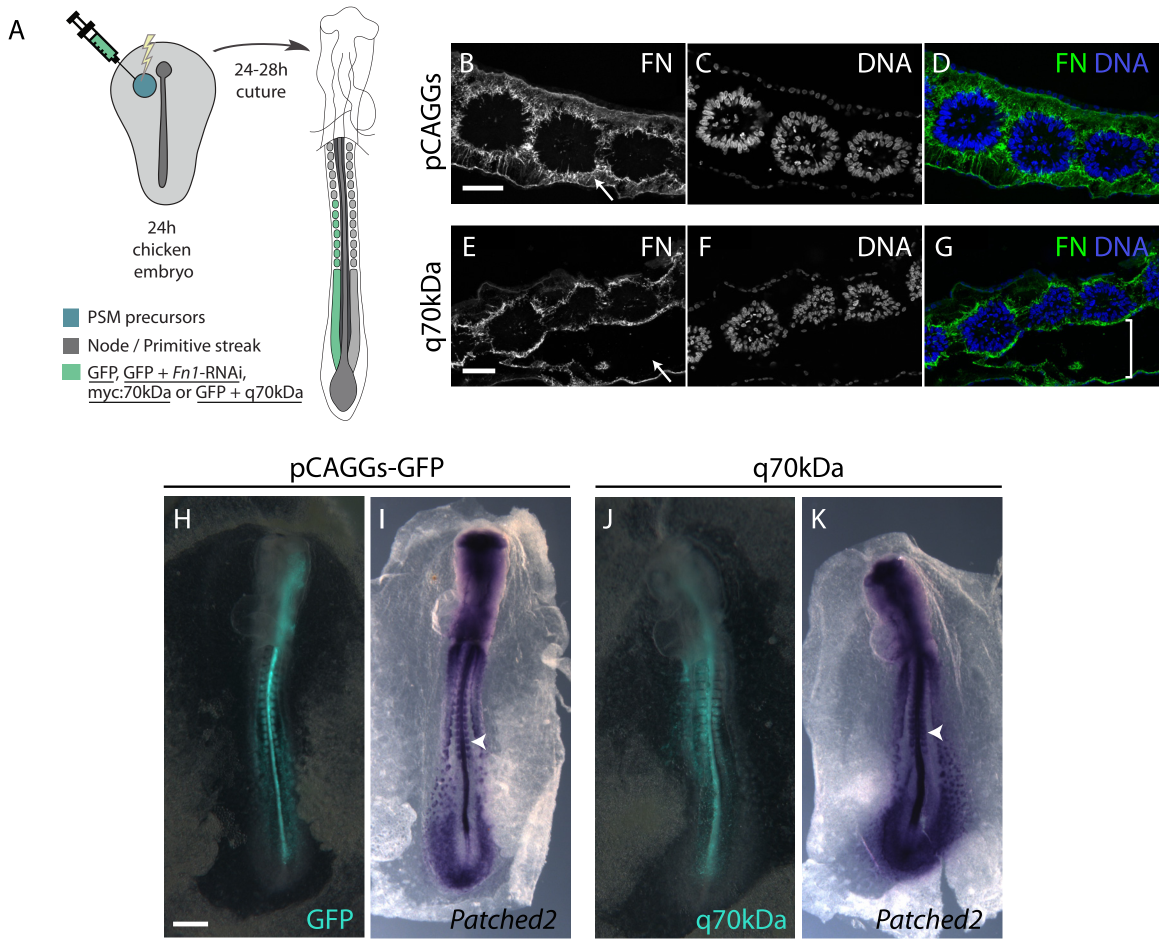


**Fig. 4.2. Electroporation with q70kDa efficiently disrupts fibronectin matrix assembly, but not *Patched2* expression. (A)** Schematic representation of the electroporation procedure. The area containing precursors of ectoderm/PSM on one side (right or left) of HH4 embryos were electroporated with either pCAGGs-GFP or co-electroporated with both pCAGGs-GFP and q70kDa. **(B-G)** Immunohistochemistry for fibronectin (FN, B, E) and DNA staining (C, F) in sagittal sections of pCAGGs-GFP (B-D) and q70kDa (E-G) electroporated embryos. Arrows point to the fibronectin ECM. Bracket shows detachment of somites from the underlying endoderm in q70kDa electroporated embryos. **(H-I)** – Embryos electroporated with either pCAGGs-GFP (H-I) or q70kDa (J-K) showing GFP (H, J) and *Patched2* (I, K) expression. Arrowheads point to *Patched2* expression in the somites. Scale bars: (B-G) 50 µm, (H-K) 500 µm.

of our 70kDa cultured explants (Fig. 4.1 B-I). These results indicate that although this approach is efficient in disrupting the normal assembly of fibronectin matrix (Fig. 4.2 B-G), it may be insufficient to interfere with Shh signaling in this experimental system (Fig. 4.2 A). Alternatively, *in situ* hybridization may not be sensitive enough to detect potential differences between pCAGGs-GFP- and q70kDa-electroporated embryos. In agreement with this hypothesis, Sato et al. (2017) detected only a slight, albeit significant, downregulation of *Patched1* by RT-qPCR (a much more sensitive technique than *in situ* hybridization) in the somites of embryos where filopodia (and consequently, the normal fibronectin matrix) are disrupted compared to control embryos (Sato et al., 2017).

Despite these technical challenges, the effects on *Patched2* expression observed when explants are cultured in the presence of 70kDa (Fig. 4.1 B-I) are consistent and in agreement with other studies (Sato et al., 2017) and, importantly, are not an artifact caused by the extra sucrose present in the commercial 70kDa preparation (Fig. 4.1 J, O-P). Thus, taken together, our results identify a previously unknown communication event during paraxial mesoderm development, implicating the fibronectin matrix surrounding PSM and somites in modulating normal Shh signaling in these tissues.

***Fn1 expression in newly formed somites is regulated by the notochord***

During somitogenesis, *Fn1* is strongly expressed by the surface ectoderm, while the PSM shows no *Fn1* expression (Rifes et al., 2007). However, as soon as the somite is formed, *Fn1* expression starts in its ventral and caudal sides (Rifes et al., 2007; Sato et al., 2017; Fig. 4.3 A). In the quail embryo, *Fn1* expression in the ventral epithelial somite and endoderm leads to the production of thick fibronectin fibrils, designated fibronectin pillars. These fibronectin pillars connect the ventral somite and the underlying endoderm and stabilize filopodia, which protrude from the ventral somitic cells and contact the endoderm (Sato et al., 2017). These filopodia are essential for normal Shh signaling in the ventral somite (Sato et al., 2017).

As soon as a new pair of somites forms, Shh produced by the notochord acts to specify the ventral somite to form the sclerotome (Fig. 4.3 B; Christ and Ordahl, 1995). Strikingly, the emergence of *Fn1* expression in the ventral somite at this stage suggests that *Fn1* expression itself may be controlled by Shh signaling during this process. Indeed, somitic expression of *Fn1* occurs in the same domains as active Shh signaling, as viewed by *Patched2* expression (Fig. 4.3 A, C, arrows).

To test if *Fn1* expression in the ventral somite is under the influence of notochord-derived Shh, posterior chick explants were bisected down the midline, removing the notochord from one explant half (Fig. 4.4 Aa, No-) while maintaining the notochord intact in the contralateral explant (No+, Fig. 4.4 Aa). Explants were then cultured for 6 to 12 hours. This manipulation effectively abolishes Shh signaling in the No- explant after 6 hours of culture, as viewed by the strong downregulation of *Patched2* expression in the No- explant compared to the contralateral notochord-containing controls (Fig. 4.4 Ab). We then assessed *Fn1* expression in the ventral somite under these conditions. In the absence of the notochord, *Fn1* expression in the ventral somite is strongly upregulated compared to that of the contralateral controls (Fig. 4.4 B-J, arrowheads, K). This is the case for 100% of analyzed explants cultured for 6 (n=11/11) and 7.5 (n=3/3) hours, while normal expression of *Fn1* is progressively restored in 25% and 50% of explants cultured for 9 (n=3/4 with increased *Fn1* expression) and 12 hours (n=3/6), respectively (Fig. 4.4 B-J, arrowheads, K). These results suggest that notochord-derived signals negatively regulate *Fn1* expression in the ventral somite for at least 7.5 hours of culture and that *Fn1* expression is partially restored, through a yet unknown mechanism, when explants are cultured for 9 and 12 hours. This increase of *Fn1* production by the ventral somite in the absence of notochord does not appear to result

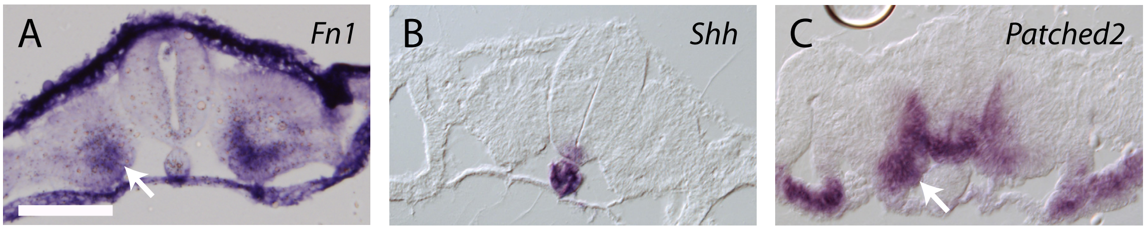


**Fig. 4.3. *Fn1* expression in the somite occurs in sites of active Shh signaling. (A-C)** Transverse sections of SII-SIII of HH12 embryos processed for *in situ* hybridization for *Fn1* (A), *Shh* (B) and *Patched2* (C). Arrows point to *Fn1* (A) and *Patched2* (C) expression domains in the somite. Scale bars 50 µm.

in evident changes in the organization or morphology of the fibronectin matrix surrounding this tissue, although an increase in fibronectin content is evident in the somitocoel of No- explants compared to contralateral No+ controls (Fig. 4.4 L-M, arrows).

*Fn1* is strongly expressed in the ventral region of somites which in HH18 embryos have already completed an epithelial to mesenchymal transition (EMT) to give rise to the mesenchymal sclerotome (Gomes de Almeida et al., 2016). Indeed, upregulation of *Fn1* expression is common in embryonic tissues undergoing EMT, including neural crest cells, primitive streak cells and endocardial cushions, possibly aiding their migration (Gomes de Almeida et al., 2016; Mittal et al., 2010). Thus, in the newly formed somite, the notochord may be negatively controlling *Fn1* expression to avoid the precocious activation of the EMT program. We could not determine if the increase in *Fn1* expression and fibronectin-content of the somitocoel in notochord-ablated explants resulted in precocious dispersal of the sclerotome, since culturing notochord ablated explants for longer periods results in increased cell-death (Hirano et al., 1995). Thus, to test this hypothesis, we attempted to overexpress *Fn1* by electroporating HH4 embryos with a pCAGGs vector expressing the full quail *Fn1* gene, with EGFP inserted between the third and fourth type III domains of the fibronectin protein (qFN-EGFP; Sato et al., 2017). However, electroporation was inefficient and no expression of qFN-EGFP was observed (data no shown), possibly due to the large size of the plasmid (~15Kb).

Nevertheless, our results strongly suggest that notochord-derived signals, possibly Shh, negatively modulate fibronectin production in the ventral somite at these stages.

### *Fn1 expression in the ventral somite is regulated by Shh*

To assess whether Shh is the notochord-derived signal regulating *Fn1* expression in the ventral somite, we added cyclopamine to the culture medium of No+ bisected explants. Cyclopamine inhibits Smoothened (Chen et al., 2002a; Chen et al., 2002b; Incardona et al., 1998), a core mediator of the Shh signaling pathway (Ingham and Placzek, 2006). Thus, while one explant half has no notochord and, thus, no source of Shh (No-), the contralateral explant half retains the intact notochord, but the added cyclopamine blocks the transduction

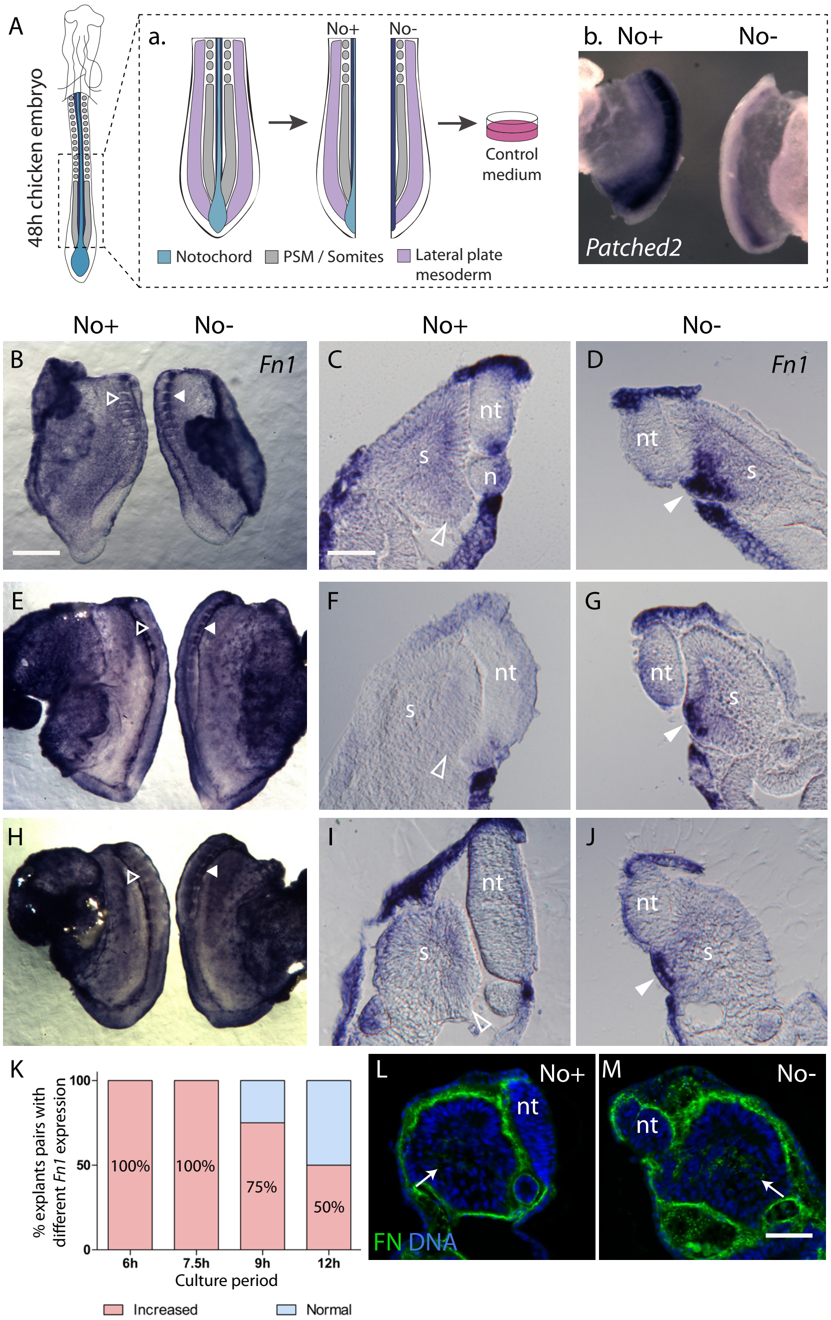


**Fig. 4.4. *Fn1* expression in the ventral somite is under the control of notochord-derived signals. (A)** (a) Schematic representation of notochord-ablated explants. Posterior chick explants were bisected down the midline removing the notochord from one of the sides (No-) while the contralateral explant half retains the tissue (No+). Both explants were cultured in control medium for 6 to 12 hours. (b) *In situ* hybridization for *Patched2* in No+/No- explants cultured for 6 hours. **(B-J)** – *In situ* hybridization for *Fn1* in No+ and No- explants cultured for 6 (B-D), 7.5 (E-G) and 9 hours (H-J). Transverse sections of contralateral explants are shown (C-D, F-G, I-J). Arrowheads point to *Fn1* expression in the ventral somite. **(K)** Percentage of analyzed explant pairs with increased *Fn1* expression in the ventral somite of No- explants at 6, 7.5, 9 and 12 hours. **(L-M)** – Immunohistochemistry for fibronectin (green) and DNA (blue) in transverse sections of No+ (L) and No- (N) contralateral explants at 6 hours. Scale bars: (B, E, H) 200 µm; (C-D, F-G, H-I, L-M) 50 µm. nt – neural tube, s – somite, e – ectoderm, en – endoderm, n – notochord, FN - fibronectin.

of the Shh signaling pathway (No+Cyclo, Fig. 4.5 Aa). Under these conditions, Shh signaling is effectively blocked, as *Patched2* expression in No+cyclo explants is downregulated to comparable levels as observed in No- contralateral halves (Fig. 4.5 B). If Shh signaling is negatively regulating *Fn1* expression in the ventral somites, its expression is also expected to be comparable between these contralateral explant halves. Indeed, 40% (n=6/15) of cyclopamine-treated explants showed similar *Fn1* expression levels in the ventral somite when compared to contralateral No- explant halves (Fig. 4.5 C-E). Furthermore, the fibronectin matrix, including the matrix in the somitocoel, was also similar between the two types of explants (Fig. 4.5 F, G). Thus, inhibiting Shh signaling recapitulates the effect of removing the notochord in *Fn1* expression of the ventral somites in these explants.

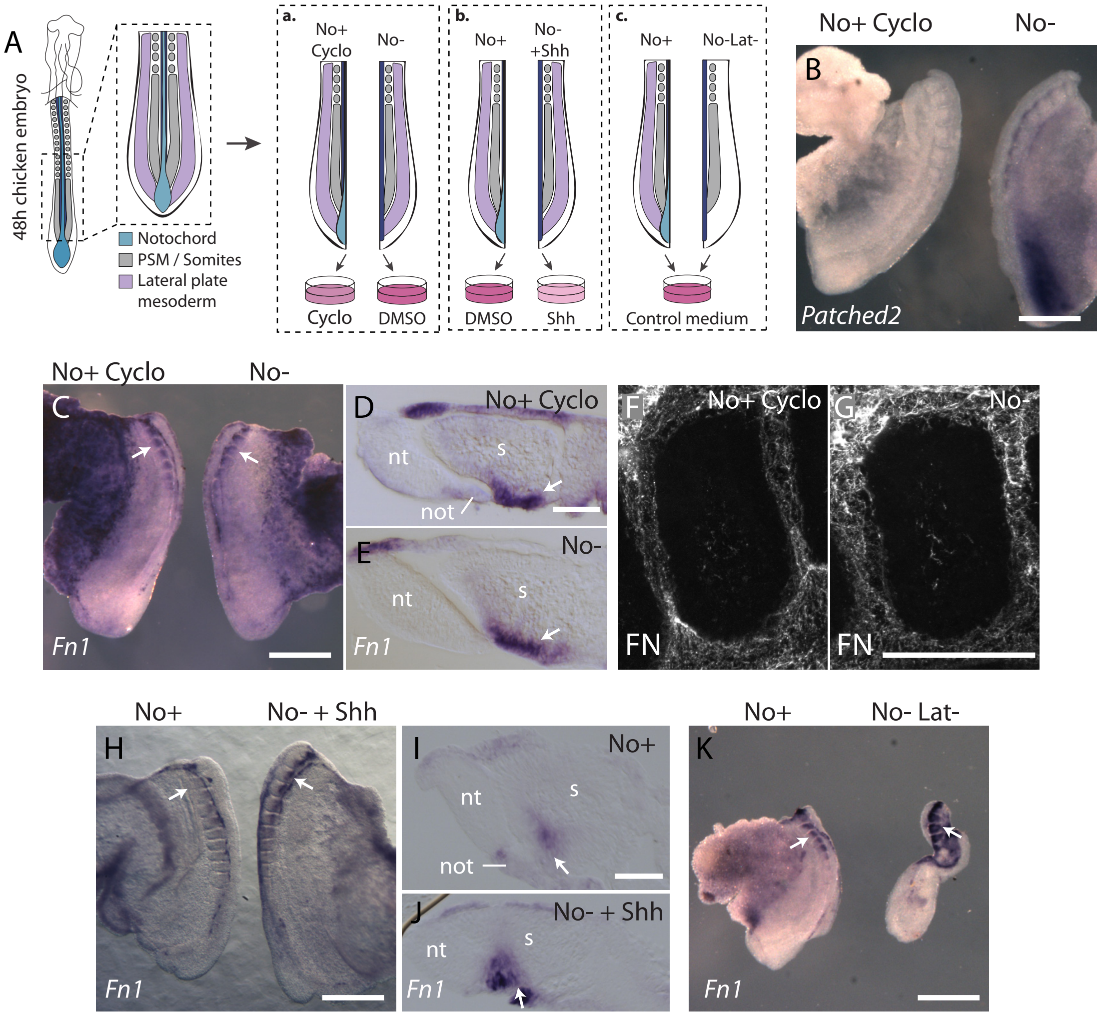


**Fig. 4.5 – One of the notochord-derived signals regulating *Fn1* expression in the somite is Shh. (A)** Schematic representation of (a) No+ explants cultured with cyclopamine (No+cyclo), (b) No- explants cultured with SHH (No- +SHH) and (c) notochord- and lateral mesoderm ablation (No-Lat-). **(B)** *In situ* hybridization for *Patched2* in No+cyclo and contralateral No- explants. **(C-E)** *In situ* hybridization for *Fn1* in No+cyclo and contralateral No- explants. Transverse sections of contralateral No+cyclo (D) and No- (E) explants are shown, arrows point to *Fn1* expression in the somite. **(F-G)** Sagittal view of whole mount immunohistochemistry for fibronectin in No+cyclo (F) and No- (G) explants. **(H-J)** *In situ* hybridization for *Fn1* in No+ and contralateral No- +SHH explants. Transverse sections of contralateral No+ (D) and No- +SHH (E) explants are shown, arrows point to *Fn1* expression in the somite. **(K)** - *In situ* hybridization for *Fn1* in No+ and No-Lat- explants. Scale bars: (B, C, H, K) 500 µm; (D-G, I-J) 50 µm**.** no – notochord, nt – neural tube, s – somite, en – endoderm, FN – fibronectin, Cyclo - cyclopamine

However, 60% of cyclopamine-treated explants (n=9/15) did not show this phenotype. Furthermore, adding exogenous Shh protein to notochord-ablated explants (Fig. 4.5 Ab) was not effective in bringing *Fn1* expression levels in the ventral somite to that of the contralateral notochord-containing controls (Fig. 4.5 H-J). These results suggest that while Shh signaling has a role in controlling *Fn1* expression in the ventral somite, and its absence results in an abnormal increase of *Fn1* production in this tissue, more notochord-derived factors are contributing to this phenotype.

One candidate for mediating this increase in *Fn1* expression in the ventral somite is BMP produced by the lateral plate mesoderm. The notochord is a known source of several BMP antagonists that counteract lateral mesoderm-derived BMP signaling in the medial structures (Dietrich et al., 1997; Nimmagadda et al., 2005). In the absence of notochord, these BMP antagonists will also be absent, possibly resulting in an increase of BMP signaling in the medial and ventral somite. To test this hypothesis, the lateral plate mesoderm from notochord-ablated explants was removed (Fig. 4.5 Ac, No-Lat-), thus removing the source of BMP. Under these conditions, *Fn1* is still upregulated in the somites of No-Lat- explants compared to the contralateral controls at 6 hours of culture (Fig. 4.5 M), suggesting that an increase of BMP signaling is not mediating this phenotype in No- explants. However, removing the lateral plate mesoderm may not result in complete absence of BMP, since cells are still gastrulating in the posterior end of the explant, thus generating new mesoderm that can potentially restore BMP signaling under these conditions. Chemical inhibition of BMP signaling in No- explants will be useful to clarify this issue.

Overall our results demonstrate that the notochord negatively regulates *Fn1* expression in the ventral epithelial somite of chick embryos and that Shh is a major player in this process.

## Discussion

### *Shh regulates Fn1 expression in the ventral somite*

Several situations where cross-talk between Shh and the ECM elicits distinct cellular responses have been described (Blaess et al., 2004; Chan et al., 2009; Fournier-Thibault et al., 2009; Pons and Martí, 2000; Witt et al., 2013). Indeed, depending on the developmental context, Shh interacts with different ECM components to promote either cell survival, proliferation, fate and differentiation. However, examples where Shh interacts with fibronectin are scarce. Shh activates fibronectin expression in cultured renal fibroblasts (Ding et al., 2012) and endocardial precursors of zebrafish embryos (Wong et al., 2012). Here we describe a novel interaction between Shh and fibronectin, whereby the fibronectin matrix plays a role in the delivery (transport and/or presentation to receptors) of Shh to ventral somitic cells, where Shh negatively regulates *Fn1* production. This is in agreement with results from zebrafish embryos where ectopic Shh inhibits *fn1b* expression in the PSM and somites (Chengtian et al., 2002), further supporting our hypothesis that notochord-derived

Shh negatively regulates fibronectin in this context.

While 40% of cyclopamine-treated chick explants recapitulate the increase in *Fn1* expression of notochord-ablated explants, 60% maintained normal *Fn1* expression levels compared to No- contralateral explants, suggesting that more notochord-derived factors negatively regulate *Fn1* in the ventral somite, or that Shh acts both through canonical (involving Smoothened) and non-canonical (not involving Smoothened) pathways (Jenkins, 2009). Although adding Shh protein to the culture medium of No- explants did not reduce *Fn1* expression to the levels seen in No+ explants, thus arguing against the hypothesis that Shh is the only notochord-derived factor repressing *Fn1* expression in the epithelial somite, experiments using a higher concentration or locally applied Shh need to be done before drawing definitive conclusions.

*What other notochord-derived signals could be regulating Fn1 expression in the ventral somite?*

Shh is one of at least three major morphogen families acting on the epithelial somite to orchestrate its dorso-ventral patterning. Wnt signals from the ectoderm counteract ventralizing signals from the notochord, specifying dorsal structures, while BMP4 produced by the lateral plate mesoderm induces the differentiation of the lateral somitic compartment (Dietrich et al., 1997). BMP signaling is inhibited in the ventral and medial somite by notochord-derived BMP antagonists, including noggin, chordin and follistatin (Nimmagadda et al., 2005). In the absence of the notochord, the ventralizing signals counteracting BMP and Wnt are also removed, and the signaling domain of these morphogens expands in the somite (Bothe et al., 2007; Dietrich et al., 1997). This may result in the ectopic or precocious over-activation of *Fn1* production of notochord-ablated explants.

Interestingly, both Wnt and BMP have been described to activate both fibronectin expression and assembly in other contexts. Wnt activates fibronectin expression in cultured *Xenopus* fibroblasts and the non-canonical Wnt Planar Cell Polarity pathway is needed for correct fibronectin assembly during *Xenopus* gastrulation (Dzamba et al., 2009; Gradl et al., 1999). Similarly, in the mouse developing lung, inhibition of Wnt signaling by ectopic expression of its antagonist Dkk1 results in decreased fibronectin deposition leading to defective branching of the tissue (De Langhe et al., 2005). BMP induces both the expression and assembly of fibronectin in cultured osteoblasts (Tang et al., 2003).

We removed the lateral plate mesoderm (and, thus, the major source of BMP) in No- explants, but this did not reduce *Fn1* expression to control levels. Future studies need to address whether BMP signaling is completely absent under these conditions. Moreover, a set of experiments using externally provided BMPs and Wnts, as well as chemical inhibitors of their signaling pathways, should be performed to systematically assess whether they regulate *Fn1* expression in this system.

Finally, it is interesting to note that in the *Xenopus* foregut precursors, BMP is needed for the correct assembly of fibronectin between the mesoderm and endoderm, which is in turn required for the maintenance of BMP signaling in these cells, promoting the correct development of pancreas, lung and liver (Kenny et al., 2012). This crosstalk between the fibronectin matrix and BMP is reminiscent of the communication between fibronectin and Shh that we describe in this study, suggesting that morphogen and ECM mutual regulation may more be common during development than previously appreciated.

*Fn1 expression and sclerotomal EMT*

Fibronectin is considered an EMT marker in both development and disease, facilitating cell migration after de-epithelialization (Kalluri and Weinberg, 2009; Pankov and Yamada, 2002; Thiery and Sleeman, 2006). During early development, fibronectin is both produced and assembled in many tissues undergoing EMTs, including the primitive streak, endocardial cushions, dermis and neural crest cells (Duband et al., 1986; Gomes de Almeida et al., 2016; Mittal et al., 2010), possibly aiding their migration and survival (Goh et al., 1997; Kalluri and Weinberg, 2009; Mittal et al., 2010).

The sclerotome of both chick and mouse embryos also assembles a fibronectin matrix in this autocrine fashion upon EMT activation, which occurs around somite stage SX in HH12 chick embryos (Gomes de Almeida et al., 2016; Rifes and Thorsteinsdóttir, 2012). This EMT has been shown to be independent of notochord-derived signals, since the ventral wall of somites separated from both the neural tube and notochord still de-epithelializes (Hirano et al., 1995). In fact, our results suggest that not only activation of sclerotomal EMT is independent of the notochord, but the notochord may actually inhibit the precocious activation of fibronectin production and, thus possibly the EMT itself, at this somitic stage. This hypothesis is further supported by the altered morphology of the somites of No- explants, which are less rounded compared to those of contralateral No+ controls (Fig. 4.4 L-M). Moreover, in HH18 chick embryos, BMP antagonists Noggin and Chordin are strongly produced by the caudal notochord at the level of epithelial somites, while the notochord from more anterior regions, where ventral somites have already undergone an EMT, Noggin and Chordin expression is reduced (Nimmagadda et al., 2005). Indeed, BMP has been found to promote the EMT of endocardial cushions in the developing heart, where fibronectin assembly is also autocrine (Gomes de Almeida et al., 2016; Ma et al., 2005). In addition, from HH20 onwards, BMP signaling must be active in the sclerotome to promote chondrogenic differentiation (Murtaugh et al., 1999; Schweitzer et al., 2001).

Altogether these results combined with the results presented in this study, are compatible with the hypothesis that the notochord near epithelial somites could attenuate both BMP signaling and *Fn1* expression to prevent precocious activation of the EMT program in the ventral somite. In the absence of notochord, both Shh protein and BMP antagonists are absent, leading to increased *Fn1* expression in the ventral somite and a precocious activation of EMT.

*Shh and fibronectin crosstalk to mediate normal somite development*

Our results strongly suggest that Shh and fibronectin extracellular matrix cooperate during somite development (Fig. 4.6). The fibronectin matrix surrounding the anterior PSM and newly formed somites is essential for normal Shh signaling in these tissues (Sato et al., 2017; this study). Shh is known to regulate the pace of somite formation in the anterior PSM (Resende et al., 2010) and, as soon as the somite is formed, it specifies the ventral somite to become the sclerotome (Ebensperger et al., 1995). Conversely, our results indicate that Shh signaling acts in concert with other yet unknown notochord- regulated pathways to attenuate *Fn1* expression in ventral somite, which we hypothesize may assure that it is maintained at low levels before activation of the EMT program and sclerotome dispersal, when *Fn1* is strongly upregulated (Gomes de Almeida et al., 2016). Thus, we propose that an intricate cross-regulation of Shh signaling in the PSM and somites and fibronectin matrix production by the somite is needed to coordinate timely somite morphogenesis and differentiation.

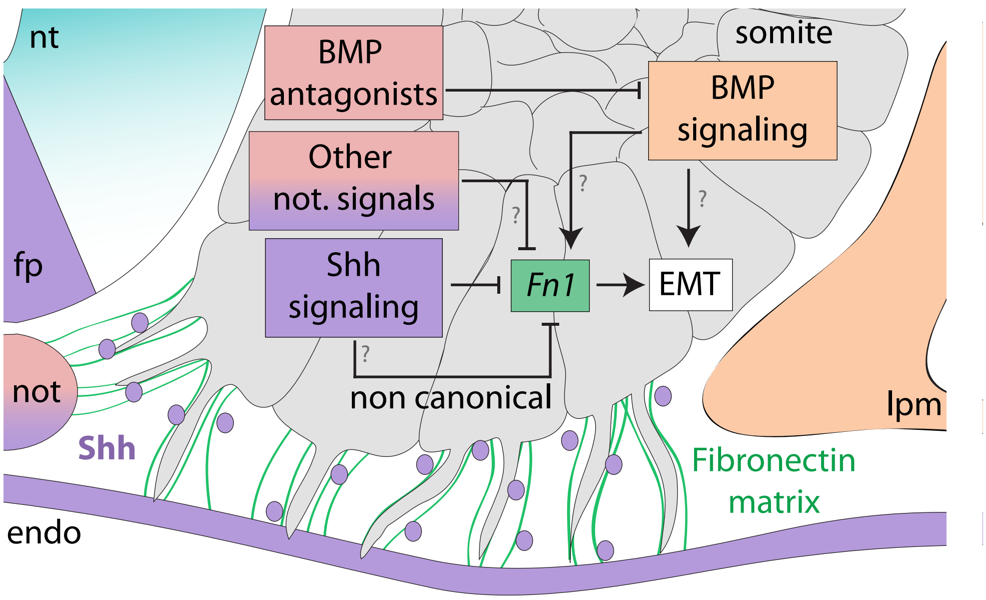


**Fig. 4.6 – Working model.** Fibronectin pillars (green) supporting filopodia from the ventral somite cells are required for normal endoderm-derived Shh (purple) signaling in this tissue (Sato et al., 2017). Conversely, Shh, through canonical and possibly also non-canonical signaling, acts in concert with other unknown notochord derived signals to negatively regulate *Fn1* expression in the ventral somite (this study). We hypothesize that the levels of *Fn1* expression are tightly controlled, as strong upregulation of *Fn1* is coincident with sclerotomal dispersal during EMT at later stages (Gomes de Almeida et al., 2016), but some *Fn1* expression is needed for producing the ventral fibronectin pillars at this stage (Sato et al., 2017). Both EMT and *Fn1* expression may be dependent on BMP signals derived from the lateral plate mesoderm (orange). Accordingly, BMP antagonists (pink) produced by the notochord, may be the notochord-derived signal cooperating with Shh to negatively regulate *Fn1* expression, by inhibiting BMP signaling. nt – neural tube, fp – floor plate, not – notochord, endo – endoderm; lpm – lateral plate mesoderm.

## Acknowledgements

We thank Manuel Koch (University of Köln, Germany) for his precious help in producing the recombinant 70kDa fragment during his sabbatical leave in our group. We also thank Yuki Sato for generously sharing the pCAGGs-q70kDa construct. This work was supported by Fundação para a Ciência e a Tecnologia (FCT, Portugal) projects PTDC/SAU-OBD/103771/2008, PTDC/BEXBID/5410/2014, UID/BIA/00329/2013, UID/BIM/04773/2013 and PPBI-POCI-01-0145-FEDER-022122 and FCT scholarship SFRH/BD/86980/2012 (PGA). We also thank all members of our laboratories for helpful discussions.

## References

**Bajanca, F., Luz, M., Duxson, M. J. and Thorsteinsdóttir, S.** (2004). Integrins in the mouse myotome: Developmental changes and differences between the epaxial and hypaxial lineage. *Dev. Dyn.* **231**, 402–415.

**Barczyk, M., Carracedo, S. and Gullberg, D.** (2010). Integrins. *Cell Tissue Res.* **339**, 269–280.

**Blaess, S., Graus-Porta, D., Belvindrah, R., Radakovits, R., Pons, S., Littlewood-Evans, A., Senften, M., Guo, H., Li, Y., Miner, J. H., et al.** (2004). Beta1-integrins are critical for cerebellar granule cell precursor proliferation. *J. Neurosci.* **24**, 3402–3412.

**Bothe, I., Ahmed, M. U., Winterbottom, F. L., von Scheven, G. and Dietrich, S.** (2007). Extrinsic versus intrinsic cues in avian paraxial mesoderm patterning and differentiation. *Dev. Dyn.* **236**, 2397–2409.

**Chan, J. a, Balasubramanian, S., Witt, R. M., Nazemi, K. J., Choi, Y., Pazyra-Murphy, M. F., Walsh, C. O., Thompson, M. and Segal, R. a** (2009). Proteoglycan interactions with Sonic Hedgehog specify mitogenic responses. *Nat. Neurosci.* **12**, 409–417.

**Chapman, S. C., Collignon, J., Schoenwolf, G. C. and Lumsden, A.** (2001). Improved method for chick whole-embryo culture using a filter paper carrier. *Dev. Dyn.* **220**, 284–9.

**Chen, J. K., Taipale, J., Young, K. E., Maiti, T. and Beachy, P. A.** (2002a). Small molecule modulation of Smoothened activity. *Proc. Natl. Acad. Sci. U. S. A.* **99**, 14071–6.

**Chen, J. K., Taipale, J., Cooper, M. K. and Beachy, P. A.** (2002b). Inhibition of Hedgehog signaling by direct binding of cyclopamine to Smoothened. *Genes Dev.* **16**, 2743–8.

**Chengtian, Z., Yu, Z. and Ying, S. U.** (2002). Somite-specific expression of a novel fibronectin variant FN3 is negatively regulated by SHH. **47**,.

**Christ, B. and Ordahl, C. P.** (1995). Early stages of chick somite development. *Anat.*

*Embryol. (Berl).* **191**, 381–396.

**De Langhe, S. P., Sala, F. G., Del Moral, P. M., Fairbanks, T. J., Yamada, K. M., Warburton, D., Burns, R. C. and Bellusci, S.** (2005). Dickkopf-1 (DKK1) reveals that fibronectin is a major target of Wnt signaling in branching morphogenesis of the mouse embryonic lung. *Dev. Biol.* **277**, 316–331.

**Dietrich, S., Schubert, F. R. and Lumsden, a** (1997). Control of dorsoventral pattern in the chick paraxial mesoderm. *Development* **124**, 3895–3908.

**Ding, H., Zhou, D., Hao, S., Zhou, L., He, W., Nie, J., Hou, F. F. and Liu, Y.** (2012). Sonic hedgehog signaling mediates epithelial-mesenchymal communication and promotes renal fibrosis. *J. Am. Soc. Nephrol.* **23**, 801–13.

**Duband, J. L., Rocher, S., Chen, W. T., Yamada, K. M. and Thiery, J. P.** (1986). Cell adhesion and migration in the early vertebrate embryo: Location and possible role of the putative fibronectin receptor complex. *J. Cell Biol.* **102**, 160–178.

**Duband, J. L., Dufour, S., Hatta, K., Takeichi, M., Edelman, G. M. and Thiery, J. P.** (1987). Adhesion molecules during somitogenesis in the avian embryo. *J. Cell Biol.* **104**, 1361–74.

**Dzamba, B. J., Jakab, K. R., Marsden, M., Schwartz, M. a. and DeSimone, D. W.** (2009). Cadherin adhesion, tissue tension, and noncanonical Wnt signaling regulate fibronectin matrix organization. *Dev. Cell* **16**, 421–32.

**Ebensperger, C., Wilting, J., Brand-Saberi, B., Mizutani, Y., Christ, B., Balling, R. and Koseki, H.** (1995). Pax-1, a regulator of sclerotome development is induced by notochord and floor plate signals in avian embryos. *Anat. Embryol. (Berl).* **191**, 297–310.

**Engler, A. J., Sen, S., Sweeney, H. L. and Discher, D. E.** (2006). Matrix elasticity directs stem cell lineage specification. *Cell* **126**, 677–89.

**Fournier-Thibault, C., Blavet, C., Jarov, A., Bajanca, F., Thorsteinsdóttir, S. and Duband, J.-L.** (2009). Sonic hedgehog regulates integrin activity, cadherin contacts, and cell polarity to orchestrate neural tube morphogenesis. *J. Neurosci.* **29**, 12506–12520.

**Frantz, C., Stewart, K. M. and Weaver, V. M.** (2010). The extracellular matrix at a glance. *J. Cell Sci.* **123**, 4195–4200.

**George, E. L., Georges-labouesse, E. N., Patel-king, R. S., Rayburn, H. and Hynes, R. O.** (1993). Defects in mesoderm , neural tube and vascular development in mouse embryos lacking fibronectin. **1091**, 1079–1091.

**Georges-Labouesse, E. N., George, E. L., Rayburn, H. and Hynes, R. O.** (1996). Mesodermal development in mouse embryos mutant for fibronectin. *Dev. Dyn.* **207**, 145–156.

**Goh, K. L., Yang, J. T. and Hynes, R. O.** (1997). Mesodermal defects and cranial neural crest apoptosis in alpha5 integrin-null embryos. *Development* **124**, 4309–4319.

**Gomes de Almeida, P., Pinheiro, G. G., Nunes, A. M., Gonçalves, A. B. and Thorsteinsdóttir, S.** (2016). Fibronectin assembly during early embryo development: A versatile communication system between cells and tissues. *Dev. Dyn.* **245**, 520–35.

**Gradl, D., Kühl, M. and Wedlich, D.** (1999). The Wnt/Wg signal transducer beta-catenin controls fibronectin expression. *Mol. Cell. Biol.* **19**, 5576–87.

**Harburger, D. S. and Calderwood, D. A.** (2009). Integrin signalling at a glance. *J. Cell Sci.* **122**, 1472–1472.

**Henrique, D., Adam, J., Myat, A., Chitnis, A., Lewis, J. and Ish-Horowicz, D.** (1995). Expression of a Delta homologue in prospective neurons in the chick. *Nature* **375**, 787–790.

**Hirano, S., Hirako, R., Kajita, N. and Norita, M.** (1995). Morphological analysis of the role of the neural tube and notochord in the development of somites. *Anat. Embryol. (Berl).* **192**, 445–57.

**Incardona, J. P., Gaffield, W., Kapur, R. P. and Roelink, H.** (1998). The teratogenic Veratrum alkaloid cyclopamine inhibits sonic hedgehog signal transduction. *Development* **125**, 3553–62.

**Ingham, P. W. and Placzek, M.** (2006). Orchestrating ontogenesis: variations on a theme by sonic hedgehog. *Nat. Rev. Genet.* **7**, 841–850.

**Jenkins, D.** (2009). Hedgehog signalling: emerging evidence for non-canonical pathways. *Cell. Signal.* **21**, 1023–34.

**Jülich, D., Geisler, R., Holley, S. a. and Tübingen 2000 Screen Consortium** (2005). Integrin alpha5 and delta/notch signaling have complementary spatiotemporal requirements during zebrafish somitogenesis. *Dev. Cell* **8**, 575–86.

**Kalluri, R. and Weinberg, R. a** (2009). Review series The basics of epithelial-mesenchymal transition. *J. Clin. Invest.* **119**, 1420–1428.

**Kenny, A. P., Rankin, S. a., Allbee, A. W., Prewitt, A. R., Zhang, Z., Tabangin, M. E., Shifley, E. T., Louza, M. P. and Zorn, A. M.** (2012). Sizzled-tolloid interactions maintain foregut progenitors by regulating fibronectin-dependent BMP signaling. *Dev. Cell* **23**, 292–304.

**Koshida, S., Kishimoto, Y., Ustumi, H., Shimizu, T., Furutani-Seiki, M., Kondoh, H. and Takada, S.** (2005). Integrin alpha5-dependent fibronectin accumulation for maintenance of somite boundaries in zebrafish embryos. *Dev. Cell* **8**, 587–98.

**Kragtorp, K. a. and Miller, J. R.** (2007). Integrin alpha5 is required for somite rotation and boundary formation in Xenopus. *Dev. Dyn.* **236**, 2713–20.

**Ma, L., Lu, M.-F., Schwartz, R. J. and Martin, J. F.** (2005). Bmp2 is essential for cardiac cushion epithelial-mesenchymal transition and myocardial patterning. *Development* **132**, 5601–11.

**Mao, Y. and Schwarzbauer, J. E.** (2005). Fibronectin fibrillogenesis, a cell-mediated matrix assembly process. *Matrix Biol.* **24**, 389–399.

**Marcelle, C., Ahlgren, S. and Bronner-Fraser, M.** (1999). In vivo regulation of somite differentiation and proliferation by Sonic Hedgehog. *Dev. Biol.* **214**, 277–287.

**Martins, G. G., Rifes, P., Amândio, R., Rodrigues, G., Palmeirim, I. and Thorsteinsdóttir, S.** (2009). Dynamic 3D cell rearrangements guided by a fibronectin matrix underlie somitogenesis. *PLoS One* **4**, e7429.

**McKeown-Longo, P. J. and Mosher, D. F.** (1985). Interaction of the 70,000-mol-wt amino-terminal fragment of fibronectin with the matrix-assembly receptor of fibroblasts. *J. Cell Biol.* **100**, 364–74.

**Mittal, A., Pulina, M., Hou, S. Y. and Astrof, S.** (2010). Fibronectin and integrin alpha 5 play essential roles in the development of the cardiac neural crest. *Mech. Dev.* **127**, 472–484.

**Murtaugh, L. C., Chyung, J. H. and Lassar, A. B.** (1999). Sonic hedgehog promotes somitic chondrogenesis by altering the cellular response to BMP signaling. *Genes Dev.* **13**, 225–237.

**Nagy, N., Barad, C., Graham, H. K., Hotta, R., Cheng, L. S., Fejszak, N. and Goldstein, A. M.** (2016). Sonic hedgehog controls enteric nervous system development by patterning the extracellular matrix. *Development* **143**, 264–75.

**Nimmagadda, S., Loganathan, P. G., Huang, R., Scaal, M., Schmidt, C. and Christ, B.** (2005). BMP4 and noggin control embryonic blood vessel formation by antagonistic regulation of VEGFR-2 (Quek1) expression. *Dev. Biol.* **280**, 100–110.

**Palmeirim, I., Henrique, D., Ish-Horowicz, D. and Pourquié, O.** (1997). Avian hairy gene expression identifies a molecular clock linked to vertebrate segmentation and somitogenesis. *Cell* **91**, 639–648.

**Pankov, R. and Yamada, K. M.** (2002). Fibronectin at a glance. *J. Cell Sci.* **115**, 3861–3863.

**Pearse, R. V, Vogan, K. J. and Tabin, C. J.** (2001). Ptc1 and Ptc2 transcripts provide distinct readouts of Hedgehog signaling activity during chick embryogenesis. *Dev. Biol.* **239**, 15–29.

**Pierschbacher, M. D. and Ruoslahti, E.** (1984). Cell attachment activity of fibronectin can be duplicated by small synthetic fragments of the molecule. *Nature* **309**, 30–3.

**Pons, S. and Martí, E.** (2000). Sonic hedgehog synergizes with the extracellular matrix protein vitronectin to induce spinal motor neuron differentiation. *Development* **127**, 333–342.

**Pourquié, O. and Tam, P. P. L.** (2001). A nomenclature for prospective somites and phases of cyclic gene expression in the presomitic mesoderm. *Dev. Cell* **1**, 619–20.

**Preibisch, S., Saalfeld, S. and Tomancak, P.** (2009). Globally optimal stitching of tiled 3D microscopic image acquisitions. *Bioinformatics* **25**, 1463–1465.

**Prieto, D., Aparicio, G., Machado, M. and Zolessi, F. R.** (2015). Application of the DNA-specific stain methyl green in the fluorescent labeling of embryos. *J. Vis. Exp.* e52769.

**Resende, T. P., Ferreira, M., Teillet, M.-A., Tavares, A. T., Andrade, R. P. and Palmeirim, I.** (2010). Sonic hedgehog in temporal control of somite formation. *Proc. Natl.*

*Acad. Sci. U. S. A.* **107**, 12907–12912.

**Riddle, R. D., Johnson, R. L., Laufer, E. and Tabin, C.** (1993). Sonic hedgehog mediates the polarizing activity of the ZPA. *Cell* **75**, 1401–1416.

**Rifes, P. and Thorsteinsdóttir, S.** (2012). Extracellular matrix assembly and 3D organization during paraxial mesoderm development in the chick embryo. *Dev. Biol.* **368**, 370–381.

**Rifes, P., Carvalho, L., Lopes, C., Andrade, R. P., Rodrigues, G., Palmeirim, I. and Thorsteinsdóttir, S.** (2007). Redefining the role of ectoderm in somitogenesis: a player in the formation of the fibronectin matrix of presomitic mesoderm. *Development* **134**, 3155–3165.

**Rozario, T. and DeSimone, D. W.** (2010). The extracellular matrix in development and morphogenesis: A dynamic view. *Dev. Biol.* **341**, 126–140.

**Sato, Y., Nagatoshi, K., Hamano, A., Imamura, Y., Huss, D., Uchida, S. and Lansford, R.** (2017). Basal filopodia and vascular mechanical stress organize fibronectin into pillars bridging the mesoderm-endoderm gap. *Development* **144**, 281–291.

**Schweitzer, R., Chyung, J. H., Murtaugh, L. C., Brent, a E., Rosen, V., Olson, E. N., Lassar, A. and Tabin, C. J.** (2001). Analysis of the tendon cell fate using Scleraxis, a specific marker for tendons and ligaments. *Development* **128**, 3855–3866.

**Tang, C., Yang, R., Liou, H. and Fu, W.** (2003). Enhancement of fibronectin synthesis and fibrillogenesis by BMP-4 in cultured rat osteoblast. *J. Bone Miner. Res.* **18**, 502–11.

**Thiery, J. P. and Sleeman, J. P.** (2006). Complex networks orchestrate epithelial-mesenchymal transitions. *Nat. Rev. Mol. Cell Biol.* **7**, 131–42.

**Trappmann, B., Gautrot, J. E., Connelly, J. T., Strange, D. G. T., Li, Y., Oyen, M. L., Cohen Stuart, M. A., Boehm, H., Li, B., Vogel, V., et al.** (2012). Extracellular-matrix tethering regulates stem-cell fate. *Nat. Mater.* **11**, 642–649.

**Vaz, R., Martins, G. G., Thorsteinsdóttir, S. and Rodrigues, G.** (2012). Fibronectin promotes migration, alignment and fusion in an in vitro myoblast cell model. *Cell Tissue Res.* **348**, 569–578.

**Voiculescu, O., Papanayotou, C. and Stern, C. D.** (2008). Spatially and temporally controlled electroporation of early chick embryos. *Nat. Protoc.* **3**, 419–426.

**Watanabe, T., Saito, D., Tanabe, K., Suetsugu, R., Nakaya, Y., Nakagawa, S. and Takahashi, Y.** (2007). Tet-on inducible system combined with in ovo electroporation dissects multiple roles of genes in somitogenesis of chicken embryos. *Dev. Biol.* **305**, 625–636.

**Witt, R. M., Hecht, M. L., Pazyra-Murphy, M. F., Cohen, S. M., Noti, C., Van Kuppevelt, T. H., Fuller, M., Chan, J. A., Hopwood, J. J., Seeberger, P. H., et al.** (2013). Heparan sulfate proteoglycans containing a glypican 5 core and 2-O-sulfo-iduronic acid function as sonic hedgehog co-receptors to promote proliferation. *J. Biol. Chem.* **288**, 26275–26288.

**Wong, K. S., Rehn, K., Palencia-Desai, S., Kohli, V., Hunter, W., Uhl, J. D.,**

**Rost, M. S. and Sumanas, S.** (2012). Hedgehog signaling is required for differentiation of endocardial progenitors in zebrafish. *Dev. Biol.* **361**, 377–91.

**Yamada, K. M. and Kennedy, D. W.** (1984). Dualistic nature of adhesive protein function: fibronectin and its biologically active peptide fragments can autoinhibit fibronectin function. *J. Cell Biol.* **99**, 29–36.

**Yang, J. T., Rayburn, H. and Hynes, R. O.** (1993). Embryonic mesodermal defects in alpha 5 integrin-deficient mice. *Development* **119**, 1093–105.

**Yang, J. T., Bader, B. L., Kreidberg, J. a, Ullman-Culleré, M., Trevithick, J. E. and Hynes, R. O.** (1999). Overlapping and independent functions of fibronectin receptor integrins in early mesodermal development. *Dev. Biol.* **215**, 264–77.

## Supplementary figures

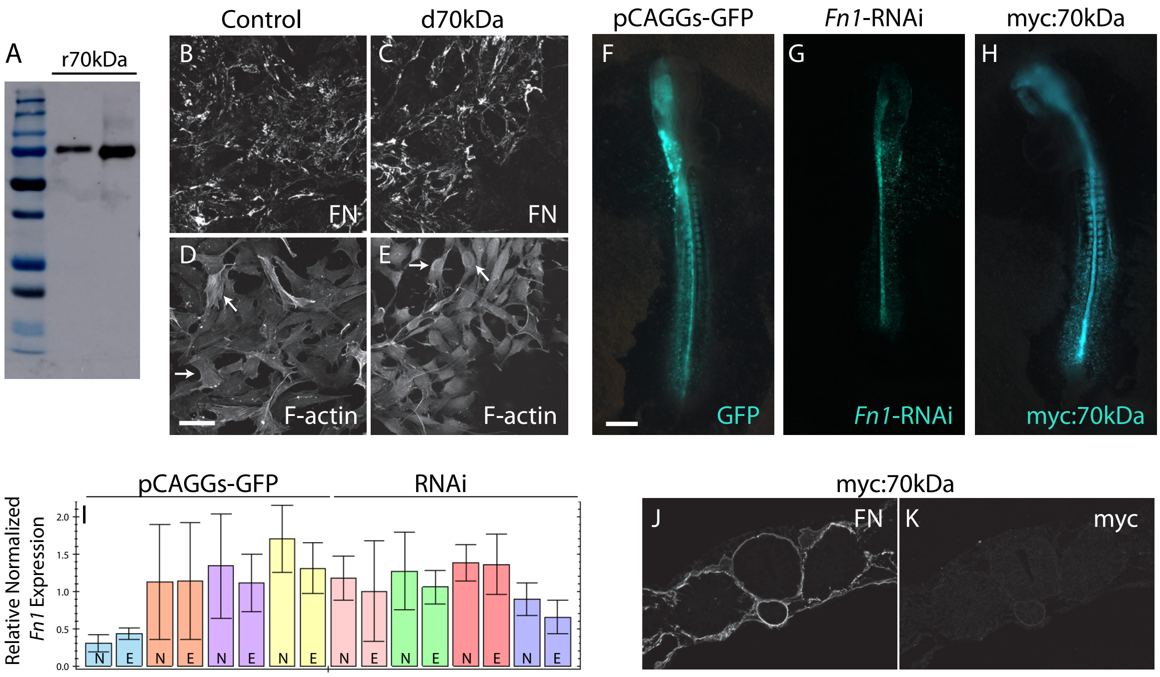


**Supplementary Fig. 1. (A)** Western blot showing the presence of recombinant 70kDa (r70kDa) in the culture medium of transfected Hek293 cells. **(B-E)** Immunocytochemistry for fibronectin (B, C) and F-actin (D, E) in control (B, D) and d70kDa-treated C2C12 cells (C, E). Arrows point to F-actin staining. **(F-H)** GFP expression in embryos electroporated with pCAGGs-GFP (F), *Fn1*-RNAi (G) and myc:70kDa (H). **(I)** RT-qPCR results showing relative normalized *Fn1* expression in the electroporated vs non-electroporated sides of pCAGGs-GFP- and *Fn1*-RNAi -treated embryos. Adjacent bars of the same color represent the two sides of one embryo, N marks non-electroporated sides, E marks electroporated sides. Bars represent the standard error of the mean. **(J-K)** Immunohistochemistry for fibronectin (FN, J) and myc (K) on a transverse section of a myc:70kDa electroporated embryo. Scale bars: (B-E, J-K) 50 µm; (F-H) 500 µm.

# Chapter 5

## Discussion

*Learn how to see. Realize that everything connects to everything else.*
— Leonardo da Vinci

# Discussion

The work presented in this thesis emphasizes the dynamic nature of fibronectin matrix assembly and function throughout early vertebrate development, particularly during paraxial mesoderm maturation and morphogenesis. Our work contributes to the increasing perception that the ECM is undoubtedly much more than just a packing material, providing structural support for cells and tissues. In fact, the ECM – and fibronectin in particular – is an active, pivotal player guiding tissue interactions and rearrangements, maintaining tissue topology, and directly participates in the genetic regulation of developmental processes, providing the cells with both chemical and mechanical cues that are transduced intracellularly to regulate cell function and behavior.

## 1. Fibronectin ECM as an active player regulating paraxial mesoderm development

Fibronectin is one of the most ubiquitous ECM components during early vertebrate development, as it closely associates with the mesoderm, including the paraxial mesoderm, during its formation and maturation (Chapter 2, Duband et al., 1987; Harrisson et al., 1984; Rifes and Thorsteinsdóttir, 2012; Rifes et al., 2007). The most striking evidence for the requirement of fibronectin for normal mesoderm development came from the analysis of *Fn1*-null mouse embryos, where the absence of fibronectin matrices correlates with severe deficiencies in most mesodermal tissues and embryos die at or before E10.5 (George et al., 1993). The work presented in this thesis provides new insights into how the fibronectin ECM regulates the formation and maturation of paraxial mesoderm. We show that fibronectin assembly, production and function is highly dynamic during early paraxial mesoderm development, from gastrulation stages to the maturing sclerotome (Chapter 2, 3 and 4). Importantly, changes in fibronectin dynamics of assembly and production are frequently correlated with morphogenetic events throughout the different stages of paraxial mesoderm maturation (Chapter 2). Here I will discuss our findings about fibronectin assembly during (1) gastrulation of mesodermal precursors, (2) PSM maturation and (3) sclerotome formation, and I will integrate these results with the current knowledge about fibronectin functions in these contexts.

### 1.1 Fibronectin dynamics during gastrulation

As previously described by Harrison et al. (1984), we confirmed that during the earliest stages of development, fibronectin separates the epiblast from the underlying mesoderm, forming a continuous sheet that is interrupted in the primitive streak, where cells are gastrulating (Chapter 2, Harrisson et al., 1984). The assembly of a fibronectin matrix is in fact important for normal gastrulation, as it is initiated both in *Fn1*$^{-/-}$/ and α5$^{-/-}$/αv$^{-/-}$ embryos, but later becomes defective (George et al., 1993; Georges-Labouesse et al., 1996; Yang et al., 1999). Moreover, both fibronectin and α5β1 integrin are necessary for the correct formation of the mammalian node (Pulina et al., 2014) and, while the disruption of this fibronectin ECM does not impair epiblast cell ingression through the streak, their subsequent lateral migration is significantly impaired, as they depend on the upper layer matrix to attach and migrate (Duband and Thiery, 1982; Harrisson et al., 1993). Thus, while the fibronectin matrix lining the epiblast is important for separating both tissues and promoting cell migration, ingression of epiblast cells is accompanied by matrix remodeling (Chapter 2, Duband and Thiery, 1982; Harrisson et al., 1993).

Strikingly, we have found that fibronectin assembly in the chick node during gastrulation is autocrine (Chapter 2). This is not the case in the mouse, where *Fn1* is expressed by cells around the node, while the ventral node expresses *Itga5* and is delimited by fibronectin matrix (Chapter 2, Pulina et al., 2011), suggesting a paracrine mode of assembly. Thus, at least in the mammalian embryo, a particular form of paracrine communication between tissues occurs where fibronectin provided by cells surrounding the node (Chapter 2) is important for node morphogenesis (Pulina et al., 2014). In the chick, although there is an autocrine mode of fibronectin assembly in the node, there is an exchange of macromolecules from the hypoblast to the basement membrane of the epiblast, highlighting the dynamic communication between both tissues during gastrulation and the involvement of extracellular components in the process (Harrisson et al., 1985).

## 1.2 Morphogenetic events in PSM maturation correlate with changes in fibronectin dynamics

In Chapter 2, we showed that paraxial mesoderm precursors ingressing from the avian primitive streak assemble fibronectin in an autocrine fashion, but once cells enter the PSM, fibronectin production drops considerably (Chapter 2). Here, both chick and mouse embryos show a paracrine form of fibronectin matrix assembly in that the PSM cells do not produce their own fibronectin matrix; rather, *Fn1* is expressed by the overlying ectoderm (Chapter 2, Rifes et al., 2007). Since the PSM expresses fibronectin-binding integrins (Chapter 2, Rifes et al., 2007) the fibronectin dimers provided by the ectoderm will be received by the cells at the PSM surface where integrins are active (Jülich et al., 2015). Moreover, integrin protein levels appear to exist in a posterior to anterior gradient (Rallis et al., 2010) and, over time, the matrix becomes increasingly more complex and dense as the PSM cells mature and become more anterior (Rifes and Thorsteinsdóttir, 2012). Our results in Chapter 3 are consistent with a model where in the anterior-most region of the PSM, fibronectin matrix signaling feeds into other pathways regulating the speed and/or intensity of segmentation clock oscillations and, consequently, *Meso1* positioning, thus defining the region where the future segment boundary will be formed. This model is further supported by studies *in vitro* where mechanical signaling though YAP was shown to dampen clock oscillations on cells grown on fibronectin (Hubaud et al., 2017). Once events downstream of *Meso1* initiate cleft formation, fibronectin assembly in the nascent cleft will help establish the individualization of adjacent somites (Chapter 3, Koshida et al., 2005; Martins et al., 2009; Rifes and Thorsteinsdóttir, 2012; Rifes et al., 2007), and together with cell-adhesion proteins which are also upregulated in this region (Chapter 3; Duband et al., 1987; Linask et al., 1998) they maintain anterior PSM cells in their respective cohort. This allows for cellular cohesion within a fibronectin matrix that has a maturation and complexity state capable of supporting the cellular rearrangements needed for somite epithelialization.

## 1.3 Fibronectin is involved in sclerotome specification and morphogenesis

Paraxial mesoderm cells reactivate *Fn1* expression once the somite epithelializes and *Fn1* expression becomes activated specifically in the most ventral and caudal region of the somite (Rifes et al., 2007). Thus, whereby cells receive and integrate fibronectin protein and signals in a paracrine fashion while still in the PSM, the epithelial somite initiates fibronectin production, thus assembling dimers from paracrine and autocrine sources (Chapter 2, Rifes et al., 2007). Fibronectin production by the caudal portion of the recently-formed somite may contribute to the matrix being assembled in the somitic cleft, further establishing the cohesion of this segment and separating the nascent somite from the anterior PSM (Chapter 2, Chapter 3, Rifes and Thorsteinsdóttir, 2012; Rifes et al., 2007). In addition, fibronectin production by the ventral somite, probably a part of the maturation program of the sclerotome, contributes to the fibronectin ECM assembled in the ventral sclerotome (Chapter 2, Chapter 4). This fibronectin is in turn crucial for Shh signaling in this tissue, as fibronectin pillars are required for the formation of the ventral somitic filopodia that receive Shh from the underlying endoderm (Sato et al., 2017). Importantly, we found that this caudo-ventral domain of fibronectin expression is under the control of notochord-derived signals, including Shh (Chapter 4).

Strikingly, the fibronectin matrix lining the ventral region of the somite is maintained even after epithelial markers are downregulated in somite SX of HH12 chick embryos (Rifes and Thorsteinsdóttir, 2012), raising the interesting possibility that it has a role in containing this compartment until the proper time for full de-epithelialization and dispersion. Why this process has to be contained is presently unclear but may have to do with other developmental events occurring in the segments, like neural crest cell migration or the formation of intersegmental blood vessels (Carmeliet, 2003; Guillory and Bronner-Fraser, 1986; Krull, 2001). Increased fibronectin production and assembly has been shown to be closely associated with EMT induction in cultured cells (Camara and Jarai, 2010; Chen et al., 2013) and EMT and invasiveness in cancer (Park and Schwarzbauer, 2014). Accordingly, we also found that *Fn1* expression is strongly upregulated in the already dispersed mesenchymal sclerotome of 3-day chick embryos and E11.5 mouse embryos and a strong, dense fibronectin matrix is found throughout the whole tissue, in close association with the mesenchymal sclerotomal cells (Chapter 2). Thus, increased fibronectin production in the ventral sclerotome and the adoption of an autocrine mode of assembly are associated with the conspicuous EMT that is the hallmark of sclerotome formation (Chapter 2, Christ et al., 2007).

To date, only a few studies have addressed the role of the ECM in sclerotome morphogenesis. It is known that the sclerotome synthetizes hyaluronic acid and chondroitin sulfate proteoglycans that allow its expansion and the dispersal of sclerotomal cells towards the notochord (Solursh et al., 1979). After sclerotome dispersal, only the posterior half maintains chondroitin sulfate production, restricting neural crest cell migration to the anterior sclerotome, as chondroitin sulfate has a repelling action in these cells (Kubota et al., 1999). Intriguingly, after sclerotomal resegmentation in the chick, only the medial and posterior sclerotomes express *Fn1* mRNA, while the anterior sclerotome contains a seemingly more complex fibronectin matrix (Chapter 2). This matrix may potentially have a role in guiding and promoting the anterior-restricted neural crest cell migration through the sclerotome (Kuan et al., 2004). Moreover, this discrepancy in fibronectin expression between the caudal and rostral halves of the sclerotome suggests that differential fibronectin production and assembly may aid establishing and separating the different regions of the tissue, necessary for proper vertebrae development (Chapter 2, Mansouri et al., 2000).

## 2. Fibronectin extracellular matrix as the missing link coordinating clock oscillations and timely somite morphogenesis

Since its first discovery in the chick embryo (Palmeirim et al., 1997), extensive efforts have been made to better understand the dynamics and functions of the segmentation clock, with particular emphasis on how the cyclic oscillations of gene expression are established and controlled (Harima et al., 2013; Herrgen et al., 2010; Hirata et al., 2004; Kageyama et al., 2012; Kim et al., 2011; Liao et al., 2016; Niwa et al., 2007; Schröter et al., 2012; Shih et al., 2015; Tsiairis and Aulehla, 2016). Another issue that is still not fully understood is how the travelling in-phase and anti-phase waves of the expression of tens to almost a hundred different Notch, Fgf- and Wnt-related genes, which sweep the PSM from caudal to rostral, are translated into the periodic morphogenesis of somites from the anterior-most end of the PSM (Krol et al., 2011; Sonnen et al., 2018; Stern and Piatkowska, 2015).

A generally unappreciated feature of somitogenesis is that it consists of the combination of distinct events, namely (1) segmentation clock oscillations, (2) segment boundary specification, (3) cleft formation and epithelialization of the posterior somitic border, and (4) the full epithelialization of all somite sides (i.e. the formation of a rosette of spindle-shaped cells), all of which span the time period from stage S-II to stage SII (Martins et al., 2009; McColl et al., 2018). These four different processes, albeit concomitant, can be experimentally uncoupled. For example, culturing isolated PSMs for 180 min in the absence of the overlying ectoderm abrogates both cleft formation and somite epithelialization, even in the presence of normal *Hairy1* oscillations and normal expression of *Meso1* and *Paraxis* (Palmeirim et al., 1997; Rifes et al., 2007). Moreover, in *Paraxis*-null mouse mutants, *Lnfg* expression is maintained and segment boundaries are formed and normally spaced, but these segments do not epithelialize (Burgess et al., 1996; Johnson et al., 2001). Remarkably, interfering with segmentation clock oscillations results in deficient rostro-caudal patterning of the formed somite-like segments, resulting in the formation of severely abnormal vertebrae (Oginuma et al., 2010). Thus, the exquisite coordination of all these different processes is necessary for both normal and timely somite morphogenesis and segment patterning.

In Chapter 3, we provide evidence that the fibronectin matrix surrounding the PSM in the avian embryo may be the missing player responsible for linking and coordinating these four processes. Notably, we found that the state of fibronectin matrix assembly and the ROCK-mediated mechanotransduction pathway of PSM cells have a role in regulating the dynamics of *Hairy1* and *Hairy2* expression and *Meso1* positioning as well as the morphogenesis of the nascent somitic boundary, suggesting that the fibronectin matrix surrounding the PSM coordinates both gene expression and morphogenesis. Although Blebbistatin-treated explants were the only one of our experimental treatments that fully blocked the epithelialization of somites, fibronectin is also likely to be required for this event. Indeed, enzymatic removal of fibronectin from isolated chick PSM leads to the same phenotype as Blebbistatin-treatment, which can be rescued by adding fibronectin to the medium (Rifes et al., 2007).

Here, our findings from Chapter 3 will be confronted with the current knowledge of how segmentation clock oscillations, boundary morphogenesis and somite epithelialization are regulated, and an integrated view of the fibronectin functions in this context will be proposed (see Fig. 5.1 for a schematic representation and summary).

## 2.1 Fibronectin ECM in control of segmentation clock oscillations

The period at which segmentation clock genes oscillate matches the period of rhythmic somite formation in all species studied, suggesting that the genetic oscillations underlie, and are translated into, periodic somite formation (Bailey and Dale, 2015; Gomez et al., 2008; Palmeirim et al., 1997; Schröter et al., 2008). However, recent studies in the zebrafish have put into evidence that the period of genetic oscillations in the PSM is not constant. Remarkably, the traveling waves of Notch-related gene expression arriving at the anterior PSM slow down before arresting, thus creating a velocity gradient in which the segmentation clock is faster in the posterior PSM relatively to the anterior portion (Shih et al., 2015). These are consistent with results from mathematical modeling in mouse studies (Niwa et al., 2011), suggesting it may be a widespread phenomenon.

Genetic oscillations of Notch-related genes in the anterior PSM are thought to periodically activate Mesp2/Meso1 expression (Saga, 2012). Our results from Chapter

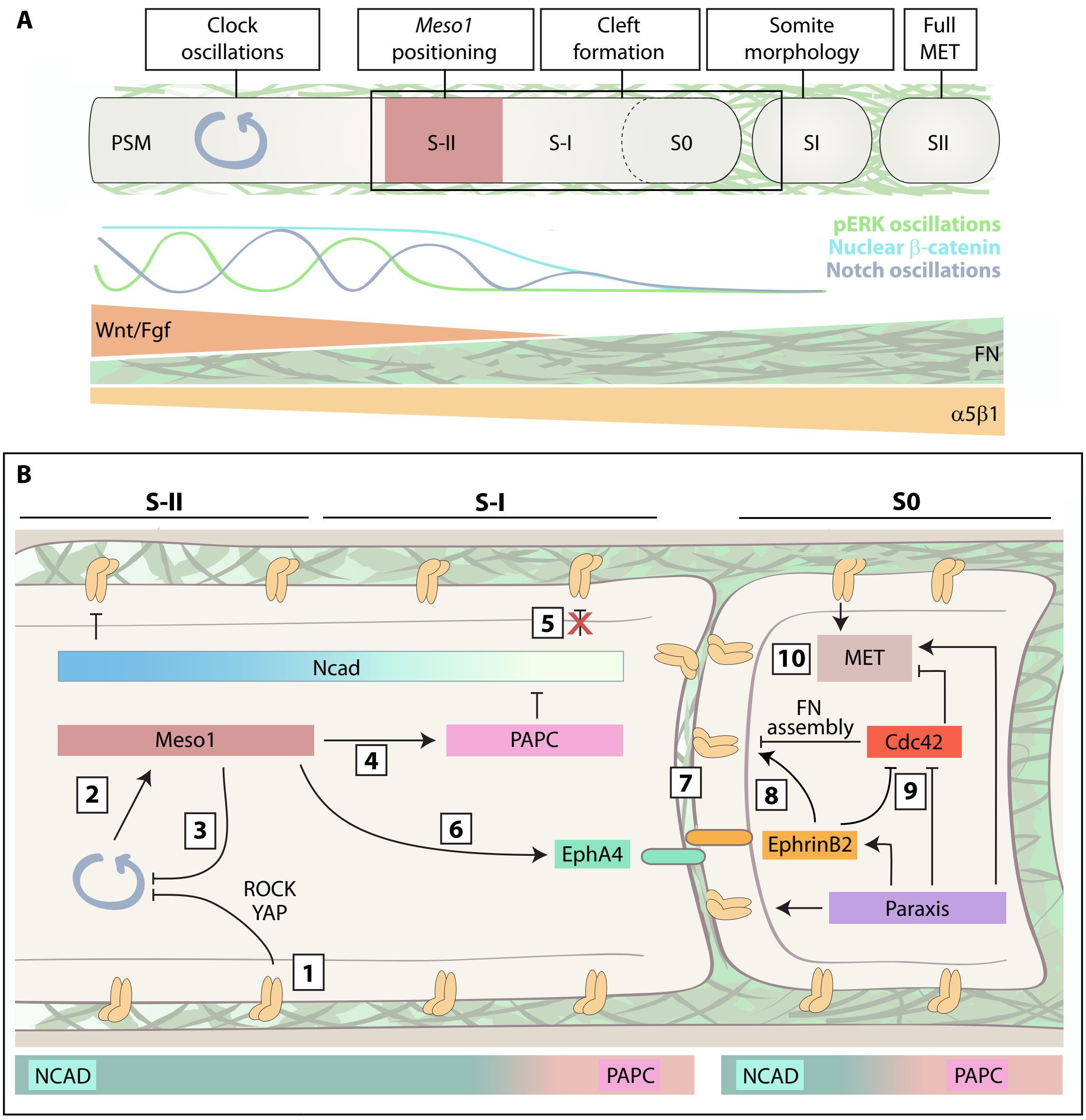


**Fig. 5.1. Schematic representation of the current understanding of the different processes underlying somite formation. (A)** Schematic representation of the gradients of Wnt, Fgf, fibronectin and α5β1 in the anterior PSM and early somites, showing pERK and Notch signaling oscillations and β-catenin nuclear localization. Note that oscillations of pERK and Notch-related clock genes are in anti-phase in the anterior third of the PSM. Moreover, this region has lower levels of Wnt and Fgf signaling and has a more complex fibronectin matrix that engages more integrins compared to the posterior region of the PSM. **(B)** Close-up of the boxed region in A. In the anterior PSM the fibronectin matrix has reached a certain complexity, which transduces mechanical signals via α5β1 and ROCK (and probably also YAP), which dampens segmentation clock oscillations [1]. Before stopping, these Notch signaling oscillations upregulate Meso1 expression in S-II [2], an area where pERK levels are low and Tbx6 is expressed. Meso1 stays expressed until S-II becomes S-I and its expression domain narrows to become restricted to the anterior region of the prospective segment. While expressed, Meso1 inhibits Notch signaling [3] and activates PAPC [4]. PAPC in the anterior region of S-I promotes endocytosis of N-cadherin (Ncad), reducing cell-cell adhesion and releasing its repression on α5β1 integrin activation [5]. Meso1 also activates the expression of EphA4 [6], which binds to EphrinB2 on the membrane of cells immediately anterior to the next segment boundary, inducing the formation of a cleft [7]. EphrinB2 further promotes α5β1 activation [8] and the subsequent assembly of fibronectin into a fibrillar matrix in the nascent cleft [7] further stabilizes the boundary. Meanwhile, EphrinB2 and Paraxis synergize to negatively regulate Cdc42 activity [9]. Lowered levels of Cdc42 activity allows for the activation of MET-inducing genes by Paraxis, which, together with increased fibronectin assembly, promotes the full epithelialization of the posterior border of S0 [10].

3 demonstrate that interfering with fibronectin matrix assembly and its downstream mechanotransduction pathway impairs clock oscillations as well as *Meso1* expression. Our results are in accordance with a recent study in cultured mouse PSM cells and explants, in which fibronectin substrate influenced the pace of *Lnfg* oscillations, as visualized by the LuVeLu reporter (a fluorescent Venus reporter driven by the promoter of *Lnfg*; Hubaud et al., 2017). Indeed, culturing these cells in the presence of fibronectin slowed down LuVeLu oscillations in a Yap-dependent manner. Fibronectin-adhesion of cultured cells has been found to activate YAP nuclear activity in other contexts, in FAK-, ROCK- and talin-dependent manners (Dupont et al., 2011; Elosegui-Artola et al., 2016; Kim and Gumbiner, 2015; Tang et al., 2013), suggesting that YAP modulation downstream of fibronectin-integrin adhesions is common and may normally occur in the PSM (Hubaud et al., 2017).

Strikingly, LuVeLu oscillations are only sustained for longer periods in the presence of ROCK inhibitors, as culturing PSM cells in their absence results in progressive dampening of LuVeLu oscillatory activity and segmentation of the self-assembled miniature PSM (Hubaud et al., 2017; Lauschke et al., 2013; Tsiairis and Aulehla, 2016), suggesting that increased ROCK activity slows down oscillations. Together, these and our results (Chapter 3) point to the possibility that an increase in fibronectin matrix complexity in the anterior PSM detected and transduced by integrins, results in both increased ROCK and YAP activity, leading to the dampening of segmentation clock oscillations in this region (Chapter 3, Hubaud et al., 2017). Another player downstream of fibronectin-integrin binding and, thus, possibly acting in this context is β-catenin (Bielefeld et al., 2011; Kim and Gumbiner, 2015), which is mostly localized in the nucleus in the posterior PSM cells as a consequence of high Wnt signaling in this region (Aulehla and Pourquié, 2008); however, in the anterior PSM, β-catenin is in the cytoplasm, where it localized in the membrane (Aulehla and Pourquié, 2008). The removal of β-catenin from the nucleus is crucial for the timely abrogation of segmentation clock oscillations, as continued nuclear β-catenin activity results in an anterior expansion of the PSM domain with oscillatory genetic activity and anteriorized *Meso1* positioning (Aulehla and Pourquié, 2008). In the rostral PSM, lower levels of Wnt signaling and, thus, decreased nuclear β-catenin activity are accompanied by an increase in N-cadherin protein-mediated cell adhesion (Linask et al., 1998; McMillen et al., 2016), β1 integrin protein (Rallis et al., 2010) and fibronectin matrix assembly and complexity (Rifes and Thorsteinsdóttir, 2012), which all potentially contribute to the maintenance of β-catenin in the cytoplasm rather than in the nucleus (Aulehla and Pourquié, 2008). Accordingly, this correlates with increased tissue tension in both zebrafish (Serwane et al., 2017) and chick (Nelemans, 2018), probably derived from increased matrix- and cell-cell adhesion in the anterior PSM (Linask et al., 1998; Rifes and Thorsteinsdóttir, 2012), where cell density and tissue compaction is also higher (Bénazéraf et al., 2017). Thus, it is conceivable that in addition to controlling of ROCK and YAP activity, thus promoting the dampening of segmentation clock oscillations in the anterior PSM, fibronectin matrix signaling also feeds into the Wnt- and N-cadherin-mediated control of β-catenin localization in these cells, progressively stabilizing its localization in cell-cell adhesions as opposed to in the nucleus, and thus contributing to the slowing down of segmentation clock oscillations (Fig. 5.1, Chapter 3, Aulehla et al., 2008; Rifes and Thorsteinsdóttir, 2012).

## 2.2. Segment boundary positioning through *Meso1* expression

The region of the anterior PSM where the next somitic boundary will be established is defined by the anterior boundary of *Mesp2/Meso1* expression. In the anterior-most region of its expression domain in the PSM, Tbx6 interacts with cyclic Notch signals to induce *Mesp2/Meso1* activation in S-I/S-II, (Saga, 2012). However, as both Tbx6 mRNA and protein and Notch signals are present throughout the A-P length of the PSM, it was unclear how *Mesp2/Meso1* activation occurs only in such a restricted domain. It appears that *Mesp2/Meso1* can only be activated in the presence of Tbx6 and in a region with low pERK activity and FGF signals (Dale et al., 2006; Delfini et al., 2005; Niwa et al., 2011; Saga, 2012). *Mesp2/Meso1* activation is thus thought to be an output of the wavefront, where Fgf and Wnt signaling drops below a certain threshold and is counteracted by increasing levels of Retinoic acid activity (Delfini et al., 2005; Dubrulle et al., 2001; Hubaud and Pourquié, 2014; Niwa et al., 2011; Saga, 2012; Sawada et al., 2001). Accordingly, constitutive activation of ERK signaling (Delfini et al., 2005) or Snail overexpression (Dale et al., 2006), which are both downstream of Fgf signaling, leads to downregulation of *Mesp2*, suggesting that high Fgf levels in the posterior PSM inhibit *Mesp2* activation through ERK. However, the role of the opposing Retinoic acid gradient is not as clear as that of Fgf – while increased levels of retinoic acid activity directly promote the activation of Mesp2 homologs in the *Xenopus* embryo, it represses Mesp activation in the zebrafish by directly activating its repressor Ripply (Moreno et al., 2008; Saga, 2012).

Another anterior to posterior decreasing gradient opposing those of Fgf and Wnt signaling is that of fibronectin matrix complexity. As already mentioned, the fibronectin matrix is much denser and more complex in the anterior compared the posterior PSM (Rifes and Thorsteinsdóttir, 2012). Accordingly, we have found that interfering with either fibronectin matrix assembly, its signaling through integrins or ROCK/NMMII activity all result in altered *Meso1* positioning in the PSM. These results are in accordance with studies where knocking out β1 integrin in the chick PSM completely abolishes *Meso1* expression, further implicating integrin-related signaling in this process (Rallis et al., 2010). Morever, integrins are known regulators of the MAPK pathway, directly modulating ERK (Schwartz and Ginsberg, 2002). Since *Mesp2* expression is only activated where pERK levels are low (Niwa et al., 2011), it is reasonable to speculate that in the S-II/S-I region, increasing fibronectin assembly and complexity results in changes in integrin-mediated intracellular signaling, which jointly with lower levels of FGF signaling result in diminished pERK levels, thus allowing for *Mesp2* activation (Fig. 5.1).

## 2.3 Segment boundary morphogenesis and epithelialization of the posterior somitic border

Segment boundary formation is induced upon EphA4 activation by Mesp2/Meso1 (Barrios et al., 2003; Watanabe et al., 2009). Interaction of EphA4 with the EphrinB2 receptor in the cells anterior to the EphA4-expressing cells are thought to induce the formation of a gap between these two cell populations. Concomitantly, cyclic activation of PAPC in the cells located immediately posterior to the nascent boundary promotes N-cadherin endocytosis, further detaching these cells from those located immediately anterior to them (Fig. 5.1, Chal et al., 2017). This in turn alleviates N-cadherin-mediated repression of integrins, which leads to integrin clustering and activation in the nascent gap, promoting fibronectin fibrillogenesis (Jülich et al., 2015). The assembly of fibronectin in this region is crucial both for boundary morphogenesis (Chapter 3) and maintenance (Jülich et al., 2005; Koshida et al., 2005). Accordingly, we found that the fibronectin assembly state, integrin-mediated signaling and downstream ROCK activity are crucial for proper morphogenesis of the segment boundaries as, even though cells polarize epithelial markers, nascent somites do not fully detach from each other (Chapter 3).

In addition to EphA4-mediated boundary induction, EphrinB2 signaling in the adjacent cells (posterior cells of S0) also contributes to the activation of fibronectin-assembling integrins and fibronectin matrix assembly in the cleft (Barrios et al., 2003; Durbin et al., 1998; Durbin et al., 2000; Jülich et al., 2009; Watanabe et al., 2009). Cdc42 activity in these cells normally inhibits MET (Fig. 5.1, Nakaya et al., 2004). By downregulating Cdc42 activity levels, EphrinB2 promotes the epithelialization of these boundary cells. Moreover this is accompanied by fibronectin-mediated polarization of these cells (Martins et al., 2009), resulting in N-cadherin, ZO-1 and F-actin accumulation on their apical side (Chapter 3, Martins et al., 2009; Rifes and Thorsteinsdóttir, 2012). This is also promoted by Paraxis, which further enhances EphrinB2 activity and fibronectin assembly, and activates MET-inducing genes (Fig. 5.1, Johnson et al., 2001; Rowton et al., 2013).

Thus, the instructive biochemical and biomechanical signals provided by increased fibronectin matrix complexity in the anterior PSM, transduced by its integrin receptors, coordinate the different cellular processes occurring during periodic somite formation. Intracellular integrin-mediated signaling resulting from increased fibronectin complexity in the anterior PSM slows down segmentation clock oscillations and establishes *Meso1* positioning (Chapter 3, Hubaud et al., 2017; Rifes and Thorsteinsdóttir, 2012), while also promoting and maintaining the nascent boundary and aiding somite epithelialization (Fig. 5.1; Chapter 3, Martins et al., 2009; Rifes et al., 2007).

# 3. Instructive signals from the ECM

## 3.1 Matrix assembly as a paracrine cell/tissue communication event

In Chapter 2, by thoroughly analyzing fibronectin production and distribution throughout early development in chick and mouse embryos, along with the distribution of its major assembly receptors, we demonstrated that fibronectin assembly can be considered a particular form of paracrine communication between different tissues in many contexts. In this form of fibronectin assembly, one cell type or tissue strongly expresses *Fn1* and thus produces the protein, while the adjacent cells or tissues, which do not express *Fn1* but express integrins capable of fibronectin assembly, sequester the protein and assemble the matrix. Thus, one tissue produces fibronectin which is assembled, and consequently also sensed, by the adjacent tissue. Other studies in the chick have demonstrated the importance of this type of paracrine communication between tissues during morphogenesis of somites (Rifes et al., 2007) and coelomic epithelium (Yoshino et al., 2014). Our data from Chapter 2 indicate that this phenomenon is not restricted to these two contexts (see below).

While we focused on fibronectin matrix assembly, there are a few other examples of paracrine assembly for other ECM components and contexts, suggesting that this type of tissue communication involving production by one tissue and assembly of matrix components by another may be a widespread phenomenon during embryogenesis, with possible implications in tissue morphogenesis. For example, an epithelial-derived laminin α5 chain-containing laminin promotes the differentiation of mesenchymal cells in the developing dermal papilla (Gao et al., 2008), while in the intestine, the epithelium and the mesenchyme secrete different laminin chains that will compose the basement membrane of the epithelial-mesenchymal interface (Simon-Assmann et al., 1998). Also, the mesenchyme of the developing kidney, lung, pancreas, mammary gland and submandibular salivary gland is responsible for producing laminins that are assembled by the adjacent epithelial cells in the epithelial-mesenchymal basement membrane (Crisera et al., 2000; Kadoya et al., 1995; Keely et al., 1995; Lee et al., 1993; Thomas and Dziadek, 1994).

As mentioned above, in Chapter 2, we describe more contexts in the early vertebrate embryo that suggest that this form of tissue communication, particularly involving fibronectin assembly, may be important for the morphogenesis of other tissues and organs. We found that the fibronectin matrix that composes the notochord basement membrane, or perinotochordal sheet, is produced solely by the surrounding sclerotome, thus representing a paracrine event (Chapter 2). Importantly, in the absence of fibronectin, the notochord degenerates shortly after its formation, (Pulina et al., 2014), highlighting its importance in the normal development and maintenance of this tissue. Interestingly, it has also been shown that at least some of the laminins assembled around the notochord, are produced by the surrounding tissues (Parsons et al., 2002). These laminins are essential for notochord differentiation (Stemple, 2005), suggesting that the paracrine assembly of the perinotochordal sheet by the notochord is required for its normal development.

Similarly, at least one of the laminins of the myotome basement membrane, laminin 111, is produced by the underlying sclerotome. If *Lama1* expression in the sclerotome is lost, myogenic precursor cells fail to activate the myogenic programme and the myotome basement membrane is not formed (Anderson et al., 2009). Fibronectin assembly in the myotome is also paracrine, being produced by the adjacent sclerotome and overlying progenitors in the dermomyotome and assembled by the myotomal myocytes (Chapter 2). This is also the case for cardiac muscle, where the fibronectin assembled in the myocardium is produced by the epicardium and endocardium (Chapter 2). Accordingly, fibronectin has long been implicated in cardiac development, particularly in the migration of the prospective myocardium to the midline in mice (George et al., 1993), chick (Linask and Lash, 1988) and zebrafish (Trinh and Stainier, 2004). In the latter case, fibronectin assembly is also paracrine, as endocardial precursors produce the fibronectin necessary for the epithelial organization of myocardial precursors, which is in turn required for myocardium migration to the midline and morphogenesis and differentiation of the heart (Trinh and Stainier, 2004). In the mouse, fibronectin is also required for the morphogenesis of the cardiac outflow tract and right ventricle (Mittal et al., 2013), and in the absence of integrin α5β1-fibronectin interactions, proliferation of pre-cardiac mesoderm, differentiation of outflow tract cells and specification of second heart field precursors are all severely impaired (Mittal et al., 2013). This suggests that the endocardium-derived fibronectin assembled in a paracrine fashion by the myocardium has crucial roles in the morphogenesis, proliferation and differentiation of myocardial tissue.

We also found that fibronectin assembly is paracrine in the developing gut of E3.5 chick embryos. While fibronectin is assembled in the basement membrane of the proventricular epithelium, which shows no *Fn1* expression, the protein is provided by the adjacent mesenchyme, which strongly expresses *Fn1* (Chapter 2). Importantly, cross-talk between epithelium and mesenchyme is essential for both gut endoderm development and mesenchyme differentiation, as signals from the proventriculus mesenchyme induce gland formation from the endodermal epithelium, but only in the presence of a basement membrane, demonstrating the importance of the ECM in this system (Fukuda and Yasugi, 2005). Fibronectin may constitute one of the signals by which the mesenchyme promotes region-specific endoderm differentiation. For example, it is required for activating BMP-receptor signaling which is necessary to maintain foregut identity of the endoderm during *Xenopus* development (Kenny et al., 2012).

Importantly, in all the contexts where we described a paracrine form of assembly of fibronectin matrices (Chapter 2), fibronectin has been described as having a crucial role in the normal development and maturation of the "assembling" tissues. This suggests that the fibronectin provided by the producing tissues conveys instructive signals to the adjacent receiving tissues, promoting their normal morphogenesis (Nelson and Bissell, 2006). In fact, the nature of fibronectin assembly is itself quite paracrine – the globular molecule is secreted by the producing cells, while the receiving cells express fibronectin-specific receptors which bind to the dimers, leading to the building of the matrix and integrin signaling. This is analogous to classical paracrine growth factor signaling, with morphogens being secreted by the producing cells, while the receiving cells in the target-tissue bind the morphogen via specific cell surface receptors, which leads to the activation of an intracellular cascade that results in the modulation of cellular responses. In addition, and similarly to what was observed in Chapter 2 for fibronectin, growth factor signaling may also be paracrine, autocrine, or both (Adams, 2002; Kaplan et al., 2007; Singh and Harris, 2005; Turner and Grose, 2010).

Thus, in addition to the classical growth factor paracrine signaling, this previously unappreciated form of tissue communication through ECM production and assembly, also has pivotal importance during embryogenesis. Together with the increasing knowledge about how the ECM conveys chemical and mechanical information to receiving cells, and how these cells transduce and integrate this information with those received through other signaling pathways, this opens new research opportunities to fully understand how the coordinated morphogenesis of different tissues is accomplished harmoniously in the developing embryo.

## 3.2 The mechanical aspect of development

The instructive signals conveyed by the extracellular environment of a given tissue are not only of biochemical nature (such as composition and concentration of ECM components), but are also biomechanical, such as ECM stiffness and elasticity, tissue cohesion and cellular adhesion (Chan et al., 2017; Eyckmans et al., 2011; Merle and Farge, 2018). Studies addressing the role of these mechanical cues in regulating the biology of cells have mostly been performed in cell culture and the recent expansion of biophysical technologies have confirmed that biomechanical cues have crucial roles in regulating normal cellular function and behavior, including proliferation and cell fate decisions (Eyckmans et al., 2011; Marjoram et al., 2014; Moeendarbary and Harris, 2014; Petridou et al., 2017). However, studies on the role of mechanical forces in regulating developmental processes *in vivo*, particularly in vertebrate embryos, are still scarce. In Chapter 3, we used chick embryo electroporation and culture to interfere with the tensional state of the fibronectin matrix by disrupting its assembly, its binding to integrins or interfering with the mechanotransduction machinery of PSM cells through impaired ROCKI/II and NMMII activity. ROCK activity has been found to have a major role in the transduction of mechanical forces downstream of cell-cell and cell-matrix adhesions (Marjoram et al., 2014), with consequences on cell differentiation. ROCK inhibition results in differentiation of cultured human embryonic stem cells into neural crest progenitors that can differentiate into multiple cell types (Kim et al., 2015), while mammary gland progenitor cells differentiate into luminal epithelial cells or myoepithelial cells depending on substrate stiffness, which they sense and respond to in a ROCK-dependent manner (Lui et al., 2012). Accordingly, we found that interfering either with fibronectin assembly or ROCK activity *in vivo* had strong effects not only in somitic boundary morphogenesis but also in the dynamics and positioning of segmentation clock oscillations (Chapter 3).

These results add to the increasing body of evidence that suggests that similarly to what has been observed in cultured cells, mechanical cues from the ECM received and transduced by developing tissues *in vivo* convey instructive information required for proper tissue morphogenesis (Linde-Medina and Marcucio, 2018; Merle and Farge, 2018; Petridou et al., 2017). Embryo development is itself quite a mechanical process, with continuous pushing, pulling, contracting and bending interactions of cells with their neighbors and surrounding ECM (Eyckmans et al., 2011; Linde-Medina and Marcucio, 2018; Petridou et al., 2017). Thus, it is of no surprise that the study and awareness of the importance of mechanical cues in developmental processes is steadily increasing, together with the development of sophisticated biophysical methodology allowing for direct observation of mechanical processes in developing embryos (Chan et al., 2017; Davidson, 2017; Merle and Farge, 2018; Moeendarbary and Harris, 2014). For example, it has recently been observed that integrin-mediated transduction of mesodermal stiffening triggers the collective migration of neural crest cells in the *Xenopus* (Barriga et al., 2018), while substrate stiffness also modulates axonal growth and spreading in these embryos (Koser et al., 2016). In the case of the PSM (Chapter 3), as cells are displaced more anteriorly, tissue tension increases considerably (Nelemans, 2018; Serwane et al., 2017) which is accompanied by an increase in density and thickness of fibronectin fibrils (Rifes and Thorsteinsdóttir, 2012). Because fibronectin assembly is a cell-mediated process, fibronectin matrices are not generally used in cell culture studies addressing tensional cues (Cukierman, 2001). However, α5β1-fibronectin bonds undergo tension-strengthening when forces are applied, transforming into tensioned and stronger adhesions to fibronectin called “catch-bonds” that mediate specific intracellular signaling events (Friedland et al., 2009). Accordingly, active fibronectin fiber alignment elicits cellular rigidity responses of cultured fibroblast as the matrix becomes increasingly stiffer (Antia et al., 2008). Thus, the fibronectin matrix surrounding the PSM is in a position to be the tension provider for these cells, as a progressively more complex fibronectin matrix may be perceived by the PSM cells as an increasingly stiffer environment that may culminate in a tissue-tensioned state capable of supporting somite formation. A similar process occurs in the blastocoel of gastrulating *Xenopus* embryos, where fibronectin assembly is accompanied by increased tissue tension, required for radial intercalation and epiboly (Dzamba et al., 2009; Rozario et al., 2009).

This increasing interest and understanding of the mechanical aspects of cell function, tissue development and tissue homeostasis is of particular importance, as cancer cells are very responsive to substrate stiffness and elasticity, changing their invasive behavior accordingly (Carey et al., 2012; Sulzmaier et al., 2014; Weaver et al., 1997) and many other diseases are related to deficient mechanotransduction, including cardiac hypertrophy and arteriosclerosis (Iozzo and Gubbiotti, 2018; Jaalouk and Lammerding, 2009). Thus, studying how cells sense and respond to mechanical cues allows for a better understanding and an integrative perspective of both developmental processes and tissue homeostasis, with considerable clinical relevance.

## 4. Final considerations

While most studies of developmental processes are focused on their chemical or genetic regulation, our work highlights the importance of considering the extracellular realm of cells and tissues and how it integrates with the intracellular dimension. The work presented in this thesis establishes the fibronectin ECM as a dynamic multi-tasking player regulating early vertebrate development. In addition to their presence or absence in a given tissue or around certain cell types, understanding the role of ECM components on a developmental process requires considering all aspects of the matrix, including assembly dynamics, rigidity, elasticity, remodeling and degradation, and their interaction with other pathways either by interfering with ligand availability or presentation, or by feeding directly into their intracellular pathway through integrin signaling. Albeit undoubtedly being challenging, the multi-dimensionality of how the ECM interacts with cells and within tissues attests for its importance during development and homeostasis, as it integrates several different aspects of the life of a cell, from its motility and shape to specific genetic regulation. Thus, the ECM is unquestionably an essential effector promoting the precision and robustness of developmental processes.

# 5. References

**Adams, G. R.** (2002). Invited Review: Autocrine/paracrine IGF-I and skeletal muscle adaptation. *J. Appl. Physiol.* **93**, 1159–1167.

**Anderson, C., Thorsteinsdóttir, S. and Borycki, A.-G.** (2009). Sonic hedgehog-dependent synthesis of laminin alpha1 controls basement membrane assembly in the myotome. *Development* **136**, 3495–3504.

**Antia, M., Baneyx, G., Kubow, K. E. and Vogel, V.** (2008). Fibronectin in aging extracellular matrix fibrils is progressively unfolded by cells and elicits an enhanced rigidity response. *Faraday Discuss.* **139**, 229–249.

**Aulehla, A. and Pourquié, O.** (2008). Oscillating signaling pathways during embryonic development. *Curr. Opin. Cell Biol.* **20**, 632–637.

**Aulehla, A., Wiegraebe, W., Baubet, V., Wahl, M. B., Deng, C., Taketo, M., Lewandoski, M. and Pourquié, O.** (2008). A β-catenin gradient links the clock and wavefront systems in mouse embryo segmentation. *Nat. Cell Biol.* **10**, 186–193.

**Bailey, C. and Dale, K.** (2015). Somitogenesis in vertebrate development. In *eLS*, pp. 1–15. Chichester, UK: John Wiley & Sons, Ltd.

**Barriga, E. H., Franze, K., Charras, G. and Mayor, R.** (2018). Tissue stiffening coordinates morphogenesis by triggering collective cell migration in vivo. *Nature* **554**, 523–527.

**Barrios, A., Poole, R. J., Durbin, L., Brennan, C., Holder, N. and Wilson, S. W.** (2003). Eph/Ephrin signaling regulates the mesenchymal-to-epithelial transition of the paraxial mesoderm during somite morphogenesis. *Curr. Biol.* **13**, 1571–82.

**Bénazéraf, B., Beaupeux, M., Tchernookov, M., Wallingford, A., Salisbury, T., Shirtz, A., Shirtz, A., Huss, D., Pourquié, O., François, P., et al.** (2017). Multi-scale quantification of tissue behavior during amniote embryo axis elongation. *Development* **144**, 4462–4472.

**Bielefeld, K. A., Amini-Nik, S., Whetstone, H., Poon, R., Youn, A., Wang, J. and Alman, B. A.** (2011). Fibronectin and beta-catenin act in a regulatory loop in dermal fibroblasts to modulate cutaneous healing. *J. Biol. Chem.* **286**, 27687–97.

**Burgess, R., Rawls, A., Brown, D., Bradley, A. and Olson, E. N.** (1996). Requirement of the paraxis gene for somite formation and musculoskeletal patterning. *Nature* **384**, 570–573.

**Camara, J. and Jarai, G.** (2010). Epithelial-mesenchymal transition in primary human bronchial epithelial cells is Smad-dependent and enhanced by fibronectin and TNF-alpha. *Fibrogenes. Tissue Repair* **3**, 2.

**Carey, S. P., D'Alfonso, T. M., Shin, S. J. and Reinhart-King, C. A.** (2012). Mechanobiology of tumor invasion: Engineering meets oncology. *Crit. Rev. Oncol. Hematol.*

**83**, 170–183.

**Carmeliet, P.** (2003). Blood vessels and nerves: common signals, pathways and diseases. *Nat. Rev. Genet.* **4**, 710–20.

**Chal, J., Guillot, C. and Pourquié, O.** (2017). PAPC couples the segmentation clock to somite morphogenesis by regulating N-cadherin-dependent adhesion. *Development* **144**, 664–676.

**Chan, C. J., Heisenberg, C.-P. and Hiiragi, T.** (2017). Coordination of morphogenesis and cell-fate specification in development. *Curr. Biol.* **27**, R1024–R1035.

**Chen, Q. K., Lee, K., Radisky, D. C. and Nelson, C. M.** (2013). Extracellular matrix proteins regulate epithelial-mesenchymal transition in mammary epithelial cells. *Differentiation* **86**, 126–132.

**Christ, B., Huang, R. and Scaal, M.** (2007). Amniote somite derivatives. *Dev. Dyn.* **236**, 2382–2396.

**Crisera, C. A., Kadison, A. S., Breslow, G. D., Maldonado, T. S., Longaker, M. T. and Gittes, G. K.** (2000). Expression and role of laminin-1 in mouse pancreatic organogenesis. *Diabetes* **49**, 936–44.

**Cukierman, E.** (2001). Taking cell-matrix adhesions to the third dimension. *Science (80-. ).* **294**, 1708–1712.

**Dale, J. K., Malapert, P., Chal, J., Vilhais-Neto, G., Maroto, M., Johnson, T., Jayasinghe, S., Trainor, P., Herrmann, B. and Pourquié, O.** (2006). Oscillations of the snail genes in the presomitic mesoderm coordinate segmental patterning and morphogenesis in vertebrate somitogenesis. *Dev. Cell* **10**, 355–366.

**Davidson, L. A.** (2017). Mechanical design in embryos: Mechanical signalling, robustness and developmental defects. *Philos. Trans. R. Soc. B Biol. Sci.* **372**,.

**Delfini, M.-C., Dubrulle, J., Malapert, P., Chal, J. and Pourquie, O.** (2005). Control of the segmentation process by graded MAPK/ERK activation in the chick embryo. *Proc. Natl. Acad. Sci.* **102**, 11343–11348.

**Duband, J. L. and Thiery, J. P.** (1982). Appearance and distribution of fibronectin during chick embryo gastrulation and neurulation. *Dev. Biol.* **94**, 337–50.

**Duband, J. L., Dufour, S., Hatta, K., Takeichi, M., Edelman, G. M. and Thiery, J. P.** (1987). Adhesion molecules during somitogenesis in the avian embryo. *J. Cell Biol.* **104**, 1361–74.

**Dubrulle, J., McGrew, M. J. and Pourquié, O.** (2001). FGF signaling controls somite boundary position and regulates segmentation clock control of spatiotemporal Hox gene activation. *Cell* **106**, 219–232.

**Dupont, S., Morsut, L., Aragona, M., Enzo, E., Giulitti, S., Cordenonsi, M., Zanconato, F., Le Digabel, J., Forcato, M., Bicciato, S., et al.** (2011). Role of YAP/TAZ in mechanotransduction. *Nature* **474**, 179–183.

**Durbin, L., Brennan, C., Shiomi, K., Cooke, J., Barrios, A., Shanmugalingam, S.,**

**Guthrie, B., Lindberg, R. and Holder, N.** (1998). Eph signaling is required for segmentation and differentiation of the somites. *Genes Dev.* **12**, 3096–3109.

**Durbin, L., Sordino, P., Barrios, A., Gering, M., Thisse, C., Thisse, B., Brennan, C., Green, A., Wilson, S. and Holder, N.** (2000). Anteroposterior patterning is required within segments for somite boundary formation in developing zebrafish. *Development* **127**, 1703–13.

**Dzamba, B. J., Jakab, K. R., Marsden, M., Schwartz, M. a. and DeSimone, D. W.** (2009). Cadherin adhesion, tissue tension, and noncanonical Wnt signaling regulate fibronectin matrix organization. *Dev. Cell* **16**, 421–32.

**Elosegui-Artola, A., Oria, R., Chen, Y., Kosmalska, A., Pérez-González, C., Castro, N., Zhu, C., Trepat, X. and Roca-Cusachs, P.** (2016). Mechanical regulation of a molecular clutch defines force transmission and transduction in response to matrix rigidity. *Nat. Cell Biol.* **18**, 540–548.

**Eyckmans, J., Boudou, T., Yu, X. and Chen, C. S.** (2011). A Hitchhiker's Guide to Mechanobiology. *Dev. Cell* **21**, 35–47.

**Friedland, J. C., Lee, M. H. and Boettiger, D.** (2009). Mechanically activated integrin switch controls alpha5beta1 function. *Science* **323**, 642–4.

**Fukuda, K. and Yasugi, S.** (2005). Review: The molecular mechanisms of stomach development in vertebrates. *Dev. Growth Differ.* **47**, 375–382.

**Gao, J., DeRouen, M. C., Chen, C. H., Nguyen, M., Nguyen, N. T., Ido, H., Harada, K., Sekiguchi, K., Morgan, B. A., Miner, J. H., et al.** (2008). Laminin-511 is an epithelial message promoting dermal papilla development and function during early hair morphogenesis. *Genes Dev.* **22**, 2111–2124.

**George, E. L., Georges-Labouesse, E. N., Patel-King, R. S., Rayburn, H. and Hynes, R. O.** (1993). Defects in mesoderm, neural tube and vascular development in mouse embryos lacking fibronectin. *Development* **119**, 1079–1091.

**Georges-Labouesse, E. N., George, E. L., Rayburn, H. and Hynes, R. O.** (1996). Mesodermal development in mouse embryos mutant for fibronectin. *Dev. Dyn.* **207**, 145–56.

**Gomez, C., Özbudak, E. M., Wunderlich, J., Baumann, D., Lewis, J. and Pourquié, O.** (2008). Control of segment number in vertebrate embryos. *Nature* **454**, 335–339.

**Guillory, G. and Bronner-Fraser, M.** (1986). An in vitro assay for neural crest cell migration through the somites. *J. Embryol. Exp. Morphol.* **98**, 85–97.

**Harima, Y., Takashima, Y., Ueda, Y., Ohtsuka, T. and Kageyama, R.** (2013). Accelerating the tempo of the segmentation clock by reducing the number of introns in the Hes7 gene. *Cell Rep.* **3**, 1–7.

**Harrisson, F., Vanroelen, C., Foidart, J. M. and Vakaet, L.** (1984). Expression of different regional patterns of fibronectin immunoreactivity during mesoblast formation in the chick blastoderm. *Dev. Biol.* **101**, 373–381.

**Harrisson, F., Van Hoof, J., Vanroelen, C. and Vakaet, L.** (1985). Transfer of extracellular matrix components between germ layers in chimaeric chicken-quail blastoderms. *Cell Tissue Res.* **239**, 643–9.

**Harrisson, F., Van Nassauw, L., Van Hoof, J. and Foidart, J. M.** (1993). Microinjection of antifibronectin antibodies in the chicken blastoderm: inhibition of mesoblast cell migration but not of cell ingression at the primitive streak. *Anat. Rec.* **236**, 685–696.

**Herrgen, L., Ares, S., Morelli, L. G., Schröter, C., Jülicher, F. and Oates, A. C.** (2010). Intercellular coupling regulates the period of the segmentation clock. *Curr. Biol.* **20**, 1244–1253.

**Hirata, H., Bessho, Y., Kokubu, H., Masamizu, Y., Yamada, S., Lewis, J. and Kageyama, R.** (2004). Instability of Hes7 protein is crucial for the somite segmentation clock. *Nat. Genet.* **36**, 750–754.

**Hubaud, A. and Pourquié, O.** (2014). Signalling dynamics in vertebrate segmentation. *Nat. Rev. Mol. Cell Biol.* **15**, 709–721.

**Hubaud, A., Regev, I., Mahadevan, L. and Pourquié, O.** (2017). Excitable dynamics and Yap-dependent mechanical cues drive the segmentation clock. *Cell* **171**, 668–682.e11.

**Iozzo, R. V. and Gubbiotti, M. A.** (2018). Extracellular matrix: The driving force of mammalian diseases. *Matrix Biol.* **71–72**, 1–9.

**Jaalouk, D. E. and Lammerding, J.** (2009). Mechanotransduction gone awry. *Nat. Rev. Mol. Cell Biol.* **10**, 63–73.

**Johnson, J., Rhee, J., Parsons, S. M., Brown, D., Olson, E. N. and Rawls, A.** (2001). The anterior/posterior polarity of somites is disrupted in paraxis-deficient mice. *Dev. Biol.* **229**, 176–187.

**Jülich, D., Geisler, R., Holley, S. a. and Tübingen 2000 Screen Consortium** (2005). Integrin alpha5 and delta/notch signaling have complementary spatiotemporal requirements during zebrafish somitogenesis. *Dev. Cell* **8**, 575–86.

**Jülich, D., Mould, a P., Koper, E. and Holley, S. a** (2009). Control of extracellular matrix assembly along tissue boundaries via Integrin and Eph/Ephrin signaling. *Development* **136**, 2913–21.

**Jülich, D., Cobb, G., Melo, A. M., McMillen, P., Lawton, A. K., Mochrie, S. G. J., Rhoades, E. and Holley, S. A.** (2015). Cross-scale integrin regulation organizes ECM and tissue topology. *Dev. Cell* **34**, 33–44.

**Kadoya, Y., Kadoya, K., Durbeej, M., Holmvall, K., Sorokin, L. and Ekblom, P.** (1995). Antibodies against domain E3 of laminin-1 and integrin ??6 subunit perturb branching epithelial morphogenesis of submandibular gland, but by different modes. *J. Cell Biol.* **129**, 521–534.

**Kageyama, R., Niwa, Y., Isomura, A., González, A. and Harima, Y.** (2012). Oscillatory gene expression and somitogenesis. *Wiley Interdiscip. Rev. Dev. Biol.* **1**, 629–641.

**Kaplan, D. H., Li, M. O., Jenison, M. C., Shlomchik, W. D., Flavell, R. A. and**

**Shlomchik, M. J.** (2007). Autocrine/paracrine TGFbeta1 is required for the development of epidermal Langerhans cells. *J. Exp. Med.* **204**, 2545–52.

**Keely, P. J., Wu, J. E. and Santoro, S. a.** (1995). The spatial and temporal expression of the alpha 2 beta 1 integrin and its ligands, collagen I, collagen IV, and laminin, suggest important roles in mouse mammary morphogenesis. *Differentiation.* **59**, 1–13.

**Kenny, A. P., Rankin, S. a., Allbee, A. W., Prewitt, A. R., Zhang, Z., Tabangin, M. E., Shifley, E. T., Louza, M. P. and Zorn, A. M.** (2012). Sizzled-tolloid interactions maintain foregut progenitors by regulating fibronectin-dependent BMP signaling. *Dev. Cell* **23**, 292–304.

**Kim, N. G. and Gumbiner, B. M.** (2015). Adhesion to fibronectin regulates Hippo signaling via the FAK-Src-PI3K pathway. *J. Cell Biol.* **210**, 503–515.

**Kim, W., Matsui, T., Yamao, M., Ishibashi, M., Tamada, K., Takumi, T., Kohno, K., Oba, S., Ishii, S., Sakumura, Y., et al.** (2011). The period of the somite segmentation clock is sensitive to Notch activity. *Mol. Biol. Cell* **22**, 3541–3549.

**Kim, K., Ossipova, O. and Sokol, S. Y.** (2015). Neural crest specification by inhibition of the ROCK/Myosin II pathway. *Stem Cells* **33**, 674–685.

**Koser, D. E., Thompson, A. J., Foster, S. K., Dwivedy, A., Pillai, E. K., Sheridan, G. K., Svoboda, H., Viana, M., Costa, L. D. F., Guck, J., et al.** (2016). Mechanosensing is critical for axon growth in the developing brain. *Nat. Neurosci.* **19**, 1592–1598.

**Koshida, S., Kishimoto, Y., Ustumi, H., Shimizu, T., Furutani-Seiki, M., Kondoh, H. and Takada, S.** (2005). Integrin alpha5-dependent fibronectin accumulation for maintenance of somite boundaries in zebrafish embryos. *Dev. Cell* **8**, 587–98.

**Krol, A. J., Roellig, D., Dequeant, M.-L., Tassy, O., Glynn, E., Hattem, G., Mushegian, A., Oates, A. C. and Pourquie, O.** (2011). Evolutionary plasticity of segmentation clock networks. *Development* **138**, 2783–2792.

**Krull, C. E.** (2001). Segmental organization of neural crest migration. *Mech. Dev.* **105**, 37–45.

**Kuan, C.-Y. K., Tannahill, D., Cook, G. M. W. and Keynes, R. J.** (2004). Somite polarity and segmental patterning of the peripheral nervous system. *Mech. Dev.* **121**, 1055–68.

**Kubota, Y., Morita, T., Kusakabe, M., Sakakura, T. and Ito, K.** (1999). Spatial and temporal changes in chondroitin sulfate distribution in the sclerotome play an essential role in the formation of migration patterns of mouse neural crest cells. *Dev. Dyn.* **214**, 55–65.

**Lauschke, V. M., Tsiairis, C. D., François, P. and Aulehla, A.** (2013). Scaling of embryonic patterning based on phase-gradient encoding. *Nature* **493**, 101–105.

**Lee, L. K., Pollock, a. S. and Lovett, D. H.** (1993). Asymmetric origins of the mature glomerular basement membrane. *J. Cell. Physiol.* **157**, 169–77.

**Liao, B. K., Jörg, D. J. and Oates, A. C.** (2016). Faster embryonic segmentation through elevated Delta-Notch signalling. *Nat. Commun.* **7**, 1–12.

**Linask, K. K. and Lash, J. W.** (1988). A role for fibronectin in the migration of avian precardiac cells. II. Rotation of the heart-forming region during different stages and its effects. *Dev. Biol.* **129**, 324–329.

**Linask, K. K., Ludwig, C., Han, M. D., Liu, X., Radice, G. L. and Knudsen, K. A.** (1998). N-cadherin/catenin-mediated morphoregulation of somite formation. *Dev. Biol.* **202**, 85–102.

**Linde-Medina, M. and Marcucio, R.** (2018). Living tissues are more than cell clusters: The extracellular matrix as a driving force in morphogenesis. *Prog. Biophys. Mol. Biol.* **137**, 46–51.

**Lui, C., Lee, K. and Nelson, C. M.** (2012). Matrix compliance and RhoA direct the differentiation of mammary progenitor cells. *Biomech. Model. Mechanobiol.* **11**, 1241–9.

**Mansouri, A., Voss, A. K., Thomas, T., Yokota, Y. and Gruss, P.** (2000). Uncx4.1 is required for the formation of the pedicles and proximal ribs and acts upstream of Pax9. *Development* **127**, 2251–8.

**Marjoram, R. J., Lessey, E. C. and Burridge, K.** (2014). Regulation of RhoA mechanotransduction activity by adhesion molecules. *Curr. Mol. Med.* **14**, 199–208.

**Martins, G. G., Rifes, P., Amândio, R., Rodrigues, G., Palmeirim, I. and Thorsteinsdóttir, S.** (2009). Dynamic 3D cell rearrangements guided by a fibronectin matrix underlie somitogenesis. *PLoS One* **4**, e7429.

**McColl, J., Mok, G. F., Lippert, A. H., Ponjavic, A., Muresan, L. and Münsterberg, A.** (2018). 4D imaging reveals stage dependent random and directed cell motion during somite morphogenesis. *Sci. Rep.* **8**, 1–10.

**McMillen, P., Chatti, V., Jülich, D. and Holley, S. A.** (2016). A sawtooth pattern of Cadherin 2 stability mechanically regulates somite morphogenesis. *Curr. Biol.* **26**, 542–9.

**Merle, T. and Farge, E.** (2018). Trans-scale mechanotransductive cascade of biochemical and biomechanical patterning in embryonic development: the light side of the force. *Curr. Opin. Cell Biol.* **55**, 111–118.

**Mittal, A., Pulina, M., Hou, S. Y. and Astrof, S.** (2013). Fibronectin and integrin alpha 5 play requisite roles in cardiac morphogenesis. *Dev. Biol.* **381**, 73–82.

**Moeendarbary, E. and Harris, A. R.** (2014). Cell mechanics : principles , practices , and prospects. **6**, 371–388.

**Moreno, T. A., Jappelli, R., Belmonte, J. C. I. and Kintner, C.** (2008). Retinoic acid regulation of the Mesp-Ripply feedback loop during vertebrate segmental patterning. *Dev. Biol.* **315**, 317–330.

**Nakaya, Y., Kuroda, S., Katagiri, Y. T., Kaibuchi, K. and Takahashi, Y.** (2004). Mesenchymal-epithelial transition during somitic segmentation is regulated by differential roles of Cdc42 and Rac1. *Dev. Cell* **7**, 425–438.

**Nelemans, B.** (2018). How to build a spine? Exploring mechanobiology of somite formation in the chicken embryo. PhD thesis. *VU Amsterdam*.

**Nelson, C. M. and Bissell, M. J.** (2006). Of extracellular matrix, scaffolds, and signaling: tissue architecture regulates development, homeostasis, and cancer. *Annu. Rev. Cell Dev. Biol.* **22**, 287–309.

**Niwa, Y., Masamizu, Y., Liu, T., Nakayama, R., Deng, C.-X. and Kageyama, R.** (2007). The initiation and propagation of Hes7 oscillation are cooperatively regulated by Fgf and Notch signaling in the somite segmentation clock. *Dev. Cell* **13**, 298–304.

**Niwa, Y., Shimojo, H., Isomura, A., Gonzalez, A., Miyachi, H. and Kageyama, R.** (2011). Different types of oscillations in Notch and Fgf signaling regulate the spatiotemporal periodicity of somitogenesis. *Genes Dev.* **25**, 1115–1120.

**Oginuma, M., Takahashi, Y., Kitajima, S., Kiso, M., Kanno, J., Kimura, A. and Saga, Y.** (2010). The oscillation of Notch activation, but not its boundary, is required for somite border formation and rostral-caudal patterning within a somite. *Development* **137**, 1515–1522.

**Palmeirim, I., Henrique, D., Ish-Horowicz, D. and Pourquié, O.** (1997). Avian hairy gene expression identifies a molecular clock linked to vertebrate segmentation and somitogenesis. *Cell* **91**, 639–648.

**Park, J. and Schwarzbauer, J. E.** (2014). Mammary epithelial cell interactions with fibronectin stimulate epithelial-mesenchymal transition. *Oncogene* **33**, 1649–1657.

**Parsons, M. J., Pollard, S. M., Saúde, L., Feldman, B., Coutinho, P., Hirst, E. M. a and Stemple, D. L.** (2002). Zebrafish mutants identify an essential role for laminins in notochord formation. *Development* **129**, 3137–3146.

**Petridou, N. I., Spiró, Z. and Heisenberg, C. P.** (2017). Multiscale force sensing in development. *Nat. Cell Biol.* **19**, 581–588.

**Pulina, M. V., Hou, S. Y., Mittal, A., Julich, D., Whittaker, C. a., Holley, S. a., Hynes, R. O. and Astrof, S.** (2011). Essential roles of fibronectin in the development of the left-right embryonic body plan. *Dev. Biol.* **354**, 208–220.

**Pulina, M., Liang, D. and Astrof, S.** (2014). Shape and position of the node and notochord along the bilateral plane of symmetry are regulated by cell-extracellular matrix interactions. *Biol. Open* 1–8.

**Rallis, C., Pinchin, S. M. and Ish-Horowicz, D.** (2010). Cell-autonomous integrin control of Wnt and Notch signalling during somitogenesis. *Development* **137**, 3591–3601.

**Rifes, P. and Thorsteinsdóttir, S.** (2012). Extracellular matrix assembly and 3D organization during paraxial mesoderm development in the chick embryo. *Dev. Biol.* **368**, 370–381.

**Rifes, P., Carvalho, L., Lopes, C., Andrade, R. P., Rodrigues, G., Palmeirim, I. and Thorsteinsdóttir, S.** (2007). Redefining the role of ectoderm in somitogenesis: a player in the formation of the fibronectin matrix of presomitic mesoderm. *Development* **134**, 3155–3165.

**Rowton, M., Ramos, P., Anderson, D. M., Rhee, J. M., Cunliffe, H. E. and**

**Rawls, A.** (2013). Regulation of mesenchymal-to-epithelial transition by PARAXIS during somitogenesis. *Dev. Dyn.* **242**, 1332–1344.

**Rozario, T., Dzamba, B., Weber, G. F., Davidson, L. a. and DeSimone, D. W.** (2009). The physical state of fibronectin matrix differentially regulates morphogenetic movements in vivo. *Dev. Biol.* **327**, 386–398.

**Saga, Y.** (2012). The mechanism of somite formation in mice. *Curr. Opin. Genet. Dev.* **22**, 331–338.

**Sato, Y., Nagatoshi, K., Hamano, A., Imamura, Y., Huss, D., Uchida, S. and Lansford, R.** (2017). Basal filopodia and vascular mechanical stress organize fibronectin into pillars bridging the mesoderm-endoderm gap. *Development* **144**, 281–291.

**Sawada, A., Shinya, M., Jiang, Y. J., Kawakami, A., Kuroiwa, A. and Takeda, H.** (2001). Fgf/MAPK signalling is a crucial positional cue in somite boundary formation. *Development* **128**, 4873–80.

**Schröter, C., Herrgen, L., Cardona, A., Brouhard, G. J., Feldman, B. and Oates, A. C.** (2008). Dynamics of zebrafish somitogenesis. *Dev. Dyn.* **237**, 545–53.

**Schröter, C., Ares, S., Morelli, L. G., Isakova, A., Hens, K., Soroldoni, D., Gajewski, M., Jülicher, F., Maerkl, S. J., Deplancke, B., et al.** (2012). Topology and dynamics of the Zebrafish Segmentation Clock core circuit. *PLoS Biol.* **10**, e1001364.

**Schwartz, M. A. and Ginsberg, M. H.** (2002). Networks and crosstalk: Integrin signalling spreads. *Nat. Cell Biol.* **4**, 65–68.

**Serwane, F., Mongera, A., Rowghanian, P., Kealhofer, D. A., Lucio, A. A., Hockenbery, Z. M. and Campàs, O.** (2017). In vivo quantification of spatially varying mechanical properties in developing tissues. *Nat. Methods* **14**, 181–186.

**Shih, N. P., François, P., Delaune, E. A. and Amacher, S. L.** (2015). Dynamics of the slowing segmentation clock reveal alternating two-segment periodicity. *Development* **142**, 1785–93.

**Simon-Assmann, P., Lefebvre, O., Bellissent-Waydelich, A., Olsen, J., Orian-Rousseau, V. and De Arcangelis, A.** (1998). The laminins: Role in intestinal morphogenesis and differentiation. In *Annals of the New York Academy of Sciences*, pp. 46–64.

**Singh, A. B. and Harris, R. C.** (2005). Autocrine, paracrine and juxtacrine signaling by EGFR ligands. *Cell. Signal.* **17**, 1183–93.

**Solursh, M., Fisher, M., Meier, S. and Singley, C. T.** (1979). The role of extracellular matrix in the formation of the sclerotome. *J. Embryol. Exp. Morphol.* **54**, 75–98.

**Sonnen, K. F., Lauschke, V. M., Uraji, J., Falk, H. J., Petersen, Y., Funk, M. C., Beaupeux, M., François, P., Merten, C. A. and Aulehla, A.** (2018). Modulation of phase shift between Wnt and Notch signaling oscillations controls mesoderm segmentation. *Cell* **172**, 1079–1090.e12.

**Stemple, D. L.** (2005). Structure and function of the notochord: an essential organ for chordate development. *Development* **132**, 2503–12.

**Stern, C. D. and Piatkowska, A. M.** (2015). Multiple roles of timing in somite formation. *Semin. Cell Dev. Biol.* **42**, 134–139.

**Sulzmaier, F. J., Jean, C. and Schlaepfer, D. D.** (2014). FAK in cancer: mechanistic findings and clinical applications. *Nat. Rev. Cancer* **14**, 598–610.

**Tang, Y., Rowe, R. G., Botvinick, E. L., Kurup, A., Putnam, A. J., Seiki, M., Weaver, V. M., Keller, E. T., Goldstein, S., Dai, J., et al.** (2013). MT1-MMP-dependent control of skeletal stem cell commitment via a β1-integrin/YAP/TAZ signaling axis. *Dev. Cell* **25**, 402–416.

**Thomas, T. and Dziadek, M.** (1994). Expression of collagen alpha 1(IV), laminin and nidogen genes in the embryonic mouse lung: implications for branching morphogenesis. *Mech. Dev.* **45**, 193–201.

**Trinh, L. a. and Stainier, D. Y. R.** (2004). Fibronectin regulates epithelial organization during myocardial migration in zebrafish. *Dev. Cell* **6**, 371–382.

**Tsiairis, C. D. and Aulehla, A.** (2016). Self-organization of embryonic genetic oscillators into spatiotemporal wave patterns. *Cell* **164**, 656–67.

**Turner, N. and Grose, R.** (2010). Fibroblast growth factor signalling: from development to cancer. *Nat. Rev. Cancer* **10**, 116–29.

**Watanabe, T., Sato, Y., Saito, D., Tadokoro, R. and Takahashi, Y.** (2009). EphrinB2 coordinates the formation of a morphological boundary and cell epithelialization during somite segmentation. *Proc. Natl. Acad. Sci.* **106**, 7467–7472.

**Weaver, V. M., Petersen, O. W., Wang, F., Larabell, C. A., Briand, P., Damsky, C. and Bissell, M. J.** (1997). Reversion of the malignant phenotype of human breast cells in three-dimensional culture and in vivo by integrin blocking antibodies. *J. Cell Biol.* **137**, 231–245.

**Yang, J. T., Bader, B. L., Kreidberg, J. a, Ullman-Culleré, M., Trevithick, J. E. and Hynes, R. O.** (1999). Overlapping and independent functions of fibronectin receptor integrins in early mesodermal development. *Dev. Biol.* **215**, 264–277.

**Yoshino, T., Saito, D., Atsuta, Y., Uchiyama, C., Ueda, S., Sekiguchi, K. and Takahashi, Y.** (2014). Interepithelial signaling with nephric duct is required for the formation of overlying coelomic epithelial cell sheet. *Proc. Natl. Acad. Sci. U. S. A.* **111**, 6660–5.